DRUG DESIGN AGAINST ANTIMICROBIAL RESISTANCE

by

Kevser Betül Kalyon

B.S., Food Engineering, Middle East Technical University, 2012

Submitted to the Institute for Graduate Studies in
Science and Engineering in partial fulfillment of
the requirements for the degree of
Master of Science

Graduate Program in Chemical Engineering

Boğaziçi University

2016

ACKNOWLEDGEMENTS

I would like sincerely thank my thesis supervisor Prof. Elif Özkırımlı Ölmez and co-supervisor Assoc. Prof. Berna Sarıyar Akbulut. Their knowledge and vision of the field have aided me to better understand my work and their guidance has helped me continuously during my thesis.

I am very grateful to my thesis committee members; Prof. Dr. Kutlu Ülgen, Assoc. Prof. Burak Alakent and Asisst. Prof. Nevra Özer for their valuable time spent on my thesis and their helpful recommendations.

I cannot thank Begüm Alaybeyoğlu enough for guiding me in times of crisis and for being an absolute source of wisdom and support. I would like to thank Hakime Öztürk for being a wonderful friend. Their emotional support and expertise was a beacon of hope when times were difficult. I would also like to express my gratitude to the members of KB407 for their kind support and help.

I would like to thank my aunts and uncles for their thoughtfulness. I would especially like to thank Gülşen Kaşka for her advices about academics and life in general.

Finally, I would like to thank my mother Güler Kalyon and my father Muammer Kalyon who have done everything they can to help me succeed throughout my life. I would like to thank my sisters, İlham Kalyon and Melike Kalyon for being pure joys in my life. I am forever grateful to you.

TUBITAK Project No.114M179 and BAP Project No.7086 are gratefully acknowledged for the funding.

The numerical calculations reported in this paper were fully/partially performed at TUBITAK ULAKBIM, High Performance and Grid Computing Center (TRUBA resources).

ABSTRACT

DRUG DESIGN AGAINST ANTIMICROBIAL RESISTANCE

Cell penetrating peptides are extensively studied due to their potential for having antimicrobial properties. The purpose of this study is to understand the mechanisms of certain cell penetrating peptides in bacterial and mammalian membranes and to research their potential in antimicrobial drug design. In this study, melittin and pVEC peptide structures along with POPC and POPE membranes were constructed in VMD and the passage of each peptide through bilayers of each membrane type were simulated using SMD simulations. MD simulations were carried out by taking snapshots of SMD simulations while the peptide was located on the top, middle, and bottom of the bilayer. The simulations were examined by following energy, force and work vs. distance profiles of peptides. The results gave insight on melittin and pVEC interactions with POPE and POPC membranes as they are transported through bilayers. Compared to POPE membrane, the electrostatic energies were higher in POPC membrane making it harder for peptides to penetrate the bilayer. Melittin helicity was higher in POPE bilayer. The observed lower helicity in POPC membrane is thought to facilitate pore formation by increasing interactions of residues with membrane lipids and effecting lipid orders. In POPE membrane another mechanism might be at work. POPE membrane thinned more which may increase the probability of leakage. The pVEC peptide lead to more water insertion inside the bilayers compared to melittin peptide. Furthermore, pVEC caused more water molecules to penetrate POPC membrane. This may increase the permeability of the membrane and increase uptake of more peptides. In MD simulations, pVEC preferred POPE membrane over POPC membrane while melittin had affinity for both membranes. When melittin center of mass was pulled, due to energy barriers melittin penetrated the upper P layer of the bilayer with difficulty but caused more water penetration into the bilayer compared to other simulations. When melittin was pulled with 1/10th velocity, it stayed in a parallel position on the upper P layer of membrane in α-helix structure before penetration. After 151.68 ns, melittin only reached the center of the bilayer while in other melittin POPE simulations it took melittin 58, 50 and 38 ns to pass through the bilayer.

ÖZET

ANTİMİKROBİYAL DİRENCE KARŞI İLAÇ TASARIMI

Hücre-delici peptitler, antimikrobik özellikler taşıma potansiyelinden dolayı birçok çalışmaya konu olmuştur. Bu çalışmada hücre-delici peptitlerin bakteriyel ve hayvansal zarlar üzerindeki işleyiş mekanizmasının anlaşılması ve antimikrobiyal ilaç tasarımında kullanılma potansyelinin belirlenmesi amaçlanmıştır. Çalışmada; melittin, pVEC peptit yapıları, POPC ve POPE zar yapıları VMD aracılığıyla oluşturulmuştur. Her peptitin farklı tip hücre zarından geçiş SMD simülasyonları gerçekleştirilmiştir. SMD simülasyonlarından, peptitin çift katmanlı hücre zarı üzerinde, ortasında ve altında bulunduğu noktalarda fotoğraf alınarak MD simülasyonları uygulanmıştır. Simülasyonların incelenmesi, peptitlerin enerji, güç ve işe karşı uzaklık profili takip edilerek gerçekleştirilmiştir. Çalışma sonucunda, tek bir melittin ve pVEC peptitinin hücre zarından geçişi hakkında detaylı bilgiler edinilmiştir. Peptitlerin elektrostatik enerjileri, POPC zarlarında daha yüksek olduğu ve çift katmanlı zardan geçişinin zorlaştığı gözlemlenmiştir. Melittin sarmal oranının POPE zarında daha yüksek olduğu tespit edilmiştir. Melittinin POPC zarında daha düşük sarmal oranına sahip olması, peptit kalıntılarının zar lipitleri ile olan etkileşiminin artmasına ve lipit düzenini etkileyerek geçici gözenek oluşmasını kolaylaştırabileceği düşünülmektedir. POPE zarının daha çok incelmesi zardan sızıntı oluşma olasılığını arttırması aşikârdır. pVEC, melittin'e göre zardan daha fazla su molekülü geçişini sağlamıştır. POPC zarından daha fazla su molekülünün geçmesine yol açan pVEC'in, zarın geçirgenliğini arttıracağı böylece daha fazla peptitin geçişine ortam sağlayacağı öngörülmektedir. MD sonuçlarında; pVEC, POPE zarını tercih ettiği, melittinin ise iki zar tipinde de yakınlaşma eğilimi olduğu görülmüştür. Kütle merkezinden çekildiğinde, melittinin enerji bariyerlerinden dolayı üst P katmanından geçişinin zor olduğu, fakat zar geçişiyle birlikte su geçişinin daha fazla olduğu gözlemlenmiştir. 1/10 (yavaş) hız ile çekildiğinde, melittin peptitinin zar geçişinden önce üst P katmanına α-sarmal şeklinde parallel yerleştiği görülmüştür. 151.68 ns süresince melittinin sadece zarın ortasına kadar ilerlediği, diğer melittin POPE simülasyonlarında melittinin zar geçişi 58, 50 ve 38 ns sürdüğü gözlemlenmiştir.

TABLE OF CONTENTS

LIST OF FIGURES

LIST OF TABLES

LIST OF SYMBOLS

a_i	Acceleration of the particle I
$\vec{F}$	Force applied
F_i	Force exerted on the particle I
fs	Femtosecond
k	Spring constant
kcal	Kilocalorie
M	Molar
m_i	Mass of the particle i and
$\vec{n}$	Direction of pulling
ns	Nanosecond
PMF	Potential of mean force
pN	Piconewton
ps	Picoseconds
$\vec{r}$	Actual position of the SMD atom
$\vec{r}_0$	Initial position of the SMD atom
$r_{i,j}$	Distance between atoms i and j.
t	Time
U	Potential energy
V	Potential energy
v	Pulling velocity
z	z coordinate of α-carbon of the chosen residue
α	Alpha
β	Beta
µM	Micromolar
Å	Angstrom

LIST OF ACRONYMS/ABBREVIATIONS

A	Alanine
Ala	Alanine
AMP	Antimicrobial peptide
Arg	Arginine
C	Carbon
CD	Circular dichroism
Chol	Cholesterol
CPP	Cell-penetrating peptide
c.o.m.	Center of mass
DMPC	1, 2-Dimyristoyl-*sn*-Glycero-3-Phosphocholine
DMPG	1, 2-Dimyristoyl-*sn*-Glycero-3-[Phospho-*rac*-(1-glycerol)]
DOPC	1, 2-dioleoyl-sn-glycro-3-phosphocholine
DOPG	Dioleoylphosphatidylglycerol
DOPS	Dioleoylphosphatidylserine
DPPC	1, 2-dipalmitoyl-sn-glycro-3-phosphocholine
DPPE	Dipalmitoylphosphatidylethanolamine
DPPG	Dipalmitoyl phosphatidyl glycerol
G	Glycine
Gln	Glutamine
Gly	Glycine
GUV	Giant Unilamellar Vesicle
h	Hour(s)
H	Histadine
His	Histadine
I	Isoleucine
Ile	Isoleucine
K	Lysine
L	Leucine
Leu	Leucine
Lys	Lysine

MD	Molecular dynamics
P	Proline
PE	Phosphodylethanolamine
PG	Phosphatidyglycerol
P/L	Peptide/Lipid
PME	Particle mesh Ewald
POPC	1-palmitoyl-2-oleoyl-sn-glycero-3-phosphocholine
POPE	1-Palmitoyl-2-oleoyl-*sn*-glycero-3-phosphoethanolamine
POPG	1-Palmitoyl-2-Oleoyl-*sn*-Glycero-3-Phosphocholine
Pro	Proline
pVEC	Vascular endothelial-cadherin protein
Q	Glutamine
R	Arginine
S	Serine
Ser	Serine
SMD	Steered molecular dynamics
T	Threonine
Thr	Threonine
TM	trans-membrane
Trp	Tryptophan
V	Valine
Val	Valine
VdW	Van der Waals
VMD	Visual molecular dynamics
W	Tryptophan

1. INTRODUCTION

The discovery of the first antibiotic, Penicilin, was in 1945. Soon after the utilization of penicilin, bacterial resistance and with it the need for new antimicrobial drugs emerged. The resistance was observed to be the result of the hydrolysis of antibiotics by β-lactamase [1]. β-lactamase is a bacterial enzyme that breaks the β-lactam bond of antibiotics. β-lactam bond is crucial for antibiotic function since it hinders the cell wall synthesis of bacteria. Without the synthesis of a new cell wall, bacteria eventually cease to exist. However, β-lactamase severs the β-lactam ring, which can no longer interfere with the bacterial cell wall synthesis. β-lactam antibiotics consequently become ineffective and the bacterial enzyme β-lactamase results in antibiotic resistance. Today, β-lactamase has caused more than 90% of nosocomial *Staphylococcus aureus* isolates to gain resistance [2]. Although we have powerful antibiotics today, in due time, the rapid evolution of bacteria may render these antibiotics ineffective [1]. Therefore studies in novel drug delivery methods are very important. Precise biological activity, acceptable pharmacokinetic profile and low immunogenicity are desired attributes in a developed antimicrobial drug. These properties should be met for a drug to be successful. Nowadays drugs that utilize antimicrobial peptides are being developed to obtain better therapeutic results. Designing drugs is not always straightforward especially when complexes of drugs and carrier peptides are involved. Vast knowledge should be gained and through experiments must be carried out to design drugs and validate for therapeutic use. Computer-based strategies are used to perform simulations and aids in gaining a theoretical idea about the mechanisms and biological modes of drugs [3].

Cell penetrating peptides (CPPs) that have antimicrobial properties are called Antimicrobial peptides (AMPs). Antimicrobial peptides are the center of many studies because of their many advantages. These advantages include low cost production, low immunogenicity because the peptide degrades to amino acids which have less toxic effects, good targeting, and acceptable pharmacokinetic effects, can

be modified without difficulty when needed and have elevated biological activity. Valuable scaffolds are identified by investigating residue interactions with membranes and their effects on cells. These scaffolds may be used in novel drug designs. [3]. Drugs must be delivered distinctly to their targets however CPPs mostly penetrate cells non-selectively. The delivery vector can be advanced by methods such as adding cell specific peptide sequences. CPPs could become tissue-specific transport vectors for various drugs [4]. In vivo studies carried out in the field of conjugated anti-cancer drugs and therapeutic peptides to cell-penetrating peptides show chances of advancement for development of targeted therapies. The pVEC peptide was used in conjunction with tumor homing drug CREKA which resulted in improved drug delivery in vitro [5].

It is hard to duplicate mechanisms such as barrier penetrations on MD time scales, which are still detained to tens of nanoseconds. To direct the system from one state onto the next external forces may be utilized. Atomic force microscopy and optical tweezers are experimental techniques that have improved the comprehension of the mechanical properties of biopolymers. The in silico state of these studies can be monitored through Steered molecular dynamics (SMD). SMD exerts external forces on molecules to explore their mechanical characteristics and to quicken mechanisms that are generally too slow. In SMD, the direction of pulling is picked before the simulation is run and introduced to the system by a couple of lines in a NAMD configuration file [6].

Powerful experimental techniques have helped advance researches of lipid-protein interactions. However, due to the complex bilayer environment the identification of these interactions is still very difficult. The collected experimental data is also limited. Therefore, any qualitative data obtained by protein membrane systems computer simulations are important in the development of studies in this field [7].

In this study, the uptake of melittin and pVEC across POPE and POPC membranes was examined using SMD and MD simulations. To investigate diverse proteins and their mechanisms in innumerable systems various studies have been carried out by employing MD simulations. Aspects such as membrane binding of proteins, hydrophilic or

hydrophobic associations, position of proteins, or free energy of binding among peptides and membranes can be monitored using MD simulations [8]. This study focuses on the effects of membrane composition, different types of cell penetrating peptides and the effect of concentration on membrane permeability. Steered molecular dynamics and molecular dynamics simulations were used to computationally examine these processes.

In the study, information on cell penetrating peptides mechanisms; cellular membrane properties; and literature research on the peptides melittin and pVEC are presented in theoretical background. The computational methods used in the study and carried out procedures during simulations are listed in the methods section. Later, the results of the SMD and MD simulations are summarized. The results are discussed and conclusions are presented. Lastly, in the future work section, prospective studies for further investigation of the field are mentioned.

2. THEORETICAL BACKGROUND

2.1. Cell Membrane Structures

Understanding the cell membrane structures is the first step to distinguishing CPP penetration mechanisms. Bacteria have prokaryotic cells while mammalians have eukaryotic cells. Prokaryotic and eukaryotic cells both have a cellular membrane. The difference is that eukaryotes have additional membrane-enclosed organelles, such as nuclei and mitochondria. The membrane's structure differs in its lipid and protein components for all type of cells. The Lipid components are phosphoglycerides and glycolipids. Hydrophilic and hydrophobic parts of lipids form the lipid bilayer of cellular membranes. The polar head groups which form the hydrophilic part and are in contact with water and the non-polar tails which are the hydrophobic part lie in the interior of the membrane. Non-covalent interactions such as van der Waals and hydrophobic interactions hold the lipid bilayer structure together. Lipid layers have mixtures of lipids in different compositions. Transport of materials through the membrane is governed by the lipid bilayer and the membrane proteins. Also during material transport, membranes act as a surface for catalysis. Enzymes can bind to membranes and enzymatic reactions can take place. Receptor property is another important function of membranes. Proteins bind to specific biologically significant substances called receptors that trigger biochemical responses in the cell. This property is crucial for drug target delivery [9].

2.1.1. Membrane Structure and Composition

Detailed information about membrane structures and compositions is crucial in drug design and delivery. The origin of the currently valid membrane model was theorized in 1972 by Singer and Nicolson and was named the fluidic membrane model [10]. The model consisted of the idea that the structural backbone of the bilayers formed of lipids. Lipids in the membrane move sideways and seldom propagate in opposite directions vertically. The membrane model also contains proteins which are heterogeneously spaced. There are different types of proteins present in membranes. The internal membrane proteins stretch

through the membrane whereas the peripheral membrane proteins may be found on the surface. It is established that the biological membranes contain lipids and proteins in roughly a 50-50 ratio [10].

Types of lipids that form biological membranes are mainly phospholipids, sphingolipids, and glycolipids. The properties of lipids immensely affect the properties of the membrane. The interactions of the lipids with water determine the permeability of the membranes. Lipids are insoluble in water and soluble in organic solvents. Lipids are formed of two parts; the hydrophilic head group and the hydrophobic tail group. Due to this structure, the phospholipids in biological membranes arrange in such a manner that the hydrophobic tail groups faces each other and the polar hydrophilic head groups face the aqueous environments. This distribution results in the formation of bilayers [10].

2.1.2. Structure of a Phospholipid

Phospholipid structure is the cause of hydrophobic and hydrophilic effects. Phospholipids have polar hydrophillic head groups and non polar hydrophobic tails. It composes of glycerol phosphate and a phosphoryl group that forms the variable head group. Polar alcohols such as choline, serine, and ethanolamine usually form the head groups. The glycerol is esterified in the C1 and C2 positions to two fatty acids and forms the tail groups. The saturated fatty acids in the C1 position have 16 or 18 carbons and the saturated fatty acids in the C2 position have 16 to 20 carbons. [10]. In the bilayer, the tails of the phosphpolipids display significant alignment [11].

In laboratories synthetic phospholipids are used to carry out experiments. Most common phospholipids used consist of dipalmitoylglycero-phosphocholine (DPPC), 1-palmitoyl- 2-oleoyl-glycerol-phosphocholne (POPC), and 1-palmitoyl-2-oleoyl-glycerophosphoethanolamine (POPE). POPC and POPE, which will be studied in this thesis extensively, have two tails; one saturated and the other unsaturated. What both POPC and DPPC have in common is the phosphocholine head group. POPE differs by having a smaller phosphoethanolamine head. All this information aids us in understanding

the membrane properties since the arrangement and constitution of lipid head and tail groups affects the packing density, surface area per lipid and the overall structure [10].

The physicochemical properties of the membranes determine its interaction with cell penetrating peptides. The head groups of the can have negatively or positively charged or neutral structures. For example, phosphatidylcholine (PC), the phosphate head group of POPC membrane, is a zwitterionic lipid. Although it is overall neutral, its internal charges causes an electric dipole within the membrane which affects the lipid interactions with CPPs [11].

Another consequence of the varying charge of polar heads is the water-lipid interface arrangement. Anionic and zwitterionic bilayers with the same acyl chains have different water-lipid interface arrangements; for example, DOPC bilayer has a relatively more relaxed water-lipid arrangement than DOPS bilayer, meaning that the water molecules can penetrate deeper into the DOPC membrane [12]. A relaxed arrangement would mean more ease for cell penetrating peptides during membrane penetration.

2.1.3. Membrane Mimics

According to experimental cell penetration studies, to mimic the cell membrane of gram negative bacteria and mammal's erythrocytes, a mixture of lipid bilayers may be used. For example following ratios were used in creating the cell mimic of erythrocyte (lipid composition of the human erythrocyte membrane taken as basis) and gram negative bacteria membrane (lipid composition of *E. coli* inner membrane taken as basis); $POPC_{114}$:$POPE_{114}$:$CHOL_{60}$ (80% POPC+POPE, 20% CHOL) and $POPE_{200}$:$POPG_{88}$ (70% POPE, 30% POPG) respectively [12].

In simulating bilayers, during most molecular dynamics simulations, membrane proteins are placed inside a membrane composed of single lipid type. Although membranes are composed of different types of lipids, the simulation is justified due to the

fact that the lipids inside the bilayer have slow lateral diffusion with a diffusion rate of an order of 10^{-8} cm^2/s [10]. Physical properties like diffusion are dependent on temperature and pressure. At particular temperature and pressure different bilayer phases may coexist. This phenomenon may be observed due to the mixed composition of lipids and proteins present in the membrane. Another phenomenon observed is that phospholipids which may have different melting temperatures affect the melting point of neighboring phospholipids inside the membrane [11].

2.1.4. Bacterial and eukaryotic membrane mimics

In mammalian cells phosphatidylcholine (PC) is the mostly found phospholipid type in the lipid bilayer. PE is the second most phospholipid type found in mammalian cells. Also the phosholipid PS is present in eukaryotic cells; however it is found in lower ratios. The percentage of PE and PS found in eukaryotic cells out of total number of phospholipids is approximately 20% and 3–15%, respectively. Therefore, since POPC is the most abundantly found phospholipid in mammalian membranes it is the most acceptable choice for mammalian cell membrane simulations. A pure phosphatidylcholine (PC) membrane was used by Zhao's group to simulate mammalian membrane. It contained 512 lipids which were split and scattered uniformly between two leaflets. Moving on to the simulation of bacterial cells, prokaryotes do not produce PC and the most phospholipid type present in bacterial membranes is PE. Zhao's group used a 3:1 phosphatidylethanolamine (POPE): phosphatidylglycerol (POPG) bilayer with 512 lipids [13]. It is stated that anionic phosphatidylglycerol (PG) or a zwitterionic phosphatidylethanolamine (PE) headgroups are found in prokaryotic cytoplasmic membrane while zwitterionic head group phosphatidylcholine (PC) makes up the outer bilayer of a eukaryotic cell membrane [8]. In computer simulations one type of lipid is also used [14]. And as mentioned earlier the slow diffusion rate of lipids in the bilayer justifies the use of a single phospholipid type in membrane simulations [11]. To mimic bacterial membranes only POPE type phospholipid is used to mimic the inner leaflet of the outer membrane of E. coli [14]. In this study, two 129-lipid membranes were constructed; one of 1-palmitoyl-2-oleoyl-sn-glycero-3-phosphoethanolamine (POPE) to mimic bacterial

membrane and the other of 1-palmitoyl-2-oleoyl-sn-glycero-3-phosphocholine (POPC) to mimic eukaryotic membranes.

Chemical Name: POPC; Palmitoyloleoylphosphatidylcholine
Molecular Formula: $C_{42}H_{82}NO_8P$
Molecular Weight: 760.076142 g/mol

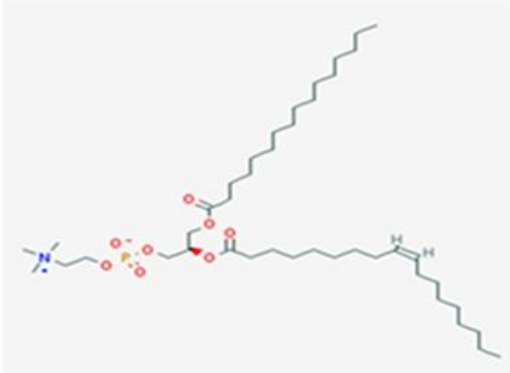

Chemical Name: POPE; 2-oleoyl-1-Palmitoylphosphatidylethanolamine
Molecular Formula: $C_{39}H_{76}NO_8P$
Molecular Weight: 717.996402 g/mol

Figure 2.1. Properties of POPC and POPE acquired from Pubchem [15][16].

The chemical representation and some of the computed properties of POPC and POPE membrane acquired from Pubchem. (Figure 2.1) POPE is observed to have a smaller molecular weight of 717.996 g/mol with respect to POPC having a molecular weight of

760.076 g/mol. The difference of the phospholipid heads can be easily observed from the chemical representation which is also shown in Figure 2.1. Especially, the energies of the CPPs with the lipid bilayer will be affected by the different phospholipid head groups of the membranes.

2.1.5. Peptide Transport Mechanisms

When the delivered cargo is large in size usually the peptide-cargo complex is internalized by endocytosis. First the cargo and carrier peptide form a complex by forming covalent bond or attaching noncovalently. The complex then reaches the membrane and interacts with the membrane which results in endocytosis. This step is followed by endosomal escape. After which the complex reaches the target. The CPP cargo complex should be designed such that after the complex has reached the center of the cell, the complex should uncouple. The bond between the complexes should be adjusted so that CPP releases the cargo inside the target [4].

Endocytosis is widely believed to be the main contributor in peptide uptake, especially if CPPs are coupled to a cargo. However, direct penetration and even receptor-mediated uptake have also been reported for specific CPPs. It is likely that CPPs without any cargo can be taken up by cells *via* multiple pathways, including direct penetration of the plasma membrane and endocytic uptake mediated by clathrin, caveolae, and/or other molecules, depending on the nature of the peptide/cell interaction. Endocytosis is a process in which the cell takes up solutes and fluids from extracellular environments. Endocytosis mechanisms are divided into two; phagocytosis and pinocytosis. Phagocytosis is the process which carries large particles whereas pinocytosis is used to transport smaller particles into the cell. There are many parameters that affect endocytosis of the CPP–cargo complexes. CPP–cargo complex uptake into the cell could be affected by the cargo; type, size, and charge, the physicochemical properties of CPPs (different molecule lengths, charge delocalization, hydrophobicity, and etc.), the cell line used as path, and the concentration of CPP. Also, fluorophores used to label peptides may affect both the uptake mechanism and intracellular distribution [4]. Figure 2.2 demonstrates the intracellular

uptake mechanisms of CPP-cargo structures. CPP make covalent or non-covalent complexes with proteins, chemotherapeutics or oligonucliotides and carry these structures into the cell through endocytosis [17].

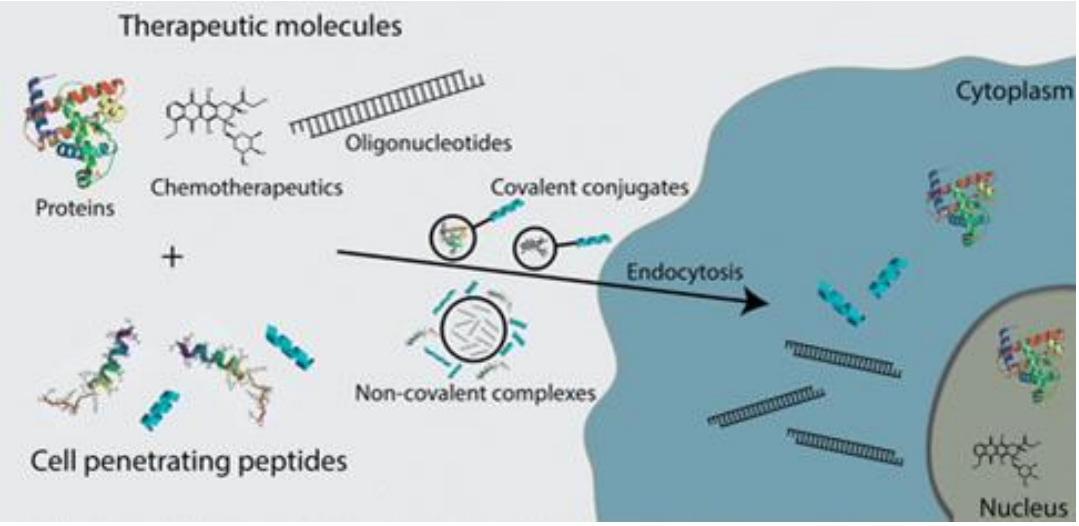

Figure 2.2. Intracellular uptake of CPP-cargo complexes [17].

Various strategies can be made use of to increase the quality of CPPs delivery into cells and tissues. Some of these strategies are altering the secondary structure, the hydrophobicity, or the charge. To prevent complications such as low synthesis yields, poor solubility, aggregation, or toxicity alterations should be considered in detail. For example, Alterations in CPPs can be made to deliver biomolecules larger in size. This can be done by adding different hydrophilic groups to a known CPP. The mechanism of cell penetrating peptides while entering cellular membranes is linked to their secondary structure, charge, helical properties, and hydrogen bonds. CPPs like asTP10 and MAP to be highly membrane-permeable. On the other hand, they are cytotoxic at elevated concentrations. Many attempts have been made with various environments to identify CPP structures. Circular dichroism (CD) and nuclear magnetic resonance (NMR) spectroscopy are the most widely used method for measuring α-helices and β-sheets in peptide structures. The structure of CPPs has been observed using the live-cell NMR technique. The result of measurements can vary greatly depending on the environment where the observation is taking place. This is because the interplay with the cellular membrane is an important factor in the CPP internalization process [4].

CD method can be used to reproduce CPP membrane interactions by using a similar medium to real cell environments. Molecular dynamics is another method used in CPP characterization, which uses thermodynamic data with data acquired from CD methods to find membrane and peptide interactions during cell penetration; electrostatic interactions, peptide orientation, secondary structure of the peptide [4].

To gain CPP-cargo complexes that are successful in vivo, novel designs or adjustments must be made. And knowing the pathway of CPP-cargo complex is imperative in achieving this goal. However, earlier studies have not shed enough light on CPP cargo pathways and uptake mechanisms. Therefore studies conducted in this area are very valuable. Up till now it is known that uptake mechanism of even analogous CPPs may differ and that varying pathways may be observed in CPP uptake without cargos [4].

2.2. Membrane Active Peptides

2.2.1. Cell Penetrating Peptides

CPPs are designed to penetrate membranes and carry antibiotics into bacterial cells. The chemical and physical reaction of the membranes towards CPPs is studied closely to determine CPPs' drug delivering properties. Cell-penetrating peptides (CPPs) can move and carry cargos (oligonucleotides, plasmids, and proteins and etc.) through cell membranes [18]. Lately, many interdisciplinary studies on CPPs and various cargos such as nucleic acids, polymers, liposomes, nanoparticles, and low molecular weight drugs have been reported. CPPs are important because of their properties such as low cytotoxicity, penetrating different types of cells, may carry any size or type of cargo and being concentration dependent. CPPs have less than 40 amino acids which makes faster at penetrating cell membranes than bigger proteins. They use different mechanisms such as endocytosis to enter cells. And they carry covalently or non-covalently attached bioactive cargos into cells. However, they must be functionalized or chemically modified for wanted purposes or else they will be passive and nonselective. Before CPPs are used in drugs, they

must be pharmacologically and toxicologically tested *in vivo* for acceptable results. From previously obtained data, CPPs are thought to become the key therapeutic instrument in molecule transport through cellular membranes with no toxic or inflammatory jeopardy. Today, CPP–cargo complexes are studied for therapeutic applications in fields such as cancer, muscular dystrophy, stroke, anti-prion, antiviral and antibacterial studies [4].

2.2.2. Antimicrobial Peptides

Antimicrobial peptides (AMP) were discovered around 30 years ago [17]. AMPs are peptides which are mostly positively charged and 10–40 residues long. The mechanism of AMP action is still researched. It is thought to have lytic abilities although pore formation in cell membranes may also be responsible for lysis. However, it is determined that AMP interacts directly with the cell membrane surface and consequently may enter the lipid bilayer. This action is noted to have resulted in cell membrane disruption. Hence AMPs cause leakage of cytoplasmic components leading to cell death. AMPs have significant effect against bacterial infections and drug resistant bacteria. For this, AMPs are considered as an alternative to antibiotics [19].

Antimicrobial peptides in nature are very diverse; however they contain conserved sequences which allow them to operate on different bacteria, membrane composition and targets. Antimicrobial peptides differentiate by their secondary structure, cationicity, hydrophobicity and amphipathicity. To determine the secondary structure of peptides Circular dichroism Spectroscopy, X-ray Crystallography and Nuclear Magnetic Resonance Spectroscopy have been used in studies. α-helices, β-sheets, mixed structures and non- α- or β- structures are the secondary structure classifications of peptides and these classifications help predict peptide mechanisms inside membranes. Another factor, amphipathicity, shows the amount and polarization of the hydrophobic and hydrophilic parts of the peptide. Cationic antimicrobial peptides mostly demonstrate a net positive charge of +1 to +7. Hydrophobic residues are found to constitute half of the overall residues. These residues aid to recognize and interfere with the membrane barrier or self-promoting uptake across the cellular membranes. melittin’s mode of action inside membranes determined to be pore formation; however, there are controversies on the type of pores formed by melittin residues in bilayers [3].

As mentioned earlier a very important factor in designing drugs is toxicity. Whether CPPs are used for Antibiotics or anticancer, the drug should not have toxicity towards normal human cells [18]. It is stated that peptides which have more toxicity towards mammalian cells as their secondary structure becomes more α-helical. Yet, the effects of secondary structures are not certain for the antibacterial activity of peptides [3].

AMPs can be found in many different lengths, sequences and secondary structures. However, they all have positive charge which makes it prone to have selectivity towards bacterial membranes which are anionic due to its negatively charged lipid content. The structures of AMPs are amphipathic, which aids the peptide in binding with the lipid bilayer [13]. AMPs are found in prokaryotes and eukaryotes and have bactericidal and/or bacteriostatic effects on different strains of bacteria. As they affect multi-drug-resistant bacteria, they do not display toxicity toward eukaryotic cells. This is because of the differences in the composition of lipids on eukaryotic cellular membrane. AMPs are cationic peptides that prefer to conjugate with anionic membranes of bacteria rather than the neutral membranes of eukaryotes. Depending on membrane composition and peptide concentration, CPPs that function as antimicrobial peptides are TP-10, pVEC, TAT, Pep-1, MAP, penetratin, ε-poly-l-lysines, and histones [4]. The electrostatic interaction between the cationic AMP and anionic bacterial membrane surfaces promotes the adsorption of the peptide inside the cell. During the adsorption on the membrane surface, a large group of AMPs transform to helical structure. They reposition themselves such that they are helical axiparallel to the surface. The next step is unclear although many experiments with different techniques have been performed to determine the prolonged interaction of the peptide membrane system. It was proposed in light of researches that in some cases that the pore formation mechanism starts when the peptide concentration reaches a critical peptide to lipid ratio (P/L). With the right peptide concentration, the peptides reorganize to a trans-membrane (TM) conformation. The TM peptides gather together to create pores inside the membrane [20].

2.2.3. CPP uptake across mammalian and bacterial cell membranes

Cell penetrating peptides are generally positively charged and they first interact with negatively charged carbohydrates (mostly glycosaminoglycans (GAGs)) and negatively charged lipids at the cell surface. Anionic lipids (*e.g.*, POPG and POPS) in eukaryotic cells are very scarce with a fraction of 10% whereas in bacterial cells the fraction may be up to 50%. However, it is known that primary amphipathic CPPs can bind to both neutral and anionic lipid membranes. It is hypothesized that the CPP interaction with the membranes forms negatively charged domains on the lipids from which the CPPs can bind to the membrane. Hydrophobic interactions are therefore thought to be the dominating factor in the CPP-membrane interactions [4].

2.2.4. pVEC

Antimicrobial peptide pVEC is attained from the murine vascular endothelial-cadherin (VE-cadherin) protein. pVEC is able to move between different cell lines with or without cargo, due to arginine and more importantly N-terminal hydrophobic residues present in its structure [21]. Table 2.1 displays pVEC sequence and properties. pVEC contains a smaller number of amino acids compared to other primary amphiphatic CPPs. The amphiphatic property of pVEC is activated when it forms an α-helix or a β-sheet structure on phospholipid membrane. Similar to other CPPs, pVEC binds to membranes with a higher fraction of anionic lipids. Thus, it is not toxic for eukaryotic cells [22].

Table 2.1. Properties of pVEC [4][22].

CPP	Origin	Sequence	Structure	Proposed mechanism
pVEC	Murine vascular endothelial cadherin	LLIILRRRIRKQAHAHSKa	Amphipathic, β-sheet	Direct penetration, transporter-mediated

Using endocytosis inhibitors decreases the cellular uptake of pVEC. At lower temperatures, with certain inhibitors, the uptake mechanism of pVEC occurs in non-

endocytotic pathways. At different conditions and with other inhibitors, different mechanisms may take place [4]. Endocytotic entry is more likely to be the rate limiting step for pVEC transport rather than endocytotic escape [21].

The studies performed on pVEC revealed that it exists as a random coil structure in pure water and neutral phospholipids. In negatively charged membranes like DOPG however, it forms a β-sheet structure. To study the effect of each residue of pVEC on cellular uptake, L-alanine mutations were performed. Mutated peptide interactions with the human Bowes melanoma cells were investigated. When the five N-terminal residues are substituted by L-alanine the cellular uptake decreased by 50% - 75%. After the three N-terminal hydrophobic residues were removed uptake stopped. The uptake of peptide ceased when all five hydrophobic residues (LLIIL) were replaced by L-alanines in the N-terminus. These results lead to the conclusion that the N-terminus is imperative for cellular uptake [23]. While the N-terminus is hydrophobic, the C-terminal of pVEC is hydrophilic while the middle is charged [24].

In the work performed by Alaybeyoğlu, a peptide based on the 45–53 loop of BLIP was modified by the addition of the five N-terminal residues (LLIIL) of pVEC to the N-terminus of the BLIP. The peptide interactions with the membrane and the antimicrobial effect on the antibiotic-resistant bacteria cells were observed to have been improved [14]. The proteins avidin, streptavidin and hexameric PNA oligomer transport into cells was also achieved by the help of pVEC peptide. pVEC was also able to penetrate gram-negative bacteria, gram-positive bacteria and fungi. It was observed to disrupt microbial cells instead of eukaryotic cells [24].

pVEC is stated to kill microbes by rendering membranes more permeable. Most AMPs destroy microbial cells by increasing the permeability of membranes through pore formation, disturbing membrane bilayer or membrane thinning. Other AMPs such as buforin 2 and PR-39 are stated to kill cells through not membrane disruption but through reaching the cell cytoplasm and disturbing internal reactions of cells such as RNA synthesis. pVEC is thought to apply the mechanism of the latter and not effect membranes but target the internal mechanisms of cells [24]. However, in another study it is stated that

pVEC forms pores in microbial membranes [25]. The divide in studies proves that more research is needed in this area.

pVEC has also been used in studies that research cell penetrating peptide and drug complexes to be used in cancer treatments. Drugs that have no cell penetrating abilities can be coupled with CPPs to increase drug targeting. PEGA which is used in cancer treatment studies were coupled with pVEC .The PEGA-pVEC complex was also coupled with chlorambucil and it was observed to increase drug efficiency and destroy tumor cells in vitro [18]. CREKA is believed to be an anti-cancer drug, when pVEC was used to carry the drug into human breast cancer cell, it was seen to be effective in targeting cancer cells instead of normal human cells. However, the uptake of the complex was lower than pVEC uptake into the cells. It is believed that the decrease of uptake was due to the drug being connected to the N-terminal which is crucial for cell penetration. This means that when designing drug complexes the point of attachment of the drug is also important [5].

It can be deduced that pVEC is a very important peptide which can be used in to design drugs for various treatments. It is researched in many studies including antimicrobial and cancer drugs [5]. Therefore understanding its mechanism may lead to extraordinary breakthroughs in drug design.

To summarize previous studies on pVEC, experimental methods such a circular dichroism, nuclear magnetic resonance, fluorescence analysis, experimental methods using endocytosis inhibitors, colocalization with endocytosis markers, LUV leakage studies, cytotoxicity measurement and etc were employed. Some of the computational methods used by earlier works are molecular dynamics simulations, steered molecular dynamics. Akdağ (2013) uses SMD simulations to study pVEC in POPE membrane. Translocations of peptides are explained to develop in three stages. Firstly the peptide is mentioned to be absorbed by means of the cationic residues followed by peptide enterance into the membrane joined by water deformity. Departure of peptide and water molecules from the bilayer is explained as the last step. Cationic, hydrophobic, and polar regions arrangements in the amphipathic pVEC peptide assist to its uptake system [23]. SMD simulations and β-lactamase activity measurements are employed by Alaybeyoğlu (2015) to study pVEC in

POPE membrane. BLIP was altered to enhance β-lactamase inhibition and uptake. The alteration was driven by a hydrophobic stretch of cell-penetrating pVEC sequence at its N-terminus. LLIIL residues were added to the inhibitory peptide BLIP N-terminus to encourage uptake. The Activity of 45–53 loop of BLIP is shown to increase inhibition. It is proposed that the peptide was a competitive β-lactamase inhibitor. LLIIL residues were demonstrated to encourage peptide associations with the membrane.The adjusted peptide is identified to have antimicrobial effect on antibiotic-resistant bacteria cells [14]. Madani (2011) reviews the studies conducted on pVEC in eukaryotic and prokaryotic cells through methods Circular dichroism, fluorescence and nuclear magnetic resonance, Molecular modeling, Fluorescence-assisted cell sorting (FACS), confocal microscopy imaging. Also methods that utilize specific endocytosis inhibitors, endocytosis markers, LUV for leakage studies are discussed. Scrambled pVEC is reported to have no uptake while pVEC translocates by utilizing a few distinct pathways for their cell uptake. endocytotic passage pursued by endosomal escape is thought to coordinate cell membrane entrance. arginine and N-terminal hydrophobic residues are proposed to effect the translocation capacity of pVEC and pVEC-cargo complexes. Diverse endocytosis inhibitors are reported to subdue the cell uptake of pVEC. Uptake at low temperatures is reported and is proposed to affirm nonendocytotic pathways in pVEC uptake. Endocytotic passage is proposed to be connected with the rate limiting step for pVEC [21]. Herbig (2006) employed Calcein Leakage Tests, Fluorescence Polarization, Dynamic Light Scattering (DLS), Circular Dichroism (CD) and atomic force microscopy AFM Imaging to study pVEC in DPPC and DOPC membranes. Peptides were reported to expand the fluidity of DPPC domains and it is thought to be the fundamental mechanism of transformation. bilayer cohesion was reported to not have been compromised by pVEC [26]. Broth micro-dilution, dye leakage methods were employed along with membrane depolarization, hemolytic activity and cytotoxicity measurements by Nan (2011) to study pVEC in gram-negative and gram-positive bacteria and PE/PG (7: 3, w/w) vesicles. The results of Trp and Arg/Lys substitution of pVEC, and antimicrobial and lipopolysaccharide-neutralizing behaviors were presented. A strong antimicrobial action yet decreasing or no hemolytic action even at high concentrations are reported. pVEC is proposed to eliminate microorganisms by framing a pore or ion channel [25]. Elmquist (2006) carried out a study by using carboxyfluorescein labelling at the N-terminus of pVEC peptides in Bowes melanoma cells. Fl-pVEC analogs were reported to enter and collect in live Bowes melanoma cells.

LL-Alanine substitution of the five residues of N-terminal hydrophobic amino acids is proposed to diminish the translocation property. Arg6, Arg8 or Ser17 substitution by Alanine improved cellular uptake. Endocytosis inhibitor Wortmannin decreased the cellular uptake. Heparinase III, Nystatin and EIPA were reported to have had no impact on the peptide uptake. N-terminal hydrophobic part of pVEC is interpreted to be essential for proficient cell translocation [24]. Microscopic analysis, toxicity studies, cellular uptake of pVEC in vitro using fluorescence microscopy was used by Mäe (2011) in human breast cancer cell lines. It was demonstrated that PEGA-pVEC conjugate is taken up by diverse breast cancer cells in vitro. Furthermore, when the anticancer medication chlorambucil is conjugated to the PEGA-pVEC chimeric peptide the potency is reported to expand more than 4 times [5]. Myrberg (2007) used fluoresceinyl-labeling method to study effects of pVEC in human breast cancer cell lines. CREKA–pVEC complex is reported to be more eligible to synthesize and better in translocating cargo particles inside canser cells when contrasted with previously published PEGA–pVEC peptide. This study shows that CREKA–pVEC and chlorambucil conjugate was significantly better at destroying cancer cells in vitro than the anticancer medication [18]. Copolovici (2014) reviewed studies that performed NMR, circular dichroism (CD) spectroscopy, CD methods combined with phospholipids and unilamellar vesicles, Isothermal titration calorimetry methods on pVEC peptide. Non-endocytotic pathways are proposed to be the pVEC uptake mechanism at lower temperatures. It is stated that a conjugate of pVEC with avidin translocates through the membrane by utilizing clathrin-dependent endocytosis. Also the existence of another mechanism is proposed to likely happen under diverse conditions. The endocytosis inhibitors are said to not have an impact on the uptake of pVEC. It was stated that pVEC diminished the viability of a yeast strain by more than 50% [4].

2.2.5. Melittin

Melittin is a lytic peptide derived from honey-bee (Apis mellifera) venom [27]. The peptide has been vastly studied and was found to exhibit high antimicrobial and antiviral activity, as well as cytotoxic activity towards mammalian cells. Melittin is a particularly interesting peptide since it can target live cells. It has been studied vastly for its anticancer properties. It causes the termination of live cells by binding and consequently rupturing

lipid membranes. As mentioned earlier, it has a broad spectrum of activity against both eukaryotic and prokaryotic cells and its activity depends on many factors. These factors include membrane composition, cholesterol content of membrane, lipid charges, lipid to peptide ratio and etc. In this work we have studied the peptide in two types of membranes; POPE and POPC [19].

Melittin constitutes of 26 amino acids which are arranged in a sequence of GIGAVLKVLTTGLPALISWIKRKRQQ. The residues 1–20 are hydrophobic and residues 21–26 are hydrophilic [19]. It is a positively charged peptide in which around the C-terminus the positive charge is more concentrated. It is believed that the salt bridges between the bilayer headgroups (negatively charged phosphates) and the peptide is anchored by the positively charged C-terminus [28]. High resolution by x-ray crystallography and NMR spectroscopy methods were used to study the structure of Melittin in earlier studies and it was found out that in different environments melittin maintains an analogous α-helical structure. The modes of action of melittin were studied more deeply and the following aspects were found to play a significant role. The protonation state of the N-terminus was found to influence membrane-peptide interactions. It was found that the proline in position 14 and the polar residues 23–26 at the C-terminus have important effects on the lysis activity. In terms of the the effects caused by different properties of membranes, it was discovered that the lysis activity is less affective on bilayers containing lipids with longer acyl chains and on membranes which are negatively charged. In negatively charged membranes the peptide binds on the membrane but does not enter the bilayer thus not resulting in lysis of the membrane. It was observed that melittin permeates zwitterionic lipids and causes lysis [7]. The residues which constitute melittin have been studied in various studies. The hemolytic activity of melittin was observed to increase when Pro14 residue was replaced with an Ala residue. While the last six residues in the C-terminal were found to causes the peptide to be hemolytic, without these residues melittin is rendered non-hemolytic. Leu6, Leu9, Leu16, Iso17 and Trp19 also promote hemolytic activity. Ala4 and Lys7 were discovered to promote antibacterial activity [3].

The mechanism of the melittin peptide has been the center of many studies. Being a lytic peptide, it is believed to form a pore in membranes by first binding to the surface then permeating further into the membrane. According to the composition of the membranes the

mechanism may differ. Such that it melittin may form pores or may inhibit the formation of pores in membranes composed of zwitterionic lipids such as phosphatidylcholine. These phenomena are a result of the binding conformation of peptide on the membrane. Melittin forms a α-helical structure when bound to the membrane. It can attach itself to a membrane within milliseconds. When the peptide directly permeates the membrane in a perpendicular conformation it forms pores. A parallel binding of the peptide is however inactive and it blocks other peptides trying to penetrate the membrane. The difference in insertion conformations is thought to have resulted from concentration differences. It is proposed that low concentrations of melittin causes the peptides to bind parallel to the membrane thus blocking pore formation. At higher concentrations the peptides are thought to bing in perpendicular conformations leading to pore formations on the membrane. This is called the two-step model for pore formation. The concentration needed to transition from parallel to perpendicular binding is determined from the ratio of melittin to lipid molecules since affinity of melittin to the membrane is caused by the attraction of PC headgroups [29]. For example, the critical peptide/lipid ratio is determined as 1/62 for a melittin POPC system [28].

In previous studies, experimental methods such as solid-state NMR, circular dichroism, UV spectra, crystallographic methods, leakage tests, cytotoxicity experiment and etc have been used to study melittin properties and mechanisms. Some of the computational methods used by earlier works are molecular dynamics simulations, umbrella sampling, PMF calculations, all-atom force field, GROMACS and coarse-grained simulations. In the study performed by Jamasbi (2014) circular dichroism (CD) spectroscopy, dye-release, hemolytic potency of peptides against human red blood cells, in vitro cytotoxicity of melittin was evaluated in POPC, POPE and POPG membranes. The antimicrobial and cytolytic activities against different cells and model membranes were investigated and proline residue was found to be necessary for antimicrobial activity and cytotoxicity. Proline absence reduced lysis of model membranes and hemolysis. The lytic activity was not found to be correlated to the secondary structure of the peptides or on the propensity to adopt helical conformation [19]. Van der Bogaart (2008) performed calcein dequenching and fluorescence-burst assay with melittin in DOPC, DOPG membranes. It was reported that the direct insertion of melittin leads to pore formation, whereas the parallel conformation is inactive and prevented other melittin molecules from inserting,

hence preventing pore formation. It was stated that melittin at low concentrations binds parallel to the membrane. Melittin shifts toward the perpendicular orientation at higher concentrations causing pore formation. It was proposed that melittin needed for pore formation is dependent on the ratio of melittin to lipid molecules [29]. Wilcox (1992) used circular dichroism, UV spectra and crystallographic methods to study melittin. It was reported that as pH increases from 4.0 to 9.5,as ionic strength increases, temperature is around 37 °C, or as phosphate is added that melittin changes from a monomeric random coil to a α-helical tetramer. The thermodynamics of folding was investigated utilizing circular dichroism. Increasing NaCl concentration in solution is reported to increase tetramer stability. It is also stated that phosphate might bind Lys 23 at the terminal of the tetramer [30]. Berneche (1998) used the experimental methods solid-state NMR and polarized attenuated total internal reflectance Fourier transform infrared (PATIR-FTIR) on melittin in DMPC membrane. Reported results included that Lys7 and Lys23, Arg24, Gln25, and Gln26 at the C-terminus have important contribution to the stability of the helix in the bilayer. melittin is stated to have effects on both layers of the membrane. The presence of melittin in the upper layer caused a local thinning of the bilayer that favors the penetration of water through the lower layer. The energetic factors involved in the association of melittin at the membrane surface were characterized using an implicit mean-field model. The influence of the protonation state of the N-terminus of melittin is proposed to be important for the penetration of water molecules into the bilayer [7]. Fluorescence and UV resonance Raman spectra and molecular dynamics simulations were used by Schlamadinger (2012) to study melittin in POPC and POPG membranes. Melittin is reported to embed profoundly into the bilayer, while antimicrobial peptide cecropin A stays limited to the lipid headgroups. CM15 is a peptide constructed by utilizing melittin and cecropin A residues. Although it is generally unfolded, CM15 is reported to be a powerful membrane-disruptor [31]. Chen (2014) studied melittin in POPC membrane by using long-timescale molecular dynamics simulations and CD spectroscopy. Melittin is reported to firmly attach itself in an unstructured conformation to the lipid bilayer. It is demonstrated that folding inside the membrane results in bilayer deformation. Helical melittin is reported to be resistant towards thermal denaturation [27]. In the review presented by Mojsoska (2015) along with experimental conclusions, molecular dynamics simulations of melittin in DPPC membrane are mentioned. It is reported that Pro14 with Ala replacement in melittin yields a 2-fold higher hemolytic peptide. Cancellation of the 6

residues from the C-terminal resulted in a non-hemolytic peptide. Removal of Leu6, Leu9, Leu16, Iso17 and Trp19 is reported to diminish hemolytic action along with removal of Ala4 and Lys7 is reported to lessen the antibacterial activity with respect to native melittin. Novel cecropin A and melittin hybrid peptides is reported to have strong antibacterial movement and no hemolytic results. cecropin A-melittin (CAM), altered by removal of Trp5,11,21,25 were reported to enhance the antibacterial action and enhance the proteolytic balance. CAM-W is reported to have 3–12 times higher antibacterial action while showing a moderate cytotoxicity. Results of molecular dynamics simulations for melittin and DPPC layers are illustrated. The peptides were reported to be situated close to the pore center while additional peptides were situated near the pore edge [3]. Santo (2013) used the computational methods coarse-grained simulations, coarse-grained to united-atom scale transformations, and molecular dynamics simulations using the united atom description of systems to investigate melittin in DPPC and POPG membrane composed in 7:3 ratio.Half of the simulations with the high Peptide/Lipid ratio were reported to have formed transient pores in the bilayer. The gathering of 3−5 melittin peptides are reported to have formed pores.In pores some peptides are reported to have adopted a trans-membrane state, a number of them formed U-shapes by having their termini residues anchored to the same leaflet. melittin peptides are described to act as a "wedge" that parts the bilayer. MD simulations are reported to demonstrate no significant change in the pore structure amid the 50 ns time interval. However, formations of water stream in the transient pores were reported to have been detected. Graded dye leakages from large vesicles are proposed to be caused translocation of peptides over the bilayer and formation of transient pores [20]. all-atom force field and molecular dynamics computer simulations were used to study melittin in POPC by Irudyam (2012). The attachment process we explained by a concurrent folding and adsorption of the peptide to the bilayer, pursued by "U shaped" orientation of melittin. The readjustment of melittin from parallel to perpendicular conformation is stated to need charged residues to transport across the hydrophobic center of the bilayer. It is proposed that with increasing concentration of melittin increasing water deformities create stable pores making it simpler for the peptide N-terminus to reorient [32]. Melittin in POPC membrane was studied by Irudayam (2013) by carrying out umbrella sampling simulations and potential of mean force (PMF) calculation. For PMFs calculated for a peptide to lipid (P/L) ratio of 1/128 and 4/128 the free energy barrier is reported to have reduced when the P/L ratio increases. It is stated that if a neighboring melittin was already in the trans-

membrane orientation, the barrier of the PMF curve is reduced for a second melittin, which is stated to confirm the presence of a cooperative effect [17]. Andersson (2013) uses the computational approach CHARMM and OPLS force fields to study melittin in DOPC membrane. A few microseconds of extended simulations were applied to monitor force-field effects. CHARMM and OPLS simulations were reported to concur for the initial couple of hundred nanoseconds. However the structural results are reported to vary radically with longer trajectories. CHARMM parameters are stated to be more agreeable with experiments. Convergence of the helix separation mechanisms are proposed to be better understood using expanded sampling [33]. The Computational method of GROMACS was used by Irudayam (2011) to study melittin in POPC membrane. Symmetric and asymmetric arrangements of melittin were studied in toroidal pore development. It is proposed that the symmetric arrangement of the peptides may be more inclined in the system than asymmetric arrangement. Helical structure is stated to be not an essential for the development of the toroidal pore [28]. Wang (2012) used NPT simulations and clustering analysis performed using GROMACS to study melittin in POPG:POPC bilayer with a 1:2 mixing ratio. Tryptophan residues in cecropin A and melittin are proposed to be the key for the action of the two AMPs. Leakage behaviors caused by the hybrid of these peptides are proposed to be evidence to the deduction they can upset certain zwitterionic lipid bilayers [34].

2.2.6. CPP induced pore formation in cellular membranes

Toxic CPPs cause destructions of cells. A way of destroying cells is to open pores on cellular membranes. Pores created by CPPs cause leakage and eventually the cell is flooded with the uncontrolled influx and destroyed. The creation of pores is different according to the CPP used. When a pore is created by peptides arranged vertically on the inner surface of the pore a barrel-stave model pore is created. Another pore model called toroidal develops when lipid headgroups and peptides unite and form the inner surface of the pore. An example of a CPP which forms barrel-stave pores is alamethicin. Melittin however creates toroidal pores in cellular membrane [20].

The carpet model in which AMPs arrange as a layer on membrane surface was proposed to explain the mechanism of other AMPs like cecropin P1. The peptide layer eventually becomes too large and tears the membrane causing the cell to be disrupted. A fourth pore formation model in which the absorbed AMPs cause disturbance in the lipids' hydrophobic and hydrophilic arrangement, leads to cell membrane losing its capabilities [20].

The melittin was observed to cause graded leakage in experiments carried out using giant unilamellar vesicles (GUV). Melittin is thought to have created transient pores. The peptides move through the membrane. Through the transient pores cell leakage was observed. Another type of leakage observed in GUV experiments with magainin was a leakage type of all-or-none. In this mechanism, the peptides cause high tension n the surface of the membrane. This causes the disruption of the membrane by opening a large channel. The occurrence of both of these mechanisms is a random process. Helicity is one of the numerous factors that effect melittin insertion into the membrane. Membrane curvature is also important; however, in computer simulations because of periodic boundary conditions membranes cannot form large curvature [20].

2.2.7. The effect of peptide concentration on membrane leakage

Cell penetrating peptides can either attach on the surface of the membrane or penetrate through the bilayer. The chance of more peptides entering the membrane is thought to increase as the peptide concentration increases. Researches in literature report that there are energy barriers for peptide insertion into membranes, however, with an increase in the concentration of peptides the energy barrier thresholds were observed to have decreased. The mechanism is hypothesized to be that as more peptides are attached to the surface of the membrane, the surface tension of the bilayer increases which causes the surface area to to increase while bilayer thickness decreases. The peptides reorient to release stress of the bilayer and this allows peptides to eventually penetrate into the bilayer. Therefore the increase in peptide/lipid (P/L) ratio causes an increase in the number of peptide insertions into bilayers. It was also reported that peptides poisoned in trans-membrane state also

decreases the energy barrier threshold making a more favorable environment for membrane penetration. [17]. The P/L concentration in which the CPPs start penetrating the bilayer is called the critical P/L ratio. Every membrane and peptide configuration reciprocates in a different manner. Therefore, the critical P/L ratio differs for different systems [28].

2.2.8. Secondary structure of CPPs in membranes

It is stated that inside the lipid bilayer of membranes, many AMPs acquire α-helical secondary structure. The secondary structure of melittin was monitored in a study carried out by Irudayam. When the peptide is pulled from the surface of the membrane to a trans-membrane state, it was observed that the melittin residues stayed α-helical. Contrarily, the residues around the terminals were observed to take on random coil as a secondary structure. In the novel computational studies in literature, it was reported that as the N-terminus is pulled through the lipid bilayer, parts of the melittin peptide was observed to fold and unfold because of the interactions with membrane lipids. The same phenomenon is also reported for diverse peptides [20].

3. METHODS

SMD simulations of melittin and pVEC peptides in POPE and POPC membrane systems are carried out in this study. The analysis includes electrostatic energy, force, work, radius of gyration, order of lipids, membrane thickness, water in membrane analysis, along with VMD visual analysis, helicity, and residue analysis.

For each SMD membrane/peptide system two simulations are carried out in which the peptide was placed above the membrane in a different initial position. The average of both simulations was considered while deducing data from the SMD simulations for each system. In total four systems were analyzed; melittin/POPE, melittin/POPC, pVEC/ POPE and pVEC/POPC systems. With the simulations we have observed eight SMD simulations in total. The results of these simulations are compared in order to find the effects of different membranes and peptides. The comparisons between POPE and POPC simulations of the same peptides helps observe the differences of peptide insertion mechanisms in different membranes. Also we get the chance of comparing the mechanism of the melittin and pVEC peptides to determine the properties of each peptide in the same membrane.

Table 3.1. demonstrates the list of SMD simulations. All peptides are placed above the membrane with 10 ±0.1 Å initial distance between the lowest point of peptide and the highest point of the phospholipid heads of the membrane. The two positions of the same peptide-membrane systems will be referred to as Pos1 and Pos2 throughout this work, for example, Pos1 and Pos2 of melittin-POPE system or Pos1 and Pos2 of pVEC-POPC system.

Table 3.1. The list of SMD simulations.

Peptide	Membrane Type	Positions
Amidated Melittin	POPE	Horizontally placed position 1 (Pos1)
		Horizontally placed position 2 (Pos2)
	POPC	Horizontally placed position 1 (Pos1)
		Horizontally placed position 2 (Pos2)
Amidated pVEC	POPE	Horizontally placed position 1 (Pos1)
		Horizontally placed position 2 (Pos2)
	POPC	Horizontally placed position 1 (Pos1)
		Horizontally placed position 2 (Pos2)

3.1. Steered Molecular Dynamics

Molecular dynamics simulations (MD) are a fundamental computational tool used to study biological molecules. It determines the time dependent behavior of a molecular system. Comprehensive information on the fluctuations and conformational changes of proteins and nucleic acids can also be achieved with this approach. Molecular dynamics simulations help investigate the structure, dynamics and thermodynamics of biological molecules and their complexes. The structures obtained from X-ray crystallography and NMR experiments can also be determined with Molecular dynamics simulations [14].

Steered molecular dynamics (SMD) presents atomic level descriptions of fundamental processes in biological phenomenon. By administering external forces, SMD employs biomolecules to obtain mechanical behavior. SMD can also model slow processes such that they can be accelerated and more easily observed [35]. In SMD simulations an external force such as constant velocity pulling or constant force pulling was applied to one or more atoms. Firstly, a dummy atom was connected to a SMD atom by means of a virtual spring. The constant velocity pulling simulation was carried out by moving the dummy atom at a constant speed. By using the following equations the force amongst the two atoms are calculated [6];

$$\vec{F} = -\nabla V$$

$$V = \frac{1}{2}k[vt - (\vec{r} - \vec{r}_0) * \vec{n}]^2$$

F: force applied

V: potential energy.

k: spring constant

v: pulling velocity of dummy atom

t: time

$\vec{r}$: Actual position of the center of mass of SMD atoms

$\vec{r}_0$: Initial position of the center of mass of SMD atom

$\vec{n}$: Direction of pulling

The outside of the membrane barrier; the middle of the membrane and the inside of the cell is made up of different concentrations. With this method, the potential force acting on the protein due to concentration differences can be simulated. Instead of constructing the exact concentrations of the real environment, the potential difference was created by using a spring constant and steering the molecule, causing the molecule to move down the concentration gradient as in the real phenomenon.

3.2. Simulations Setup

3.2.1. Constructing the Melittin structure

The crystal structure of melittin was downloaded from the PDB databank (PDB ID: 2MLT). The coordinates of chain A of the crystal structure were used to set up the system [32]. The C-terminus was amidated with the help of VMD. The PSF file was generated using the psfgen module of VMD. The amidated melittin structure was placed in a water

box of 20x20x20 Å dimensions. Water molecules within 2.8 Å of the protein are deleted. The amidated melittin was prepared and equilibrated at 310 K. The peptide was constrained with harmonic constraints (k = 1kcal/mol/ Å ^{2}) and the system was minimized for 1000 steps and equilibrated for 2 ns. The constraints were removed and the system was again equilibrated for 2 ns [23]. Resulting melittin structure was used in the MD and SMD simulations. The amidated melittin was placed in POPE and POPC membrane in different horizontal positions for SMD simulations.

3.2.2. Constructing the pVEC structure

The pVEC pdb and psf file was generated by coding the peptide's sequence LLIILRRRIRKQAHAHSK in VMD. The pVEC structure was amidated. The amidated melittin structure was placed in a water box of 20x20x20 Å dimensions. Water molecules within 2.8 Å of the protein are deleted. The steps above for minimization and equilibration are repeated for amidated pVEC water box system. The amidated pVEC will be placed in POPE and POPC membrane in different horizontal positions. After the MD simulations are complete, SMD simulations will be carried out.

3.2.3. Constructing the POPC membrane

The POPC membrane was created using the membrane package in VMD. The dimensions of the membrane were constructed 69 Å in x- and 69 Å in y-directions such that there were 129 phospholipids present. The membrane was placed in a water box with its minimum and maximum coordinates at {{-34.5 -34.5 -80} {34.5 34.5 80}} Å Clashing water molecules with the membrane were deleted. The water-membrane system was equilibrated for 0.5 ns with harmonic constraints (k = 1kcal/mol/ Å ^{2}) and for 0.5 ns without constrains [23]. The system results in the following dimensions: 77.861 Å X 79.560 Å X 181.271 Å with a lipid area of 6194.700 Å ^{2}.

3.2.4. Constructing the POPE membrane

The POPE membrane was also created using the membrane package in VMD. The dimensions of the membrane were constructed 69 Å in x- and 69 Å in y-directions such

that there were 129 phospholipids present. The membrane was placed in a water box with its minimum and maximum coordinates at {{-34.5 -34.5 -80} {34.5 34.5 80}} Å. The water-membrane system was equilibrated for 0.5 ns with harmonic constraints (k = 1kcal/mol/Å ^{2}) and for 0.5 ns without constrains [23]. The system results in the following dimensions: 76.552 Å X 81.414 Å X 180.339 Å with a lipid area of 6232.486 Å^2

3.2.5. Equilibration Simulations

The previously equilibrated peptide was placed in the membrane-water box system such that the distance between the peptide and the lipids are 10 Å initially. The clashing water molecules are deleted. The system was ionized to a concentration of 0.1 M NaCl. The system was equilibrated for 0.5 ns with harmonic constraints (k = 1kcal/mol/ Å ^{2}) and for 0.5 ns without constrains [23]. Simulations are carried out at 310 K.

3.2.6. SMD Simulations

After the minimization and equilibration steps SMD can be performed. Force was applied on the N-terminal Cα atom of the peptide (melittin/pVEC) in order to move the peptide in the negative z direction. The spring constant value which was used in the simulations was 10 kcal/mol/Å^2. Constant pulling velocity was used at a value of 2.5 Å/ns with timestep 2.0 fs, which is equal to the value 0.0000050 Å/timestep [14]. The simulation temperature and pressure were constant with values of 310K and 1 atm, respectively.

CHARMM22 force-field parameters were used along with NAMD molecular dynamics package [23]. The phosphorous heads were constrained in the z direction. The P heads can move in the x and y direction whilst pore formation and the applied constraint causes minimal disturbance to the membrane bilayer [14]. A cutoff value of 12 Å was used on nonbond interactions and 10 Å of switching distance. To modify the system size Periodic boundary conditions with Particle Mesh Ewald (PME) method were used. To keep the system at a constant temperature of 310 K Langevin dynamics were used along with 5/ps damping coefficient. The pressure of the system was kept constant at 1 atm by utilizing Langevin piston. The period of the piston was set at 200 fs [23]. In every 20 steps

(40 fs) the SMD forces were printed and in every 2 ps the coordinate sets were saved [11]. All SMD simulations were repeated two times with a different initial peptide position. The results were averaged for analysis [14]. NAMD2 program and CHARMM22 force field were used in the MD and SMD simulations.

In literature most AMP simulations use a pre-folded α-helix as initial structure placed in a parallel orientation close to the membrane (<10) [34]. In this study the peptides are placed at least 10 Å away from the membrane. Also the initial α-helical peptide was equilibrated in 0.1 M NaCl solution before being placed into the membrane system and equilibrated again and does not unfold. Since most AMPs, including melittin, have a coil structure in aqueous solutions transforms into an α-helical secondary structure near the membrane and orients itself in a parallel position on the membrane [6]. Also melittin tetramers are known to have helical melittin monomers which dissociate in the presence of phospholipids [34]. It was more logical to start the simulation in an α-helical structure since the peptide was placed not close enough to interact initially with the membrane but also not too far away from the membrane.

The list of SMD simulations and simulation lengths are given in Table 3.3. SMD simulations were conducted to observe the effects of different SMD pulling point and velocity of melittin in POPE membrane. (Table 3.2). In one of the simulations the SMD force was applied to melittin center of mass and in the other simulation the melittin peptide was pulled from the N-terminus however the SMD pull velocity was 1/10th the velocity of the previous simulations. So, the velocity of pulling was 0.25 Å/ns with time step 2.0 fs. (0.0000005 Å/time step).

Table 3.2. The list of additional SMD simulations.

#	**Simulation Type**	**Simulation length**
SMD Simulation 1	Melittin pulled from center of mass.	38.24 ns
SMD Simulation 2	Mellittin pulled from N-terminus with 1/10th velocity.	151.68 ns

Table 3.3. The list of SMD simulations and simulation lengths.

#	Simulation Type	Simulation length
1	Melittin POPE position1	53 ns
2	Melittin POPE position2	58 ns
3	Melittin POPC position1	60 ns
4	Melittin POPC position2	64 ns
5	pVEC POPE position1	42.8 ns
6	pVEC POPE position2	50 ns
7	pVEC POPC position1	50 ns
8	pVEC POPC position2	50 ns

The results of the SMD simulations were analyzed by monitoring electrostatic energy, force, work, radius of gyration, order of lipids, membrane thickness, water in membrane analysis, along with VMD visual analysis, helicity, and residue analysis. The analyses were carried out with respect to the position of the α-carbon of the first residue of the peptide. The outputs obtained from the SMD simulations in the form of .log files contained information on the SMD forces applied in the simulation. And NAMD energy plugin was used to obtain the electrostatic, VDW and total nonbond values between the peptide and the lipids during the simulation in the form of the output file energy_profile.txt. Energy_coor.m script was used along with energy_profile.txt file obtained from NAMD Energy plugin to plot the energy profiles. SMD forces were determined at each SMD step by NAMD. The SMD forces lines which contained SMD force values along with first residue α-carbon z coordinates in the .log file were saved as smdforces.txt output file. smdforces.txt output file was used by force_coor_av.m file to plot the SMD force profiles in MATLAB. In the obtained trajectories, the force profile and the electrostatic energy profile was plotted in the negative axis because the SMD pull is in the negative z direction. Therefore, lower force values in the plot indicate more force applied by SMD in the –z direction. The energy and force trajectories were interpreted accordingly. Work was determined by multiplying the puling velocity over time by the integral of force.

Work_z_50.m script used smdforces.txt file in the calculations and produced the work profiles. Timeline tool of VMD was used to view the secondary structure of the simulation components [23]. Electrostatic energy profile gives information about the energies of the peptide with lipid molecules. Monitoring the electrostatic, VdW and non-bond energy trajectories by obtaining their profiles via scripts helped to determine which of these interactions play an important role in peptide penetration into the bilayer. High energy observed at the top of the bilayer may suggest an energy barrier or high energy observed inside the bilayer may be a sign of energy potential which may pull the peptide inside the bilayer. Therefore the energy profies were analyzed along with force and work profiles to obtain a clearer picture of the ongoing phenomena during penetration. Force profiles show the force applied by SMD to keep the pull velocity of the peptide constant. The force analyses showed the points where additional force was applied by the system to move the peptide in the –z direction with a constant velocity. These points indicated where energy barriers existed. Work analysis shows the amount of work done in the system. Radius of gyration analysis gave a better understanding about the peptide by demonstrating the dispersion of the peptide atoms around its center of mass. Radius of gyration values of the peptide with respect to time frames were acquired by using the rgyr.tcl script. The order of lipids analysis showed the relative order of the hydrocarbon tails [31]. It was useful for determining the peptide and water penetration effects on the membrane because the lipid carbon order changes as membrane lipids are disturbed. Orderc3_vs_frame.tcl script was used to obtain the order of lipid carbons with respect to time frames. Order_vs_z_subplot.m was used to plot the lipid order profile with respect to z coordinate of the α-carbon of the first residue of the peptide. The membrane thickness analysis helps monitor the changes such as membrane thinning caused by peptide and water insertion. Thickness_of_memb.tcl script was run to obtain the minimum and maximum coordinates of lipid molecules with respect to time frames of the SMD and MD simulations. The water in membrane analysis helps determine when and how much water enters and leaves the membrane. Count_water_in_membrane.tcl script was run to calculate the number of water molecules between the two phosphate headgroup layers. The visual analysis performed in VMD helps to understand the system and detect visual changes in the system as the peptide moves through the membrane. The residue energy analysis shows the energies of individual residues of the peptide with the membrane lipids. This analysis aids in determining which residues act dominantly and what they cause in the simulations. Residue

energy analysis was performed similar to energy analysis except in NAMD Energy plugin the two molecules were chosen as protein and residue number vs. lipid. Lastly, the helicity analysis showed when and how helical a peptide was during the simulations. Helicity.tcl script was run to obtain the secondary structure of peptide with respect to time frames. It helped to monitor the winding and unwinding of helical peptides.

3.3. Equilibrium MD Simulations of melittin and pVEC in membranes

The object of this study was to further analyze the performed SMD simulations of melittin and pVEC in POPC and POPE membranes by taking snapshots from the SMD trajectories when the peptide was situated at the top, middle and bottom of the membrane and run 10 ns equilibrium MD simulations to observe the peptide when the SMD forces were released. A total of 24 MD simulations were performed for three snapshots from each of the eight SMD simulations. An additional MD simulation was performed on a snapshot from the pVEC SMD simulation in POPE (the simulation was previously performed by Begüm Alaybeyoğlu). The simulations were run at 310 K. The melittin MD simulations prepared are summarized in Table 3.4. The MD simulations of pVEC are shown in Table 3.5. (*300 K snapshot was obtained from Alaybeyoğlu)

MD Simulations of amidated melittin and amidated pVEC in POPC and POPE are prepared by taking snapshots of the SMD simulations of the peptide in the various membranes when its first residue was situated at the top, middle and bottom of the membrane. After the MD simulations are completed; visual descriptions analysis; energy analysis vs. frame; helicity percentage vs. frame; and distance between the first residue and the center of mass of lipids vs. frame analysis are made in order to obtain the results. The distance between the first residue and the center of mass was calculated through getzdata.tcl script which produced the coordinates of the α-carbon of the first residue of the peptide with respect to time frames then z_center_of_mass.tcl script was run to obtain the center of mass of lipids with respect to time frames. The two output files acquired from these scripts were used by distance_vs_frame.m file which calculated the distance between the α-carbon of the first residue of the peptide and the center of mass of lipids in each time frame and produced the distance vs. time profile. The MATLAB and tcl codes used in the analysis of the simulations are presented with more detail in Appendix C.

Table 3.4. The MD simulations of amidated melittin in POPC and POPE membranes. SMD position refers to the initial position of SMD simulations. Snapshot positions column refers to the location of peptide when MD simulations snapshots are acquired.

Peptide	**Membrane Type**	**SMD Positions**	**Snapshot Positions**
Amidated Melittin	POPE	Position 1	Top of membrane
			Middle of membrane
			Bottom of membrane
		Position 2	Top of membrane
			Middle of membrane
			Bottom of membrane
	POPC	Position 1	Top of membrane
			Middle of membrane
			Bottom of membrane
		Position 2	Top of membrane
			Middle of membrane
			Bottom of membrane

Table 3.5. The MD simulations of amidated pVEC in POPC and POPE membranes. SMD position refers to the initial position of SMD simulations. Snapshot positions column refers to the location of peptide when MD simulations snapshots are acquired.

Peptide	**Membrane Type**	**SMD Positions**	**Snapshot Positions**
Amidated Melittin	POPE	Position 1	Top of membrane
			Middle of membrane
			Bottom of membrane
		Position 2	Top of membrane
			Middle of membrane
			Bottom of membrane
	POPE	Alaybeyoğlu*	Bottom of membrane
	POPC	Position 1	Top of membrane
			Middle of membrane
			Bottom of membrane
		Position 2	Top of membrane
			Middle of membrane
			Bottom of membrane

4. RESULTS AND DISCUSSION

Before SMD and MD simulations were carried out the peptides used in this study melittin and pVEC were amidated and equilibrated. The resulting equilibrated amidated peptide structures before SMD simulations are shown in Figure 4.1 and Figure 4.2. The RMSD between the initial and final states of equilibration was 1.541 Å.

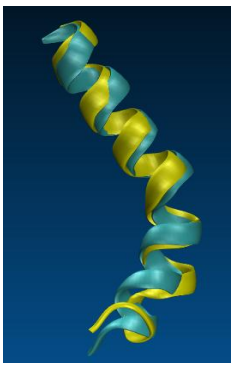

Figure 4.1. Melittin structure at the beginning (green) and end (yellow) of the simulations.

Amidated pVEC was prepared and equilibrated at 310 K. The RMSD between the initial and final states of equilibration was 4.571 Å.

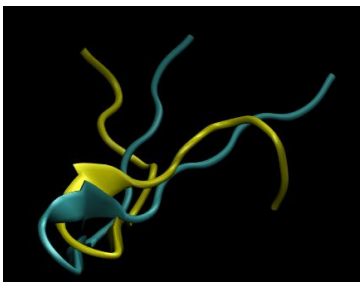

Figure 4.2. pVEC structure at the beginning (green) and end (yellow) of the simulations.

4.1. Peptide Transport across Membranes Examined by SMD Simulations

The SMD simulation results were analyzed. Firstly, the results of the systems containing the same peptide and membrane type but different initial peptide positions were compared. The results of these simulations were expected to resemble each other since the components of the system are the same. Later the results of different peptide membrane systems were compared to further understand the actions of different peptides in different membranes.

4.1.1. Melittin Transport across the POPE Membrane Examined by SMD Simulations

The SMD simulation trajectories of melittin in POPE membrane were observed visually with the help of VMD. The snapshots in Figure 4.3 and Figure 4.4 showed that melittin entered the POPE membrane in a vertical position in both simulations. The peptide started to unfold inside the membrane and continued to unfold as the peptide left the membrane through the lower P layer.

The electrostatic energy was monitored with respect to the z coordinate of α-carbon of Gly1 during the simulation (Figure 4.5). Both melittin simulations in POPE exhibited similar energy trends in the form of three regions. The first region started where the peptide entered the membrane until the moment when Gly1 reached the lower half of the membrane; the electrostatic energy increased suggesting that the resistance to peptide insertion has increased. The second region started from the moment Gly1 reached the lower P heads until the last residue was pulled from the upper P heads; the electrostatic energy increased (from-200kcal/mol to about -600kcal/mol) and so did the resistance against peptide insertion. And the third region started from the moment the Gly26 left the upper P heads until it leaves the lower P heads; the electrostatic energy decreased and the resistance against the peptide moving in the –z direction decreased.

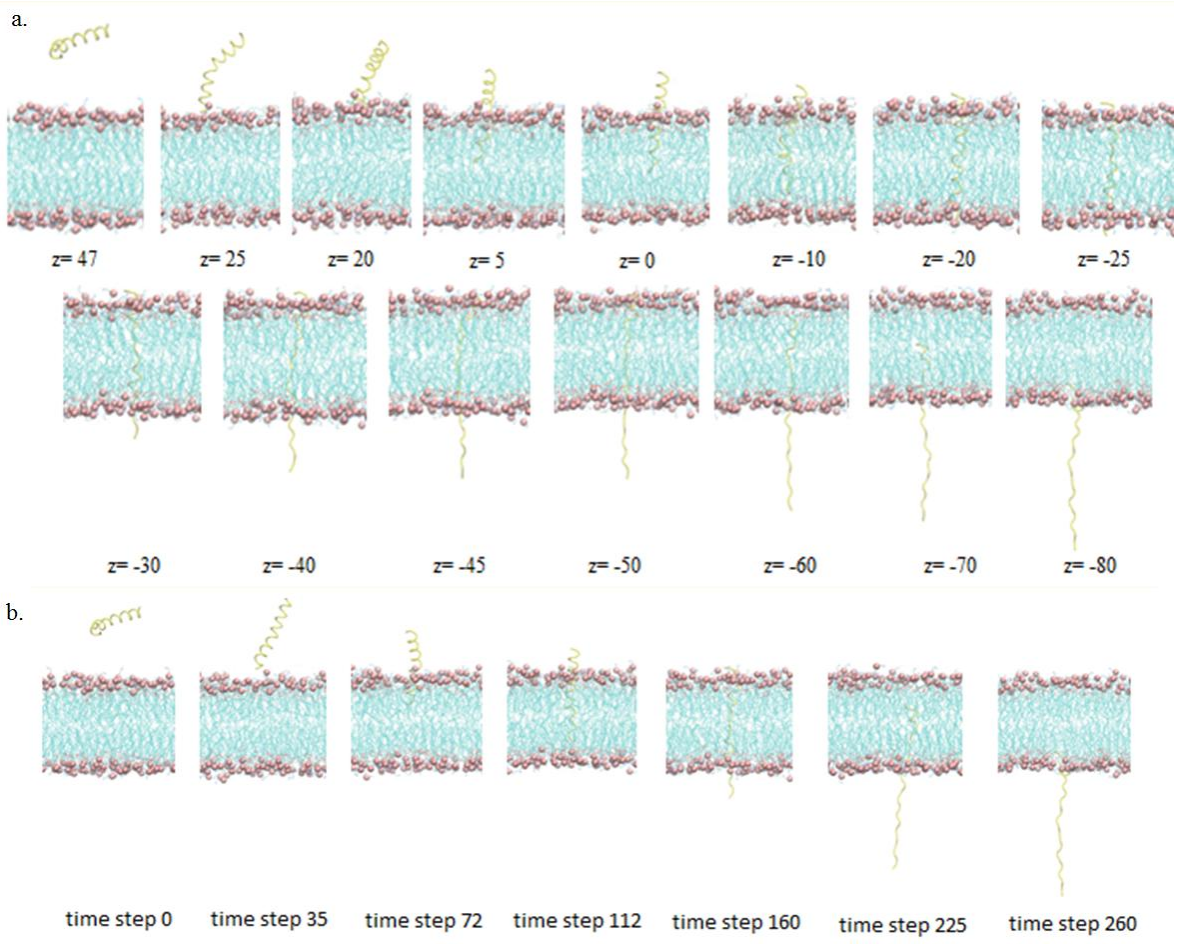

Figure 4.3. Snapshots acquired from the first melittin POPE SMD simulation. (a) Snapshots at different z values (the distance between Gly1 and the center of the SMD system, units: Å). (b) Snapshots captured at different time steps.

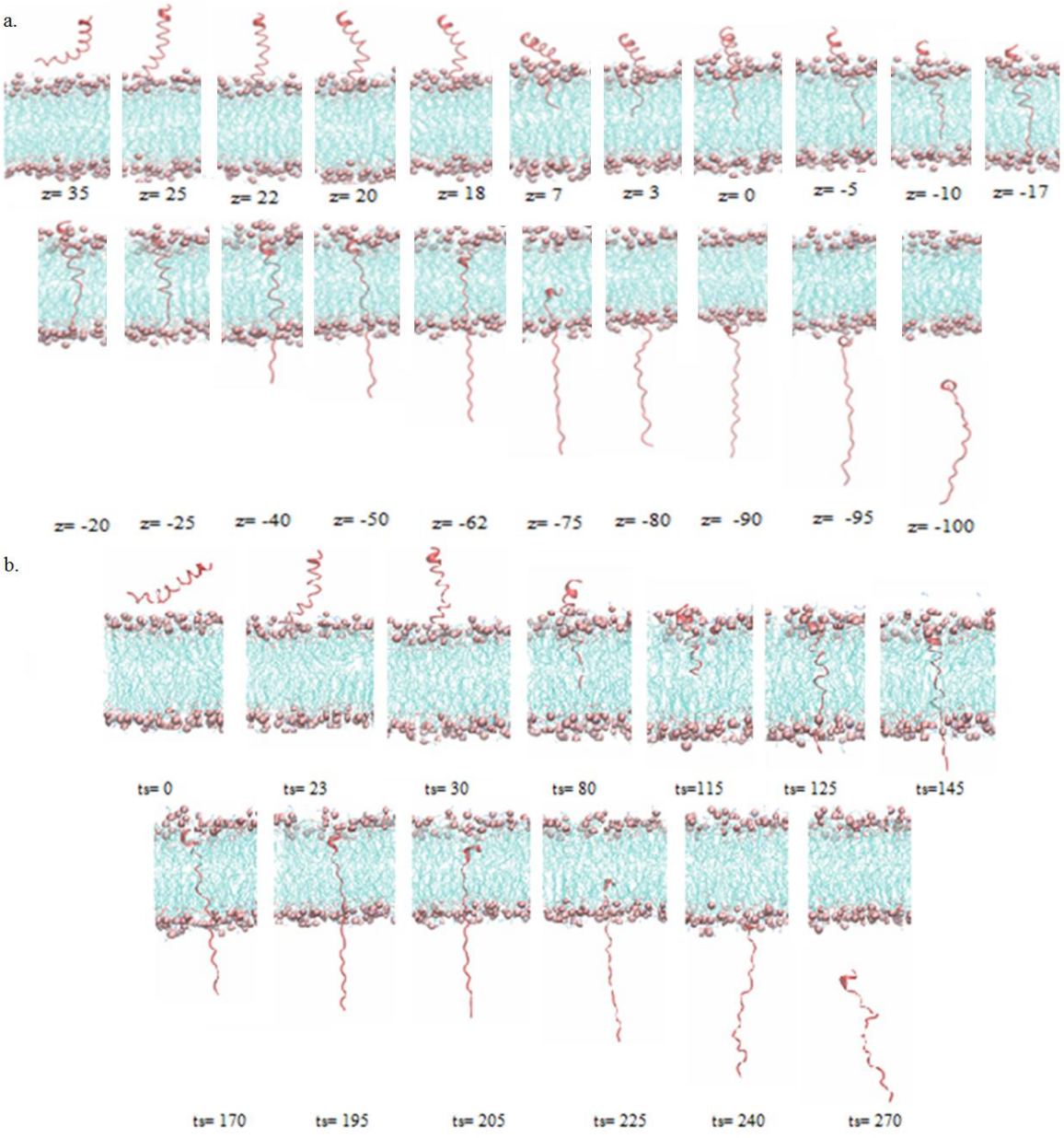

Figure 4.4. Snapshots acquired from the second melittin POPE SMD simulation. (a) Snapshots at different z values (the distance between Gly1 and the center of the SMD system, units: Å. (b)Snapshots captured at different time steps.

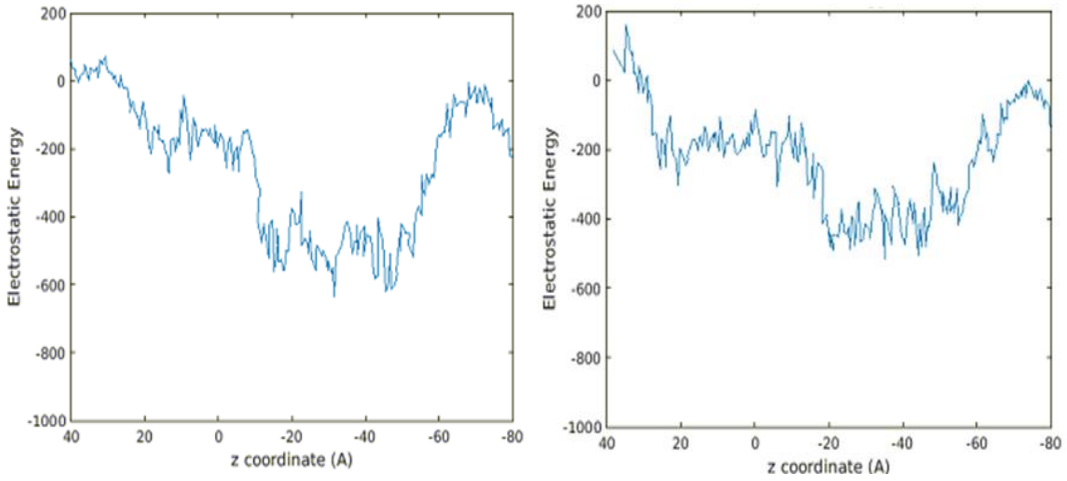

Figure 4.5. The electrostatic energy profiles of melittin in POPE Pos1 and Pos2 SMD simulations as a function of the z coordinate of the SMD atom.

The three regions of similar trends were also observed in the force profiles (Figure 4.6a). The difference in forces was that in the second position at z=20 Å (when the Gly1 reached the upper P heads), there was an increase in the force which decreased shortly. This lead to an energy barrier which was overcome with increased force. The work profiles were similar for the two simulations. The final work was between 1300-1400 kcal/mol (Figure 4.6b). A different trend was at z=20 Å in the second simulation where there was a steep increase in work. The fact that at z=20 Å the electrostatic energy between the peptide and the lipids showed no significant increase while a peak of -800 pN of force and a sharp increase in work was observed lead to the conclusion that the force barrier observed at this point was not due to peptide lipid interactions but more probably to the secondary structure of the peptide itself. The helicity profile showed that indeed the helicity percentage of the peptide remained 90% while in Pos1 the helicity percentage has dropped to about 75% at the same point. In Pos2 helicity percentage started to drop after Gly1 has passed z=20 Å barrier.

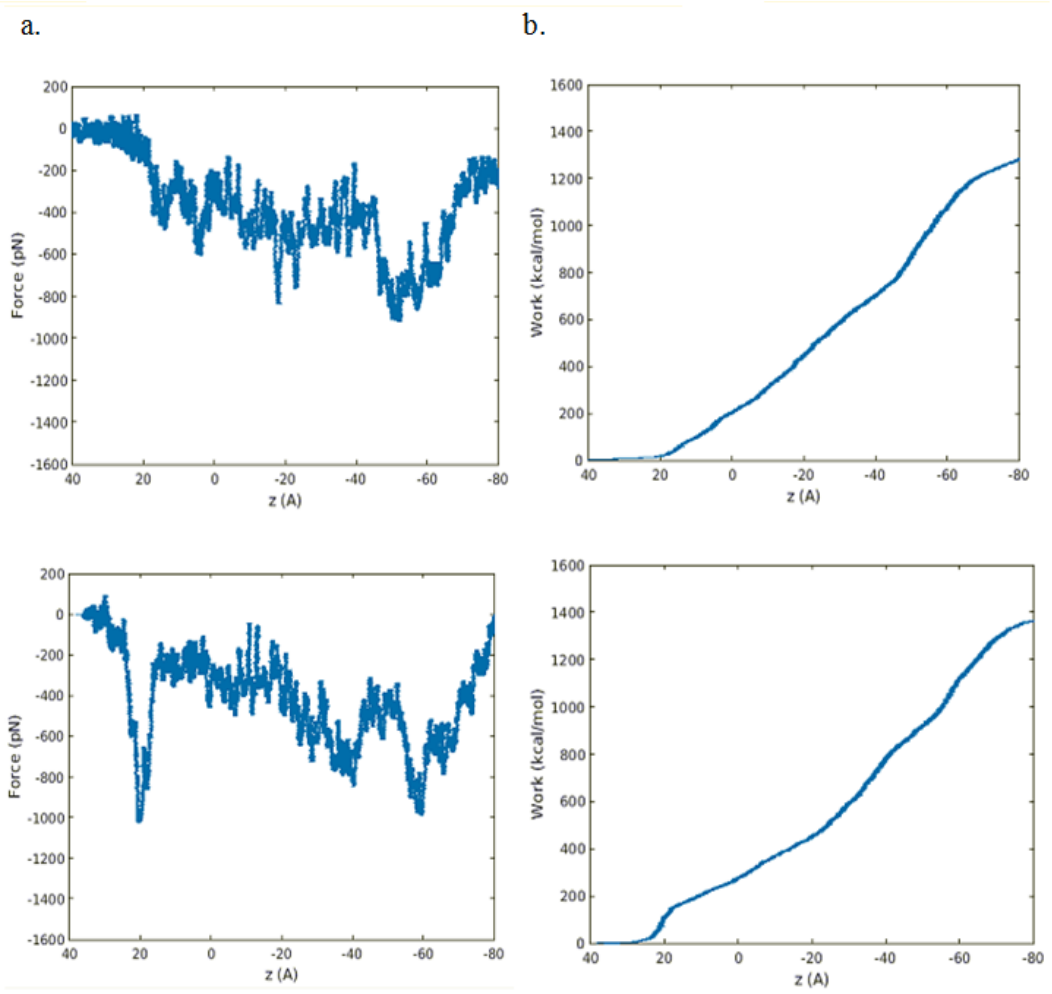

Figure 4.6. Melittin POPE SMD simulation: a) The force vs. z profile of Gly1 graph and b) the work vs. z profile of Gly1 of Pos1 and Pos2

Figure 4.7 displays the radius of gyration vs. z coordinate and helicity percentage vs. z coordinate graphs for melittin POPE SMD simulations. The 'radius of gyration' profiles for both simulations were very similar. The radius of gyration increased from 13 to 25. Higher radius of gyration values mean that the protein was packed more loosely [36]. A different trend was observed after z=-70 Å in the second simulation where there was a steep decrease in the radius of gyration. The helicity profiles showed that the helicity of the peptide was zero at these points. It was concluded that the peptide becomes more compact however does not assume α-helix structure.

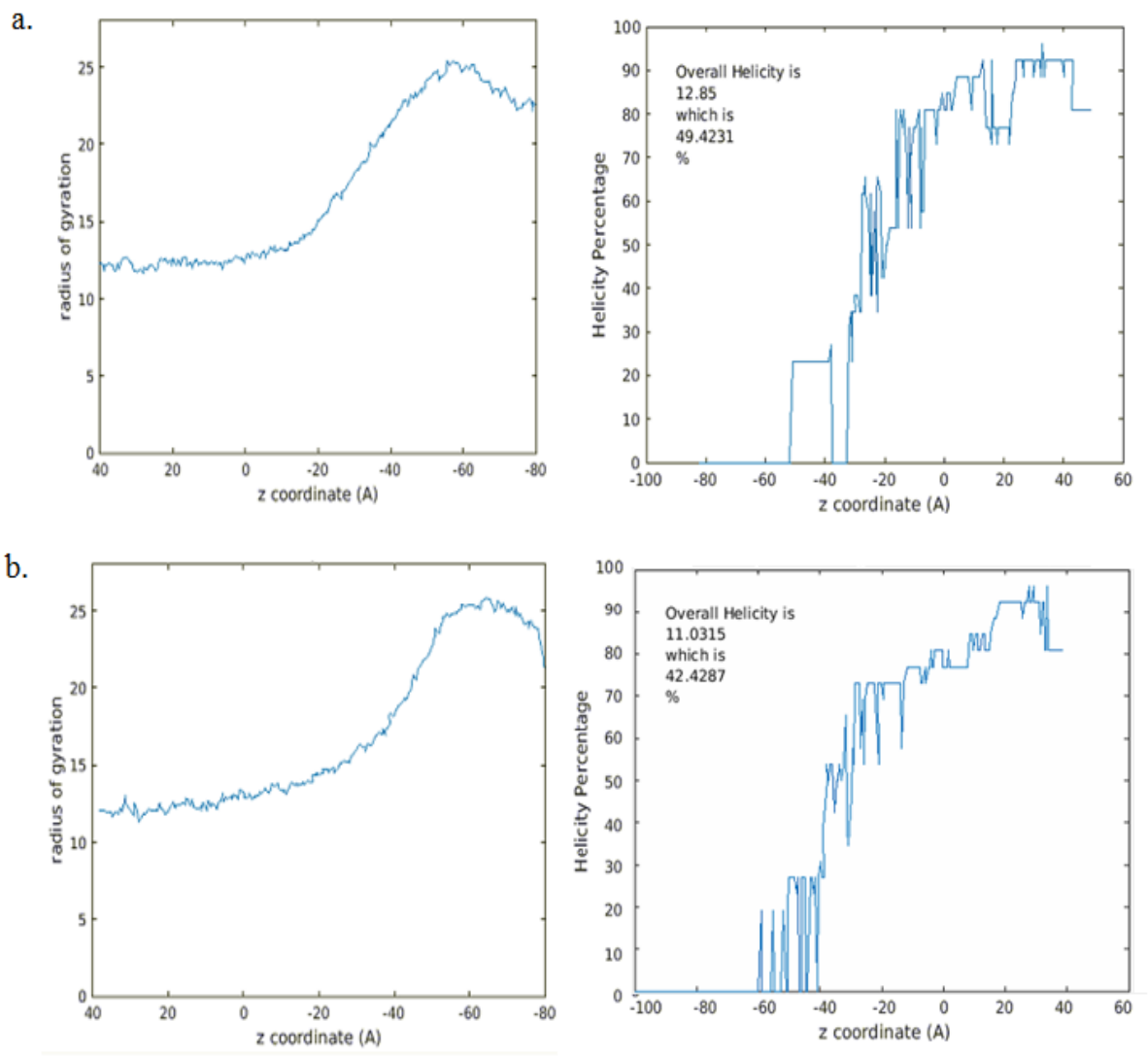

Figure 4.7. Melittin POPE SMD simulation radius of gyration vs. z profile and helicity percentage vs. z profile for a) Pos1 b) Pos2

The order of lipids is displayed in Figure 4.8 for both simulations. In the first simulation the change of order was random whereas in the second position the order changed at z 7 Å (where the order was most random), -20 Å (where the lipids were more aligned) and at z 50 Å the order of lipids were disordered again. At z -20 Å the peptide is in a trans-membrane state inside the lipid bilayer and the lipid order is not disturbed as much as at z 7 Å and z -50 Å where the lipids are disordered due to peptide entering and leaving the membrane respectively.

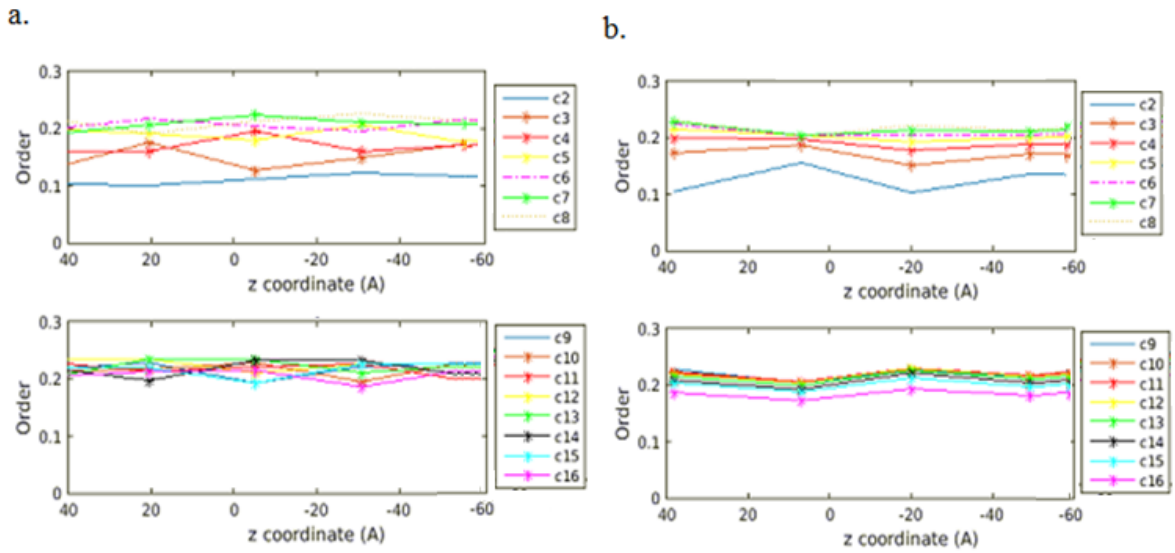

Figure 4.8. The carbon order vs z profile of melittin in POPE a) Pos1 and b) Pos2 SMD simulations.

The change in membrane thickness throughout the simulation is shown in Figure 4.9. At the start, the thickness of Pos1 and Pos2 were 55.5 & 54 Å respectively. These values were close to each other. In both simulations the membrane was the thickest at around z 60 Å when Gln26 is on the upper P heads; the values were 60 & 60.5 Å respectively. The difference between these simulations was that Pos1 was thinnest at z -10 & -60 Å with a value of 53 Å, while Pos2 was thinnest at z 3 Å with a value of 52.5 Å. Membrane thinning was caused by the increase in stress of the membrane caused by peptide binding [17]. Membrane thinning at different points shows that the stress was applied at different points. There were three z values at which the size of the water bubble within the membrane increased. The number of water molecules increased as the peptide entered the membrane until Gly1 left the lower membrane. The peptide started leaving through the lower P heads and the number of water molecules decreased. The last residue that left the membrane caused an increase from around 30 water molecules to 50 molecules after z -60 Å. The difference between the simulations was that in Pos1 there was an increase of water molecules at z 5 Å. Val5 entered the membrane at this point. Val5 residue should be observed more closely.

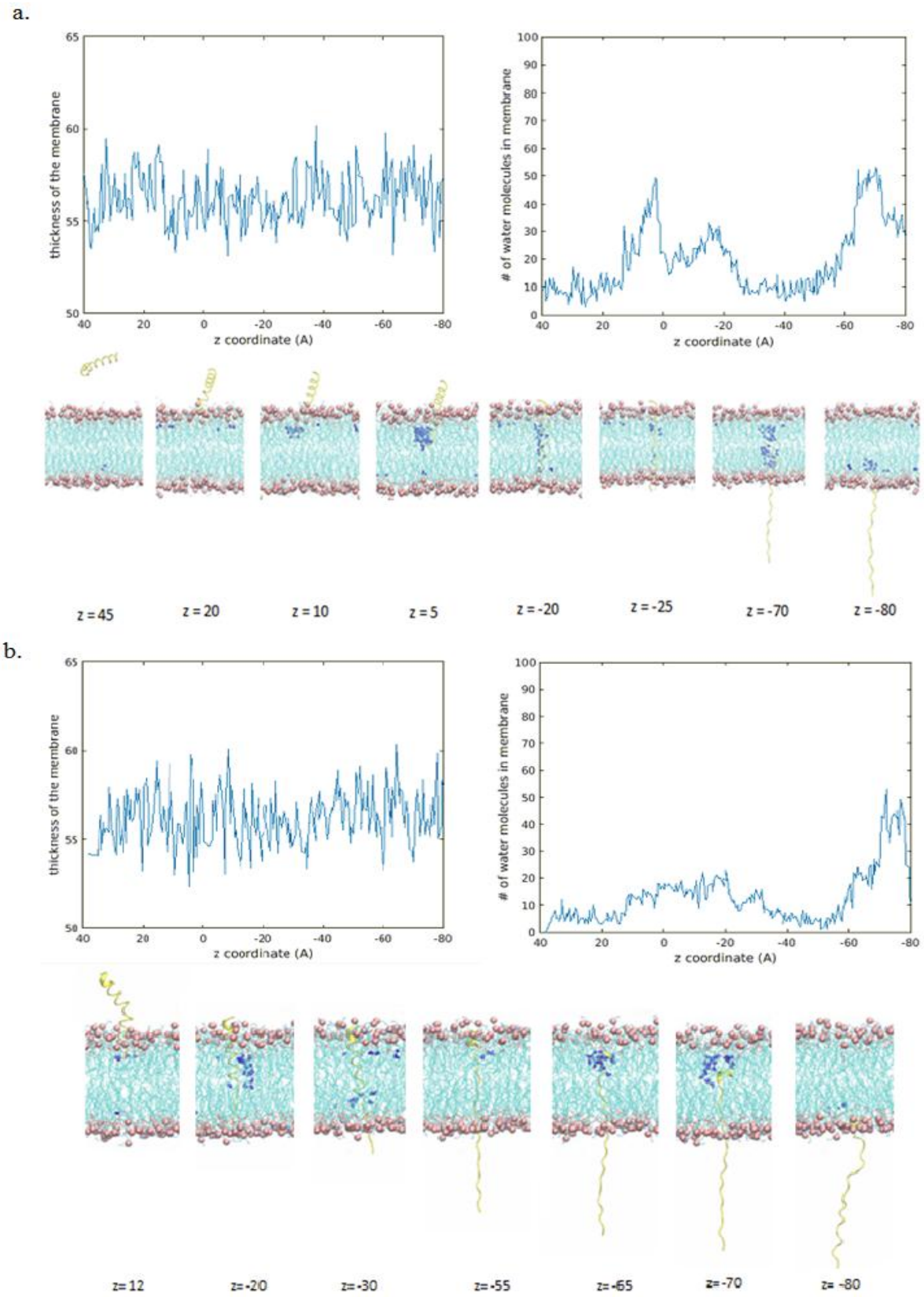

Figure 4.9. Melittin POPE SMD simulation thickness of membrane vs. z, water in membrane vs. z profiles of Gly1 and snapshots for a) Pos1 b) Pos2

Important details about the peptide's trajectory inside the membrane system of the SMD simulations were observed through visual analysis. Figure 4.10 shows the snapshots acquired for the melittin POPE position 1. The peptide positioned itself in a vertical position prior to penetration into the membrane.Thr10-Thr11-Gly12 formed a kink in the simulations. When the melittin peptide binds to a membrane, the positive charges in melittin might affect the lipid structure through interacting with the phosphate groups [34]. Water penetration into the membrane started as Val5 entered the membrane. At that point Lys7 was inside the upper P heads. In trans-membrane state, in Pos1, the peptide helicity dropped. The secondary structure of melittin in trans-membrane position is important because the trans-membrane state was suggested to be an important orientation in the melittin's pore formation and consequently antimicrobial action [17]. As helicity drops the residues of the peptide have more exposure to the lipid molecules, therefore more interaction might initiate antimicrobial properties.

In Pos2, (Figure 4.11) Thr10-Thr11-Gly12 anchored on the upper P heads as the residues inside the membrane unwind. Thr10-Thr11-Gly12 had high energies in the residue energy analysis. In Pos1, Leu6-Lys7-Val8 did not unwind while the rest of the residues in trans-membrane state started unwinding. Trp19-Ile20-Lys21-Arg22-Lys23-Arg24-Gln25-Gln26 had anchoring effects in Pos1 in addition in Pos2 residues Gly12-Leu13-Pro14-Ala15-Leu16 also had anchoring effects. The kink between Leu6-Lys7-Val8 unwinds as half of the peptide left through the bottom. Residues Leu6-Lys7-Val8 and Lys21-Arg22-Lys23-Arg24-Gln25-Gln26 (which moved as a block inside the membrane) carried more water molecules into the membrane. Ala15 caused an opening in the lower P heads. The peptide and water molecules left the membrane swiftly at the end of the simulations.

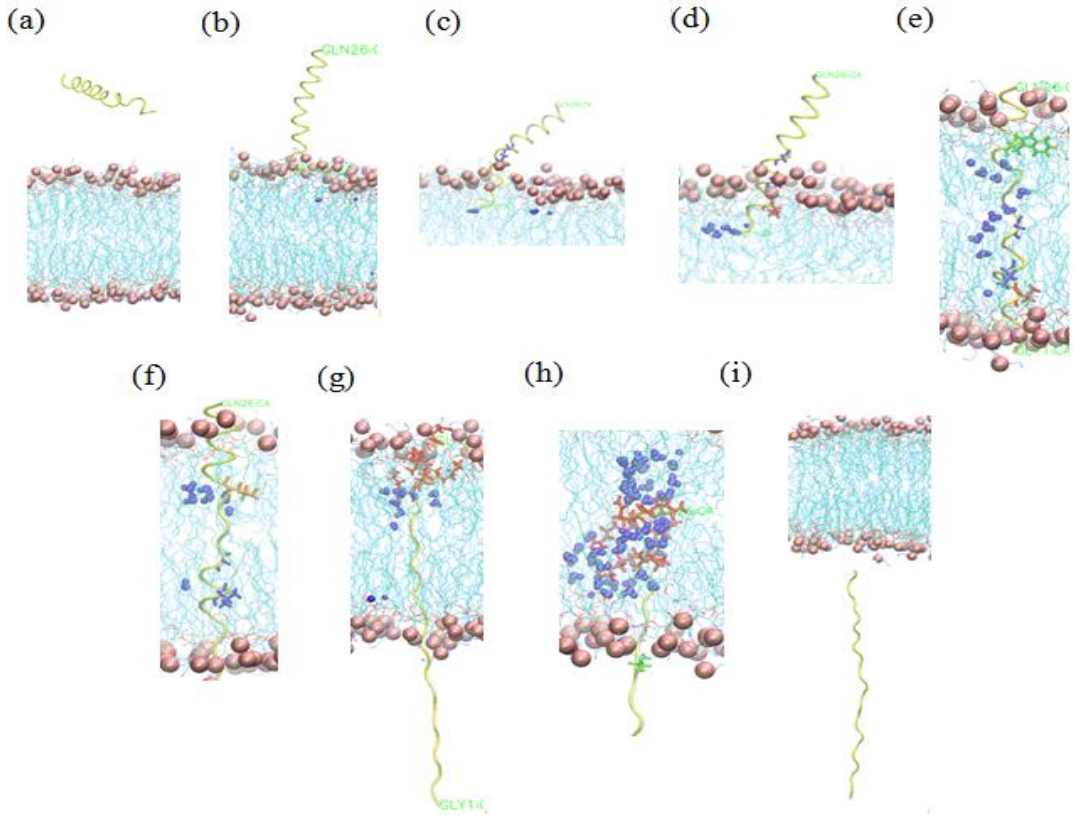

Figure 4.10. Snapshots of melittin POPE SMD simulation Pos1. Z is the distance between center of mass of lipids and center of mass of Gly1. (a) z=44.66 Å (b) z= 21.53 Å (c) z=13.45 Å (d) z=10.35 Å, Val5 is shown in red. (e) z= -23.88 Å, Trp19 is shown in green. (f) z= -29.82 Å, Leu6 and Val8 are shown in blue while Leu16 is shown in orange. (g)z=-58.76 Å, Lys21-Arg22-Lys23-Arg24-Gln25-Gln26, all represented in red (h) z=-72.24 Å, Ala15 is shown in green. (i) z=-93.83 Å

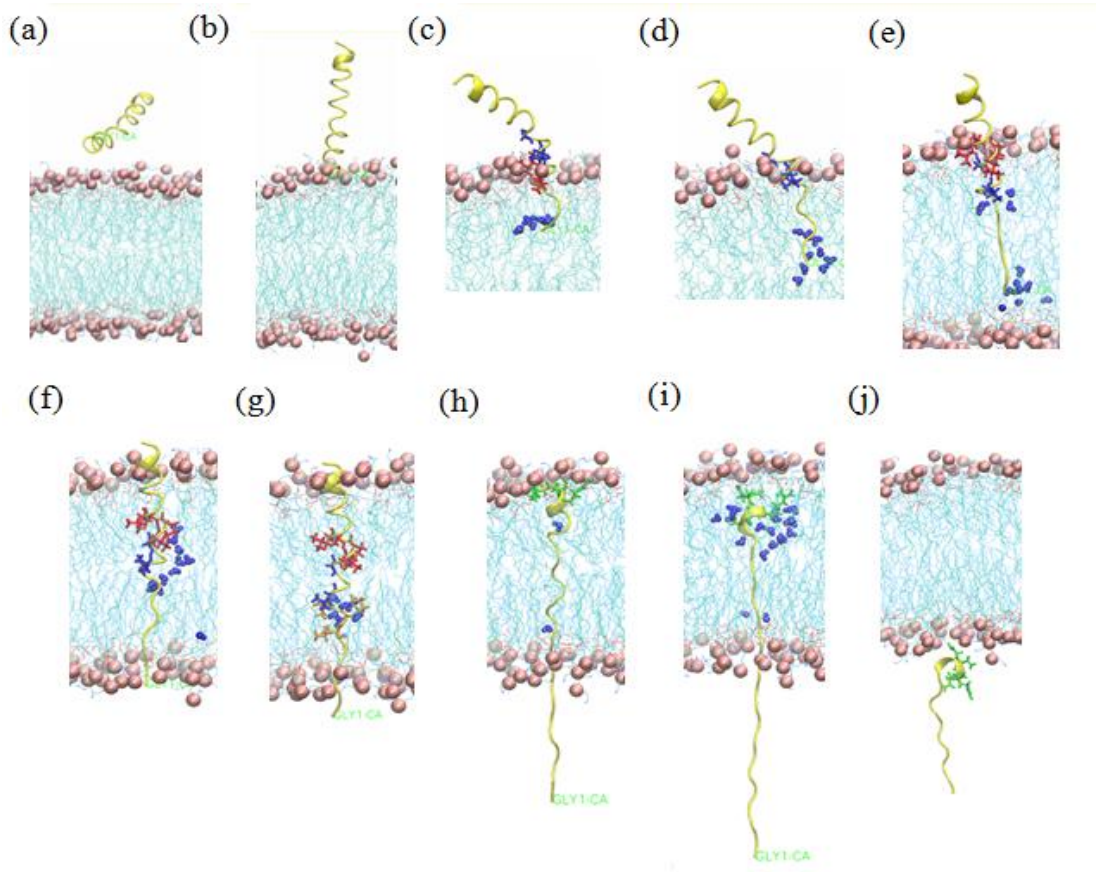

Figure 4.11. Snapshots of melittin POPE SMD simulation Pos2. Z is the distance between center of mass of lipids and center of mass of Gly1. (a) z= 34.47 Å (b) z= 20.52 Å (c) z= 9.59 Å, Val5-Leu6-Lys7-Val8 are shown in red sticks, Thr10-Thr11-Gly12 are shown in blue. (d) z=1.78 Å (e) z=-10.13 Å, Gly12-Leu13-Pro14-Ala15-Leu16 are shown in red. (f) z= -23.17 Å (g)z=-27.60 Å, Leu6-Lys 7-Val8 are shown in orange (h) z= -49.85 Å, Arg24-Gln25-Gln26 are shown in green (i) z= -65.13 Å (j) z=-95.60 Å

4.1.2. Melittin Transport across the POPC Membrane Examined by SMD Simulations

Melittin in POPC membrane was also observed and the results were found similar to the POPE simulations, however, there were a few notable differences. Figure 4.12 and Figure 4.13 displays the snapshots acquired from the melittin POPC SMD simulations.

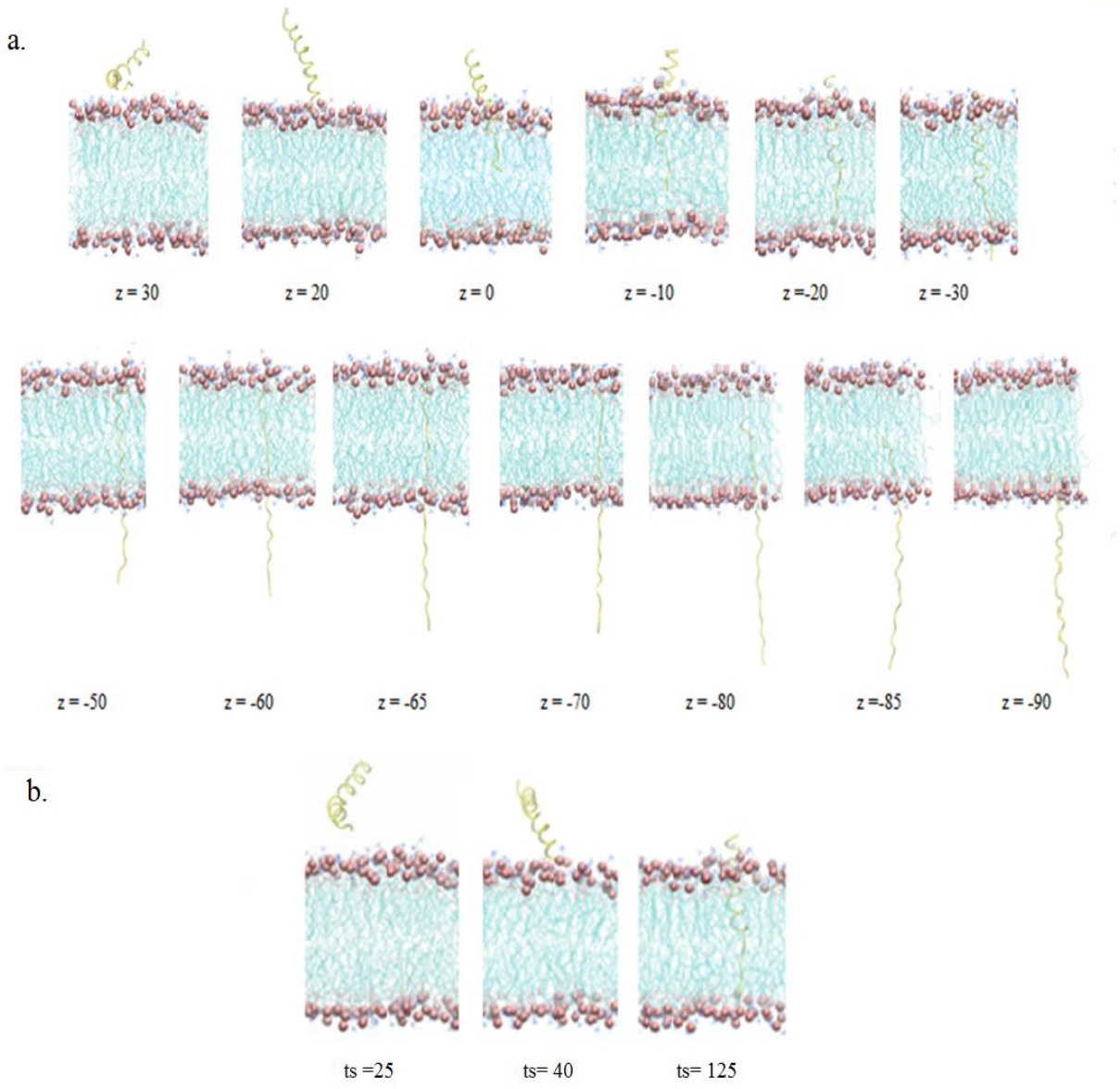

Figure 4.12. Snapshots acquired from the first melittin POPC SMD simulation. (a) Snapshots at different z values (the distance between Gly1 and the center of the SMD system, units: Å (b)Snapshots captured at different time steps.

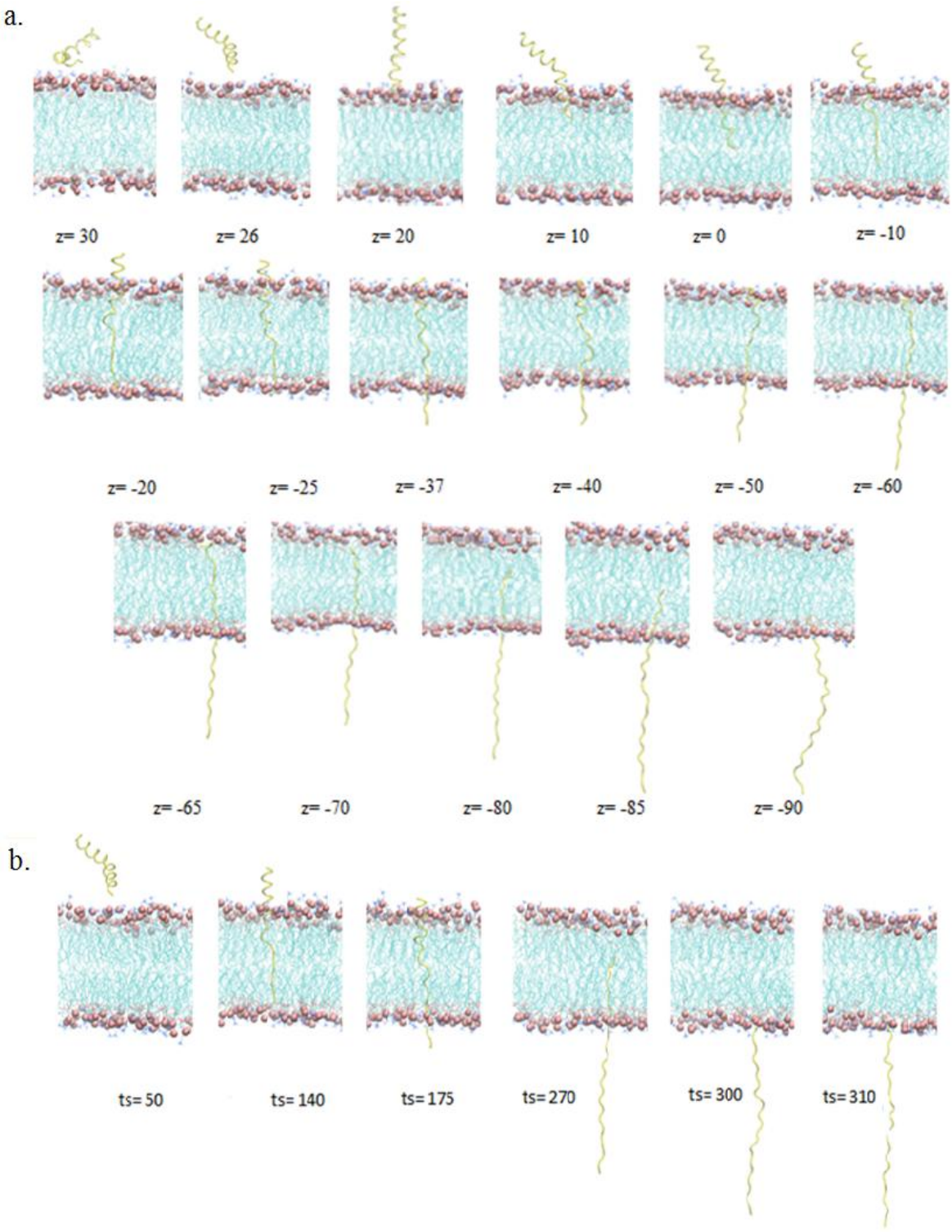

Figure 4.13. Snapshots acquired from the second melittin POPC SMD simulation. (a) Snapshots at different z values (the distance between Gly1 and the center of the SMD system, units: Å). (b) Snapshots captured with time steps.

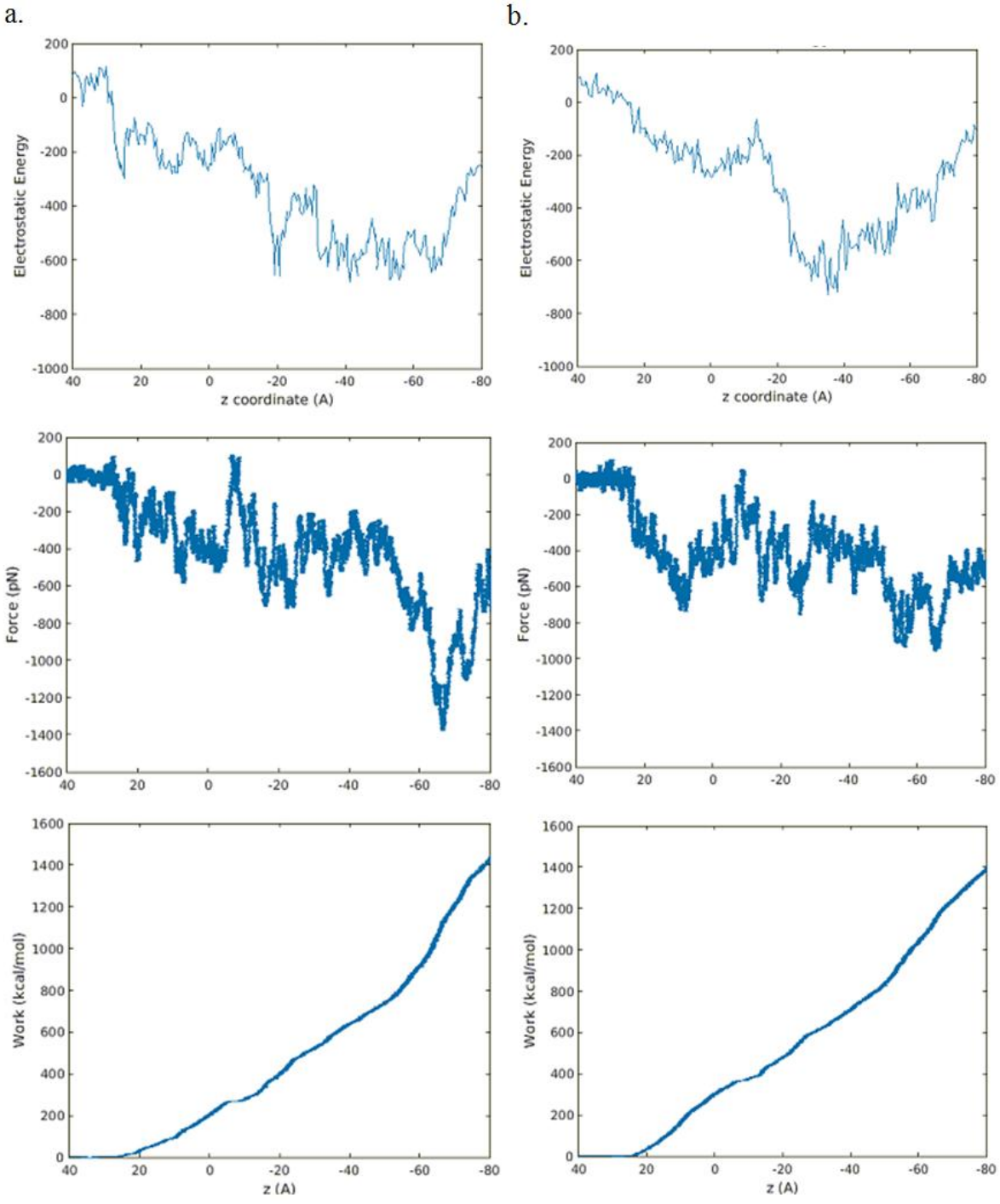

Figure 4.14. Melittin POPC SMD simulation: electrostatic energy vs. z, force vs. z & work vs. z profiles of Gly1 graph of a) Pos1 b) Pos2

Radius of gyration vs. z coordinate and helicity percentage vs. z coordinate graphs of melittin POPC SMD simulations can be seen in Figure 4.15. The energy vs. z graphs showed three regions of energy fluctuations. Except, at Pos1, between z -20 Å and -40 Å

there was a decrease in energy. At this point the peptide was in a trans-membrane state and as Gly1was pulled through the lower membrane the energy profile showed no resistance. In the force graphs, the simulations acted in a similar fashion except at z -65 Å in Pos1 more force was applied. This force is thought to have aroused due to the energy barrier caused by Lys7, Arg22, Gln25 and Gln26. Both positions showed similar work trends. And the 'radius of gyration' trends and the changes in the order of lipids were very similar when both positions are compared.

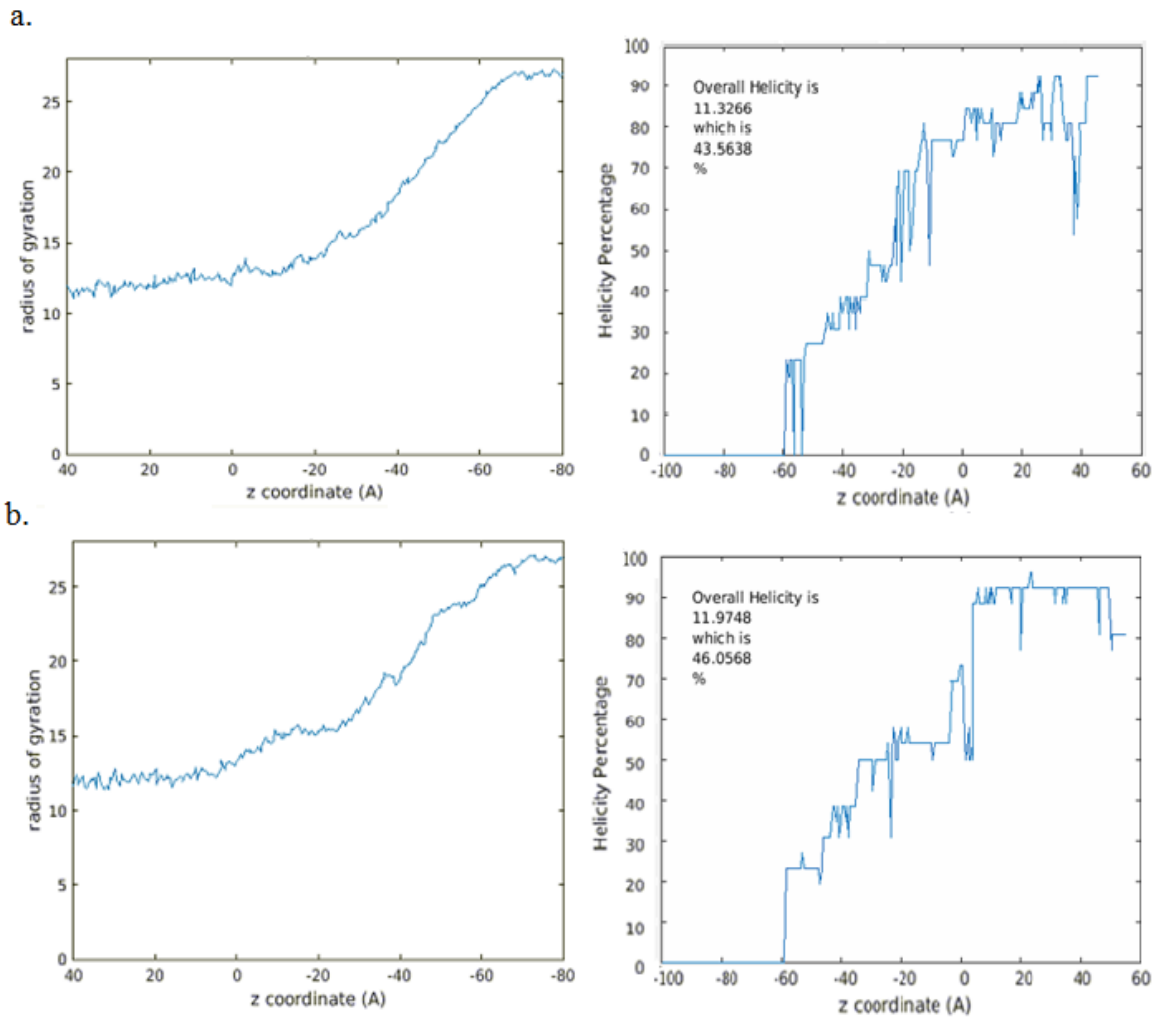

Figure 4.15. Melittin POPC SMD simulation a) Pos1 b) Pos2. Radius of gyration vs. z and helicity percentage vs. z profiles of Gly1.

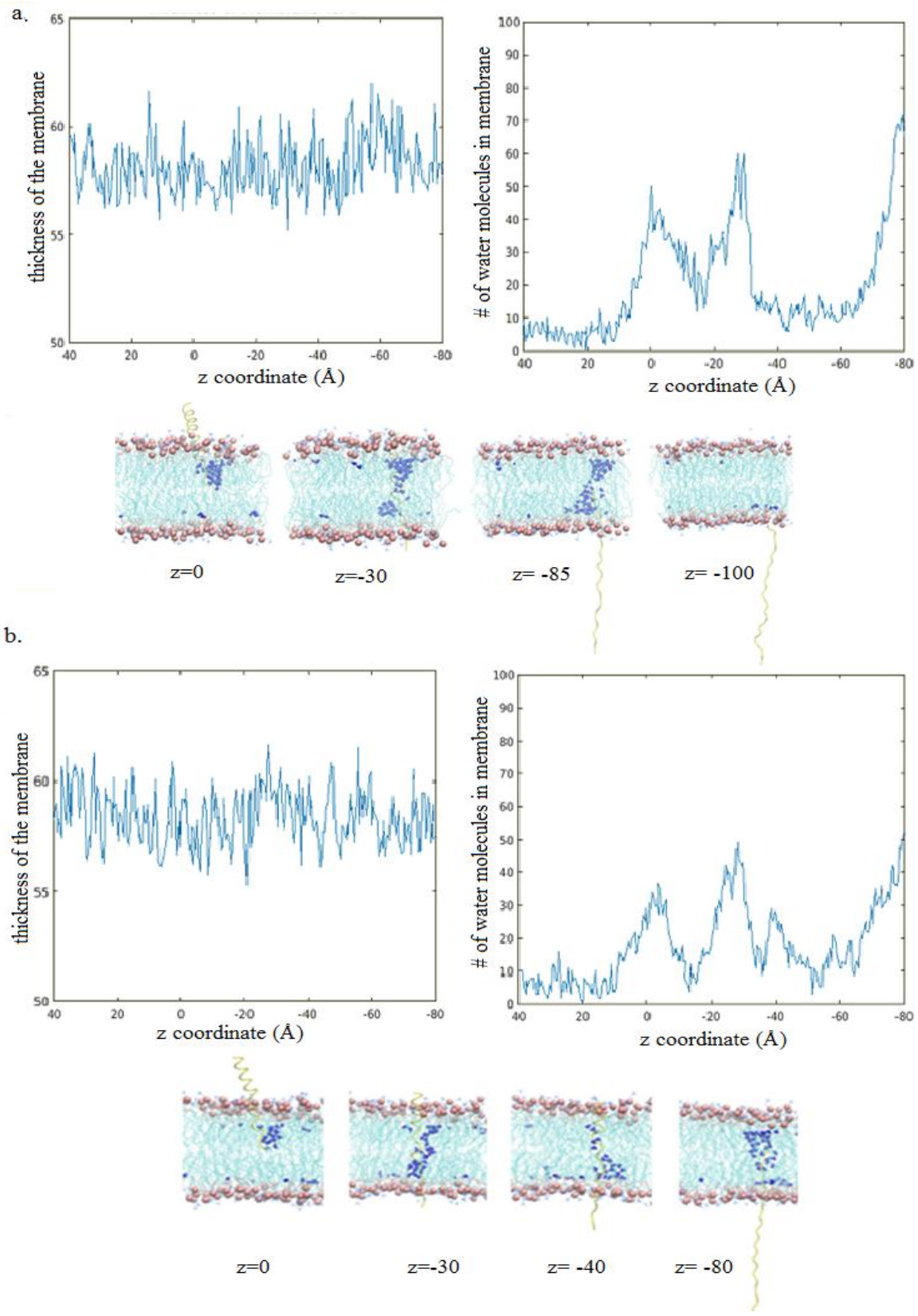

Figure 4.16. Melittin POPC SMD simulation a) Pos1 b) Pos2. Thickness of membrane vs. z, water in membrane vs. z profiles of Gly1 along with snapshots.

Thickness of membrane vs. z graphs, water in membrane vs. z graphs along with snapshots is given in Figure 4.16. The value of the thickest and the thinnest values were 62 and 55 Å respectively in both membranes. However, for Pos1 the thinnest value was at z -30 Å and thickest was at z -60 Å, whereas for Pos2 it was at z -20 Å and z -25 Å respectively. At the end of the simulations the thickness values were similar 57 & 58.5 Å for Pos1 and Pos2 respectively. The intake of water molecules was very similar in both simulations, with just a slight difference in Pos2. At z -40 Å there was an increase in the number of water molecules. At this point the peptide was in a trans-membrane position and the last residues (C-terminus) were being pulled through the upper P heads. Membrane thickness and water in membrane profiles showed that both simulations exhibited similar reactions to peptide penetration. The membranes thinned mostly while the peptide was in a transmembrane state. And most water intake was observed as the peptide left the membrane.

In the melittin POPC visual analyses in Figure 4.17 just before penetration, the peptide positioned itself in a vertical position with respect to the membrane however as the peptide moved inside the membrane the part of the peptide that's left outside took a parallel position with the membrane. Both tips of the peptide were in close proximity with the P heads. Gly1 and Arg24 were the closest residues to the membrane. This was not observed in the POPE simulations. From the residue energy profiles apart from Gly1, Lys21 was also active at this point. Arg24 was pushed away from the membrane as the peptide was pulled by Gly1 towards the membrane by the SMD simulation. The peptide was in a vertical state as the peptide starts penetrating the membrane. Melittin binding in parallel and vertical orientations are suggested to be competing mechanisms. Mellittin oriented in a parallel position at low peptide concentrations [32]. Similar to simulations in POPE, the water penetration initiated as Val5 enters the membrane. At this point Lys7 was inside the upper P heads and it was detected that from the residue energy analysis the energy of Lys7 was very high at this point. Although the helicity dropped as the peptide entered the membrane until the trans-membrane state was achieved the peptide radius of gyration increased from 15 to 20. This means that the peptide did not unfold fully because the radius of gyration continued to increase past trans-membrane position. Leu6-Lys 7-Val8-Leu9-Thr10-Thr11 anchored the peptide and held its helical structure inside the membrane. In

Pos1 Thr11-Gly12-Leu13-Pro14 form a kink, which later unwinded. A kink is the secondary structure that connects the two helical structures which composes the peptide.

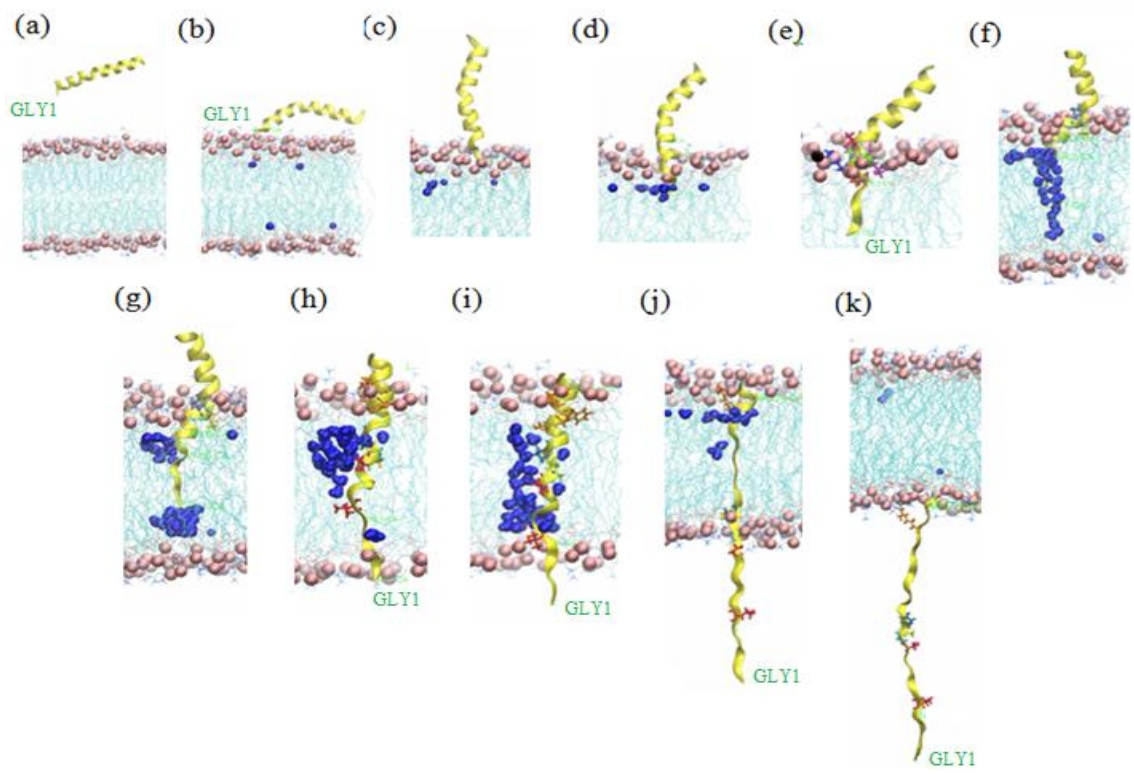

Figure 4.17. Snapshots of melittin POPC SMD simulation-position 1. Z is the distance between center of mass of lipids and center of mass of Gly1. (a) z=43.58 Å (b) z=25.96 Å (c) z= 18.27 Å (d) z=7.91 Å (e) z=2.20 Å (f) z= 1.42 Å, Lys7 (blue), Val8 (green), Leu9 (purple) and Thr10 (lime). (g)z=-3.23 Å (h) z=-23.26 Å, Leu6-Lys7-Val8-Leu9-Thr10-Thr11 (red) , Trp19-Ile20-Lys21-Arg22 (orange). (i) z= -30.83 Å (j) z= -62.55 Å, Arg22(orange) (k) z= -100.44 Å

Snapshots of melittin POPC position 2 SMD simulation are given in Figure 4.18.In Pos2, Leu9-Thr10-Thr11-Gly12 formed a kink which carried water molecules inside the membrane. Trp19-Ile20-Lys21-Arg22 acted as an anchor. Lys21-Arg22-Lys23-Arg24 had high electrostatic energies in the residue energy analysis. Also Trp19 had higher energy at this point although it was relatively much lower, it increased from a value of 0 to 20 kcal/mol. Trp is known to play an important role in the melittin insertion mechanism.

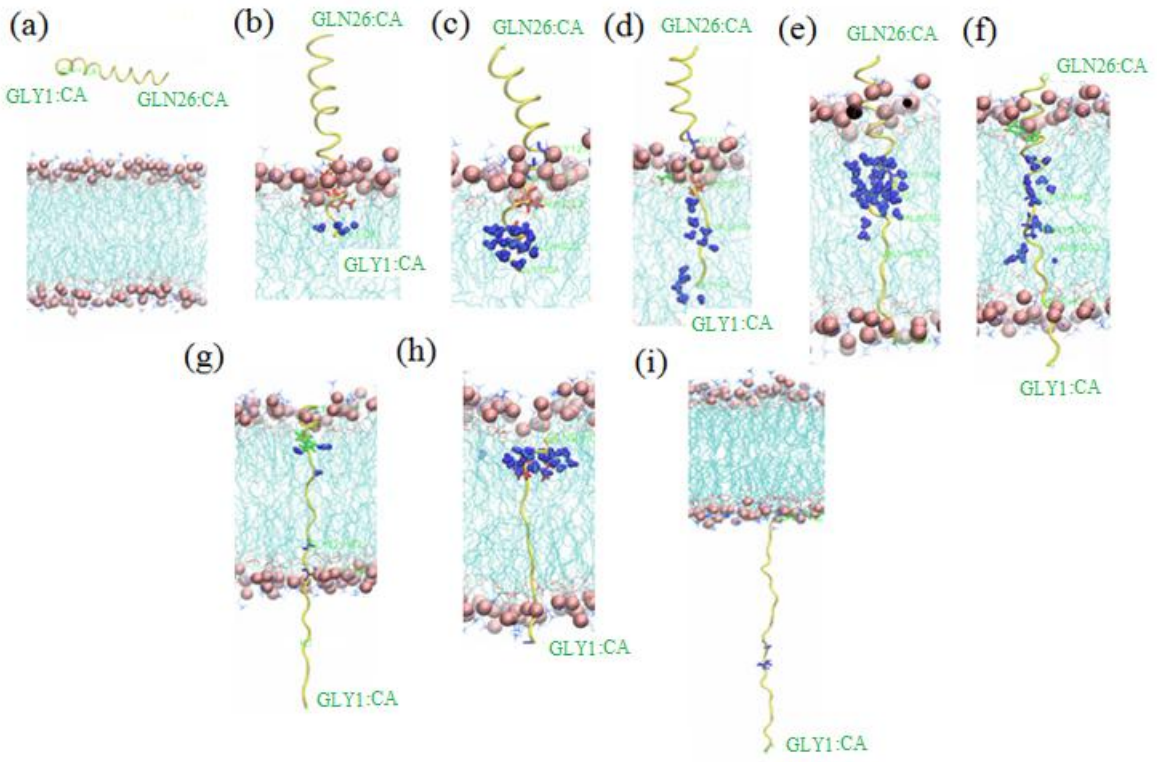

Figure 4.18. Snapshots of melittin POPC SMD simulation-position 2. Z is the distance between center of mass of lipids and center of mass of Gly1. (a) z=53.39 Å (b) z= 10.15 Å, Val5-Leu6-Lys 7-Val8 (red sticks) (c) z=4.35 Å, Thr10-Thr11-Gly12 (blue) (d) z= -0.06 Å, Leu9 (green) Gly12 (blue) (e) z= -24.53 Å (f)z=-31.40 Å Trp19 (green) (g) z= -52.50 Å (h) z= -68.01 Å (i) z=-103.27 Å.

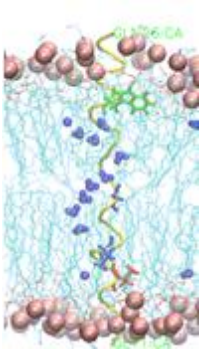

Figure 4.19. Trans-membrane melittin snapshot in POPE membrane. Trp19 residue is shown in green.

With the intrinsic circular dichroism method with the interactions of phospholipids, the NMR relaxation properties of Trp19 protons changed. Also the aliphatic chains of the phospholipid were immobilized by the insertion of melittin who's solely Trp19 residue

moves to a hydrophobic environment [37]. The deletion of Trp19 was found to reduce melittin activity in experimental results. The immersion of the Trp19 residue to a zwitterionic membrane (ex. POPE, POPC) was observed to be less than an anionic vesicle. Trp19 residue was also discovered to act as an anchor. It is known to affect the positioning of the peptide inside the membrane and subsequently play an important part in antibiotic channel peptides. When Trp19 was in an inter-membrane state, it was observed to stabilize the overall thermodynamics of a membrane protein. The insertion levels of Trp and other residues depend on many factors such as system temperature, environmental pH, the initial position of the peptide, etc [31]. This might be the reason why the Trp19 residue did not show much interaction with lipids in both POPC and POPE membrane SMD simulations or the fact that it had low lipid interactions showed that it has less resistance against moving in the –z direction. Arg22-Lys23-Arg24-Gln25-Gln26 had really high electrostatic energies and caused increase in water molecules inside the membrane. Especially Arg22 interacted with the lower P heads. The peptide and water molecules left the membrane at the end of the simulations.

In Figure 4.19, melittin was in a trans-membrane state in POPE membrane; the Trp19 residue is shown in green licorice and acted as an anchor during the SMD simulation. Trp19 acted as an anchor due to increased electrostatic energies with the lipids at this point. Trp19 was observed closely in POPE and POPC simulations. Figure 4.20 shows the z coordinate of Trp19 α-Carbon vs. time step in the Melittin POPE and POPC SMD simulations. The areas in the graphs that show a steady z-coordinate was observed visually. It can be seen from Figure 4.21 that in the POPE simulations, Trp19 had interactions with the upper P layer at time step 150. Between time steps 150-200 Trp19 stood stationary as the C-terminus residues anchored the peptide onto the upper P layer. Trp19 also had interactions with the upper P layer. Similarly, in Figure 4.22, in one of the POPC simulations between time steps 150-200, Trp19 interacted with the upper P head layer along with the C-terminus of the peptide, causing the peptide to be anchored on the upper P heads as the N-terminus was unfolded. In the plateaus observed between time steps 0-100 Trp19 was situated outside the membrane therefore has no interactions with the membrane at these points.

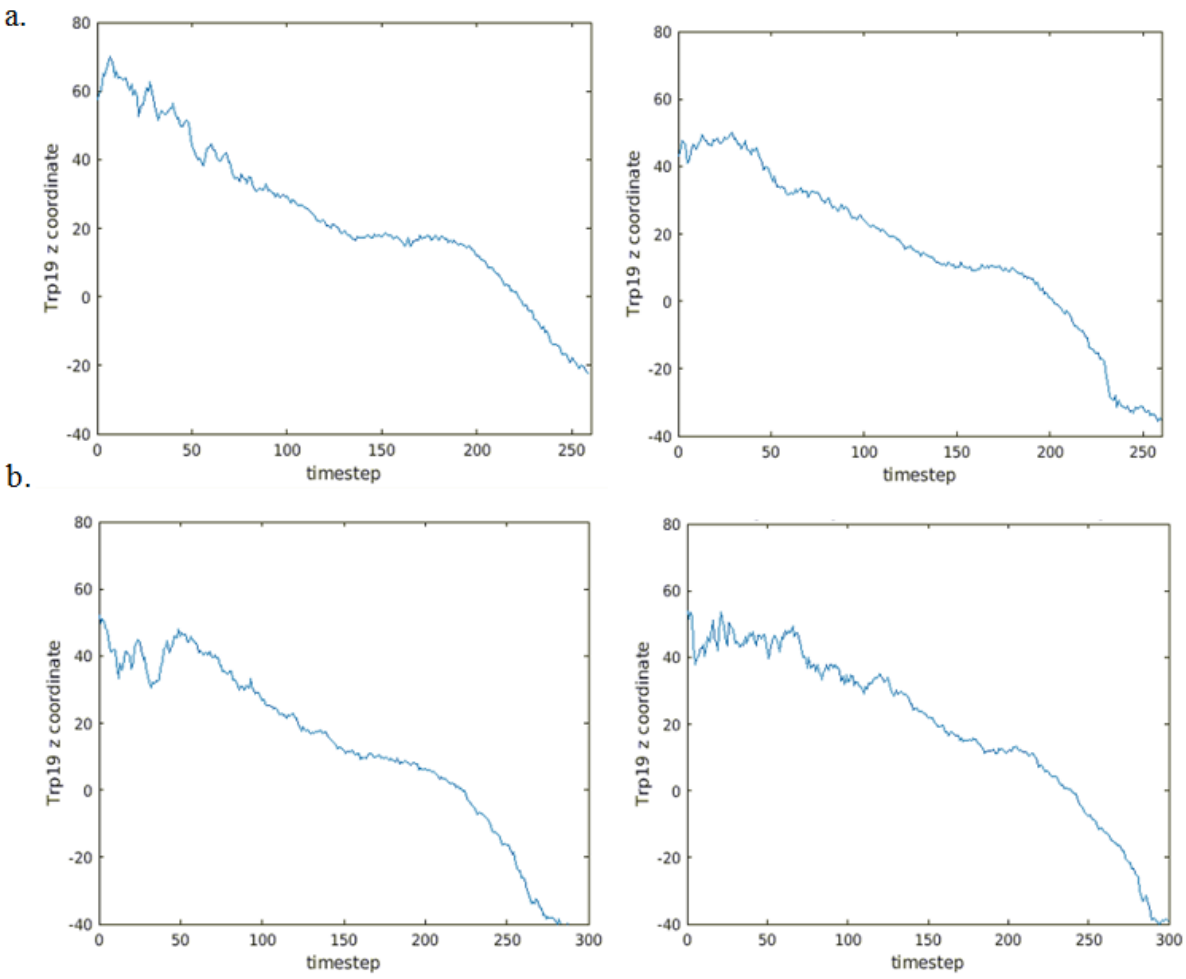

Figure 4.20. Trp19 residue trajectory vs. time in a) POPE b) POPC membrane SMD simulations.

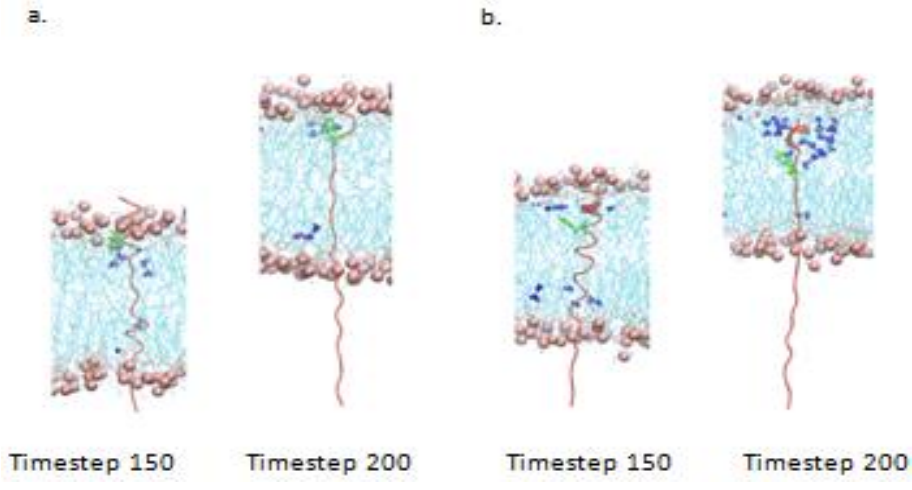

Figure 4.21. Trp19 in melittin POPE SMD simuations a) Pos1 b) Pos2. Trp19 is shown in green.

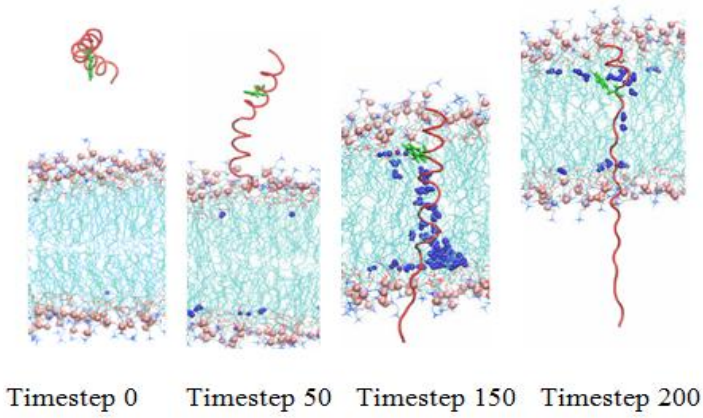

Figure 4.22. Trp19 in melittin POPC membrane SMD simulation. Trp19 is shown in green.

In the melittin POPE and POPC simulations the residues that have interactions with the membrane were found to be the same residues. However there are a few differences observed between the two membrane systems. The average of maximum electrostatic energies of melittin residues in POPE and POPC membrane SMD simulations are shown in Figure 4.23. The residues with the most interactions with the membranes were found to be Gly1, Lys7, Lys21, Arg22, Lys23 and Arg24. Residues Thr10, Thr11, Ser18, Gln25 and Gln26 had interactions with the membrane however less intense with an electrostatic interaction of below -50 kcal/mol.

When the electrostatic energies of all residues of melittin were compared in terms of POPE vs. POPC, the electrostatic energies were slightly higher in POPC. Significant differences in energy were observed in residues Lys21 and Arg24 whose electrostatic energies were higher in POPC. Also Gln25 and Gln26 were more active in POPC. It was proposed that melittin would not enter the membrane due to the charged and polar amino acids Lys7, Thr10, Thr11 and Ser18 which would not want to be placed in a hydrophobic environment. It was counter proposed that a hydrogen bond between residues Lys7 and Thr11 in the α-helical orientation may be the cause of the melittin translocation to a trans-membrane state [32]. All of the mentioned residues had considerable lipid interaction in the simulations. Lys 7, Thr10, Thr11 and Ser18 having around -150, -25, -20, -20 kcal/mol in POPE and -200, -40, -40, -30 kcal/mol in POPC membrane respectively.

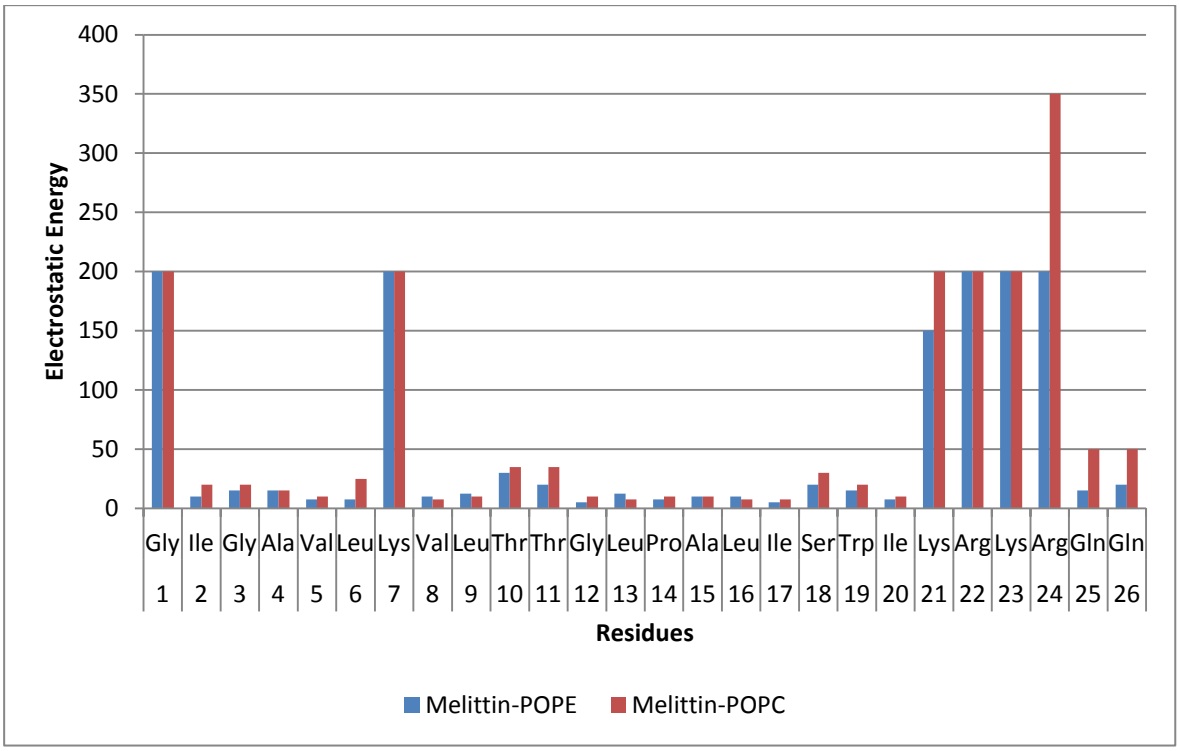

Figure 4.23. The average of maximum electrostatic energies of melittin residues in POPE and POPC membrane SMD simulations.

In the residue energy analysis Pro14 had scarce energies with the membranes. It was discovered that the Pro14 was not needed for lytic activity however it was detected to be more active against bacterial membranes compared to Pro14 mutated non-native analogs [19].

The sequence of melittin is GIGAVLKVLTTGLPALISWIKRKRQQ. Residues 1-6 are hydrophobic. Residues Ile2, Val5 and Leu6 faces towards the inner or upper side of the bent rod structure of melittin while Ala4 chain faces the opposite side making the peptide somewhat apolar. Val-8, Leu-9, Leu-13, Leu-16, Ile-17, Trp-19, and Ile-20 which are the most apolar residues are placed on the inner surface or the upper surface of the chain while Lys-7, Thr-10, Thr-11, and Ser-18 which are hydrophilic residues are placed on the outer surface of the bent rod. Pro14 was a large apolar side chain and contrary to other apolar residues it was placed on the outer surface of the bent rod. The last six residues are all hydrophilic. The helix was charged in this region because the Lys and Arg side chains

which are positively charged are placed such that they cover the whole circumference of the helix. And the remaining two residues Gln25 and Gln26 are polar [38]. Apart from Gly1 the residues with high electrostatic energies with the lipids are uncharged/ polar or charged residues.

The helicity analyses of the SMD simulations gave information about the secondary structure of the peptides throughout the simulations. The melittin peptide has α-helix structure. The pVEC peptide was in β-sheet form before the penetration into the membrane. As the melittin peptide locates into a trans-membrane state the secondary structure becomes a random coil and moved through the membrane in the form of a chain [23]. Melittin is known to have a folded structure in aqueous environments where it was found as a tetramer. It is presumed that the interactions with phospholipids cause the melittin tetramer to disassociate an separate into monomeric melittin peptide [37]. Melittin is composed of three regions; a hydrophobic N-terminus region, a center with hydrophobic and hydrophilic parts, and a hydrophilic C-terminus region. The secondary structure of melittin constitutes of two α-helical rods connected at residues 11 and 12. Residues 1-10 make up the first part of the α-helical structure and residues 13-16 make up the longer α-helical rod. NMR methods have shown that melittin is mainly in a flexible (non-helical) constitution, however residues 5-9 and 14-20 are found to be helical. The backbone of melittin is considered to be %90 α-helical [38]. In the simulations carried out in this study, for Melittin in POPE membrane simulations, the initial helicity percentage of melittin was about 80% which corresponds to 20.8 helicity. The helicity increased to about %90 while the peptide was still in the water solution. When Gly1 reached the upper P layer the helicity dropped to about its initial helicity. In Pos1 the helicity increased to about 90% when the peptide was inside the membrane then slowly decreased. When in Pos2 helicity dropped slowly. After Gly1 reached the lower P layer where the helicity was about 70%, the helicity started to drop more radically. This trend was similar in both simulations. The helicity dropped to zero as the peptide moved out of the membrane. This may be caused by the pull velocity applied by the SMD simulation. By using a lower pull velocity this problem may be overcome. In trans-membrane position the helicity percentage was about 70-80%.

In the melittin POPC membrane simulations the trends were similar for both positions. The starting helicity was 90% for Pos1 while it was 80% for Pos2. In a study the melittin helicity was reported as 100% in 2M NaCl buffer and 89% in zwitterionic lipids [31]. Both POPC and POPE are zwitteroinic lipids and the helicity percentage was found to be between 80%-90% in the simulations. The difference was caused by the equilibration and the minimization step applied before the SMD simulation. While in Pos2 the helicity increased in the solution and continued to be at 90% inside the membrane, in Pos1 the helicity dropped to almost 50% then increased back to 90% before Gly1 reached the upper P heads. The helicity dropped to about 80% when Gly1 started to penetrate the membrane and stayed constant for a while. In Pos 2 the helicity dropped drastically when Gly1 reached the middle of the membrane to about 55%. In a study performed with melittin in POPC membrane the peptide was in a α-helical confirmation in the trans-membrane state with the residues at the two termini being in random coil confirmation. The peptide folded and unfolded as it travelled inside the membrane [17]. In Pos1 the helicity was about 70% when Gly1 reached the lower P heads. In a UA (united atom) simulation the initial helicity of melittin was chosen as 88% and dropped as the peptide entered the membrane. When wholly absorbed on the surface of a pure POPC membrane the helicity of melittin was 73% [20]. Experimental values are reported to be about 70% helicity [32]. In both simulations the helicity dropped further until the peptide has left the membrane. Again this may have been caused by the pull velocity of the SMD simulations. In all simulations the peptide totally unwinds. In trans-membrane position the helicity percentage was on average about 70%. It was suggested that the melittin peptide may stay at a low helicity percentage when forming pores and might fold once the pore is stabilized. While forming a toroidal pore, with a less helical melittin structure the residues are freer to interact with the lipid headgroups. With more interaction, the melittin peptide might pave the lipid headgroups more easily and create pores more effectively [28]. The helicity of melittin was higher in the POPE membrane compared to the POPC membrane simulations. All of the analysis graphics for the SMD simulations can be found in Appendix A. The residue energy analysis graphics are given in Appendix B.

4.2. Melittin Transport across the POPE Membrane Examined by Additional SMD Simulations

4.2.1. Melittin Transport across the POPE Membrane Examined by SMD Simulations Pulled by Center of Mass

The visual analysis in VMD showed that for SMD simulation 1, at time step 0 the peptide was positioned above the membrane. (Figure 4.24) By time step 43, the peptide reached the membrane and positioned in a horizontal state. At time step 62, melittin entered the membrane in a parallel orientation. There was no visible water penetration although most of the peptide passed through the upper P layer. Water started to enter the membrane at time step 70 just as Ile20 passed the upper P heads and Ile20-Lys21-Arg22-Lys23-Arg24-Gln25-Gln26 were embedded in the P layer. At time step 76, the peptide was anchored on the upper P layer by Ile20-Lys21-Arg22-Lys23-Arg24-Gln25-Gln26 and Gln1. As the center of the peptide moved to the middle at time step 87, the peptide pulled more water molecules into the membrane. The center of the peptide almost reached the lower P heads. The water molecules continued to enter the membrane through the top at time step 104. At time step 122, the center of the peptide reached the bottom P layer. It caused a vortex of water molecules inside the membrane. At time step=133, the center of the peptide moved through the lower P layer the water vortex started to disappear. Val8 and Thr11 are shown in green. Around time step 135, the water in the upper half of the membrane left. At time step 139, the peptide unfolded further as more residues passed through the lower P layer. Water continued to leave the membrane at time step 151. Gly1 was in contact with the lower P heads along with the C-terminus of the peptide. The N-terminus left the membrane at time step 155, so the peptide started to move in a vertical orientation as it moved out of the membrane. Gln26 also left the membrane. Pro14-Ala15-Leu16 and Ile20-Lys21-Arg22-Lys23-Arg24-Gln25 were embedded in the lower P layer. Residues Ile17-Ser 18-Trp19 were above the lower P layer. 14 is shown in green, 17 is shown in purple while Trp19 is shown in yellow. At time step182, Trp19 is the last residue to leave the membrane. Around time step 186, the C-terminus had final interactions with the lower P layer. And finally at time step 191, both the peptide and water molecules left the membrane.

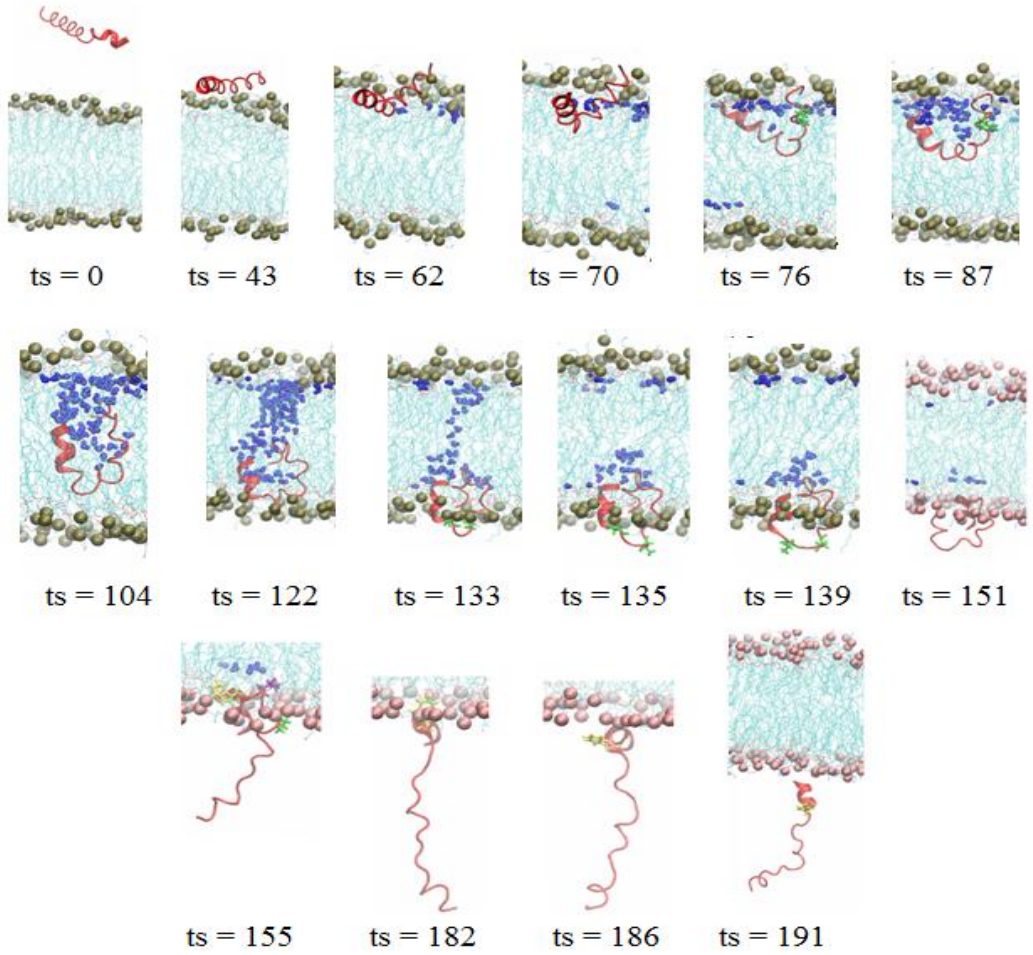

Figure 4.24. SMD Simulation 1- melittin in POPE pulled from the center of mass of the peptide.

The electrostatic energy started to increase at z 30 Å. (Figure 4.25). The peptide neared the membrane in a horizontal position. The residues in the center of the peptide reached the membrane and started to interact with the upper P layer while Gly1 was situated at z 30 Å. The force profile and work profile also showed that force and rate of work started to increase around z 30 Å. The electrostatic energy reached a maximum of -650 kcal/mol at z 18 Å. And maximum force of -1250 pN was applied at z 18 Å. At this point all the two termini of the peptide were embedded on the upper P layer while the center of the peptide was inside the bilayer. The extra force was applied to overcome the anchor caused by the two termini. The energy started to decrease as the c.o.m. of the peptide moved toward the center of the membrane, the force applied also started to decrease after this point. After z 0 Å the energy stayed around -200 kcal/mol. At z -11 Å a

force peak was observed. The peptide reached the lower P layer and an extra force was applied to pull the c.o.m. of the peptide through the lower P layer. Around z -20 Å another force peak was observed as more force was applied to pull the the residues around the c.o.m. of the peptide through the lower P layer. Also there was a change in the rate of work around z -20 Å. The force applied dropped from this point forward. At z -40 Å the c.o.m. of the N-terminus of the peptide moved through the lower P layer and the energy increased to -350 kcal/mol because the C-terminus of the peptide was still embedded in the lower P layer. Around z -50 Å, the energy decreased to 0 and the peptide left the membrane. The VdW energy increased as the peptide moved through the membrane. The major contributor to the total energy, however, was electrostatic energies. At the end of the simulation the maximum work reached was 1200 kcal/mol.

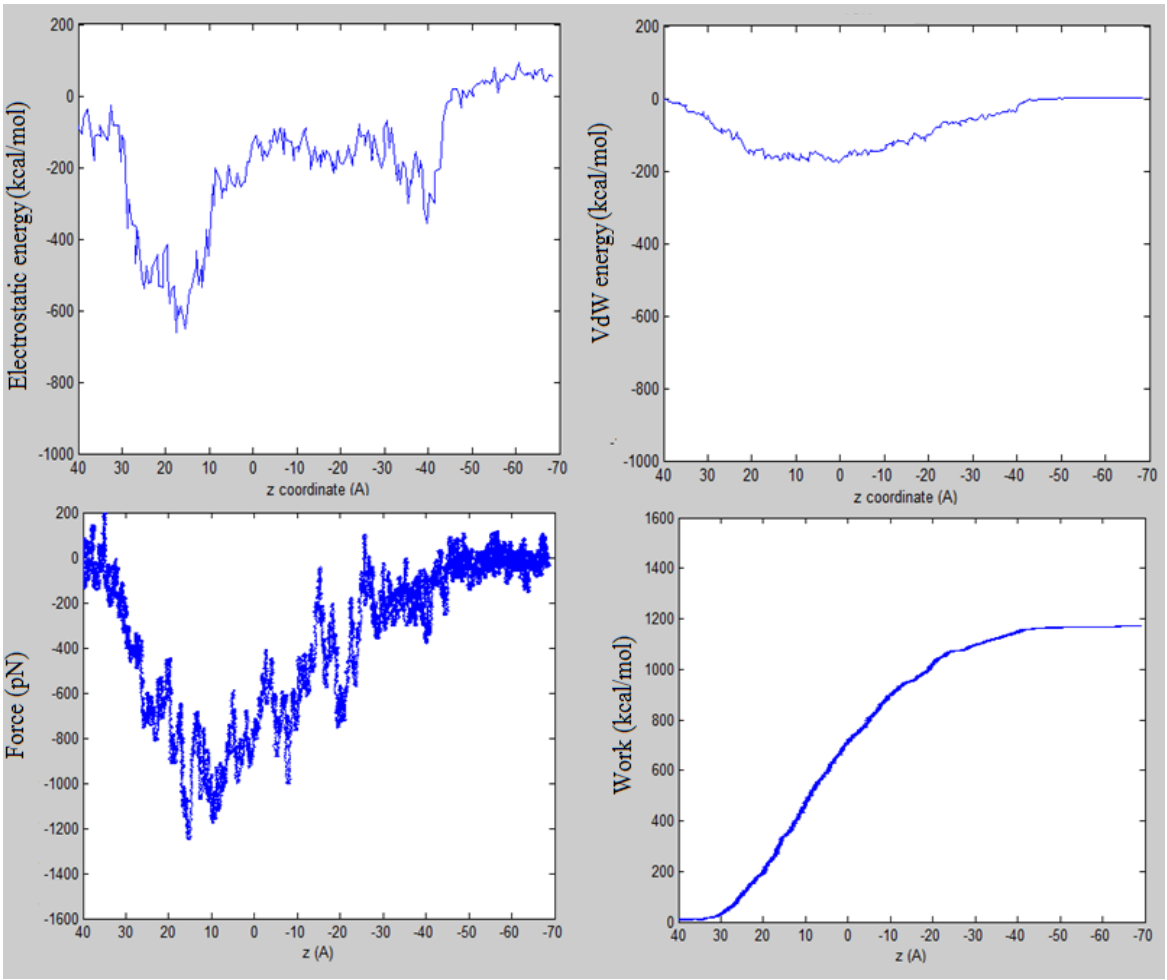

Figure 4.25. The electrostatic energy, VdW energy, force and work vs. z profiles of Gly1 for melittin in POPE membrane SMD simulation pulled by c.o.m.

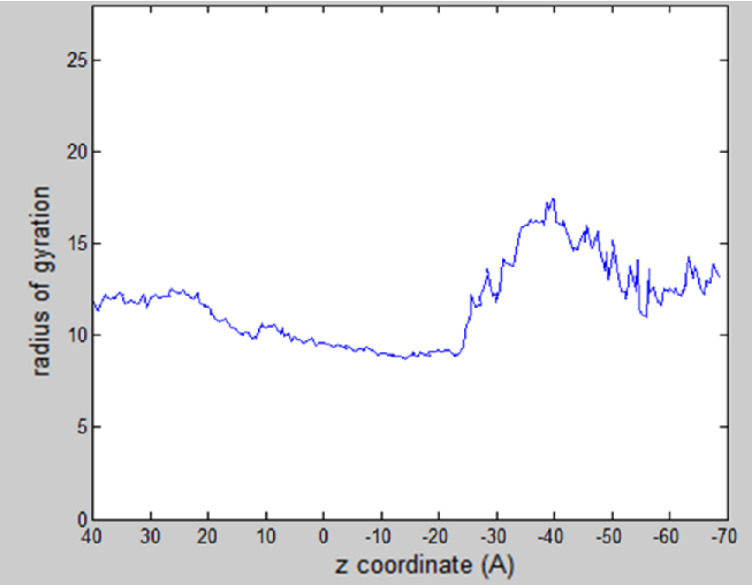

Figure 4.26. Radius of gyration vs. z profile of Gly1 for Melittin in POPE membrane SMD simulation pulled by c.o.m.

The radius of gyration dropped as the peptide moved inside the membrane. (Figure 4.26) The peptide was pulled from the center and the peptide was folded into two thus the radius of gyration decreased. After z -25 Å, radius of gyration increased, the N-terminus left the membrane through the bottom of the membrane and the peptide was attached to the membrane through the C-terminus. As the C-terminus anchored the peptide, the peptide unfolded and the radius of gyration continued to increase. A maximum value of 17 was reached around z -40 Å. After this point the C-terminus also left the membrane and the peptides folded back to two as the peptide was pulled from the center in the –z direction.

Water started to enter the membrane around z 20 Å, which was the point where the peptide was embedded on the upper P layer by the two termini while the c.o.m. of the peptide was situated in the bilayer. (Figure 4.27) The minimum thickness was observed at z -5 Å, when the peptide was inside the membrane and the c.o.m. of the peptide reached the lower P layer. Meanwhile at z -5 Å, maximum amount of water molecules was reached inside the membrane. Water molecules started to leave the membrane from this point forward. At z -20 Å, the peptide left the membrane through the lower P layer and caused the water molecules to also leave the membrane. The maximum membrane thickness was

62.384 Å, at z -19 Å, as the peptide was embedded inside the lower P layer. The average membrane thickness was 56.288 Å with a standard deviation of 1.510 Å.

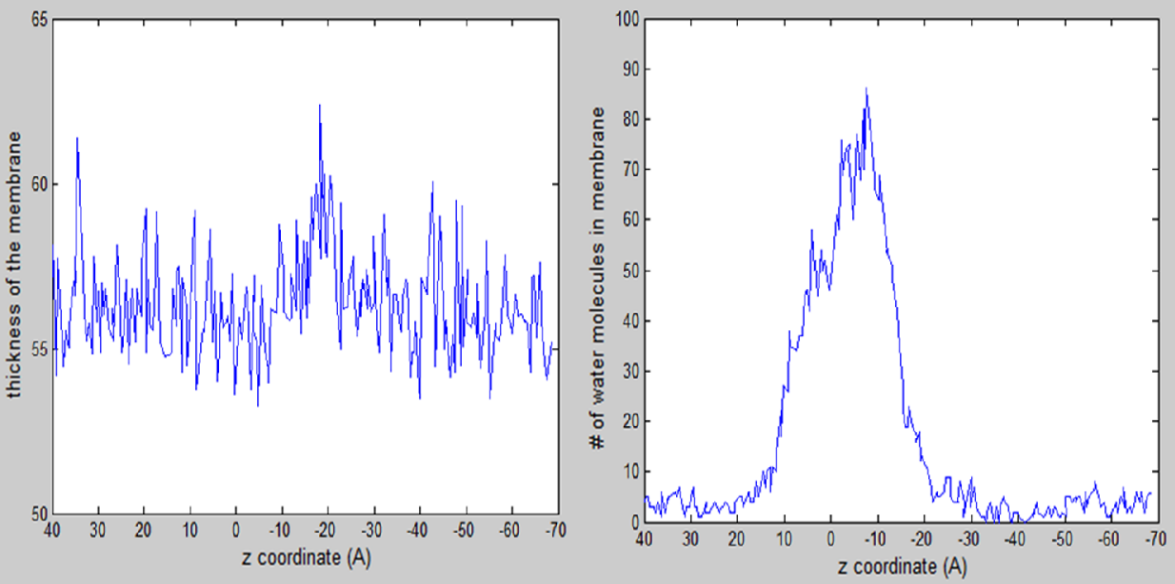

Figure 4.27. Thickness of membrane and water in membrane vs. z profiles of Gly1 for melittin in POPE membrane SMD simulation pulled by c.o.m.

4.2.2. Melittin Transport across the POPE Membrane Examined by SMD Simulations with 1/10th Velocity Pulling

The simulation was carried out until the peptide reached the center of the membrane due to shortage of resources. However, the simulation still gives an overall picture of the peptide insertion mechanism at a lower velocity. The visual analysis of Simulation 2 showed that by time step 417, the peptide reached the membrane and was positioned in a horizontal state. (Figure 4.28) At time step 574, melittin entered the membrane in a parallel orientation. The peptide moved more slowly and took a long time to enter the membrane because the SMD pull velocity was 1/10th of the other SMD simulations. At time step 586, the peptide embedded itself, up to Pro14, in a horizontal position inside the P layer. Water insertion started at time step 701 and the peptide entered the membrane in a slant position. At time step 775, the water bubble inside the membrane grew. During time step 836, the N-terminus started to unfold as Lys7 and Val8 anchored the peptide on the upper P layer. At time step 882, Lys7 and Val8 continued to anchor the peptide and the N-terminus travelled

as far as the center of the membrane. The water bubble extended to the center of the membrane also.

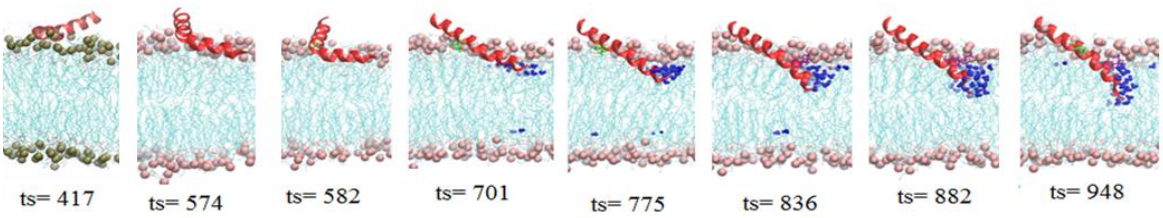

Figure 4.28. Snapshots of melittin in POPE pulled with 1/10th velocity by the N-terminus. Pro14 is shown in green. Lys7 and Val8 are shown in purple sticks.

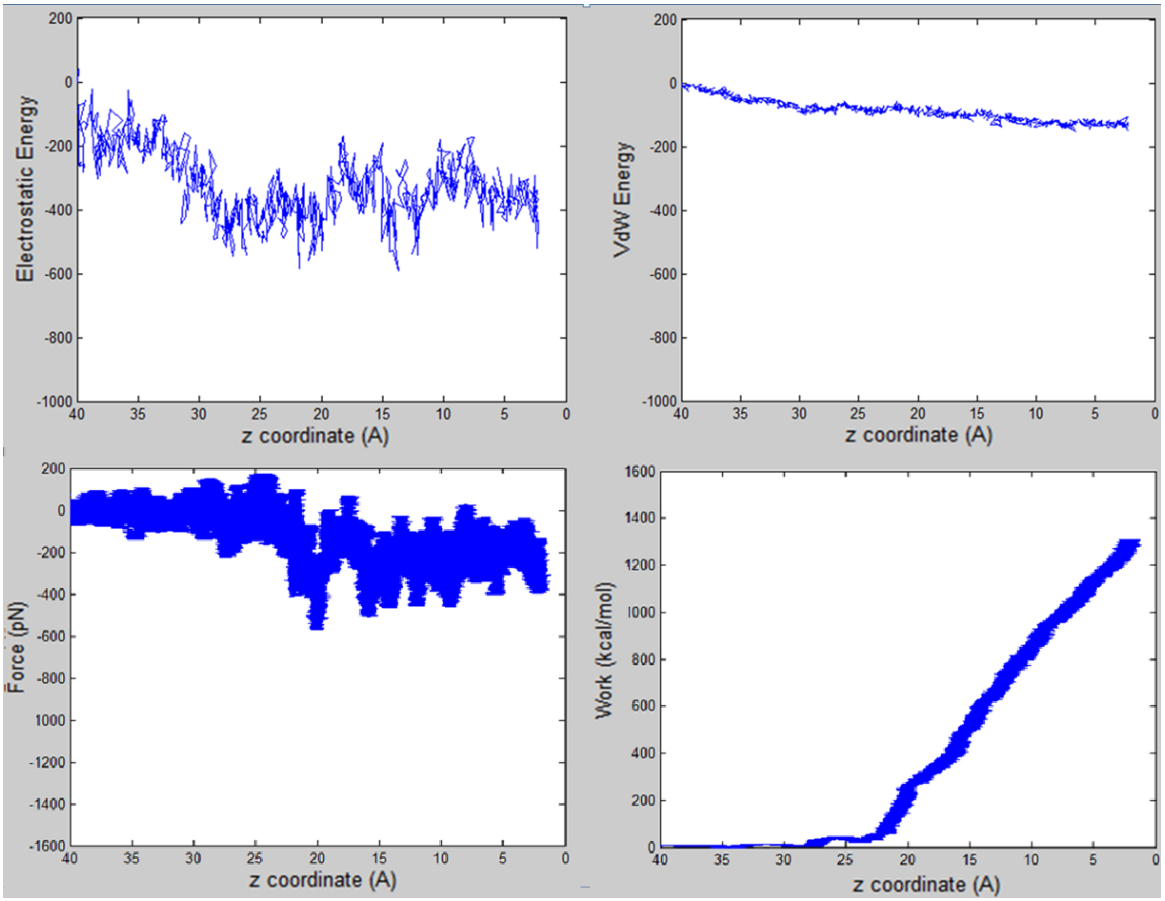

Figure 4.29. The electrostatic energy, VdW energy, force and work vs. z profiles of Gly1 for melittin in POPE membrane SMD simulation pulled with 1/10th velocity by the N-terminus.

The electrostatic energy started to increase around z 30 Å. (Figure 4.29). Until z 22 Å it reached an energy level of -600 kcal/mol. The force started to increase around z 27 Å and the work profile showed an increase of work. The peptide was above the membrane at this point. The peptide reached the top of the membrane in and assumed a horizontal position above the membrane. The interactions of the residues with the upper P layer started before the peptide started to enter the membrane. The rate of increase of work increased at z 22 Å where the peptide was in a parallel position and embedded inside the upper P layer. There was a force peak at z 20 Å, where the force applied increased to -600 pN. At this point the peptide was on the upper P layer and extra force was applied to move the peptide further into the membrane. The rate of increase in work decreased at z 20 Å. The energy dropped after z 20 Å. At z=20 Å the peptide was embedded up to Pro14 inside the P layer, explaining the increase in electrostatic energy up till this point. At z 18 Å the energy dropped to -200 kcal/mol as the peptide moved towards the center of the membrane. As Gly1 escaped the upper P layer, the applied force dropped to 0 pN. The force increased again around z 17 Å. This is thought to have occurred due to Lys7 and Val8. The two residues anchored the peptide to the upper P layer and extra force was applied to pull the peptide in the –z direction. electrostatic energy increased around z 15 Å and the rate of increase of work increased again. The rate of work stayed constant until Gly1 reached the center of the membrane. After z 13 Å the energy started to decrease again. The electrostatic energy value was -400 kcal/mol near the center of the membrane. The VdW energies increased slightly as the simulation continued, which showed that the major contribution to the total energy was given by electrostatic energies. The radius of gyration stayed constant around the value 12. (Figure 4.30) This means that the peptide did not unfold significantly as it moved inside the membrane.

The maximum membrane thickness was 62.714 Å around z 34 Å, and the average membrane thickness was 56.423 Å with a standard deviation of 1.448 Å. The minimum thickness of 53 Å was observed around z 5-3 Å. (Figure 4.31). From the water in membrane profile the water started to increase around z 23 Å however the water leaved the membrane at z 20 Å. Water bubble started to form inside the membrane at z 17 Å. The water bubble continued to grow as Gly1 reached the center of the membrane. From these

profiles it is deduced that the thickness of membrane decreased as more water molecules entered membrane while the peptide moved towards the center of the bilayer.

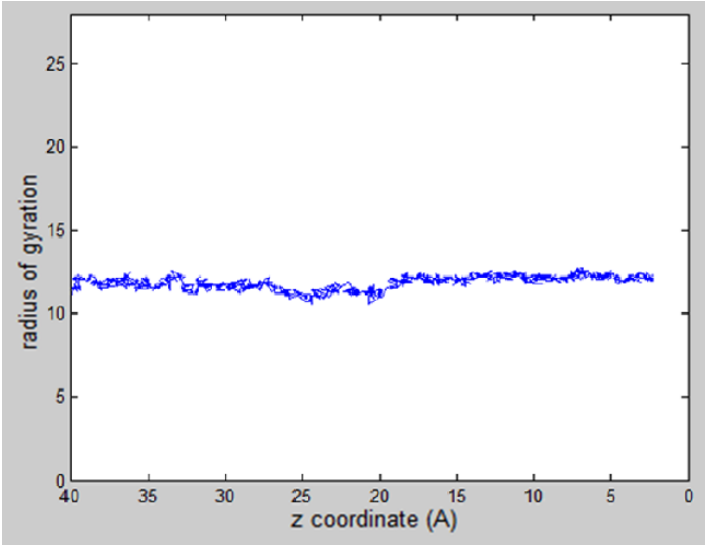

Figure 4.30. Radius of gyration vs. z profile of Gly1 for melittin in POPE membrane SMD simulation pulled with 1/10th velocity by the N-terminus.

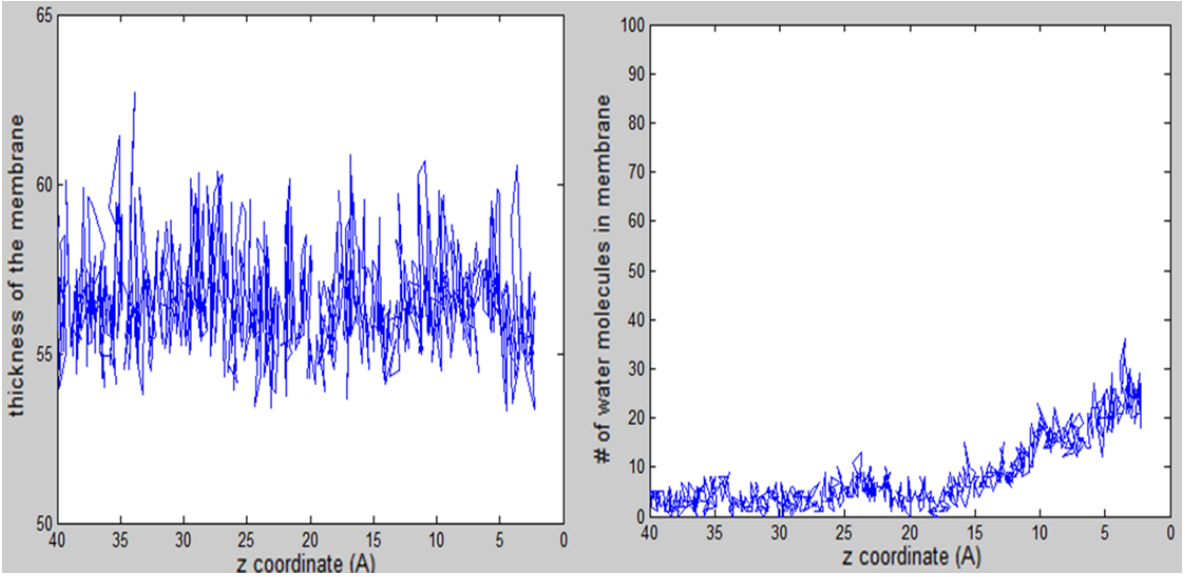

Figure 4.31. Thickness of membrane and water in membrane vs. z profiles of Gly1 for melittin in POPE membrane SMD simulation pulled with 1/10th velocity by the N-terminus.

4.3. pVEC Transport across Membranes Examined by SMD Simulations

4.3.1. pVEC Transport across the POPE Membrane Examined by SMD Simulations

The SMD simulation trajectories of pVEC in POPE membrane were observed visually with the help of VMD. Figure 4.32 and Figure 4.33 show snapshots obtained from pVEC in POPE simulations that show that the pVEC peptide entered the POPE membrane in a vertical position in both simulations. The peptide started to unfold as it passed through the upper P layer and left the membrane through the lower P layer in a random coil formation.

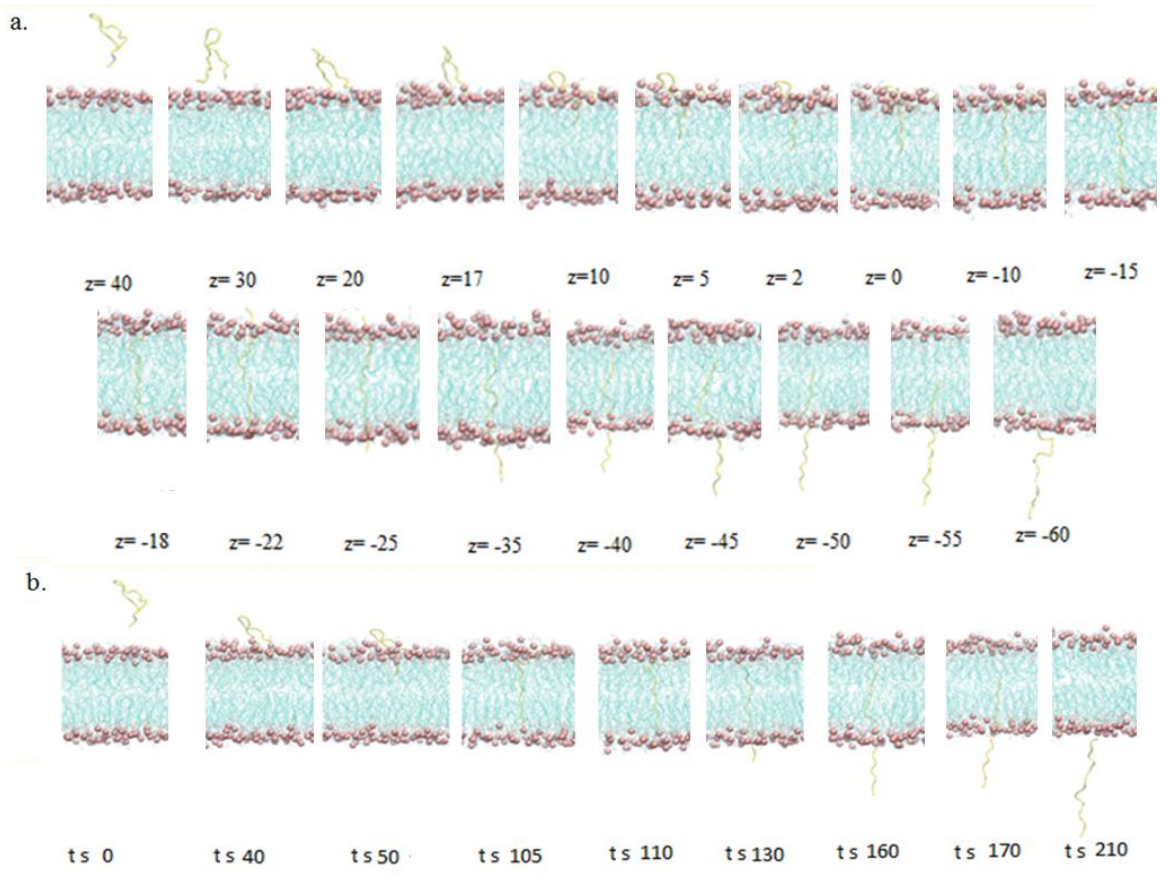

Figure 4.32. Snapshots acquired from the first pVEC POPE SMD simulation. (a) Snapshots at different z values (the distance between Leu1 and the center of the SMD system, units: Å. (b). Snapshots captured at different time steps.

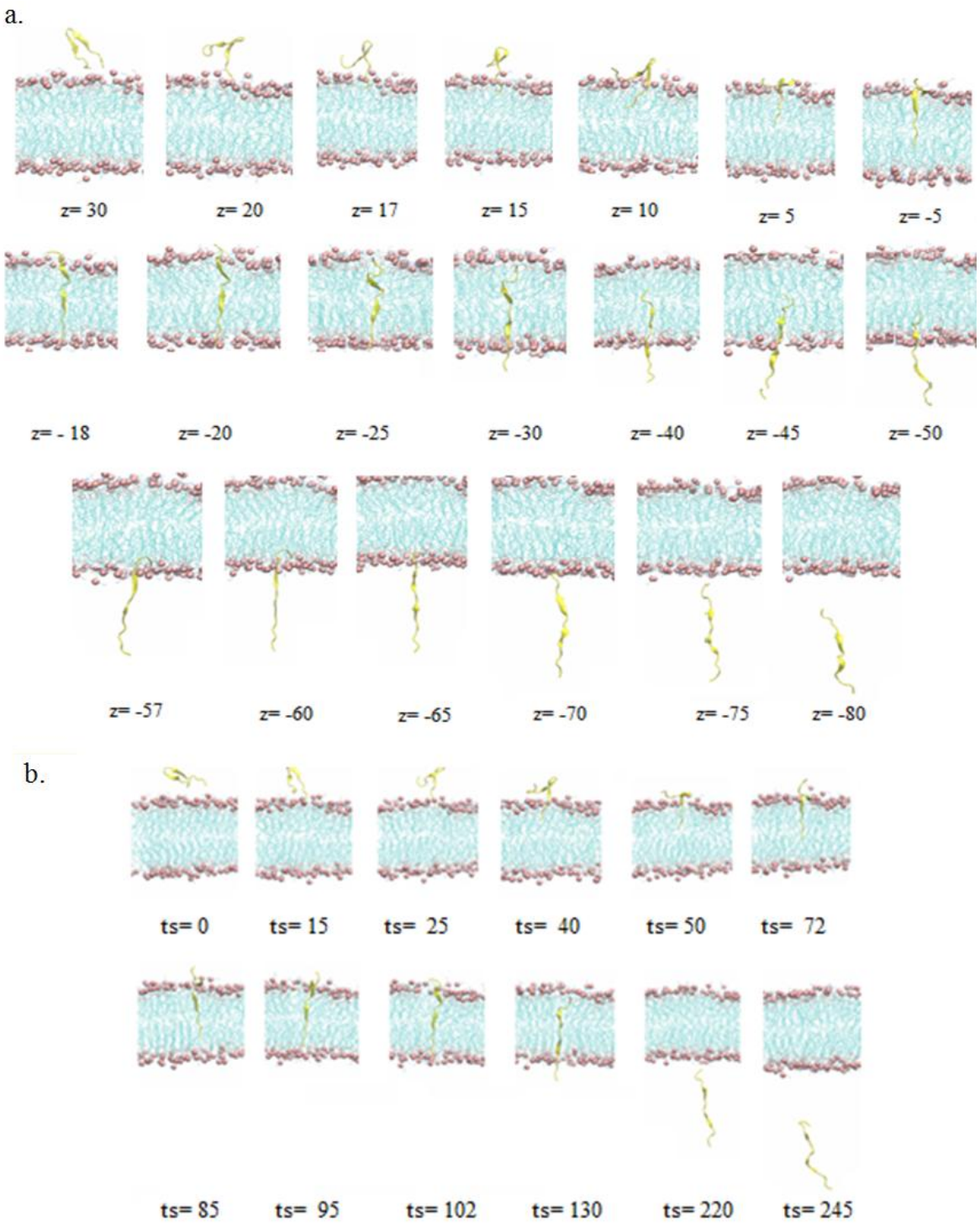

Figure 4.33. Snapshots acquired from the second pVEC POPE SMD simulation. (a) Snapshots at different z values (the distance between Leu1 and the center of the SMD system, units: Å (b) Snapshots captured with time steps.

In the energy vs. z graphs (Figure 4.34), the energy trends were very similar showing 5 regions of energy fluctuations in both positions with an exception in Pos2 at z 30 Å energy increased before the peptide reached the membrane. In the snapshots both ends of the peptide are positioned such that they are in close proximity with the upper P heads of the membrane. Both ends interacting with the membrane might be the reason behind the increase in energy at this point.

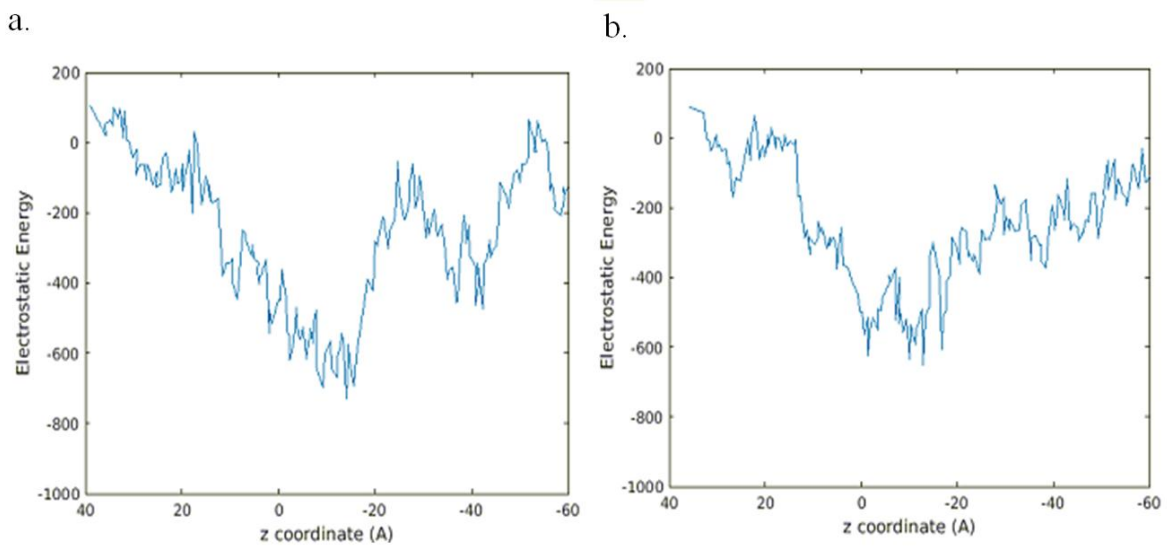

Figure 4.34. pVEC POPE SMD simulation: electrostatic energy vs. z profiles of Leu1 of a) Pos1 b) Pos2

The energy started to rise as the peptide started moving in the –z direction. The energy increased before peptide reached the membrane. There was a decrease in the energy when Leu1 reached the upper P heads. The energy started to increase as Leu1 pierced through the upper P heads. The energy continued to increase until it reaches the lower P heads of the membrane and as it pierced through the energy started to decrease. The energy continued to decrease until the peptide left the membrane and stabilized when it was fairly away from the membrane.

The force applied showed a similar trend as can be seen in Figure 4.35, in both simulations in the form of three regions. These regions show the translocation of the peptide inside the membrane and are observable by the increase in the force applied by the

SMD simulation. The insertion of the N-terminus, the complete insertion of the peptide and the complete extraction of the peptide from the membrane are the three stages of peptide translocation [23]. The differences between the positions are that the force applied was greater in Pos1 and in Pos2 at z -65 Å there appears to be an extra force applied. At this point the last residues were in contact with the lower P heads and extra force was applied to pull the peptide in the –z direction. Both positions showed a similar work trend with the rate of increasing and decreasing work happening around the same points. However, in position1 more work was done, 1200 vs. 1000 kcal/mol.

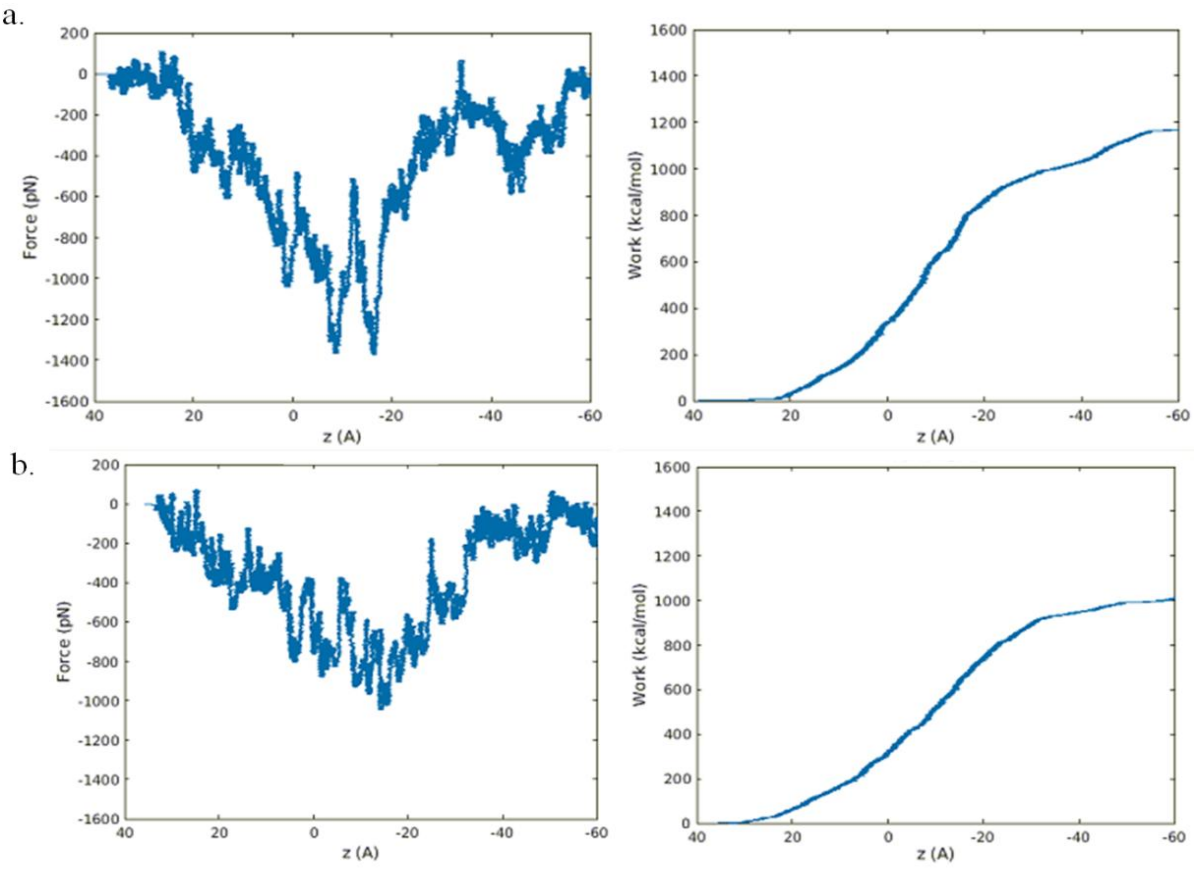

Figure 4.35. pVEC POPE SMD simulation: force vs. z & work vs. z profiles of Gly1 of a) Pos1 b) Pos2

The radius of gyration in both simulations showed a similar trend. In Figure 4.36, the radius of gyration increased until Leu1 reached the lower P layer stayed somewhat constant until the last residue left the membrane then decreased as the peptide traveled away from

the membrane. This means that the peptide unpacks, stays somewhat in a constant secondary structure, then packs more tightly again as the peptide moves further away from the membrane. Both positions showed a similar trend of increasing disorder in lipids. However, at z -18 Å for Pos1 the order parameter decreased meaning that the lipids were ordered as the peptide started to enter the membrane from the top and the order parameter increased for Pos2 for some of the carbons at this point, meaning that the peptide disordered lipids as it entered through the top of the membrane. Other carbons however stayed at a constant order. The thickness of membrane vs. z was also checked for pVEC in POPE membrane in Figure 4.37. The thickest value for Pos1 was 60.5 Å at z 0 Å while for Pos2 it was 59.5 Å at z -18 Å. At these points the peptides were placed in a trans-membrane state. The thinnest value Pos1 was 52.5 at z -45 Å and for Pos2 it was 53 Å at z -70 Å.

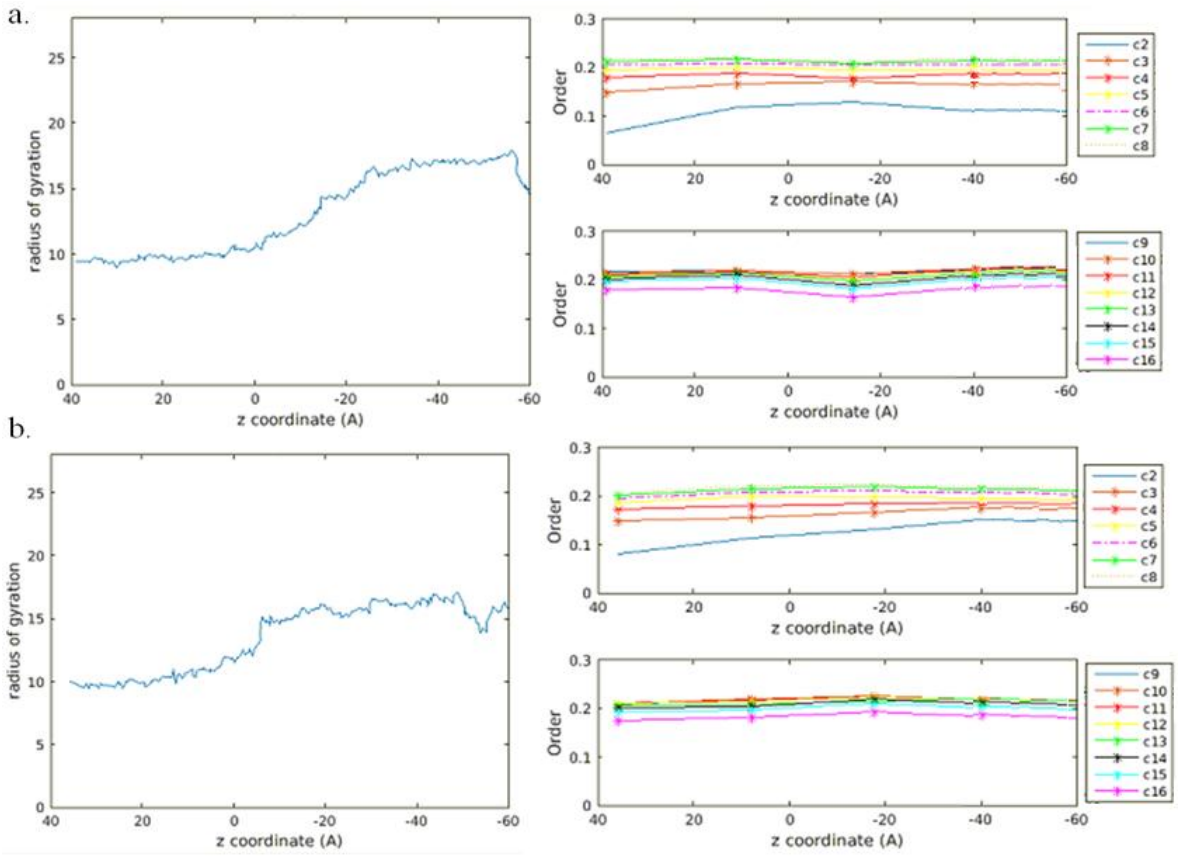

Figure 4.36. pVEC POPE SMD simulation: radius of gyration vs. z & lipid order vs. z profiles of Gly1 of a) Pos1 b) Pos2

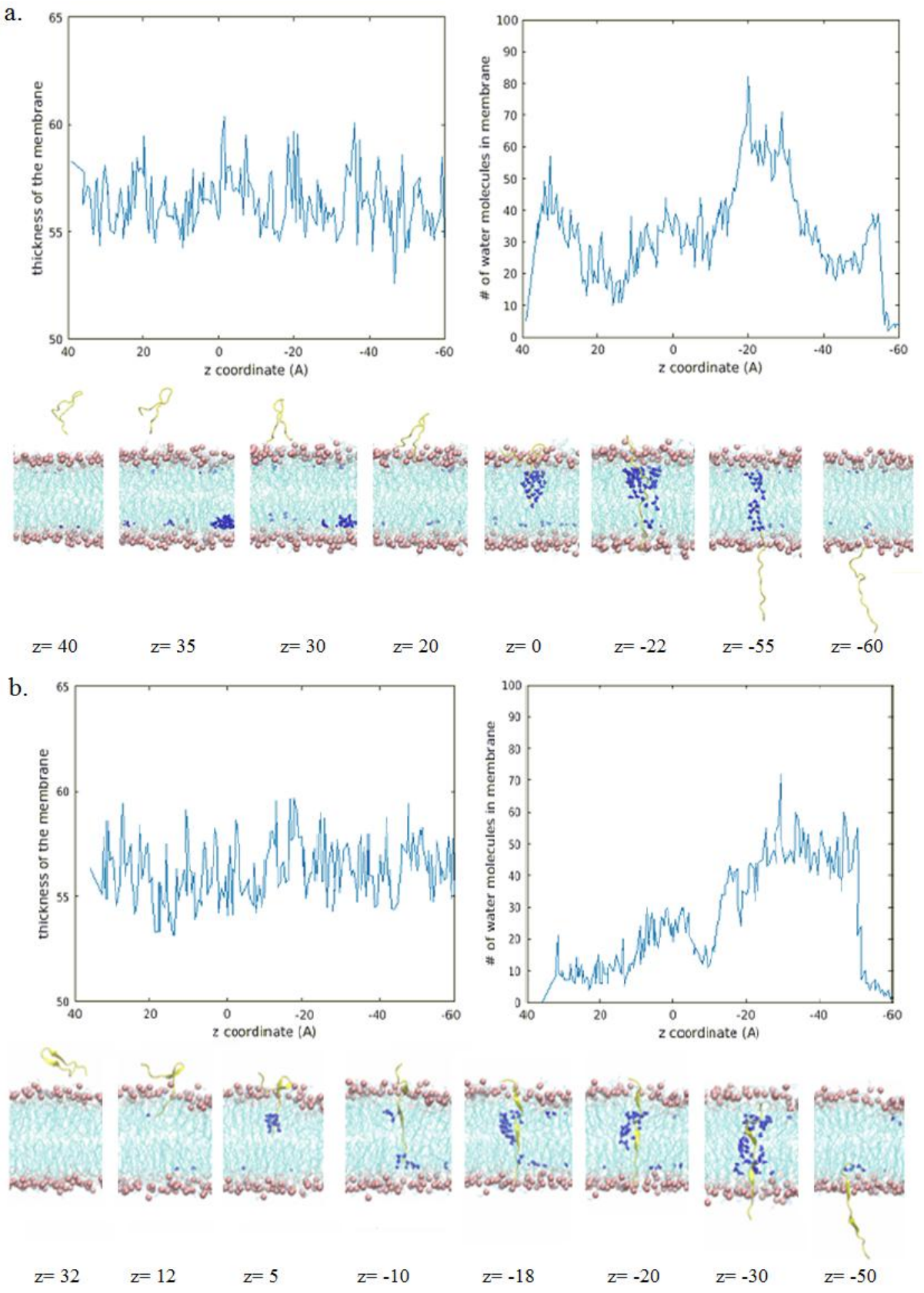

Figure 4.37. pVEC POPE SMD simulation thickness of membrane vs. z, water in membrane vs. z profiles of Leu1 and snapshots for a) Pos1 b) Pos2

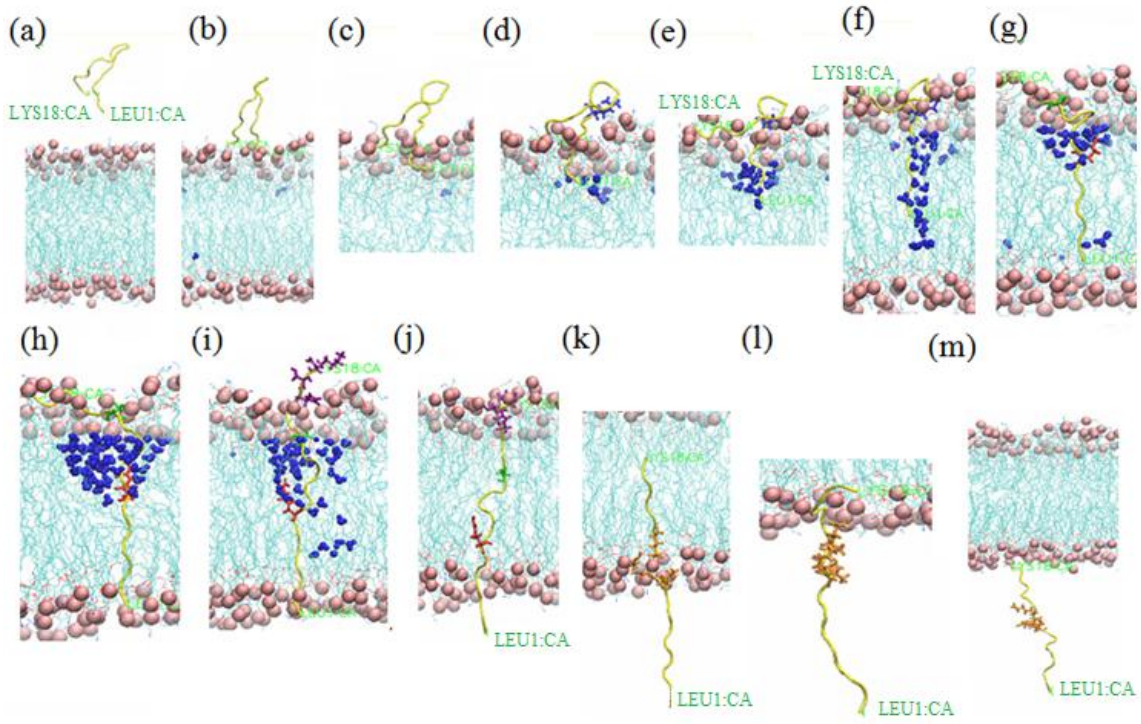

Figure 4.38. Snapshots of pVEC POPE SMD simulation Pos1. Z is the distance between center of mass of lipids and center of mass of Leu1. (a) z=33.61 Å (b) z=19.50 Å (c) z=13.73 Å (d) z=10.22 Å, Arg7-Arg8-Ile9-Arg10-Lys11-Gln12-Ala13 (blue) (e) z=3.82 Å (f) z=-4.22 Å (g)z=-15.49 Å, Arg7 (red) (h) z=-20.36 Å (i) z=-24.80 Å, His16-Ser17-Lys18, (purple), Arg7 (red) (j) z=-32.59 Å, Ala13 (green) (k) z=-52.11 Å, Ile9-Arg10-Lys11 (orange sticks) (l) z=-60.58 Å (m) z=-69.58 Å.

The values were really close to each other; however, the states of the peptides in the membranes were different. The trend of water intake was similar in both simulations except for the region z -35 Å to -55 Å. In Pos1, around z -40 Å the number of water molecules decreased while it increased at Pos2. In both simulations the peptides were halfway through the lower P heads of the membrane. The profiles showed that the membrane thickness was highest while the peptide traveled from the center of the bilayer towards the lower P layer. The membrane thickness decreased the most as the peptide was leaving the membrane. This was also when most water molecules entered the bilayer. However in the end of the simulations water left both membranes.In the visual analyses of pVEC simulations with the POPE membrane, from snapshots in Figure 4.38 and Figure 4.39, the peptide was positioned in a vertical state as the peptide entered the membrane. Leu1 contacted the

upper P heads while the Lys18 was in contact with the membrane in one of the simulations. Water penetration initiated as Leu5-Arg6 entered the membrane. It was proposed that the initial contact of Arginine might promote water intake into the lipid bilayer [23]. This phenomenon was observed visually in the simulations.

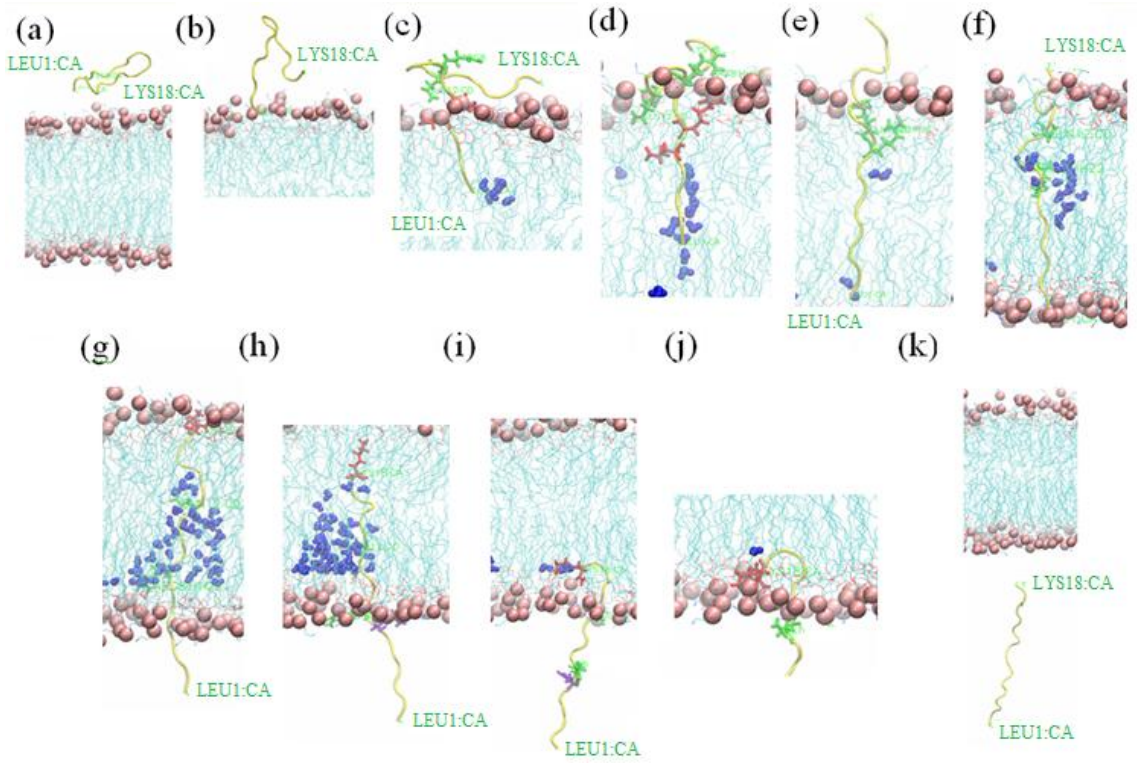

Figure 4.39. Snapshots of pVEC POPE SMD simulation Pos2.Z is the distance between center of mass of lipids and center of mass of Leu1. (a) z=30.91 Å (b) z=20.02 Å (c) z=5.42 Å, Leu5-Arg6 (red sticks), Arg8-Ile9-Arg10-Lys11-Gln12(green) (d) z= -3.89 Å (e) z=-13.39 Å (f) z=-23.09 Å (g)z=-32.84 Å, Lys18 (red) (h)z=-44.08 Å, Arg 7 (violet) (i) z= -54.48 Å (j) z= -61.93 Å, Gln12 (green), Lys18 (red) (k)z =-80.20 Å

As the simulations continue both ends of the peptide entered the membrane while the hairpin structure stayed embedded in the membrane. While the hairpin acted as an anchor. Arg7 pulled more water molecules into the membrane. The hairpin structure unwinds as Leu1 was pulled in the –z direction. In the trans-membrane state, Lys18 acted as an anchor. The interaction energy of Lys18 was high at this position. Residues Arg7 and Gln12, whose electrostatic energies were high, anchored the peptide to the lower P layer. As

residues His16-Ser17-Lys18 reached the lower P heads water molecules started to leave the membrane. Gln12 and Lys18 formed a U-shape on the lower P head layer, while the peptide attached to the lower P layer in both sides. At the end of the simulation the peptide and the water molecules left the membrane.

4.3.2. pVEC Transport across the POPC Membrane Examined by SMD Simulations

In the POPC membrane simulations, pVEC assumes a parallel position with respect to the membrane as Leu1 started to enter the membrane. The snapshots can be observed from Figure 4.40 and Figure 4.41.

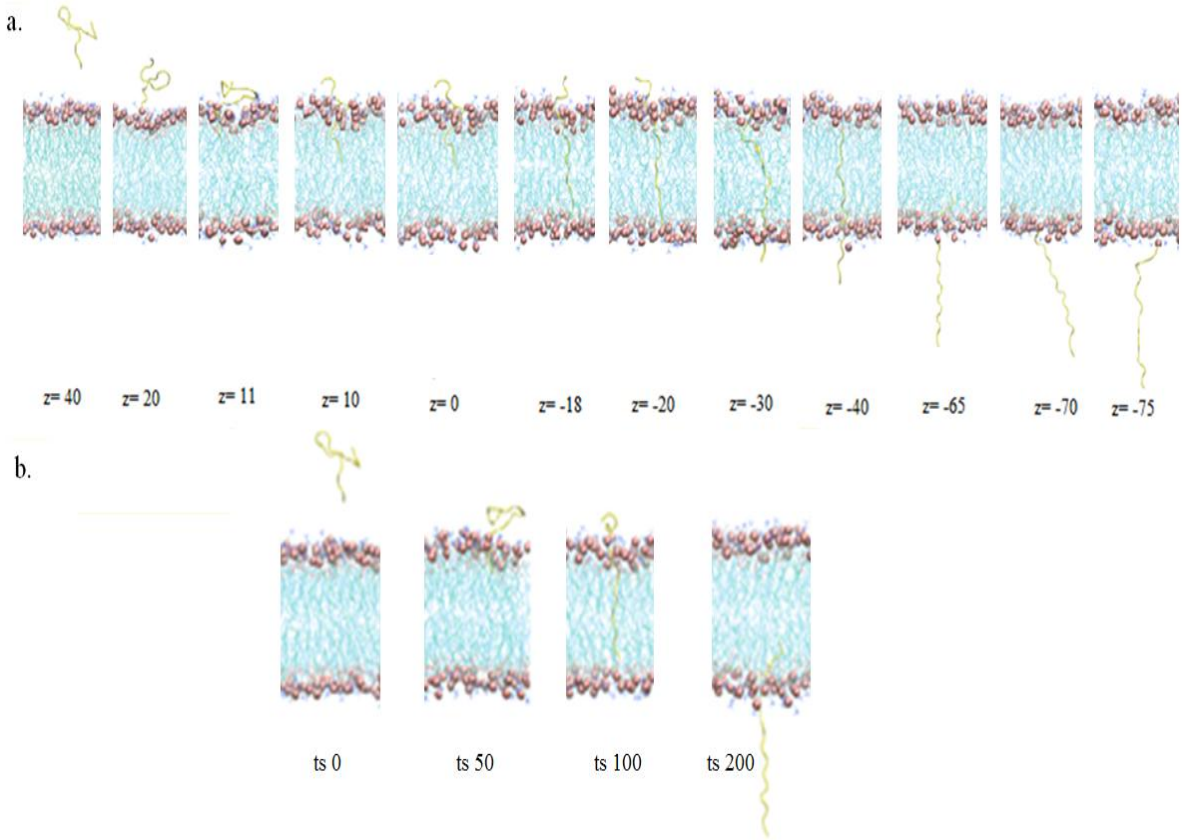

Figure 4.40. The figures show snapshots acquired from the first pVEC POPC SMD simulation. (a) Snapshots at different z values (the distance between Leu1 and the center of the SMD system, units: Å (b) Snapshots captured with time steps.

a.

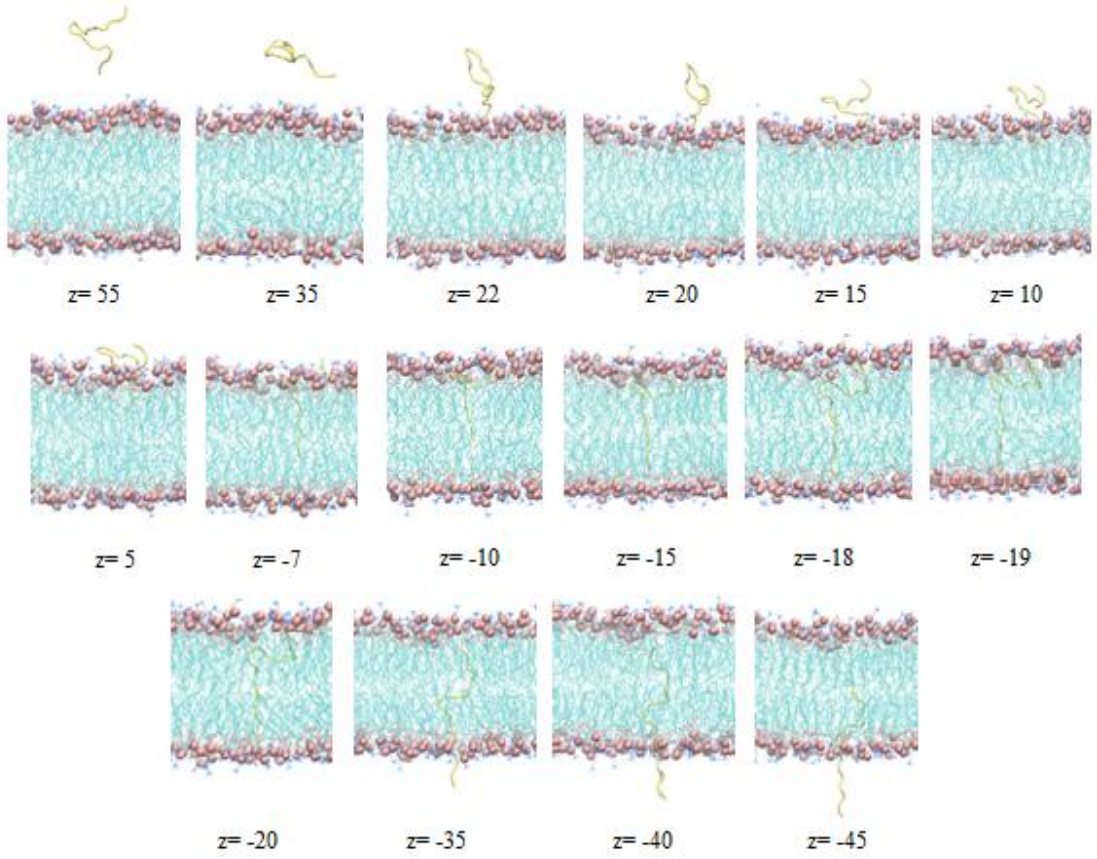

b.

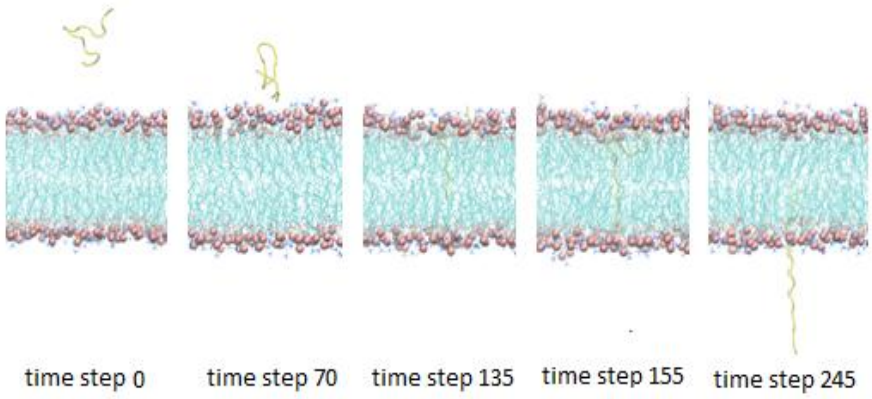

Figure 4.41. Snapshots acquired from the second pVEC POPC SMD simulation. (a) Snapshots at different z values (the distance between Leu1 and the center of the SMD system, units: Å (b) Snapshots captured with time steps.

For pVEC in POPC in both positions, (Figure 4.42), the energy behaved in a similar fashion. A difference is that in Pos1 the energy between z -20 Å and -40 Å was higher than Pos2. The energy increased as Leu1 moved towards the lower P heads to about -800kcal/mol. The energy decreased to about -200kcal/mol as the peptide started moving out of the membrane.

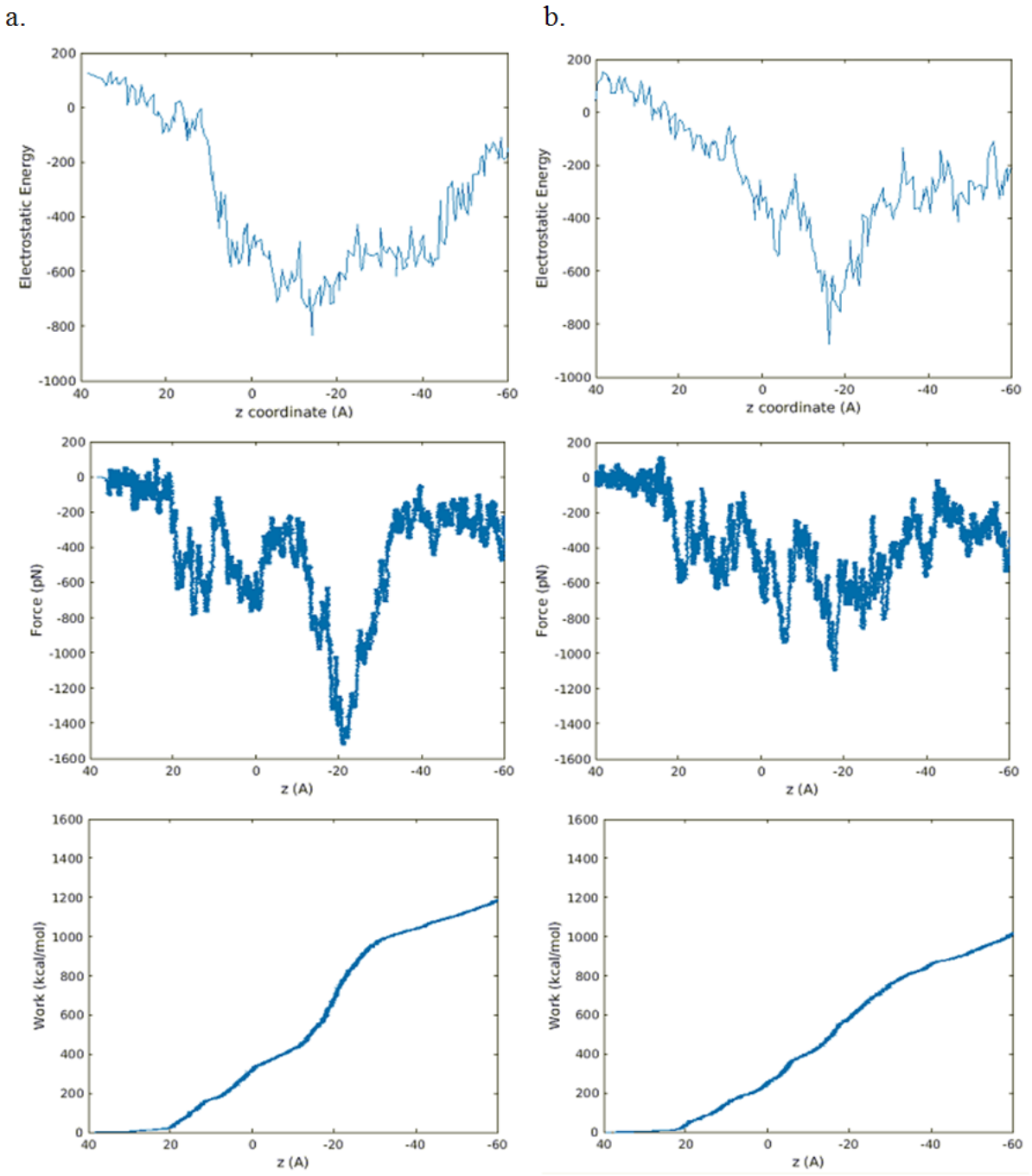

Figure 4.42. pVEC POPC SMD simulation: electrostatic energy vs. z, force vs. z & work vs. z profiles of Leu1 of a) Pos1 b) Pos2

The force applied in Pos1 at z -20 Å was higher than Pos2, which was -1400pN and -1000pN respectively.. The trends in forces were similar. The rate of work in Pos1 changed very frequently while in Pos2 the rate of work was steadier.

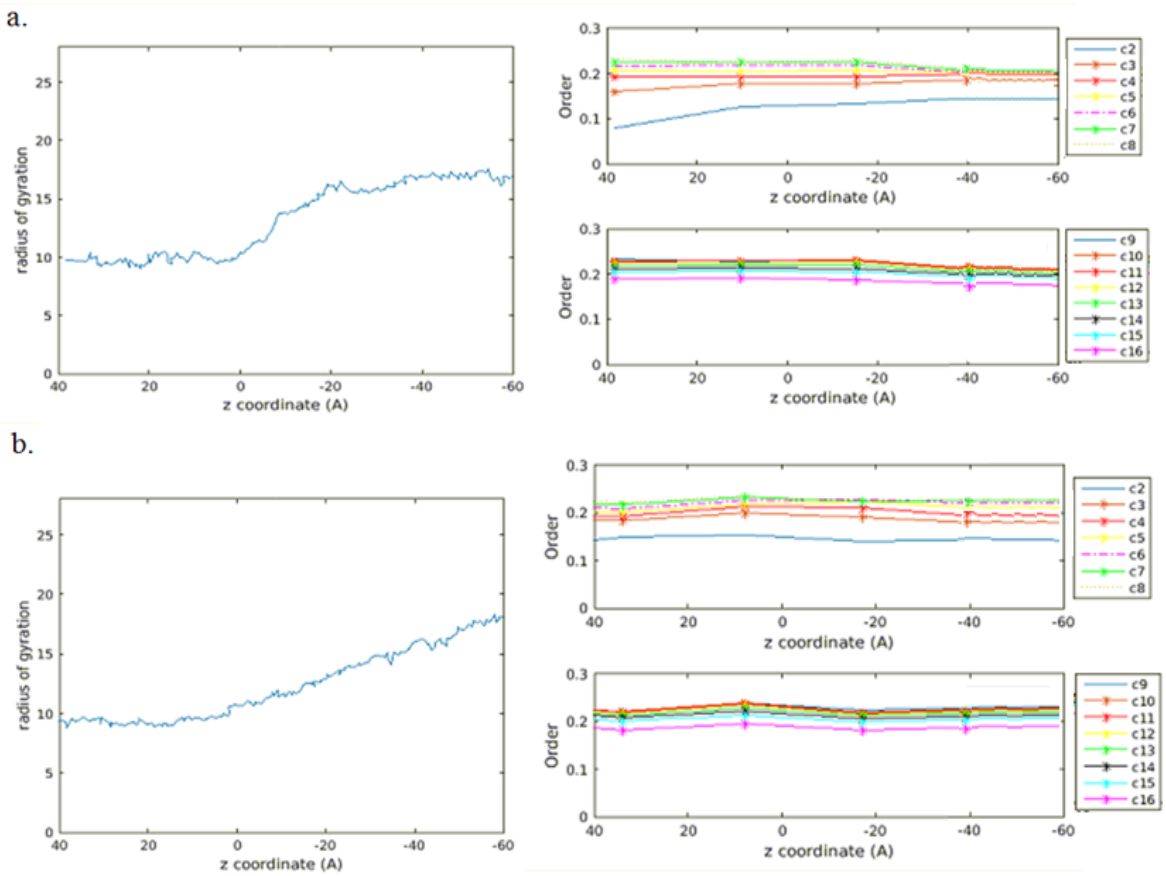

Figure 4.43. pVEC POPC SMD simulation: radius of gyration vs. z & lipid order vs. z profiles of Leu1 of a) Pos1 b) Pos2

The radius of gyration graphs (Figure 4.43), are very different. The most difference was observed between z 0 Å and -20 Å. The radius of gyration increased very steeply for Pos1, meaning that the peptide was packed more loosely; however, for Pos2 the radius of gyration change was low in this range. For carbons 2-8 in Pos1 the lipid order was disturbed as the simulation continued while in Pos2 the lipid order stayed somewhat constant. For the other carbons the orders parameters stayed somewhat constant during the simulations. However in Pos2 there was a disturbance around z 8 Å. The peptide was

moving towards the center of the bilayer. Also at this point the number of water molecules inside the bilayer increased which might also have caused the sudden disorder in lipids.

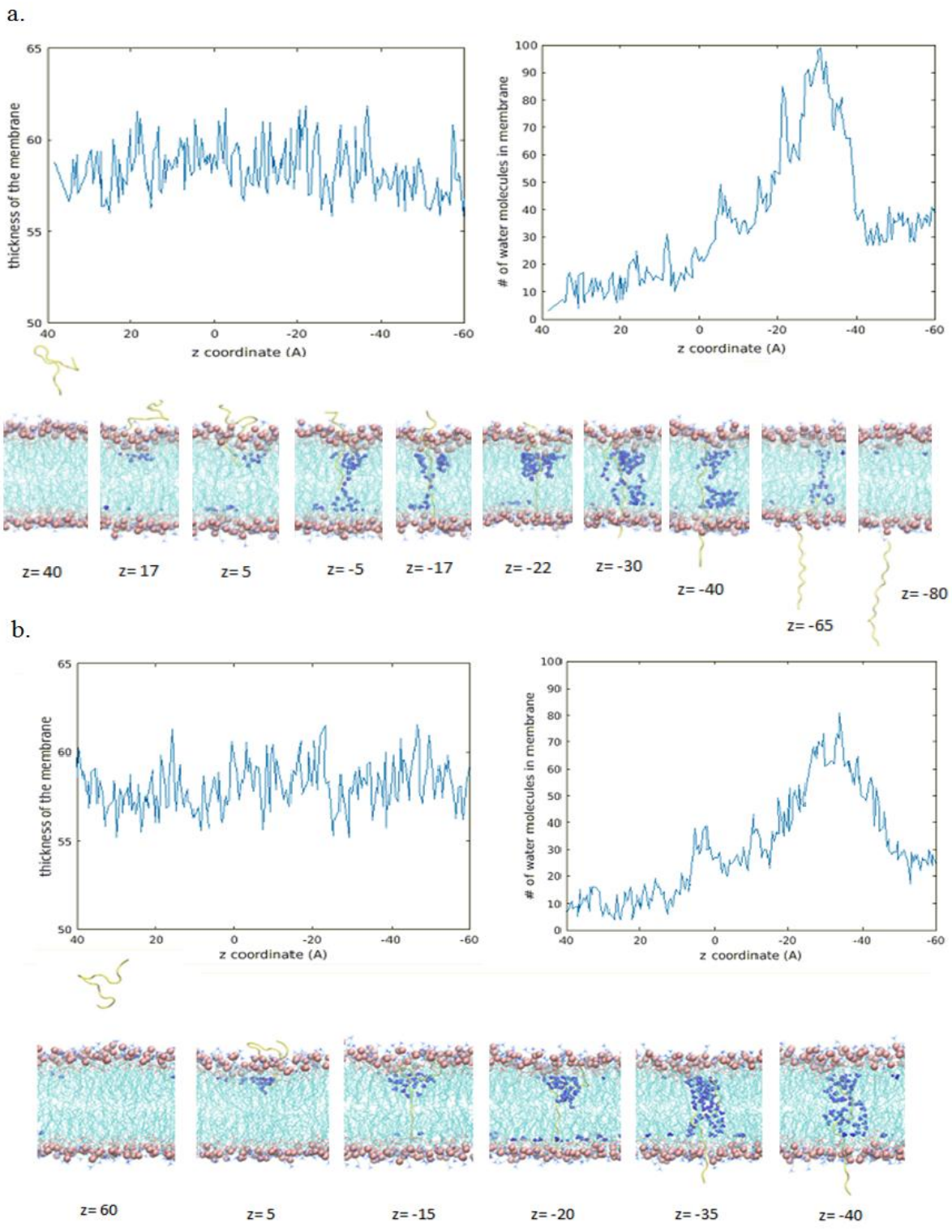

Figure 4.44. pVEC POPC SMD simulation thickness of membrane vs. z, water in membrane vs. z profiles of Leu1 and snapshots for a) Pos1 b) Pos2

The thickness of membrane vs. z graphs in Figure 4.44 showed that the thinnest values of the membrane for both simulations were close with values of 55.5 Å and 54.5 Å for Pos1 and Pos2 respectively. However these values were achieved at different z positions, z -60 Å and z -30 Å respectively. These values were achieved outside the membrane after the peptide left the membrane for Pos1 and while the peptide was in a trans-membrane state in Pos2. The thickest values of the membranes were 62 Å and 61.5 Å for Pos1 and Pos2 respectively. These values were achieved at close positions; at z-37 Å and -22 Å for Pos1 and z -45 Å and z -22 Å for Pos2. At these points the peptide was positioned inside the membrane. From the water in membrane vs. z graphs the most water molecules entered at range z -20 Å to -40 Å for both simulations. Therefore it can be said that the while the peptide was in a trans-membrane position the number of water molecules inside the bilayer increased and simultaneously the membrane thickness values also increased. The difference was that for Pos2 there was an increase in water molecules observed between z 40 Å to z 60 Å as the peptide moved out of the membrane through the bottom P layer.

Lastly, the visual analyses of the pVEC in POPC membrane, in Figure 4.45 and Figure 4.46 showed that the peptide was in a vertical position. With Lys18 positioned away from the membrane when the peptide started to penetrate the membrane. Water permeation started as Ile4 started to enter the membrane. Residue energy analysis confirmed the role of Ile4 as its energy increases at this point. Residues 8-12 form the hairpin structure. These residues anchored the peptide on the upper P layer. Also residues Arg6-Arg7 anchored the peptide and had exceptionally high electrostatic energies around -200 kcal/mol at that position. Water was carried inside the membrane with Leu1, Ile4, Arg6, and Arg7. His14-Ala15-His16-Ser17 moved as a block and caused water molecules to enter the membrane. The hair-pin structure unwinded in the trans-membrane state. Lys18 anchored on the top P head layer. While the peptide exited the membrane Arg10 and Gln12 interacted with the lower P layer for a long time and were observed to have elevated electrostatic energies of -200 kcal/mol and -50 kcal/mol respectively in the residue energy analysis. The peptide and water molecules left the membrane at the end of the simulation. In the residue analysis for pVEC in POPE and POPC membrane the residues with the most interaction with the membranes were Leu1, Arg6, Arg7, Arg8, Arg10, Lys11 and Lys18. Residues Leu2,

Gln12, His14, His16, and Ser17 also had interactions with the membrane. This can be seen in Figure 4.47. When the electrostatic energies were compared for pVEC in terms of POPE vs. POPC, the electrostatic energies were slightly higher in POPC. Most differences were in residues Leu1 and Lys18, with -125 and -150 kcal/mol difference in maximum electrostatic energy with the lipids.

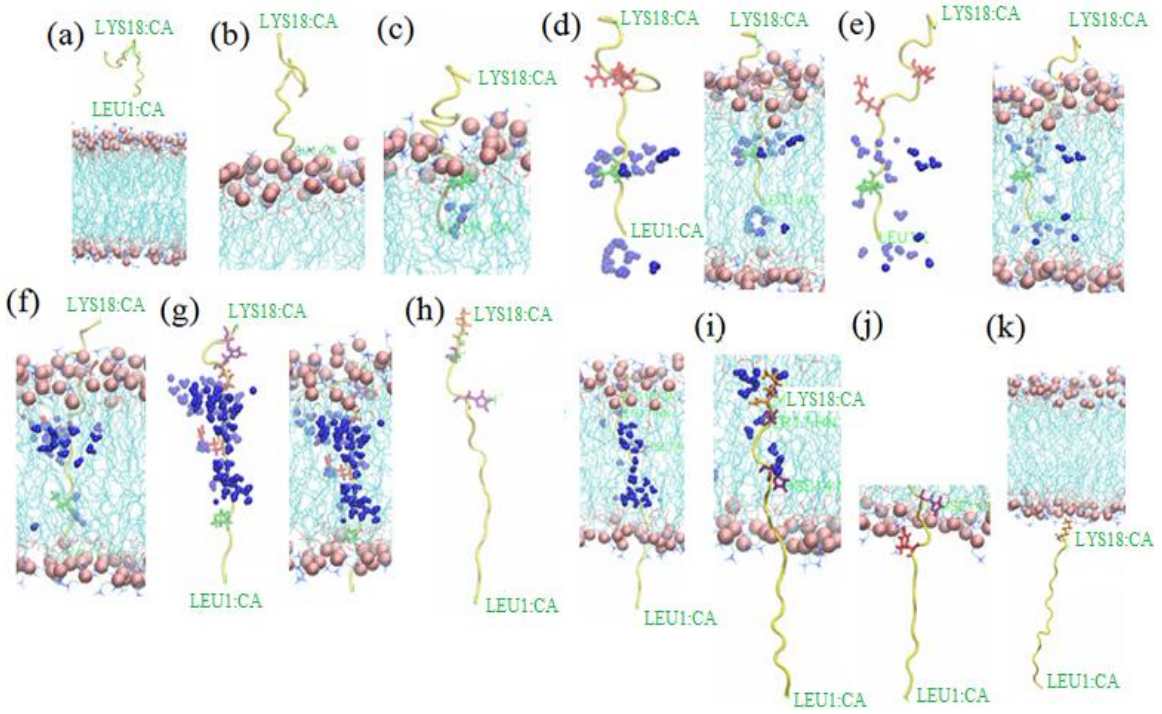

Figure 4.45. Snapshots of pVEC POPC SMD simulation Pos1. Z is the distance between center of mass of lipids and center of mass of Leu1. (a) z=36.80 Å (b) z=24.28 Å (c) z=4.84 Å, Ile4 (green) (d) z= -5.98 Å, Arg8,Gly12 (red) and Ile4 (green). (e) z=-9.33 Å (f) z=-19.39 Å (g)z= -28.66 Å, His14, Ser17 (purple). (h) z= -39.65 Å, Lys18 (orange) (i) z= -49.18 Å (j) z=-58.89 Å, Arg10 (red) (k) z=-79.19 Å, Lys18 (orange).

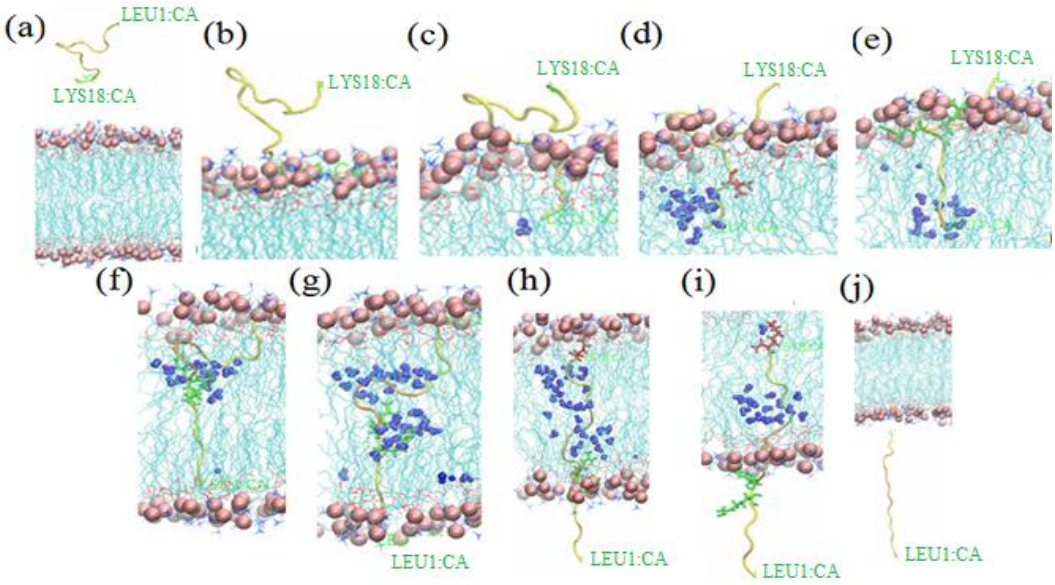

Figure 4.46. Snapshots of pVEC POPC SMD simulation Pos2. Z is the distance between center of mass of lipids and center of mass of Leu1. (a) z=61.80 Å (b) z=21.84 Å (c) z=9.33 Å, Ile4 (red) (d) z=2.12 Å (e) z=-2.32 Å, Arg6-Arg7 (green) (f) z= -16.3 Å, Arg8-Ile9-Arg10-Lys11-Gln12-Ala13 (orange) (g)z=-24.85 Å (h) z= -39.72 Å (i) z=-47.15 Å (j) z=81.5 Å.

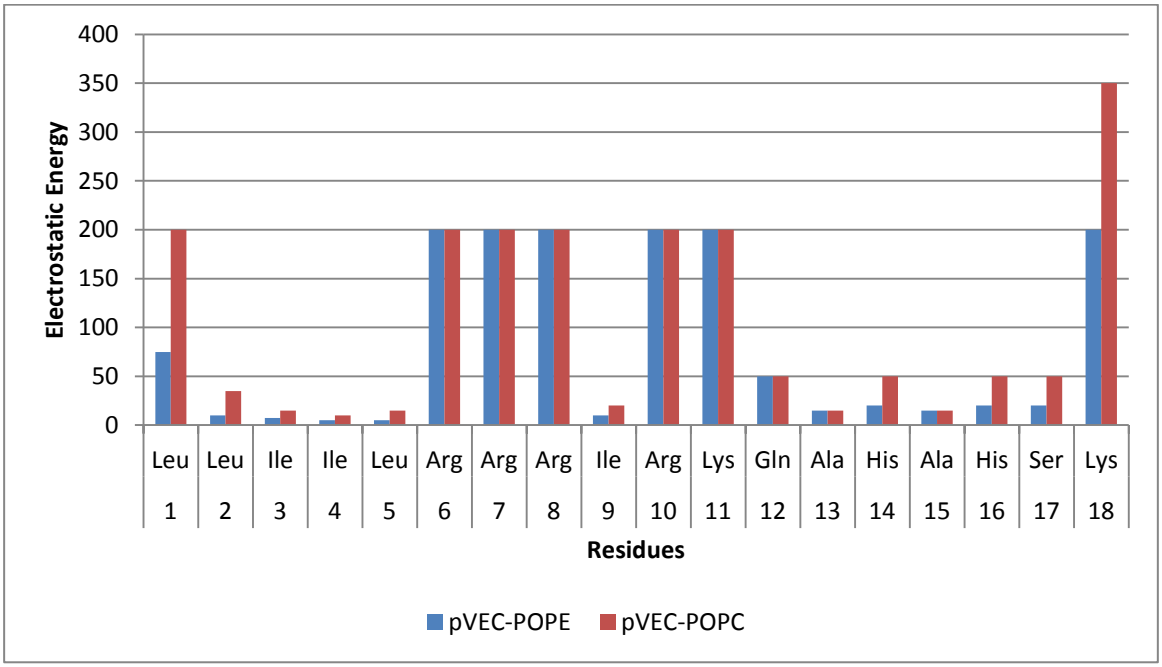

Figure 4.47. The average of maximum electrostatic electrostatic energies of pVEC residues in POPE and POPC membrane SMD simulations.

The N-terminus of the pVEC peptide played an important role in the penetration of cellular membranes, such when the first five residues Leu1-Leu2-Ile3-Ile4-Leu5 were replaced by L-alanine and the peptide did not enter the membrane [23]. The high energy of Leu1 was therefore anticipated. As stronger interactions cause energy barriers they may also propel the peptide forward in the SMD simulations [23]. Residues Leu2, Gln12, His14, His16, and Ser17 had elevated energies. The Leu and Ile residues are suggested to have contributions to the penetration of the N-terminus of the peptide because of their highly hydrophobic nature [23]. Leu1 had high energy while Leu2, Leu5 and the Ile residues showed low interactions with the lipids. Low interactions may mean that the residues show no resistance towards moving through the membrane. When the electrostatic energies are compared for pVEC in terms of POPE vs. POPC, the electrostatic energies are slightly higher in POPC. This is asked for, since higher energy means more resistance and the designed drug delivering peptides are desired to affect the bacterial membranes (represented by POPE) while having no effect on the mammalian membranes (represented by POPC) [34]. Most differences in energy were seen in residues Leu1 and Lys18 which are higher in the POPC membrane with -150 kcal/mol difference in maximum electrostatic energy.

4.4. Peptide Trajectory in Membranes Examined by MD Simulation

4.4.1. Melittin Trajectory in Membranes Examined by MD Simulation

Melittin POPE top MD simulations snapshots in Figure 4.48 showed that as the MD simulation continued, the peptide assumed a parallel position at the top of the membrane. Gly1-Ile2-Gly 3-Ala4 played an important part in the repositioning of the peptide. In Figure 4.51, the energy started to increase halfway through (after the peptide tilted to a more parallel position with the membrane) while in the second position the interactions with the lipids was constant. In both simulations the average energy was about -300 kcal/mol. The helicity and distance analysis for the POPE melittin simulations revealed that for the top positions the overall the helicity percentage was higher when the peptide was in a vertical position above the upper P heads. (≈86 % vs. 90 %).

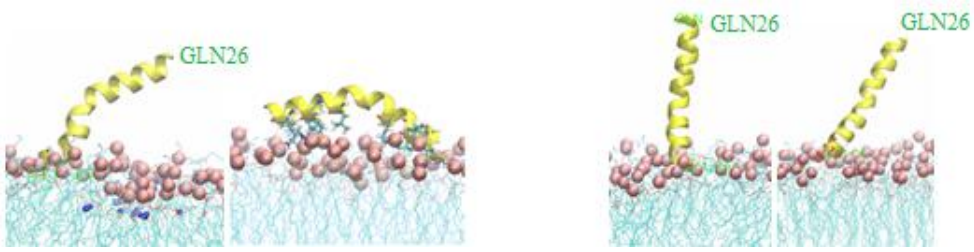

Figure 4.48. Melittin POPE MD top position: initial and final snapshots.

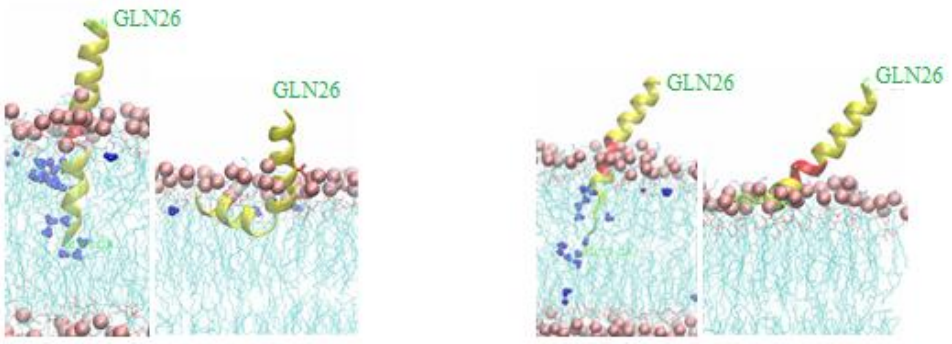

Figure 4.49. Melittin POPE MD middle position: initial and final snapshots.

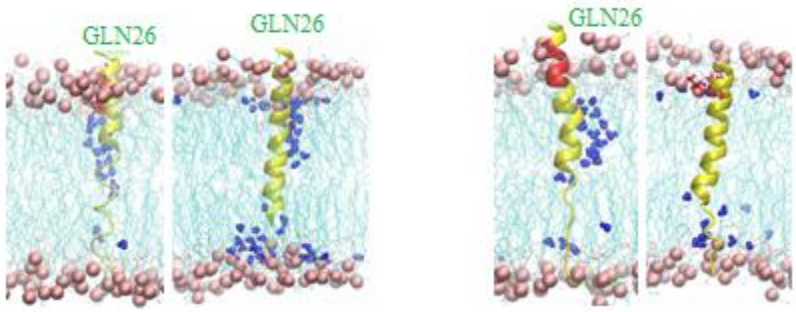

Figure 4.50. Melittin POPE MD bottom position: initial and final snapshots.

In the melittin POPE middle simulations the peptide entered the membrane. Figure 4.49 shows the initial and final snapshots of the simulations. Gly1-Ile2-Gly 3-Ala4-Val5-Leu6-Lys7-Val8-Leu9-Thr10 had an important role in peptide insertion into the membrane.

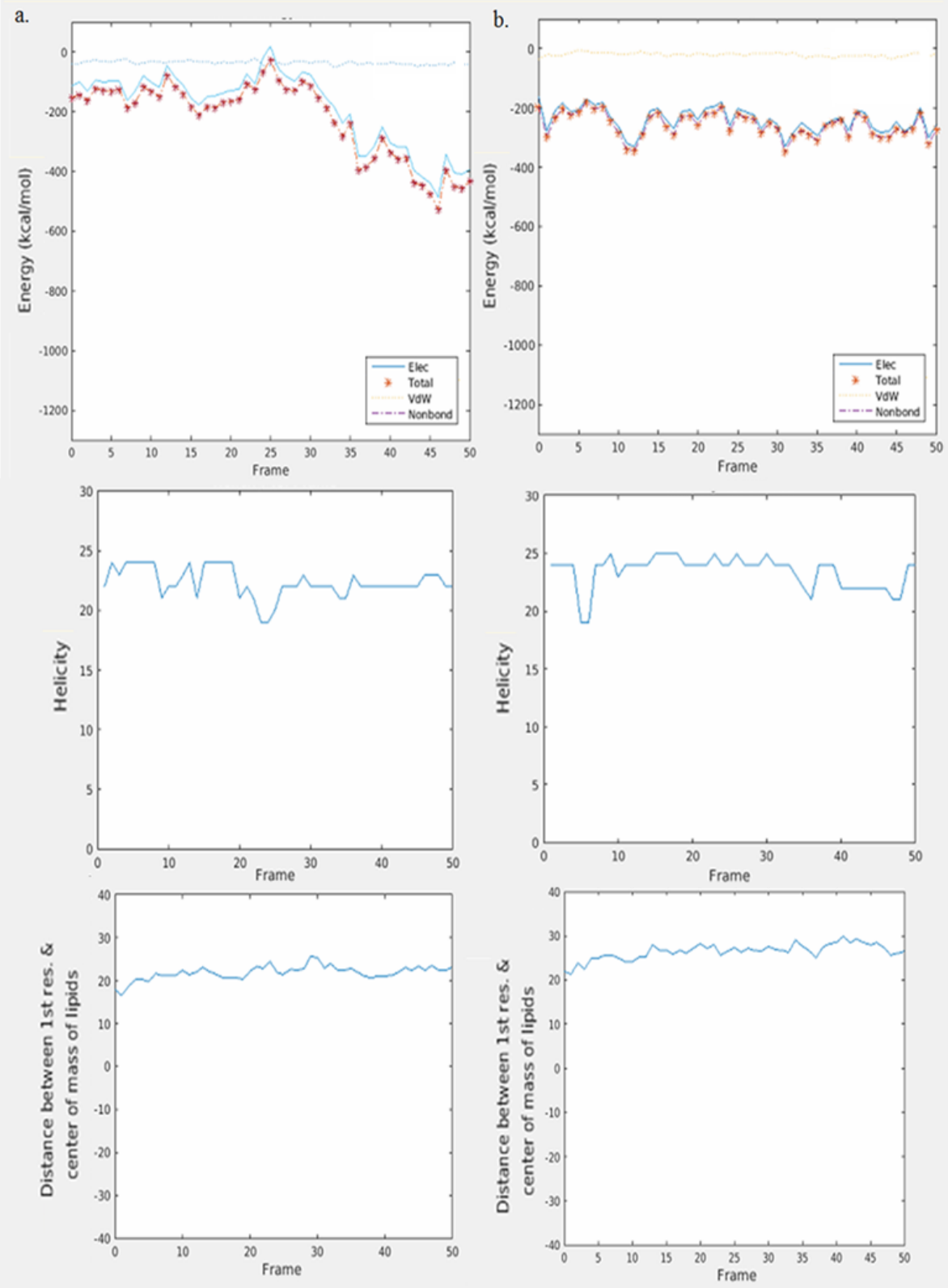

Figure 4.51. Melittin POPE MD top position: energy plot, helicity plot and distance* plot for Pos1 & Pos2. * Distance between the 1st residue and the center of mass of lipids.

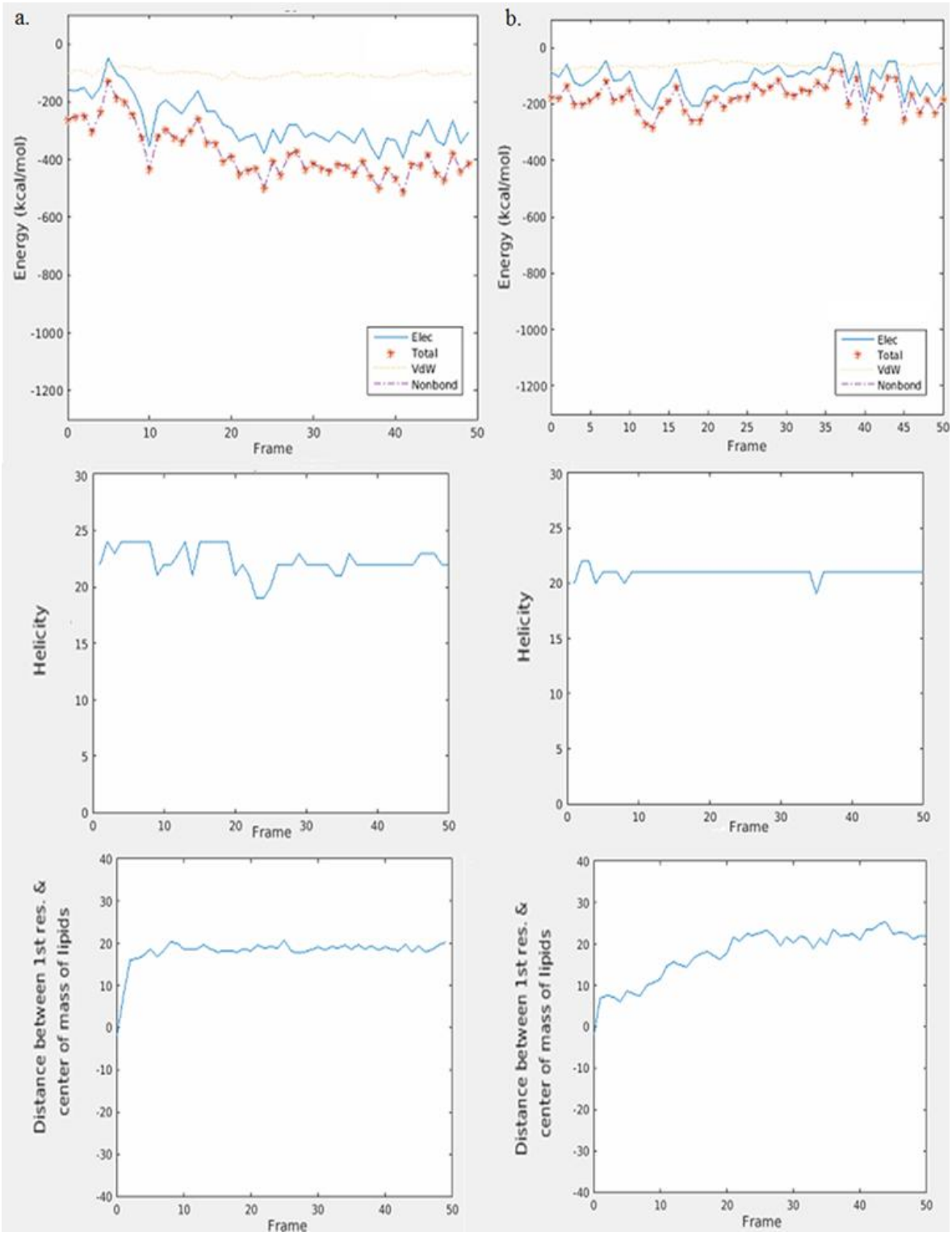

Figure 4.52. Melittin POPE MD middle position: energy plot, helicity plot and distance* plot for Pos1 & Pos2. * Distance between the 1st residue and the center of mass of lipids.

In Figure 4.52, in the first position, the peptide started at -160 kcal/mol interactions, however, interactions increased and became constant at around -400 kcal/mol. The peptide moved inside the membrane in the visual analysis and the increased energy did not contradict this. In the second position the interaction with lipids started at -80 kcal/mol then increased to -225 kcal/mol then droped to a value of zero. The peptide moved out of the membrane however Gly1-Ile2-Gly 3-Ala4-Val5-Leu6-Lys 7-Val8-Leu9-Thr10 anchored the peptide. After this point the interaction of the peptide with lipids increased again, however, it was not a significant increase as the final value of electrostatic energy was -125 kcal/mol. The overall helicity was higher in Pos 1 (≈86 % vs. 80 %). At Pos1 simulation Gly1 spent more time anchored between the upper P layer while the peptide in Pos2 left the membrane through the top.

In melittin POPE bottom MD simulations, the peptide took a trans-membrane position by moving further into the membrane. Figure 4.50 shows the initial and final snapshots of the simulations. If the interaction of Gly1 with the lower P heads was not enough the peptide may move out of the membrane through the top. If the interaction is strong enough the peptide moves inside the membrane.

Both MD simulations, started with a high initial energy around -350 to -425 kcal/mol, which can be seen in Figure 4.53. The interaction increased as the simulation continued and reached a maximum of about -800 kcal/mol. When compared with the top and middle simulations the bottom simulation has the highest interactions between the peptide and the lipids. This was understandable as the peptide was in a trans-membrane state and most of the residues are in contact with the membrane. At the end of the second simulation the value started to drop and from the visual and helicity analysis the helicity of the peptide increased around the end. Meaning that as the structure folds once more, the residues have less contact with lipids thus interaction energy between the peptide and the lipids decreased. The peptide prefered to stay inside the membrane in a helical structure. For the second position, the helicity percentage became lower as Gly1 was embedded in the lower P layer. (≈91 % vs. 72 %).

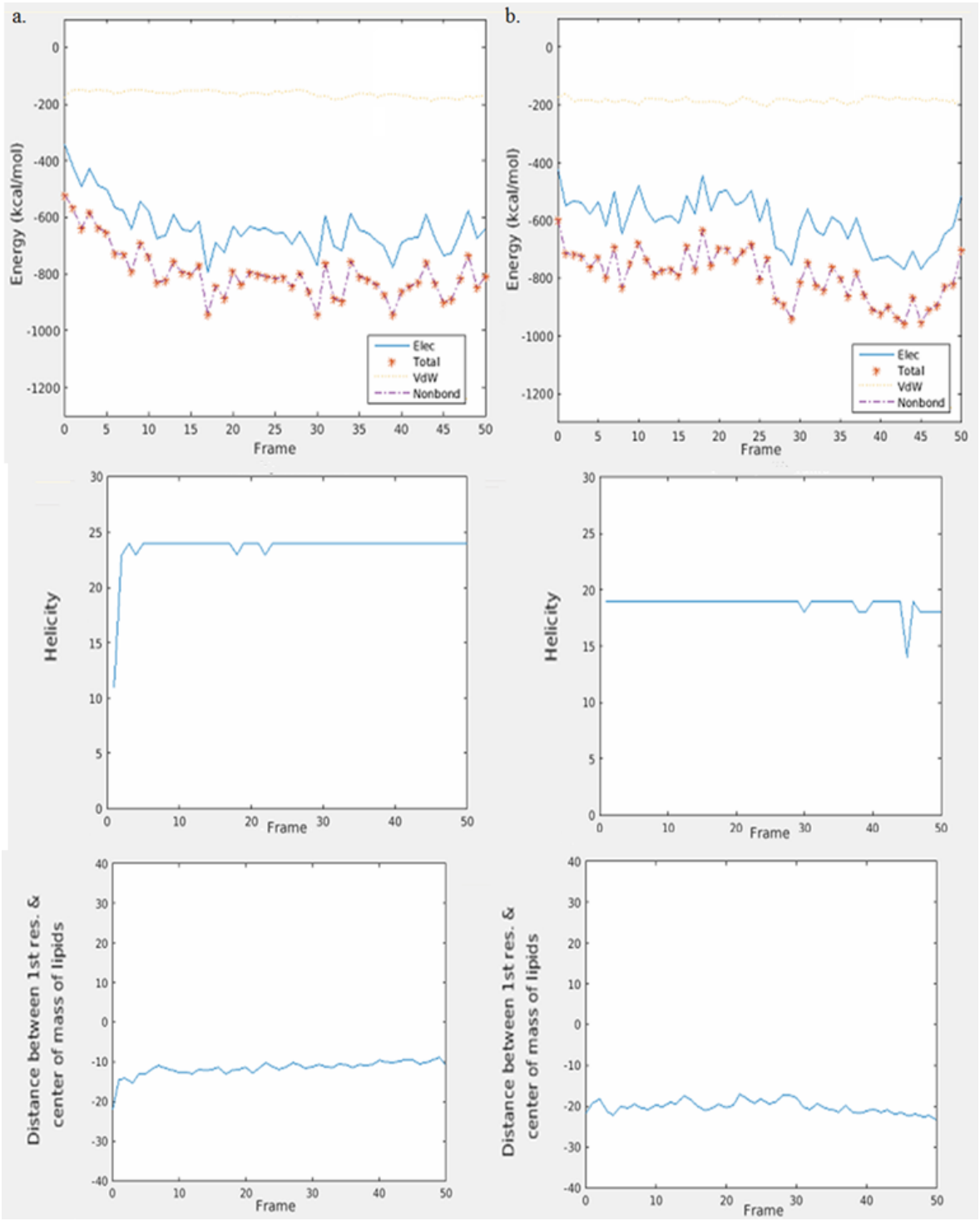

Figure 4.53. Melittin POPE MD bottom position: energy plot, helicity plot and distance* plot for Pos1 & Pos2. * Distance between the 1st residue and the center of mass of lipids.

In Figure 4.54, Melittin POPC MD top simulations results showed that the peptide stayed on top of the membrane and may possibly enter the membrane as the simulation continues. Leu16, Trp19, Ile20 and Lys23 played an important role in the attraction of the peptide towards the membrane. The initial positioning of these residues was also extremely important. When these residues do not face the membrane at a certain angle, the attraction of the peptide and the membrane did not occur.

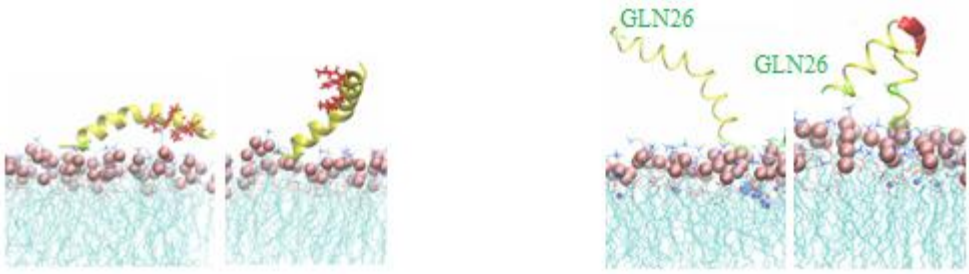

Figure 4.54. Melittin POPC MD top position: initial and final snapshots.

In Figure 4.55 electrostatic energies started at -225 and -75 kcal/mol in Pos1 and Pos2 respectively. In Pos1, many fluctuations were observed in the interactions between the protein and the lipids. In the visual analysis the peptide moved out of the membrane. The interaction of the helical peptide with the P layer of the membrane caused fluctations since each residue had different interactions with the P head layer. At frame 35 the energy reached a maximum of -280 kcal/mol. In the second position the energy droped to a value of zero at frame 5.

The interaction increased after this point and although the energy fluctuated throughout the simulation at the end highest interaction of -330 kcal/mol was achieved. From the visual analysis the peptide changed position from a vertical state with respect to the membrane to a position in which both ends of the peptide interacted with the upper P head layer. This explains the increased electrostatic energies at the final frame of the simulation. The electrostatic energy for both simulations were in the range 0 to -300 kcal/mol. The helicity analysis showed that for top positions the distance stayed at a constant range. Helicity was also in the same range. The overall helicity values were close. (≈87.7% vs. ≈ 92%).

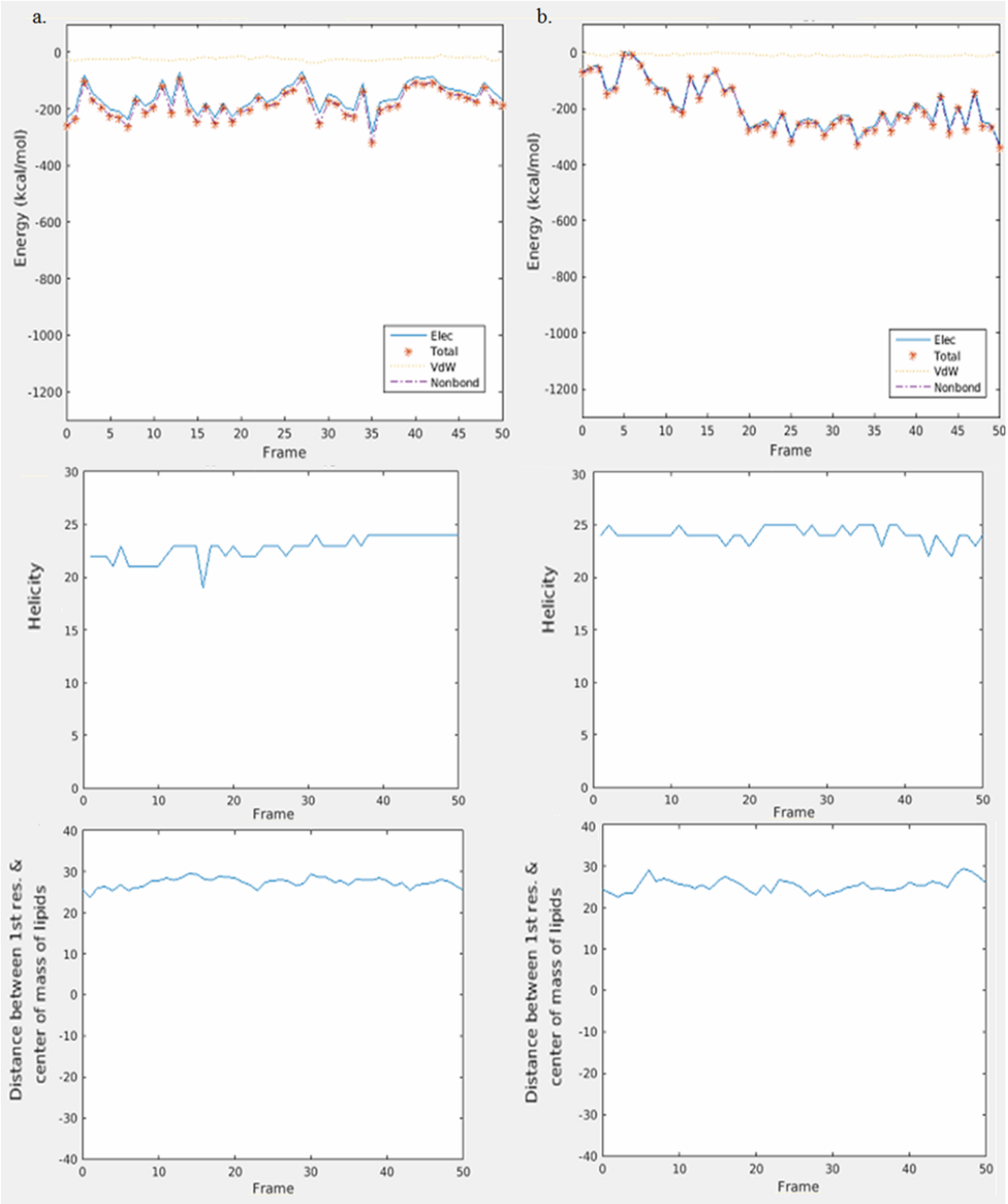

Figure 4.55. Melittin POPC MD top position: energy plot, helicity plot and distance* plot for Pos1 & Pos2. * Distance between the 1st residue and the center of mass of lipids.

The peptide started to leave the membrane from the top in melittin POPC middle MD simulations. Figure 4.56 shows the initial and final snapshots of the simulations. Gly1 had

high interaction with the upper P heads. However that might not be enough to hold the peptide inside the POPC membrane.

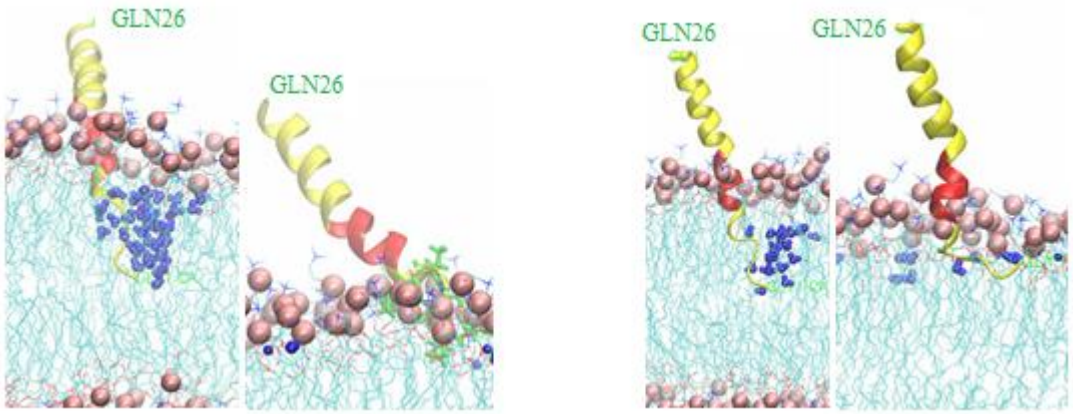

Figure 4.56. Melittin POPC MD middle position: initial and final snapshots.

Figure 4.57 shows the energy plot, helicity plot and distance plot for melittin POPC MD middle position simulations. The interaction between the peptide and the lipids was high at the start of about -300 kcal/mol, however, the interactions dropped and continued at a lower rate until the end of the simulation. The visual analysis showed that the peptide moved out of the membrane which explains the decreased interaction between the peptide and the lipids as the simulation continued. For this simulation the average energy was about -200 kcal/mol. In the second simulation the interaction increased. The electrostatic energy started at -300 and increased to a value of -480 by frame 15. In the visual analysis, the first residue moved inside the membrane and interacted with the upper P head layer. After this point the interaction with lipids dropped drasticly as the peptide moved out of the membrane. As the simulation continued the interactions with lipids started to increase again. And reached a maximum.Until this point the peptide was readjusting its position inside the upper P head layer and the interaction of different residues at different conformations with the lipids yielded an increase in interaction energy. When majority of the residues left the membrane a decrease was observed at the end of simulation. For this simulation the average energy was about -400 kcal/mol.

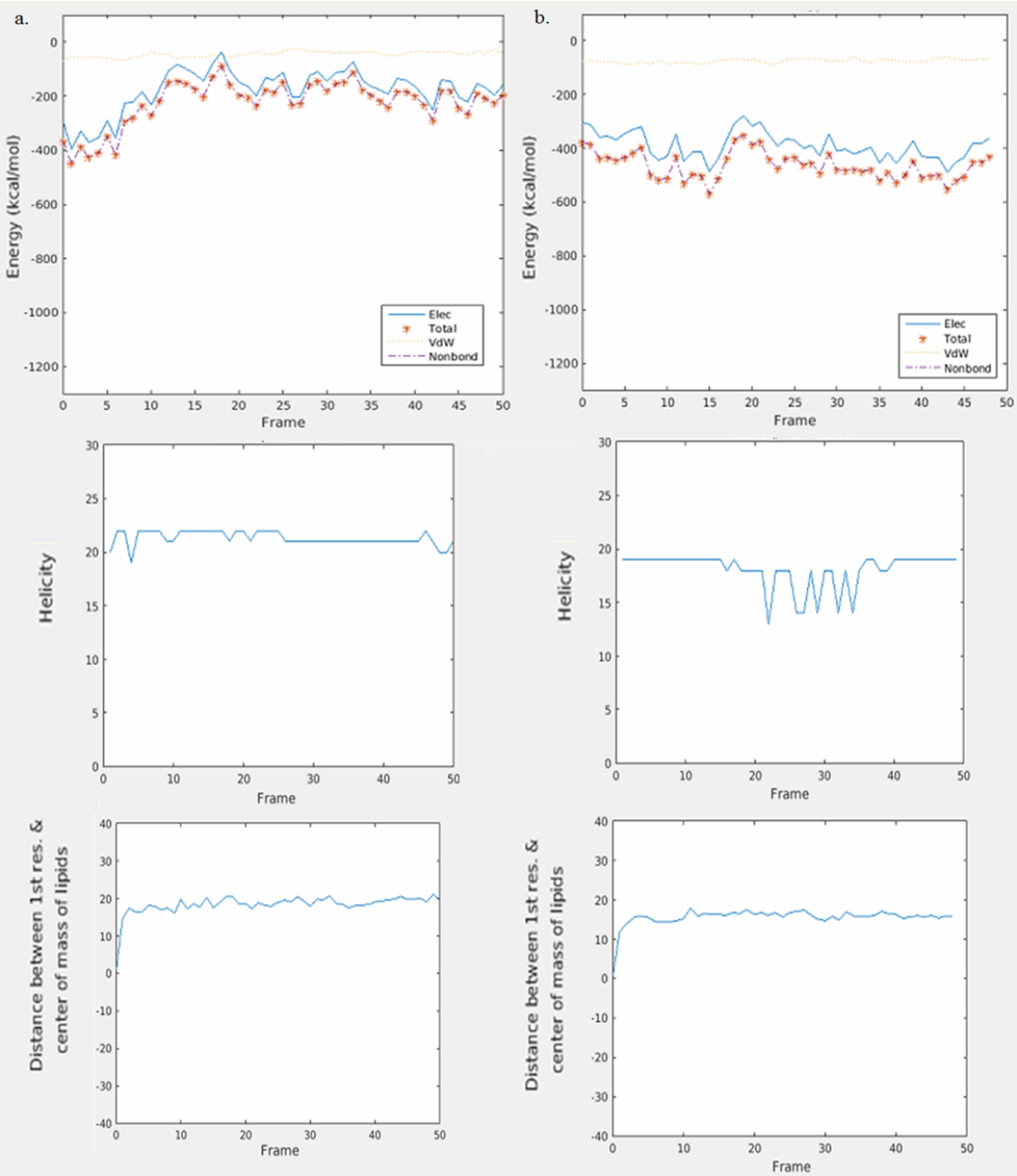

Figure 4.57. Melittin POPC MD middle position: energy plot, helicity plot and distance* plot for Pos1 & Pos2. * Distance between the 1st residue and the center of mass of lipids.

In the middle simulations for the first position, the distance increased immediately and the helicity increased but stayed at a constant range afterwards. The distance slowly declined which means that the peptide moved since helicity stayed constant. From VMD

visualizations the first few residues moved to the upper P heads but the overall structure of the peptide did not change. For the second position there was an immediate increase in the distance in the first few frames. Then, the distance stayed constant until the end. The helicity only changed when the peptide reoriented itself in the P heads and droped to 50%, and then assumeed its original helicity percentage. Helicity in Pos1 was higher than Pos2 (81% vs 69%). This showed that when the peptide was anchored inside the P layer the helicity dropped.

Melittin POPC MD bottom simulations showed that the peptide moved further inside the membrane. Figure 4.58 shows the initial and final snapshots of the simulations. Gly1 had high interactions with the lower P heads. Also high interaction of residues Lys7 and Thr11 with the upper P heads was observed. The membrane disrupted as the P heads were pulled towards the center of the lipid membrane by residues. While in the first simulation the peptide inserted itself further into the membrane, in the second simulation the peptide stayed in its original place, not going out or into the membrane.

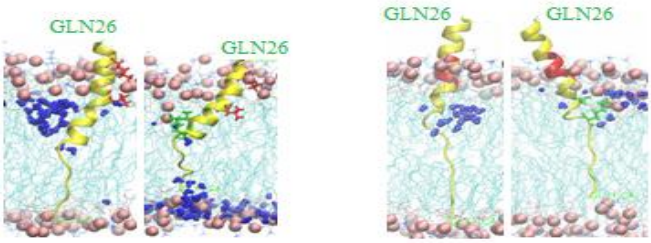

Figure 4.58. Melittin POPC MD bottom position: initial and final snapshots.

In Figure 4.59 the electrostatic energy started at -550. The energy increased to -800 in 5 time steps. Until time frame 44 the energy continued in a fluctuating manner in the energy range of -700 and -900. After frame 44 the energy increased further and at the end of the simulation the value of the electrostatic energy reached -1100. From the visual analysis the peptide stayed in a trans-membrane state throughout the simulation. Also residues Gly1, Lys7, Thr10 and Thr11 pulled the P heads of the phospholipid layers towards the middle of the membrane. Since the P heads were not fixed in the MD simulations the effect of the interactions were clearly observed. For this simulation the average energy was about -800 kcal/mol. For the second position, compared to the Pos1

simulation the peptide was initially placed with more residues outside of the membrane, therefore the lower energy observed was understandable.

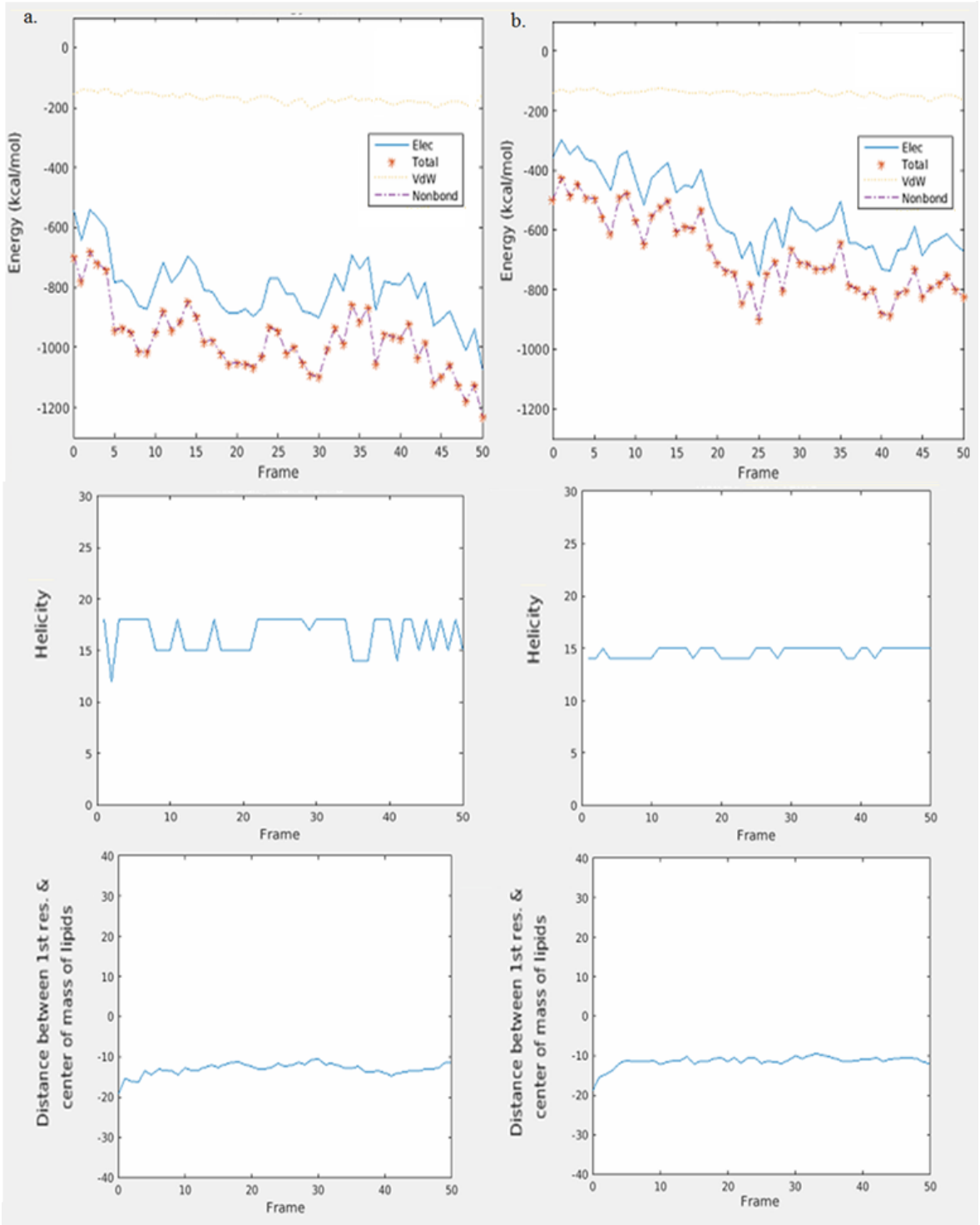

Figure 4.59. Melittin POPC MD bottom position: energy plot, helicity plot and distance* plot for Pos1 & Pos2. * Distance between the 1st residue and the center of mass of lipids.

For this simulation the average energy was about -600 kcal/mol.The interaction reached a maximum as Gly1 interacted with the lower P layer. Residues Lys7 and Thr11 anchored the peptide by interacting with the upper P layer. Overall, the interaction of the peptide was high compared to the top and middle simulation.In the first position Gly1 had interactions with the lower P layer as the peptide moved in the +z direction. This caused the peptide to stretch and loose its helical structure. Helicity increased when the peptide was in a trans-membrane state and the peptide was loosely present inside the lipid. Lys7 and Thr11 pulled the peptide towards the lower P layer and caused the peptide to lose its helicity. In the second position as Gly1 moved downward the helicity did not change. The overall helicity percentage of Pos1 was greater than Pos2 (≈64% vs. 56%).

4.4.2. pVEC Trajectory in Membranes Examined by MD Simulation

The pVEC POPE top MD simulations showed that the peptide continued to interact with the upper P layer as the simulation continued. Figure 4.60 shows the initial and final snapshots of the simulations. In position 1, at the initial frame the peptide was placed inside the membrane such that Leu1-Leu2-Ile 3-Ile4 are embedded inside the membrane and also Lys18 was in contact with the upper P head layer. The peptide started to leave the membrane. The peptide assumed a parallel position with respect to the membrane. Leu1-Leu2-Ile 3 and Ser17-Lys18 on the other end were embedded inside the membrane at the end of the simulation. This means that these regions had great electrostatic energies with the P-heads. In the second position, the peptide was positioned above the membrane such that Leu2-Ile3-Ile4 (shown in red sticks) was embedded in the P heads. Ile3-Ile4 started to leave the membrane. Leu1-Leu2 was located inside the upper P heads. At the end of the simulation, Leu1 and Leu2 were still in contact with the membrane. The tip of the peptide with Lys18 moved further away from the membrane.

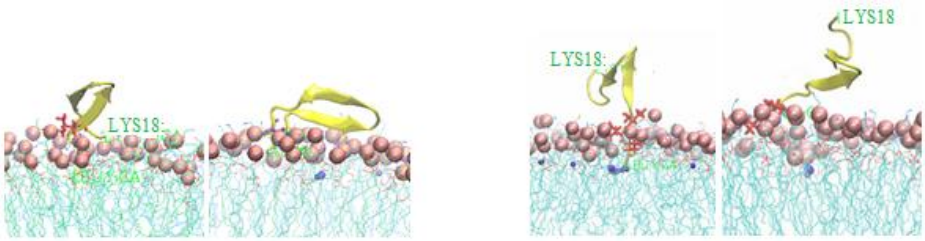

Figure 4.60. pVEC POPE MD top position: initial and final snapshots.

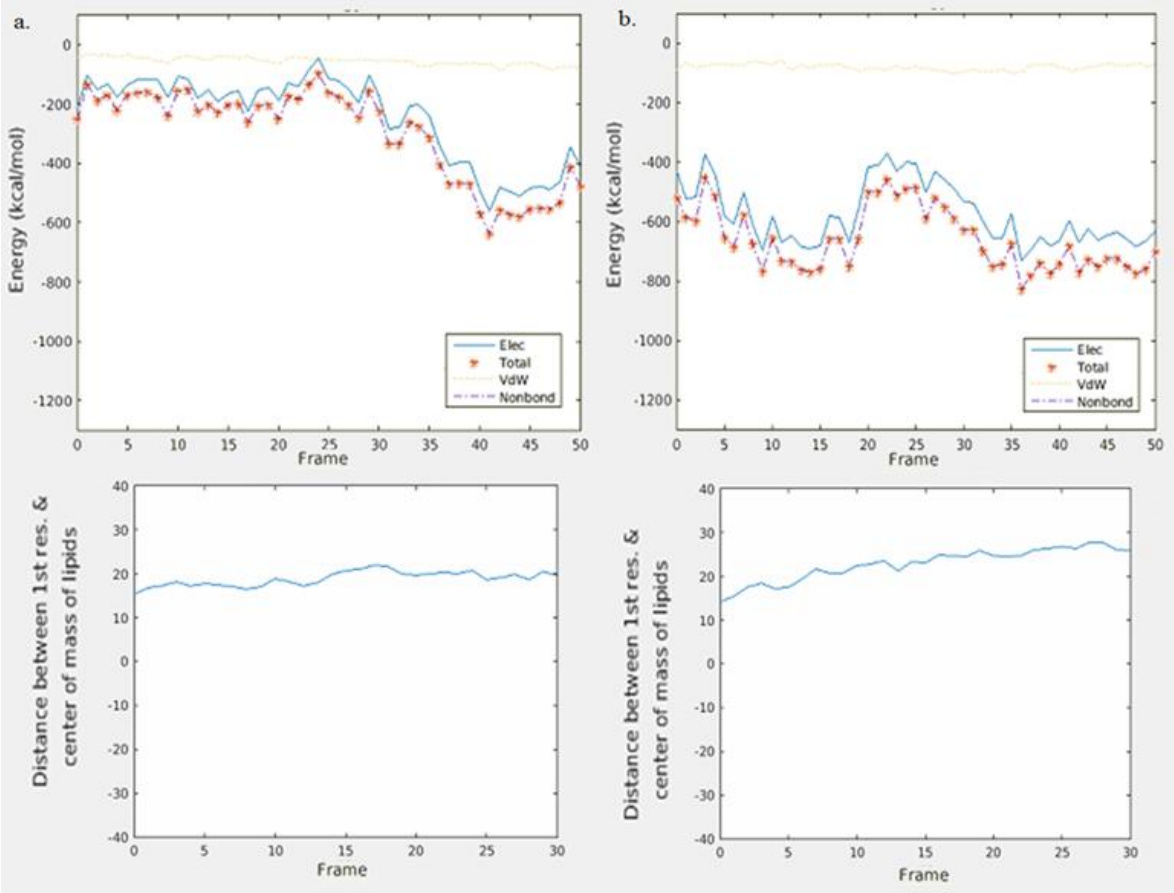

Figure 4.61. pVEC POPE MD top position: energy plot and distance* plot for Pos1 & Pos2. * Distance between the 1st residue and the center of mass of lipids

In Figure 4.61, the electrostatic energy started at -200 kcal/mol and dropped to zero around frame 25 as the peptide moved out of the membrane . The distance between Leu1 and the center of mass of lipids increased to about 20 from 15 Å. Leu1 moved away from the center of mass of lipids. Meaning that the peptide started to move away from the membrane through the top however it was attached to the upper p heads and could not leave the membrane. Energy started to increase as the peptide was anchored by Leu1-Leu2-Ile3 and Ser17-Lys18 and reached a maximum of -550 kcal/mol at frame 40. On the last frame the energy dropped to -400 kcal/mol. The secondary structure of the pVEC peptide did not assume a helical structure throughout both simulations.

The pVEC POPE middle MD simulations showed that the peptide started to move out of the membrane. The initial and final snapshots are shown in Figure 4.62. The distance between Leu1 and the center of mass of lipids increased in the first 2 frames drastically, meaning that the peptide prefered to move out of the peptide through the top. Leu1 reached the upper p heads, however it did not leave the membrane. Initially Arg6-Arg 7-Arg8-Ile9-Arg10-Lys11-Gln12-Ala13-His14-Ala15-His16-Ser17-Lys18 were embedded inside the membrane. The hair-pin structure was composed of Arg8-Ile9-Arg10-Lys11-Gln12. Immediately Leu1 was pulled up by the electrostatic energies of the upper P heads of the membrane. The water molecules also started to leave the membrane. The peptide moved in the +z direction. The hairpin structure between Arg8-Ile9-Arg10-Lys11-Gln12 was not disturbed as the peptide moved through the membrane. At the end of 10 ns of simulation; Arg8-Ile9-Arg10-Lys11-Gln12-Ala13-His14-Ala15-His16-Ser17-Lys18left the membrane. In the second simulation, the peptide was positioned inside the membrane such that Arg8-Ile9-Arg10-Lys11-Gln12-Ala13-His14- Ala15 were embedded in the P heads. Immediately the tip of the peptide with Leu1 moved toward the upper P heads and the water molecules started to leave the membrane. Also the kink composed of Lys11-Gln12-Ala13-His14 started to leave the membrane. At the end of the simulation, Gln12-Ala13 anchored the upper part of the peptide on the P heads. Ile4 and Leu5 were embedded in the membrane. Leu1 was in contact with the inner part of the upper P heads.

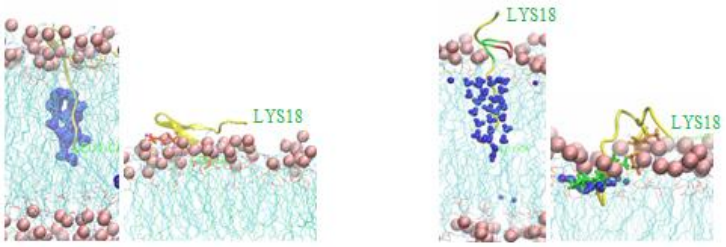

Figure 4.62. pVEC POPE MD middle position: initial and final snapshots.

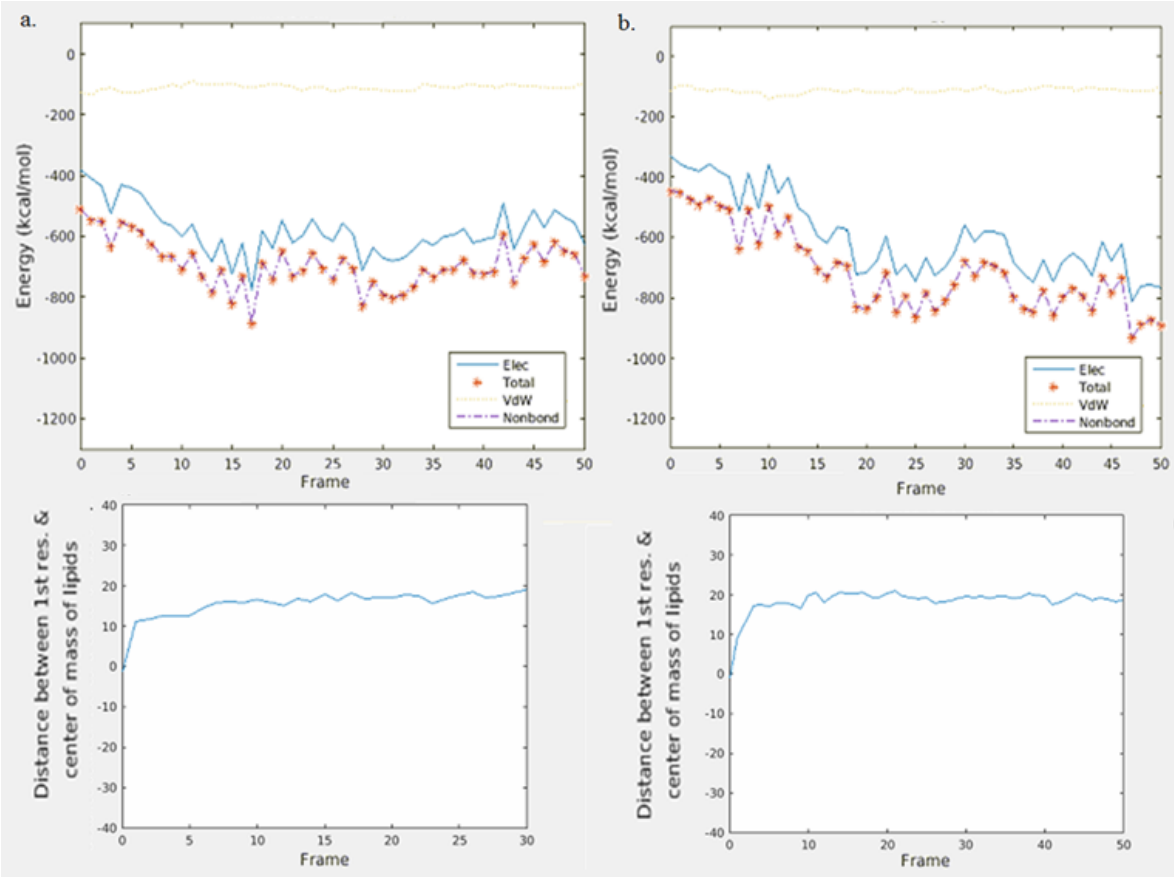

Figure 4.63. pVEC POPE MD middle position: energy plot and distance* plot for Pos1 & Pos2. * Distance between the 1st residue and the center of mass of lipids.

In Figure 4.63, the electrostatic energy started at around a value of -400 to -500 kcal/mol. The energy increased as the hairpin structure Arg8-Ile9-Arg10-Lys11-Gln12-Ala13 moved inside the upper P head layer. It reached a maximum energy of -700 kcal/mol. After the hairpin structure left the membrane the energy dropped since less residues were in contact with the membrane, energy started to decline. Toward the end of the simulation the peptide anchored to the membrane by Ile4- Leu5 and Lys18. The secondary structure of the pVEC peptide did not assume a helical structure throughout both simulations.

The pVEC POPE bottom MD simulations showed that the peptide started to move out of the membrane. Figure 4.64 shows the initial and final snapshots of the pVEC POPE MD bottom positions including the MD simulation carried out from the snapshot acquired from Alaybeyoğlu. In all the pVEC POPE bottom MD simulations, the hair-pin structure

composed of Arg8-Ile9-Arg10-Lys11-Gln12 was surrounded by water molecules. The peptide started to migrate back in the +z direction. The water molecules started to leave the membrane. The peptide moved up, and Ala13-His14-Ala15-His16 formed a hair-pin like structure on the upper part of the P heads. As the peptide moved up the lower P heads were pulled into the lipid part of the membrane due to the vacuum caused by the retreat. In SMD simulations the P heads were restricted in the z direction; however, in MD simulation this restriction was not applied so as to see the reaction of all structures in the system. The interactions between Arg8-Ile9-Arg10-Lys11-Gln12-Ala13-His14 caused the peptide to linger inside the membrane.

As can be seen in Figure 4.65, the electrostatic energy started at a value of -350 to -400 kcal/mol. The distance between Leu1 and the center of mass of lipids increased in the first 2 frames, meaning that the peptide prefered to move out of the peptide through the top. Ala13-His14-Ala15-His16 which formed a hairpin like structure resisted moving out of the membrane. Arg8-Ile9-Arg10-Lys11-Gln12- anchored the peptide inside the mebrane. Leu1 moved towards the middle of the membrane and lingered about -10 Å away from the middle of the membrane until the end of the simulation

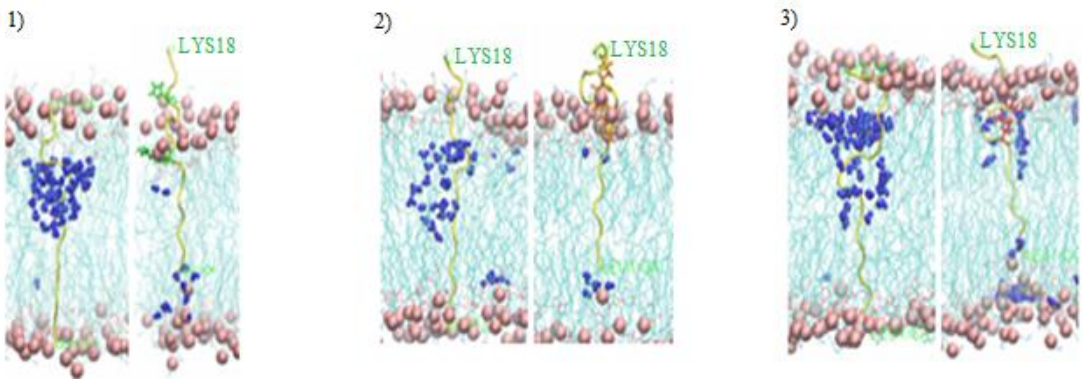

Figure 4.64. pVEC POPE MD bottom position: initial and final snapshots. *The third set of snapshots is from Alaybeyoğlu.

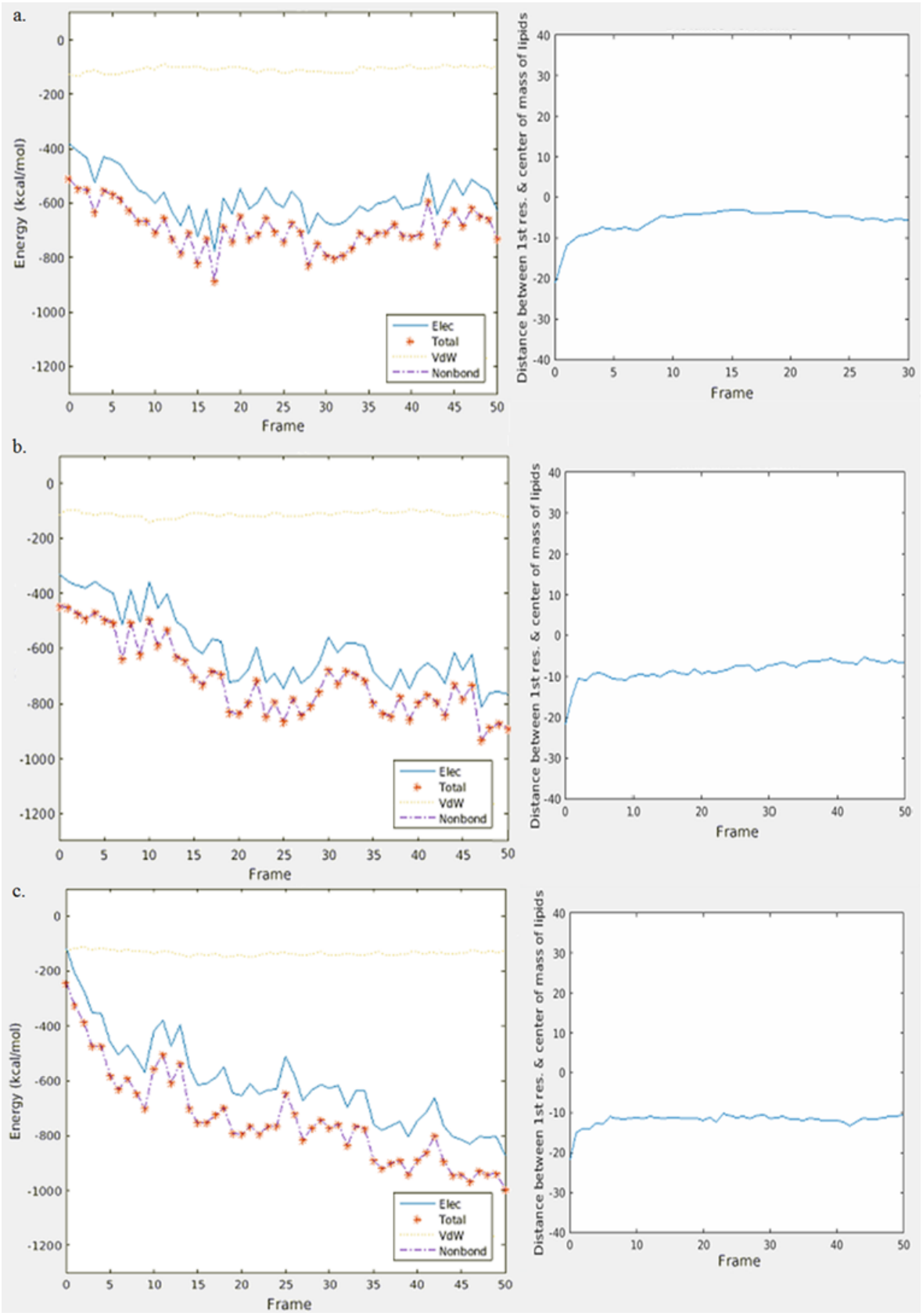

Figure 4.65. pVEC POPE MD top position: energy plot and distance* plot for Pos1, Pos2 & Pos3. * Distance between the 1st residue and the center of mass of lipids.

The energy increased and reached a maximum value of about -800 kcal/mol at frame 17. The residues left inside the membrane strecthed between the bilayer. The residues were in contact with the lipids and the electrostatic energy stayed at a high rate of about -600 to -700 kcal/mol. The secondary structure of the pVEC peptide did not assume a helical structure throughout both simulations.

The results of Alaybeyoğlu snapshot showed that the electrostatic energy started at a value of -100kcal/mol and similar to the bottom simulations of the pVEC in POPE, the distance between Leu1 and the center of mass of lipids increased in the first frames drastically meaning that the peptide preferred to move out of the peptide through the top. Energy increased as the upper residues left the membrane through the top. Leu1 moved towards the middle of the membrane and lingered at -10 Å away from the middle of the membrane until the end of the simulation. The rest of the residues stretched between the lipid bilayer due to the pull of lower P heads. Similarly, Arg8-Ile9-Arg10-Lys11-Gln12 (which formed the hairpin structure) had higher interaction with the upper P layer. The energy reached a maximum value of -850 kcal/mol at the end of the simulation. The secondary structure of the pVEC peptide did not assume a helical structure throughout the simulation. The three simulations showed the same result, which means that our simulations were consistent with the simulations carried out by Begüm Alaybeyoğlu.

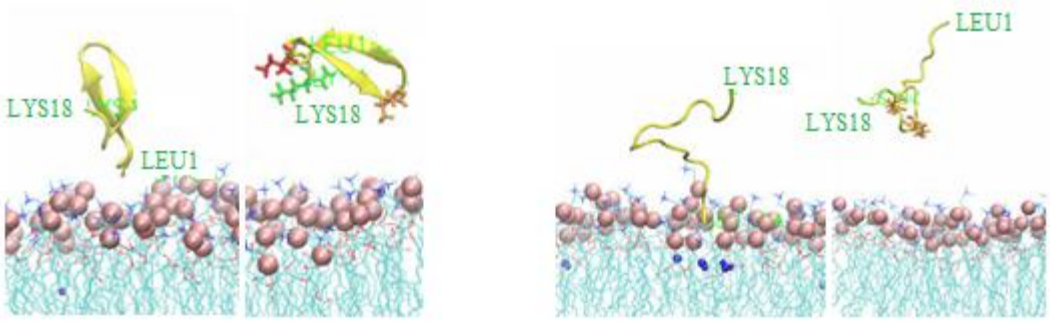

Figure 4.66. pVEC POPC MD top position: initial and final snapshots.

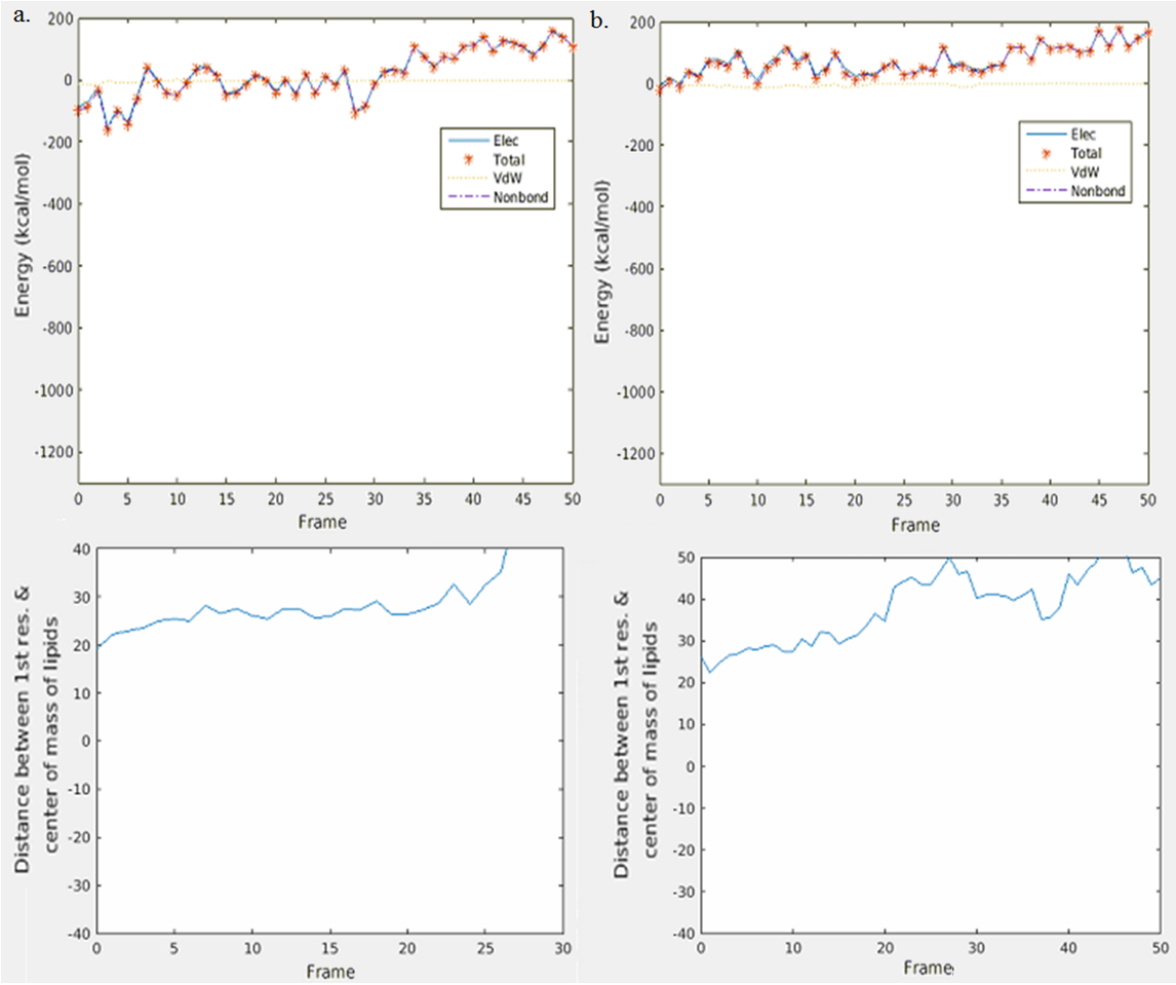

Figure 4.67. pVEC POPC MD top position: energy plot and distance* plot for Pos1 & Pos2. * Distance between the 1st residue and the center of mass of lipids.

pVEC POPC top MD simulations demostrated that the peptide moved away from the membrane as the simulation continued. Figure 4.66 shows the initial and final snapshots of the MD simulations. The peptide was vertically positioned with respect to the membrane, such that Leu1 was closest to the P heads. There are no water molecules in the membrane. The peptide took a horizontal position with respect to the membrane, however, the distance between the center of mass of lipid and Leu1increased. Ile3 and Lys18 interacted with the membrane however, the distance between the center of mass of lipid and the first residue increased further meaning that the energies of the system pushed the peptide away from the membrane despite these attractions.

In Figure 4.67, the electrostatic energy started at around 0 to -100 kcal/mol. The distance between Leu1 and the center of mass of lipids increased continuously. The energy dropped from this point forward. The peptide left the membrane completely and continued to move further away from the membrane. The secondary structure of the pVEC peptide did not assume a helical structure throughout both simulations.

The pVEC POPC middle MD simulations showed that the peptide started to move out of the membrane as the simulation continued. The initial and final snapshots of the simulations are shown in Figure 4.68. The peptide was positioned inside the membrane such that Leu5-Arg6-Arg 7-Arg8-Ile9-Arg10-Lys11-Gln12-Ala13-His14 was embedded in the P heads. Immediately the peptide started to move in the +z direction. The water molecules started to leave the membrane. Leu1 was pulled by the P heads. The hairpin structure was not disturbed. Leu5 acted as an anchor. In the second position, the residues embedded inside the membrane Leu1-Leu2-Ile 3-Ile4-Leu5-Arg6-Arg 7 acted as an anchor. Therefore the hairpin structure could not leave the membrane.

In Figure 4.69, the electrostatic energy started at a value of about -350 to -400 kcal/mol and similar to the POPE simulation results, the distance between Leu1 and the center of mass of lipids increased in the first frames meaning that the peptide prefered to move out of the peptide through the top. The energy increased in the first three frames and reached a maximum of about -700 kcal/mol. The energy dropped as the peptide moved out to a minimum of -150 kcal/mol at frame 30. The energy increased towards the end where Leu1-Leu2-Ile3-Ile4-Leu5-Arg6-Arg7 anchored Leu5 being more dominant and held the peptide attached to the membrane. Leu1 reached the upper P heads, however it did not leave the membrane. The energy reached -700 kcal/mol and continued at this energy level until the end of the simulation. In pos1 the final value was about -350 kcal/mol. The secondary structure of the pVEC peptide did not assume a helical structure throughout both simulations.

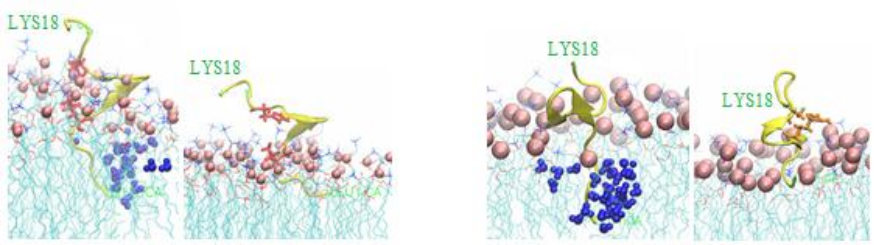

Figure 4.68. pVEC POPC MD middle position: initial and final snapshots.

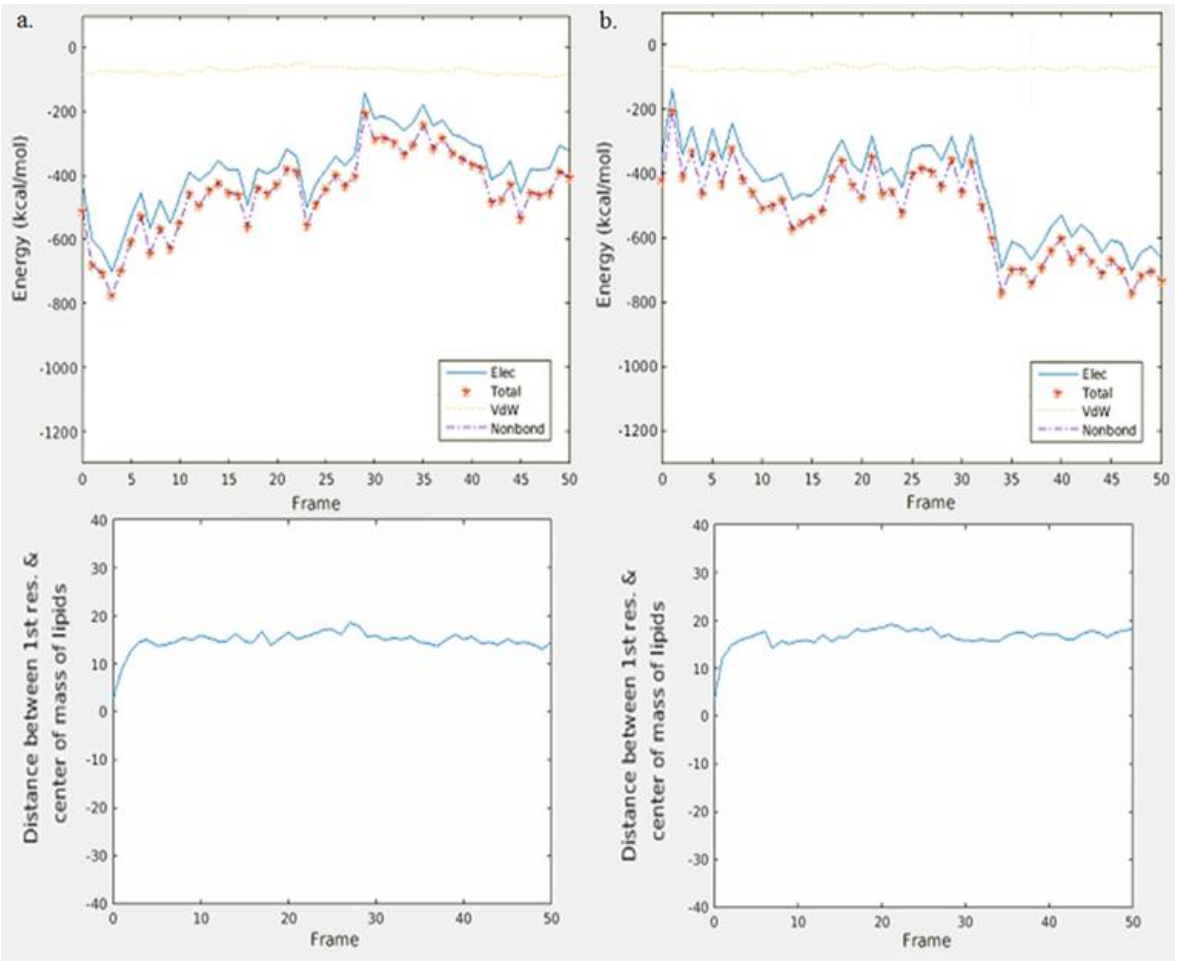

Figure 4.69. pVEC POPC MD middle position: energy plot and distance* plot for Pos1 & Pos2. * Distance between the 1st residue and the center of mass of lipids.

The pVEC POPC bottom MD simulations showed that the peptide started to move out of the membrane in the +z direction. The initial and final snapshots of the simulations are shown in Figure 4.70. In the initial frame, the peptide was placed such that Leu1 was

embedded in the lower P heads of the membrane. Ala15-His16-Ser17-Lys18 were outside the membrane. There was a considerable amount of water molecules inside the membrane. Immediately the peptide started moving in the +z direction. The water molecules started to leave the membrane. Leu1 pulled water molecules as the peptide moved upwards. Arg7-Arg8-Ile9-Arg10 acted as an anchor. As the peptide moved up, Leu1 pulled the lower P head layer and caused the distance between the two P head layers to decrease. In the second position, at the final snapshot Arg8-Ile9-Arg10-Lys11-Gln12-Ala13-His14-Ala15-His16-Ser17-Lys18 were embedded inside the membrane, with the hairpin structure intact. Leu1 was pulled by the lower P heads of the membrane.

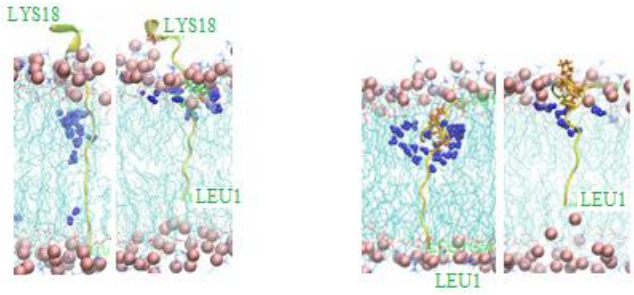

Figure 4.70. pVEC POPC MD bottom position: initial and final snapshots.

In Figure 4.71, the electrostatic energy started at -500 to -600 kcal/mol. The energy started to rise, there was a peak around frame 8. The energy increased as the simulation continued and oscilated between -800and -1000 kcal/mol. Ala15 had extra interaction with the upper P heads. This residue might be the reason for the increase energy peak around frame 8. The residue left the P heads as the simulation continued however it was attracted to the upper P heads once more. The energy started to rise again after the drop and continued to increase until the end of the simulation. The peptide tried to leave the membrane through the top but was anchored by Arg7-Arg8-Ile9-Arg10 on the upper P heads while Leu1 was pulled by the lower P heads. The peptide stretched along the membrane was unlikely to leave the membrane. Arg8-Ile9-Arg10-Lys11 -Gln12-Ala13-His14-Ala15-His16-Ser17-Lys18 stayed embedded in the top P head layer.This might be the cause of the increased energy. The energy of the bottom simulation was higher than the top and middle simulation, this was understandable as more residues were in contact with

the lipids in the bottom simulation. At the last frame the energy value was -900 to -1000 kcal/mol.

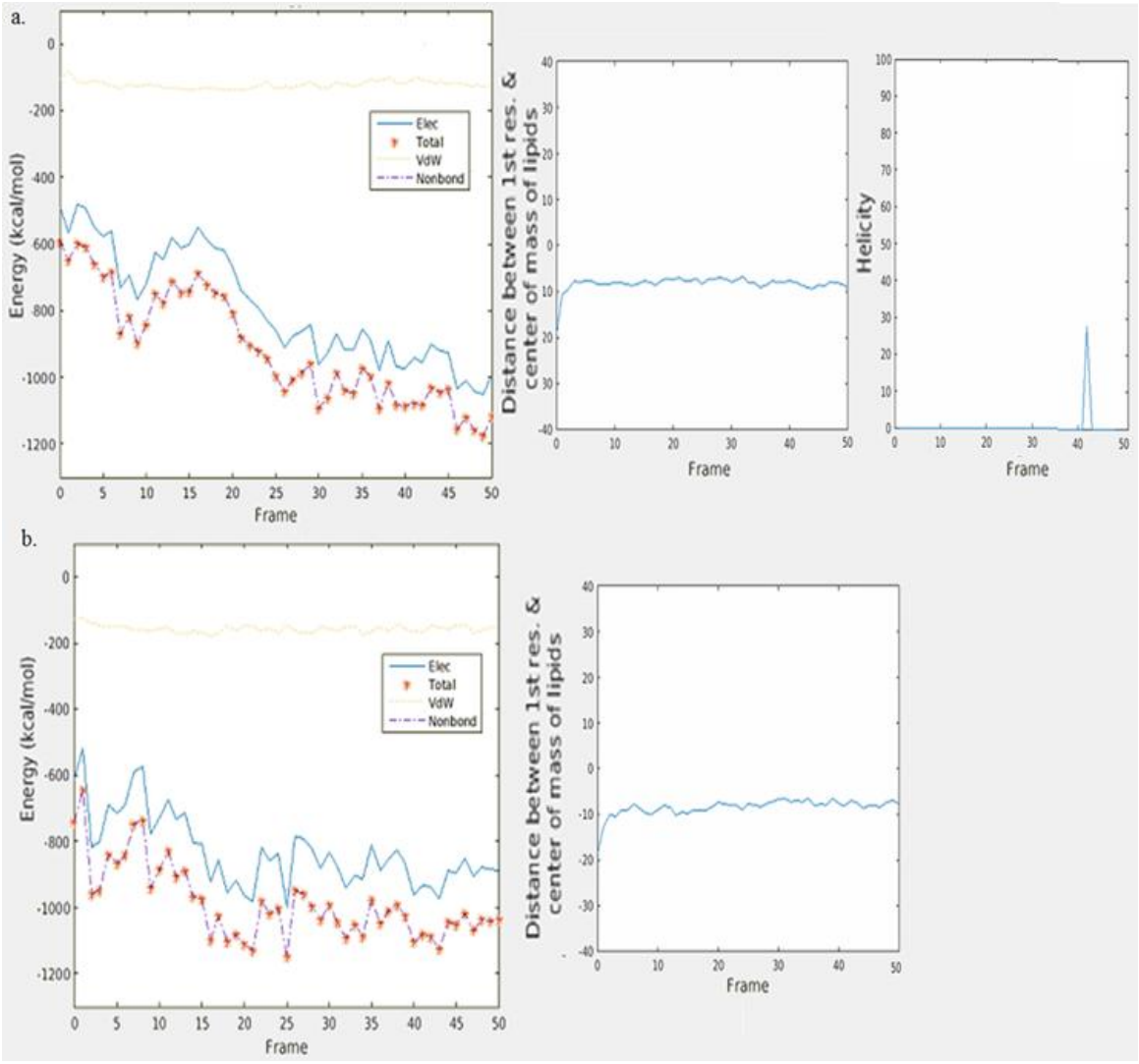

Figure 4.71. pVEC POPC MD top position: energy plot, helicity plot and distance* plot for Pos1 & Pos2. * Distance between the 1st residue and the center of mass of lipids.

Unlike the other simulations, in Pos1 the peptide assumed a helical structure between frames 41-43, with a maximum value of 30% helicity. This means that 5.4 out of 18 the residues had helical structure at this point. The helicity droped to zero as the simulation continued. The second simulation, however, did not assume a helical structure.

5. CONCLUSION

5.1. Conclusions Deduced from the SMD Simulations

The data obtained from each system was compared further to understand the actions of melittin and pVEC in POPE and POPC membranes. Through comparison, the differences between melittin and pVEC peptides and POPE and POPC membranes were observed. The SMD simulations showed that the duplicate system simulations with different initial peptide positions showed similar trends. This was anticipated as the systems had identical components. The differences observed are thought to arise because of the differences in the initial positions of the peptides. The initial position of the peptide effected the initial contact interactions of the peptide residues with the upper P layer. In the melittin SMD simulations the initial water insertion started as Val5-Leu6-Lys7 are in the upper P layer. Also as the C-terminus left the lower P heads, increase in the number of water molecules inside the membrane were observed. As Gly1 entered the membrane a force barrier was observed. So the water insertion was thought to be related with Val5-Leu6-Lys7 and the C-terminus interactions with the lipid P layers. As the simulations continued residues Thr10-Thr11-Gly12-Leu13-Pro14-Ala5-Leu16, Lys21-Arg22-Lys23-Arg24-Gln25-Gln26 were seen to anchor the peptide inside the membrane showing that these residues have an important role in peptide penetration mechanism in POPE and POPC membranes. The melittin in POPE and POPC membrane simulations were found to be similar but with a few differences.

In POPE and POPC simulations, a similarity observed was that Trp19 was seen to have increased electrostatic interactions with the lipids. It also acted as an anchor. However, compared to the C-terminus residues, it was less interactive. The role of Trp19 in antibiotic action was mentioned [31]. Its mode of action might be that the non-polar residues which have the most electrostatic interaction with Trp19 faces less resistance towards moving in the –z direction and propels the peptide through the membrane aiding peptide insertion. It is known that Tryptophan disturbs membranes by an indole ring present in its side chain. Hydrogen bonding, and attributes such as dipole and quadrupole

moments which Trp residue is capable of is due to this side chain. Tryptophan can bind to water molecules through hydrogen bonding. As tryptophan enters interfacial region of the membrane (which tryptophan prefers) the bonds with the water molecules break. Tryptophan anchors and inserts the peptide through the membrane barriers [3].

The melittin residues which have the most electrostatic interactions with POPE and POPC membranes were Gly1, Lys7, Lys21, Arg22, Lys23 and Arg24. Other residues with less electrostatic energy levels were Thr10, Th11, Ser18, Gln25 and Gln26. The rest of the residues had close to no electrostatic interactions with the lipids. Apart from Gly1, the residues with high electrostatic interactions were either non-charged/polar or charged. The electrostatic energies of residues were observed to be higher in POPC. Especially Lys21, Arg24, Gln25 and Gln26 had higher electrostatic energies in POPC. This means that in the POPC membrane, the melittin peptide faced more energy barriers and more force was needed to pull the peptide through the membrane. It can be concluded that POPC membrane was more impenetrable than POPE membrane. This is important in drug design, as it is wanted for the CPP to penetrate bacterial membranes (POPE) and not harm mammalian membranes (POPC).

The helicity of the melittin peptide was also monitored in the simulations. In POPE and POPC membranes the melittin peptide had 80-90% helicity before entering the membrane. It was found that at the upper P layer the helicity continued at the same percentage. As the peptide assumed a trans-membrane position the helicity decreased to 70%. The residues interacted with the lipids and as the peptide was pulled downward the peptide unfolded. It was observed that in the POPE membrane the helicity was higher. Low helicity is thought to encourage pore formation. Melittin in POPC having low helicity might facilitate pore formation. Table 5.1. Summary of the simulations carried out with melittin, the results were found as the following for POPE vs. POPC simulations. Consequently, more water molecules were observed in POPC than POPE with about 70 and 50 water molecules respectively.

Table 5.1. Summary of the simulations carried out with melittin, the results were found as the following for POPE vs. POPC simulations.

Energy	The energy graphs were very similar. They showed a trend of three regions.
Force	Similarity: more force was applied around z -50 Å, -60 Å. Force application started around z 20 Å. The melittin peptide stayed in a trans-membrane state. This might initiate a pore. Difference: the force trends differed in all the simulations with small peaks at different z coordinates. In POPE simulation at z 20 Å a large peak was observed. The force increased to -1000 pN from -200 pN. This showed that melittin faced a resistance in POPE membrane. It moved through POPC more easily.
Work	More work was done in POPC. In POPC=1600 kcal/mol was applied while in POPE=1400 kcal/mol was applied.
Radius of Gyration	Shows similar trends with respect to z coordinates. The highest value was observed around z [-80, -60] Å. The maximum radius of gyration value was higher in POPC=27 while POPE=26. This means that the peptide was more loosely packed in POPC, confirming the low helicity percentage of melittin in POPC.
Order of Lipids	The lipid order trends are different. Order range was between 0.25-0.1 in all simulations. This means that the lipids were positioned randomly, which was the case in real membranes.
Membrane Thickness	The values were very close however the POPC values were higher. Average minimum was 52.75 Å for POPE while it was 55 Å for POPC. Average maximum was 60.25 Å for POPE while it was 62 Å for POPC. When melittin binds to a membrane it causes stress that leads to the membrane area to increase and membrane thickness to decrease. Membrane thinning caused by melittin binding to a membrane was observed to eventually lead to pore formation [17]. The POPE membrane was observed to have thinned more which means that leakage was more likely to happen in the POPE membrane which represents the bacterial membrane.
Water in membrane	In both membranes water usually started to enter the membrane around z 10 Å. And most water molecules were observed at z -60, -80 Å. Where the peptide started to leave the bilayer through the lower P layer. Around 50 water molecules entered POPE the most, while in POPC membrane it was around 70 molecules.

The evidences suggest that melittin causes membrane thinning in POPE and initiate pore formation in POPC by decreasing its helicity. It is known that melittin is disruptive in

both membranes [19]. However, the mechanism observed in both membranes varied in our SMD simulations.

The SMD simulation results of pVEC in POPE membrane showed that the peptide inserted itself in a vertical manner. Leu1 and Lys18 interacted with the upper P layer and inserted the peptide through both tails. Water insertion started as Leu5 and Arg6 entered the membrane. Arg6 was a charged residue and is thought to initiate water penetration in literature which was also observed in our simulations [23]. Arg7 also pulled more water molecules into the membrane. In the pVEC POPC membrane simulations, most water insertion was observed between z -20 Å and -40 Å. At these points the peptide was in a trans-membrane state. Water insertion started as Ile4 started to enter the membrane. Water was carried inside the membrane by Leu1, Ile4, Arg6 and Arg7. The residues Arg7, Arg10, Gln12, His14, Ala15, His16, Ser17 and Lys18 acted as an anchor at certain points during the simulations. Table 5. summarizes the SMD simulation results in terms of POPE results vs. POPC results. The residue electrostatic energies were detected to be high. Apart from Ala15, the mentioned residues were either Uncharged/polar or charged. The residue electrostatic energies were higher in POPC. Similar to the melittin results, the pVEC peptide faced more force barriers in the POPC membrane (mammalian) making it more impenetrable. The residues Leu1, Arg6, Arg7 Arg8, Arg10, Lys11 and Lys18 had the highest electrostatic interactions with the lipids. Leu2, Gln12, His14, His16 and Ser17 also had interactions, however, less than the prior residues. The rest of the residues had almost no electrostatic interactions with the membrane lipids. For SMD simulations; in the electrostatic energy analysis of melittin and pVEC residues Lys 21 and Arg24 residue of melittin and Leu1 and Lys18 residue of pVEC exhibited higher electrostatic energy levels in POPC membrane. In previous researches electrostatic energies were observed between Lys and Arg and bacterial membranes. The difference between Arg and Lys residues is that Arginine has a guanidinium group in its side which distributes positive charge. It may lead to hydrogen bonding with surrounding water molecules. Arginine may have multiple interactions whereas lysine has mono charge and substitution of arginine with lysine decreased antimicrobial activity. When arginine and asparagines were substituted with lysine and *C*-terminus amidation, antibacterial activity was not much affected while hemolytic activity was observed to have decreased. Substituting Arg residues with Lys also decreased the cellular uptake of peptides. Lysine and arginine show antimicrobial activity

in proteins. Arginine residues added to the *C*-terminus end of antimicrobial peptides causes salt-resistance. Electrostatic interaction among the peptide and bacterial membranes are increased as a result [3].

Table 5.2. Summary of the SMD simulations carried out with PVEC, POPE vs POPC simulations are compared.

Energy	The energy trends were different. Most energy was around z -18 Å in all simulations. In POPC the electrostatic energy was higher around 800 while in POPE it was around 700. This means that the peptide showed more resistance against moving through the POPC membrane.
Force	The regions observed were similar in all simulations. Most force was applied around z -20 Å, to move the peptide through the lower P heads. This means that the peptide wanted to stay at a trans-membrane state in all simulations.
Work	The trends and values were very similar.
Radius of Gyration	The trend was similar for three of the simulations. And the value of the highest radius of gyration for all simulations was 18. This value was lower than the melittin values meaning that the pVEC peptide was packed more tightly than the melittin peptide.
Order of Lipids	The values of order for carbons in POPE was between [0.1, 0.22] while in POPC it was between [0.1, 0.24].
Membrane Thickness	The POPC values were higher. Average maximum was 60 Å for POPE while 61.75 Å for POPC. Average minimum was 52.75 Å for POPE while 55 Å for POPC. The POPE membrane thinned slightly more, therefore it is more likely that leakage may happen in a POPE membrane.
Water in membrane	For both membranes the water molecules were found inside the membrane during z [-20, -30] Å with a quantity of 70 molecules for POPE and around 90 molecules for POPC. More water molecules entered the POPC membrane. The water entering the membrane may affect the permeability of the membrane. These changes to the bilayer may boost the uptake of peptides [23].

If more peptides can pass through the bilayer this might mean that there is more chance of drug delivery.

Table 5.3. The table shows the, initial, maximum thickness values and average thickness along with standard deviation values of membranes in each SMD simulation.

Simulation	Initial Membrane Thickness (Å)	Maximum Thickness (Å)	Average Thickness (Å)	Standard Deviation (Å)
Melittin POPE Pos1	55.631	60.179	56.196	1.356
Melittin POPE Pos2	54.103	60.360	56.331	1.458
Melittin POPC Pos1	59.331	62.022	58.132	1.278
Melittin POPC Pos2	56.810	61.821	58.386	1.259
pVEC POPE Pos1	58.277	60.369	56.365	1.328
pVEC POPE Pos2	56.363	59.666	56.235	1.410
pVEC POPC Pos1	58.755	61.861	58.332	1.345
pVEC POPC Pos2	57.890	61.583	58.119	1.382

The POPE and POPC membrane were constructed of 129 lipids in 69 x 69 Å x- and y- coordinates. Water was added in the -80 Å and 80 Å z directions. The system was equilibrated and the resulting system sizes were 76.552 Å X 81.414 Å X 180.339 Å for POPE and 77.861 Å X 79.560 Å X 181.271 Å for POPC. The lipid area of POPE was 6232.486 $Å^2$ and for POPC the lipid area was 6194.700 $Å^2$. As SMD simulations continued the lipid area and membrane thickness changed. (Table 5.3) The average thickness of the POPE membrane was lower than the POPC membrane, with about the average thickness of 56 and 58 Å, respectively. When the deviations were compared the POPE membrane deviated more. This means that the POPE membrane thickness changed more.

From the graphs in Figure 5.1, the pVEC peptide caused more water molecules to enter the membrane when compared with the melittin simulations. Also, more water molecules penetrated the POPC membrane when compared with the POPE membrane simulations. Figure 5.1 is an example which demonstrates the different profiles the amidated melittin and pVEC peptides show in different membranes. For example the

melittin peptide showed a large peak around z=-80 Å in POPE and POPC. From the residue energy analysis, residues Lys21,Arg22, Lys23 and Arg24 had increased levels of interaction of about 150-200 kcal/mol with the P heads of the lower membrane at this point. However, this interaction caused more water molecules to enter the POPC membrane when compared with the POPE membrane profile. This might lead to a theory of POPC being more prone to leakage however from experimental studies it is known that pVEC enters both mammalian and bacterial membranes and it is known to have no toxicity on mammalian cells [33].

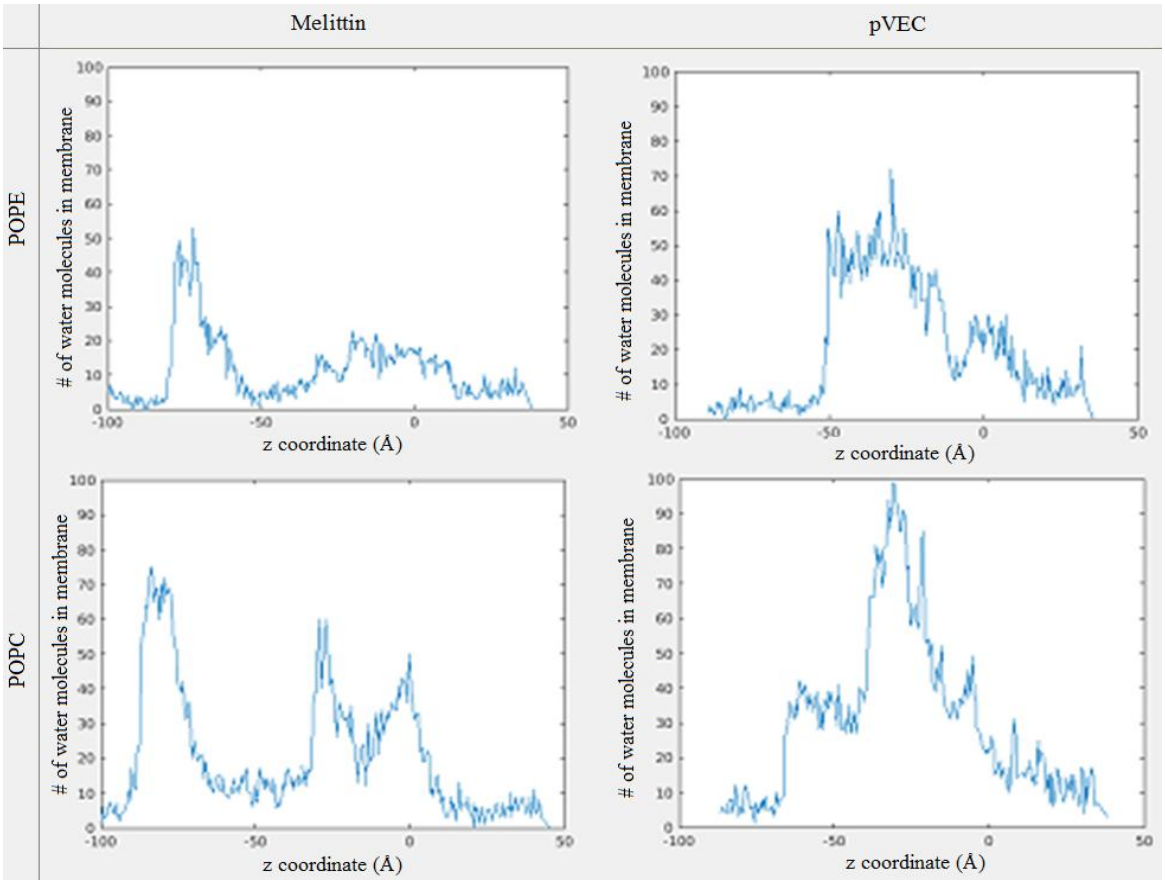

Figure 5.1. A summary of the number of water molecules profiles in each SMD system as a function of the z coordinate of the SMD atom.

The maximum electrostatic energy, force, number of water molecules in membrane and total work for all the SMD simulations were compared in Table 5.. When compared with the melittin SMD simulation results, pVEC exhibited higher electrostatic energy with the

membrane lipids. The high electrostatic energy caused barriers and more force was applied to overcome these higher energy barriers. Overall less work was done by the system which means that overall pVEC faced less resistance and this makes pVEC more suitable at drug delivery. The pVEC peptide also penetrated the membranes in a shorter amount of time when compared to melittin.

Table 5.4. The maximum Interaction energy, force, number of water molecules in membrane and total work for all the SMD simulations.

Simulations	Max Electrostatic Energy (kcal/mol)	Maximum Force (pN)	Total Work (kcal/mol)	Max Number of water Molecules in Membrane
pVEC in POPE				
Position 1	-728.53	-1371.75	1175.78	82
Position 2	-650.20	-1045.54	1071.00	72
pVEC in POPC				
Position 1	-832.30	-1524.66	1230.55	99
Position 2	-876.67	-1097.03	1039.25	81
Melittin in POPE				
Position 1	-635.59	-920.34	1301.41	53
Position 2	-514.80	-1024.35	1406.55	53
Melittin in POPC				
Position 1	-681.03	-1377.86	1552.75	75
Position 2	-728.81	-955.02	1513.94	66

The shortest times were observed as 42.8 and 53 ns for pVEC and melittin SMD penetrations, respectively. More water molecules penetrated when pVEC passed through both type of membranes. This means that pVEC was more efficient than the melittin peptide. However, the fact that pVEC has caused more leakage in POPC membrane would have meant that it might be disruptive for mammalian cells. However, in experimental studies it has been proven that, pVEC has no toxic effects on mammalian cells [26]. Therefore the water insertion observed here might not be enough to create cell leakage. As mentioned earlier, it is also believed that increase in water molecules might assist more peptides to enter the bilayer increasing the chances of drug delivery by the pVEC peptide in POPC membranes to find its target [23]. Overall the SMD simulations show that the

pVEC peptide proved to be more potent than the melittin peptide in bacterial cells. pVEC in POPE membranes exhibited low work and lower energy barriers compared to POPC membrane simulations. Also considering that the membrane thickness deviated more in POPE it might be more prone to leakage. Therefore, the pVEC penetration of POPE (bacterial) membranes might be more spontaneous. The MD simulation results shed more light to the natural occurrence of events in these systems.

The MD simulation results of melittin-POPE, melittin-POPC, pVEC-POPE and pVEC-POPC systems were also observed in this study. Melittin-POPE and melittin-POPC systems were prepared by taking snapshots of the SMD simulations when Gly1 was at the top, middle and bottom of the membrane. The results of visual analysis, energy, and distance and helicity plots gave further insight on the differences of behavior of the melittin peptide inside the POPC and POPE membrane which represent mammalian and bacterial membranes respectively. The analysis showed when the peptide prefers to enter or leave the membrane. The preferred secondary structure of the peptide at different positions was also observed. For melittin MD simulations, the initial position of the peptide was crucial for peptide insertion. The effects of certain residues were visible in the simulations. Gly1-Ile2-Gly3-Ala4-Val5-Leu6-Lys7-Val8-Leu9-Thr10 in POPE membrane had an important role in melittin peptide insertion. For both membranes the interaction of Gly1 with the lower P layer was crucial for further peptide insertion into the membrane. In POPC simulations Leu16, Trp19, Ile20 and Lys23 played an important role in attracting the peptide towards the membrane and to assume a parallel position. Also, residues Lys7 and Thr11 had high interaction with the P heads of the membrane. The effects of these phenomena were also observed from the energy, helicity and Distance analysis. The POPC membrane had higher interaction with the lipids in the energy analysis. Helicity was observed to be higher when the peptide was inside the membrane. When compared with POPC, the peptide in POPE had higher helicity. The MD simulations gave a better understanding of the peptide-membrane interactions since no outside force was applied contrary to the SMD simulations.

5.2. Conclusions Deduced from SMD Simulations carried out by Pulling from Center of Mass and 1/10th Velocity Pulling

Melittin in POPE pulled by c.o.m. simulation analysis showed that the peptide entered the membrane horizontally and that water insertion started with Ile20. Residues Ile20-Lys21-Arg22-Lys23-Arg24-Gln25-Gln26 and Gly1 were observed to have anchoring effects on the membrane. These residues also had anchoring effects in the melittin POPE simulations pulled by the N-terminus. Unlike the N-terminus pulled simulations, the peptide was observed to unfold mostly when it reached the lower P layer. In the N-terminus pulled simulations the peptide started unfolding as it entered through the upper P layer. However in both simulations the peptide left the membrane through the lower P layer unfolded and in a vertical position. The last residue that left the membrane was Trp19. The anchoring effects of Trp19 were discussed earlier. This simulation once again demonstrated these effects. Overall from the electrostatic energy, force and work profiles most resistance was seen in the upper P layer. The high electrostatic electrostatic energies were overcome by the applied force.

The melittin simulation in POPE membrane carried out with $1/10^{th}$ velocity and pulled by the N-terminus, demonstrated that the melittin peptide takes parallel position with respect to the membrane on the upper P layer. And similar to the previous simulations the peptide entered the bilayer vertically. Lys7 and Val8 residues played an important part in water bubble formation inside the membrane. The simulation was carried out until the N-terminus reached the center of the bilayer therefore only the mechanisms up to that stage were observed. The electrostatic energy, force and work profiles showed that the upper P layer showed resistance. And extra force was applied to move the peptide through the energy threshold. Gly1 was observed to have important anchoring effects on the upper P layer, which was also seen in the other simulations carried out in this study. Unlike other simulations, the peptide started unfolding as it passes through the upper P layer. This simulation was important for simulating pore formation of melittin peptides. In literature it

is stated that melittin forms α-helix structures inside the membrane after forming pores to stabilize pore structure [28].

When the maximum electrostatic energy, maximum force, total work, and maximum number of water molecules are compared for all melittin SMD simulations performed in POPE membrane (Table 5.), the simulation with melittin pulled by c.o.m. showed most resistance. The peptide is unlikely to enter the membrane in this conformation as more force was applied to pull the peptide through the upper P layer compared to other simulations. However, the total work was less than all the other simulations.

Table 5.5. The maximum interaction energy, force, number of water molecules in membrane and total work for melittin POPE SMD simulations.

Simulations	Max Electrostatic Energy (kcal/mol)	Maximum Force (pN)	Total Work (kcal/mol)	Max Number of water Molecules in Membrane
Melittin in POPE pulled by N-terminus				
Position 1	-635.59	-920.34	1301.41	53
Position 2	-514.80	-1024.35	1406.55	53
Melittin in POPE pulled by c.o.m.				
Position 1	-659.72	-1252.08	1172.38	88
Melittin in POPE pulled by N-terminus with $1/10^{th}$ velocity (half simulation)				
Position 1	-590.50	-572.48	1307.56	36

Earlier, melittin membrane penetration mechanisms were discussed and it was mentioned that melittin either stays on the upper P layer with α–helix secondary structure positioned horizontally or enters the membrane in a random coil structure vertically positioned when a certain critical P/L concentration was achieved [29][28]. The radius of gyration vs. z profile showed that the peptide did not unfold until Gly1 reached the lower P layer. From the data gathered, it was deduced that it is unlikely for melittin to penetrate POPE membrane in this manner. On the other hand, melittin pulled by N-terminus with $1/10^{th}$ velocity showed about half resistance when penetrating the upper P layer with respect to other simulations. The force applied to move the peptide in –z direction was -590

pN which was smaller than -920 pN observed in melittin simulation pulled with initial speed. The electrostatic electrostatic energies are in the same range. Total work, however, was about 1300 kcal/mol although the peptide has only reached the center of the bilayer. This means that if the simulation was carried on, the total work would have been around 2600 kcal/mol.

When the membrane thickness profiles were compared for these simulations (Table 5.) it was observed that in melittin pulled with $1/10^{th}$ velocity the average membrane thickness and standard deviation was in the same range with the other N-terminus pulled simulations. The most change was observed in melittin pulled by c.o.m. with a standard deviation of 1.510 Å.

Table 5.6. Maximum thickness values and average thickness along with standard deviation values of membranes in melittin POPE SMD simulations.

Simulation	Maximum Thickness (Å)	Average Thickness (Å)	Standard Deviation (Å)
Melittin POPE pulled by N-terminus Pos1	60.179	56.196	1.356
Melittin POPE pulled by N-terminus Pos2	60.360	56.331	1.458
Melittin POPE pulled by c.o.m.	62.384	56.288	1.510
Melittin POPE pulled by N-terminus with $1/10^{th}$ velocity	62.714	56.423	1.448

To sum up, melittin pulled by c.o.m. showed higher resistance while entering membrane, however, once it has moved through more water molecules entered the membrane compared to N-terminus pulled melittin simulations. The membrane thickness was observed to fluctuate more compared to other simulations. Lastly, the total work was 1200 kcal/mol which was lower than the other simulations. This profile shows that although it was difficult for the peptide to penetrate the cell through c.o.m., once through, it is more probable that it may make the membrane more permeable.

The melittin peptide pulled from the N-terminus in $1/10^{th}$ velocity showed less resistance towards penetrating the upper P heads, however, the work profile showed that

the work done to move the peptide through the bilayer was almost double the amount seen in the other simulations. Therefore, it is more likely that this peptide will stay on the upper P layer in α–helical structure and prevent the entrance of other peptides as mentioned in earlier studies [29].

5.3. Conclusions Deduced from Melittin MD Simulations

The melittin MD simulations reveal that in top simulations Gly1 played an important role in peptide parallel positioning in the POPE and POPC membrane. While in the POPC membrane, the residues Leu16, Trp19, Ile20 and Lys23 caused the first interactions for the peptide to position itself in a parallel position with the membrane. In the middle simulations for POPE membrane Gly1-Ile2-Gly3-Ala4-Val5-Leu6-Lys7-Val8-Leu9-Thr10 assisted the insertion of the peptide inside the membrane while in POPC although the attraction of Gly1 was high, the peptide choose to move out of the membrane through the top. In the bottom simulations for both membranes, the peptide inserted itself or moved out of the membrane or stayed inside the membrane according to the attractions of Gly1 with the lower P heads. In POPC membrane attractions between the P heads and residues Lys7 and Thr11 were high.

When the electrostatic energies were compared between POPE and POPC membrane melittin MD simulations, the top simulations electrostatic energies were close. In the middle and bottom simulations the energy levels were higher in the POPC membrane simulations. This was expected as more residues were in contact with the membrane in the middle and bottom simulations. The helicity percentage was higher in the POPC membrane. In the middle simulations for the POPE membrane the helicity increased when the peptide in anchored inside the P heads, whereas in POPC membrane the helicity dropped when the peptide was anchored in the P heads. This was also observed in the SMD simulations and it presses the assumption of different mechanisms observed in POPC and POPE simulations. Overall the helicity was higher in the POPE membrane. In the bottom simulations for both membranes the helicity was higher when the peptide stayed inside the membrane and the helicity dropped as Gly1 embedded itself into the lower P heads. The

difference was that the helicity was lower in the POPC membrane compared to POPE membrane. These analyses have given us further insight in the differences of behavior of the melittin inside the POPC and POPE membrane. Since information on the AMPs is scarce, new understandings of the behavior of peptides at different environments may open new forefronts in drug design.

5.4. Conclusions Deduced from pVEC MD Simulations

The visual analysis of snapshots of pVEC in POPE and POPC membranes were analyzed. The snapshots were taken from the SMD simulations when Leu1 was situated at the top, middle and bottom of the membrane. The results of two positions of the same peptide-membrane combinations were compared. The MD simulations of the same systems gave similar results, which were expected as the components are identical. In the POPE membrane systems top position the peptide started to leave the membrane. However, it was stopped by Leu1-Leu2-Ile3. Ser17-Lys18 anchored in the first simulation while the peptide moved out of the membrane in the second simulation. The initial position of the peptide with respect to the membrane was known to have a significant effect on the protein-lipid interactions and Ser17-Lys18 might have shown this alternative behavior due to this fact. The electrostatic energy increased to -550 kcal/mol as Leu1-Leu2-Ile3 and Ser17-Lys18 anchored the peptide. And the peptide did not assume an α-helix secondary structure during the simulations. In the POPE-pVEC middle simulations the peptide started to move out through the top. Leu1 had high electrostatic electrostatic energies with the P layer. Leu1, Ile4-Leu5, Gln12-Ala13 and Lys18 anchored the peptide to the membrane depending on the initial position within the membrane. The kink between Lys11-Gln12-Ala13-His14 was conserved meaning that the lipid interactions did not affect the secondary structure of the peptide in this area. And in the bottom MD simulations of the POPE-pVEC system including the SMD snapshot taken from Begüm Alaybeyoğlu (simulation carried out at 300 K) the peptide started moving out of the membrane through the top. The peptide was anchored by Arg8-Ile9-Arg10-Lys11-Gln12-Ala13-His14. And Leu1 had high interaction with the lower P heads. The results of Alaybeyoğlu and the bottom simulations of the pVEC in POPE showed that the distance between Leu1 and the center of mass of lipids increased in the first frames. Energy increased as the upper residues left the membrane

through the top. Leu1 moved towards the middle of the membrane and stayed at -10 Å away from the middle of the membrane until the end of the simulation, the rest of the residues stretched between the lipid layers due to the pull of lower P heads. Similarly, Arg8-Ile9-Arg10-Lys11-Gln12 (which formed the hairpin structure) had higher interaction with the upper P layer. In all simulations, the secondary structure of the pVEC peptide did not assume an α-helical structure. The three simulations showed similar results, which means that the simulations were consistent with the simulations carried out by Begüm Alaybeyoğlu.

In the visual analysis of pVEC POPC MD simulations, in the top positions the residues that show interaction with the membrane differed. However; in both cases the peptide left the membrane through the top. Arg8-Ile9-Arg10-Lys11 formed a hairpin and the residues Leu1, Ile3 and Lys18 interacted with the membrane. The electrostatic energy between the peptide and the membrane lipids was initially low and continued to drop as the peptide moved away. In the middle simulations the peptide started to leave the membrane through the top. The energy increased towards the end where Leu1-Leu2-Ile3-Ile4-Leu5-Arg6-Arg7 anchored with Leu5 being more dominant. In both simulations the hairpin structure between Arg8-Ile9-Arg10-Lys11-Gln12 stayed intact. And in the bottom MD, the peptide started to leave the membrane through the top and had high interaction with the lower P layer. The hairpin structure composed of Arg8-Ile9-Arg10-Lys11 in the second simulation was not disturbed and these residues had high interaction with the membrane. Arg7-Arg8-Ile9-Arg10-Lys11 acted as an anchor. The energy increased as the simulation continued and oscilated between -800and -1000 kcal/mol. Ala15 had high interactions with the membrane. Arg8-Ile9-Arg10-Lys11-Gln12-Ala13-His14-Ala15-His16-Ser17-Lys18 stayed embedded in the top P head layer and caused increased energy. At the last frame the energy value was -900 to -1000 kcal/mol. Unlike the other simulations, in Pos1 the peptide assumed a helical structure between frames 41-43, with a maximum value of 30% helicity. This means that 5.4 out of 18 the residues had helical structure at this point. The helicity dropped to zero again as the simulation continued. The second simulation, however, did not assume a helical structure.

Table 5.7. The MD simulations peptide final positions.

		POPE Membrane	**POPC Membrane**
Melittin	Top	The peptide stays on the membrane.	The peptide stays on the membrane.
	Middle	The peptide starts moving out of the membrane through the top.	The peptide starts moving out of the membrane through the top.
	Bottom	The peptide stays in the membrane.	The peptide starts moving further into the membrane.
pVEC	Top	The peptide stays on the membrane.	The peptide moves out of the membrane through the top.
	Middle	The peptide starts moving out of the membrane through the top.	The peptide starts moving out of the membrane through the top.
	Bottom	The peptide starts moving out of the membrane through the top.	The peptide starts moving out of the membrane through the top.

From Table 5.7, overall the MD simulations showed that melttin was highly attracted to the POPE membrane P layer. In POPC membrane bottom simulations, melittin inserted itself further into the lipid membrane, which means that it voluntarily entered the POPC membrane. The pVEC peptide however started to move out of the membrane through the top in the POPC membrane even in the top simulation. In the POPE membrane pVEC stayed attached to the upper P layer in the top simulation whereas in POPC top simulation the peptide broke free and moved away from the membrane. In experimental studies, pVEC peptide did not have toxic effects on mammalian membranes [22]. Consequently, keeping the SMD simulation results in mind, it can be concluded that the pVEC peptide was more effective than melittin in bacterial cells.

6. FUTURE WORK

In future work, the effect of peptides on mammalian and bacterial cells can be investigated when in critical peptide/lipid ratio. These simulations would aid in understanding collective peptide actions and optimizing drug delivery systems. Also the results of SMD simulations showed differences between c.o.m. and N-terminus and slower velocity pulled simulations of melittin in POPE membrane. PMF calculations of these simulations may lead to a better understanding of the peptide penetration mechanisms.

REFERENCES

1. K. Lewis, “Platforms for antibiotic discovery,” *Nat Rev Drug Discov*, vol. 12, no. 5, pp. 371–387, 2013.

2. O. Skold, *Antibiotics and Antibiotic Resistance*. Portland, US.: John Wiley & Sons., 2011.

3. B. Mojsoska and H. Jenssen, “Peptides and Peptidomimetics for Antimicrobial Drug Design,” *Pharmaceuticals*, vol. 8, no. 3, pp. 366–415, 2015.

4. D. M. Copolovici, K. Langel, E. Eriste, and U. Langel, “Cell-Penetrating Peptides: Design, Synthesis, and Applications,” *ACS Nano*, vol. 8, no. 3, pp. 1972–1994, 2014.

5. M. Mäe, H. Myrberg, S. El-Andaloussi, and Ü.¨Langel, “Design of a tumor homing cell-penetrating peptide for drug delivery,” *Int. J. Pept. Res. Ther.*, vol. 15, pp. 11–15, 2009.

6. J. C. Phillips*, R. Braun*, W. Wang*, J. Gumbart*, E. Tajkhorshid*, E. Villa*, and K. , Christophe Chipot†, Robert D. Skeel‡, Laxmikant Kalé‡, and Schulten*, “NIH Public Access,” vol. 15, no. 10, pp. 1203–1214, 2008.

7. S. Bernèche, M. Nina, and B. Roux, “Molecular dynamics simulation of melittin in a dimyristoylphosphatidylcholine bilayer membrane.,” *Biophys. J.*, vol. 75, no. 4, pp. 1603–1618, 1998.

8. C. I. E. von Deuster and V. Knecht, “Antimicrobial selectivity based on zwitterionic lipids and underlying balance of interactions.,” *Biochim. Biophys. Acta*, vol. 1818, no. 9, pp. 2192–201, 2012.

9. S. H. Campbell, M. K.& Farrell, *Biochemistry*, 7th editio. CA,USA: Brooks/Cole, 2010.

10. R. B. Gennis, *Biomembranes: Molecular Structure and Function*, 1st editio. Springer, 1989.

11. S. Mashaghi, T. Jadidi, G. Koenderink, and A. Mashaghi, *Lipid Nanotechnology*. 2013.

12. A. a Polyansky, P. E. Volynsky, A. S. Arseniev, and R. G. Efremov, "Adaptation of a membrane-active peptide to heterogeneous environment. I. Structural plasticity of the peptide.," *J. Phys. Chem. B*, vol. 113, no. 4, pp. 1107–19, 2009.

13. X. Zhao, H. Yu, L. Yang, Q. Li, and X. Huang, "Simulating the antimicrobial mechanism of human β-defensin-3 with coarse-grained molecular dynamics," *J. Biomol. Struct. Dyn.*, no. February 2015, pp. 1–8, 2015.

14. B. Alaybeyoglu, B. Sariyar Akbulut, and E. Ozkirimli, "A novel chimeric peptide with antimicrobial activity," *J. Pept. Sci.*, vol. 21, pp. 294–301, 2015.

15. "National Center for Biotechnology Information. PubChem Compound Database; CID=5497103." [Online]. Available: http://pubchem.ncbi.nlm.nih.gov/compound/5497103 . [Accessed: 12-May-2015].

16. "National Center for Biotechnology Information. PubChem Compound Database; CID=5282290." [Online]. Available: http://pubchem.ncbi.nlm.nih.gov/compound/5282290 . [Accessed: 12-May-2015].

17. S. J. Irudayam, T. Pobandt, and M. L. Berkowitz, "Free energy barrier for melittin reorientation from a membrane-bound state to a transmembrane state," *J. Phys. Chem. B*, vol. 117, pp. 13457–13463, 2013.

18. H. Myrberg, L. Zhang, M. Mäe, and Ü. Langel, "Design of a Tumor-Homing Cell-Penetrating Peptide," *Bioconjug. Chem.*, vol. 19, no. 1, pp. 70–75, 2008.

19. E. Jamasbi, S. Batinovic, R. a Sharples, M.-A. Sani, R. M. Robins-Browne, J. D. Wade, F. Separovic, and M. A. Hossain, "Melittin peptides exhibit different activity on different cells and model membranes.," *Amino Acids*, vol. 46, no. 12, pp. 2759–66, 2014.

20. K. P. Santo, S. J. Irudayam, and M. L. Berkowitz, "Melittin creates transient pores in a lipid bilayer: Results from computer simulations," *J. Phys. Chem. B*, vol. 117, pp. 5031–5042, 2013.

21. F. Madani, S. Lindberg, Ü. Langel, S. Futaki, and A. Gräslund, “Mechanisms of Cellular Uptake of Cell-Penetrating Peptides,” *J. Biophys.*, vol. 2011, pp. 1–10, 2011.

22. E. Koren and V. P. Torchilin, “Cell-penetrating peptides: Breaking through to the other side,” *Trends Mol. Med.*, vol. 18, no. 7, pp. 385–393, 2012.

23. I. O. Akdag and E. Ozkirimli, “The Uptake Mechanism of the Cell-Penetrating pVEC Peptide,” *J. Chem.*, vol. 2013, pp. 1–9, 2013.

24. A. Elmquist, M. Hansen, and U. Langel, “Structure-activity relationship study of the cell-penetrating peptide pVEC.,” *Biochim. Biophys. Acta*, vol. 1758, no. 6, pp. 721–729, 2006.

25. Y. H. Nan, I.-S. Park, K.-S. Hahm, and S. Y. Shin, “Antimicrobial activity, bactericidal mechanism and LPS-neutralizing activity of the cell-penetrating peptide pVEC and its analogs.,” *J. Pept. Sci.*, vol. 17, no. 12, pp. 812–7, 2011.

26. M. E. Herbig, F. Assi, M. Textor, and H. P. Merkle, “The cell penetrating peptides pVEC and W2-pVEC induce transformation of gel phase domains in phospholipid bilayers without affecting their integrity,” *Biochemistry*, vol. 45, pp. 3598–3609, 2006.

27. C. H. Chen, G. Wiedman, A. Khan, and M. B. Ulmschneider, “Biochimica et Biophysica Acta Absorption and folding of melittin onto lipid bilayer membranes via unbiased atomic detail microsecond molecular dynamics simulation ☆,” *BBA - Biomembr.*, vol. 1838, no. 9, pp. 2243–2249, 2014.

28. S. J. Irudayam and M. L. Berkowitz, “Influence of the arrangement and secondary structure of melittin peptides on the formation and stability of toroidal pores,” *Biochim. Biophys. Acta - Biomembr.*, vol. 1808, no. 9, pp. 2258–2266, 2011.

29. G. Van Den Bogaart, J. V. Guzmán, J. T. Mika, and B. Poolman, “On the mechanism of pore formation by melittin,” *J. Biol. Chem.*, vol. 283, no. 49, pp. 33854–33857, 2008.

30. W. Wilcox and D. Eisenberg, “Thermodynamics of melittin tetramerization

determined by circular dichroism and implications for protein folding.," *Protein Sci.*, vol. 1, no. 5, pp. 641–53, 1992.

31. D. E. Schlamadinger, Y. Wang, J. A. McCammon, and J. E. Kim, "Spectroscopic and computational study of melittin, cecropin A, and the hybrid peptide CM15," *J. Phys. Chem. B*, vol. 116, no. 35, pp. 10600–10608, 2012.

32. S. J. Irudayam and M. L. Berkowitz, "Binding and reorientation of melittin in a POPC bilayer: Computer simulations," *Biochim. Biophys. Acta - Biomembr.*, vol. 1818, no. 12, pp. 2975–2981, 2012.

33. M. Andersson, J. P. Ulmschneider, M. B. Ulmschneider, and S. H. White, "Conformational states of melittin at a bilayer interface," *Biophys. J.*, vol. 104, no. 6, pp. L12–L14, 2013.

34. Y. Wang, D. E. Schlamadinger, J. E. Kim, and J. A. McCammon, "Comparative molecular dynamics simulations of the antimicrobial peptide CM15 in model lipid bilayers.," *Biochim. Biophys. Acta*, vol. 1818, no. 5, pp. 1402–9, 2012.

35. B. Isralewitz, M. Gao, and K. Schulten, "Steered molecular dynamics and mechanical functions of proteins," *Curr. Opin. Struct. Biol.*, vol. 11, no. 2, pp. 224–230, 2001.

36. M. I. Lobanov, N. S. Bogatyreva, and O. V Galzitskaia, "Radius of gyration is indicator of compactness of protein structure," *Mol. Biol. (Mosk).*, vol. 42, no. 4, pp. 701–706, 2008.

37. L. G. and F. P. Roberto STROM+, Carlo CRIFO+, Vincenza VITI, "Variations in circular dichroism and proton-NMR relaxation properties of melittin upon interaction with phospholipids," vol. 96, no. 1, 1978.

38. T. C. T. and D. Eisenberg, "The structure of melittin," *Eur. J. ...*, vol. 257, no. 11, pp. 6016–6022, 1988.

APPENDIX A: PROFILES OF SMD SIMULATIONS

A. SMD Simulations Snapshots and Graphs

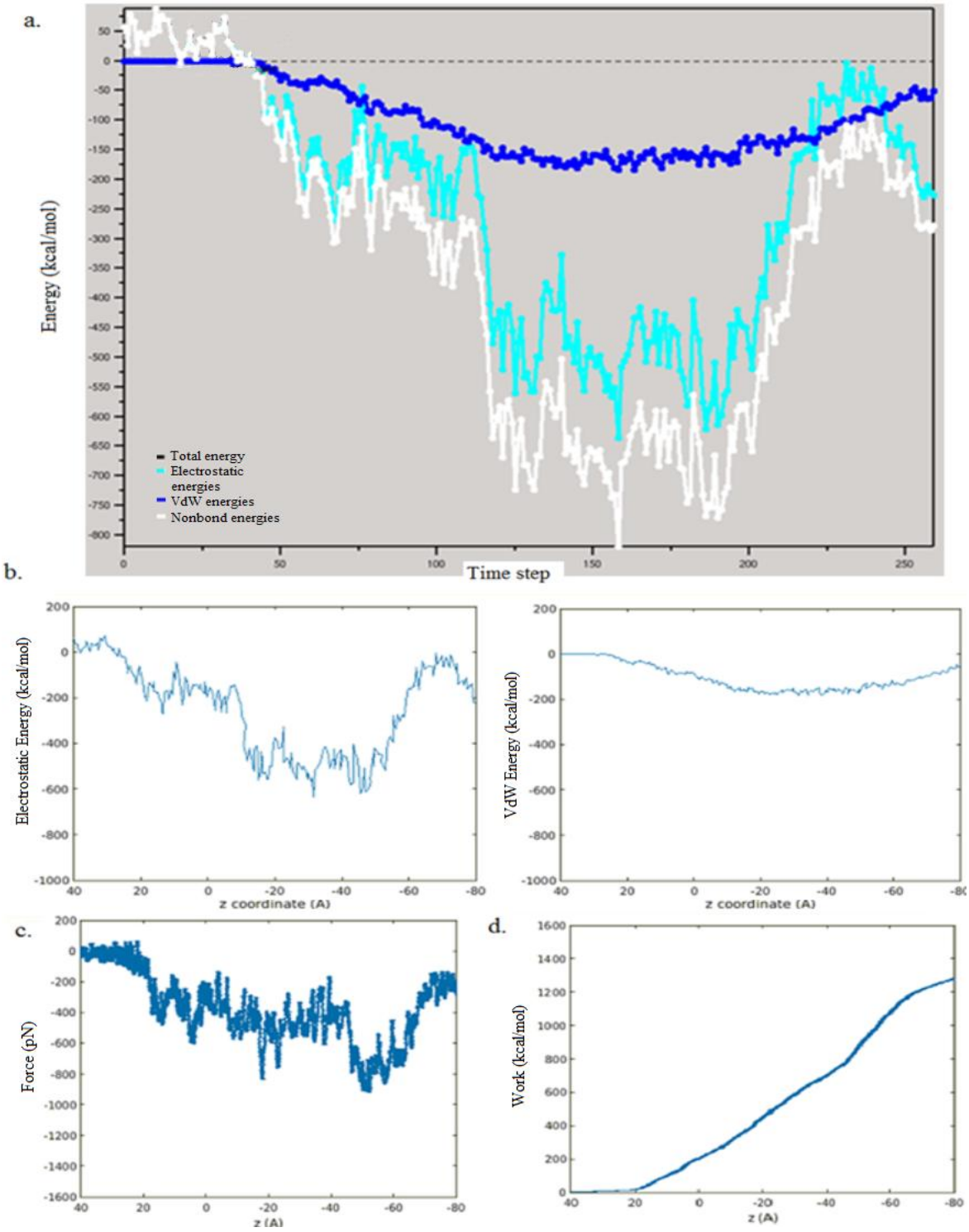

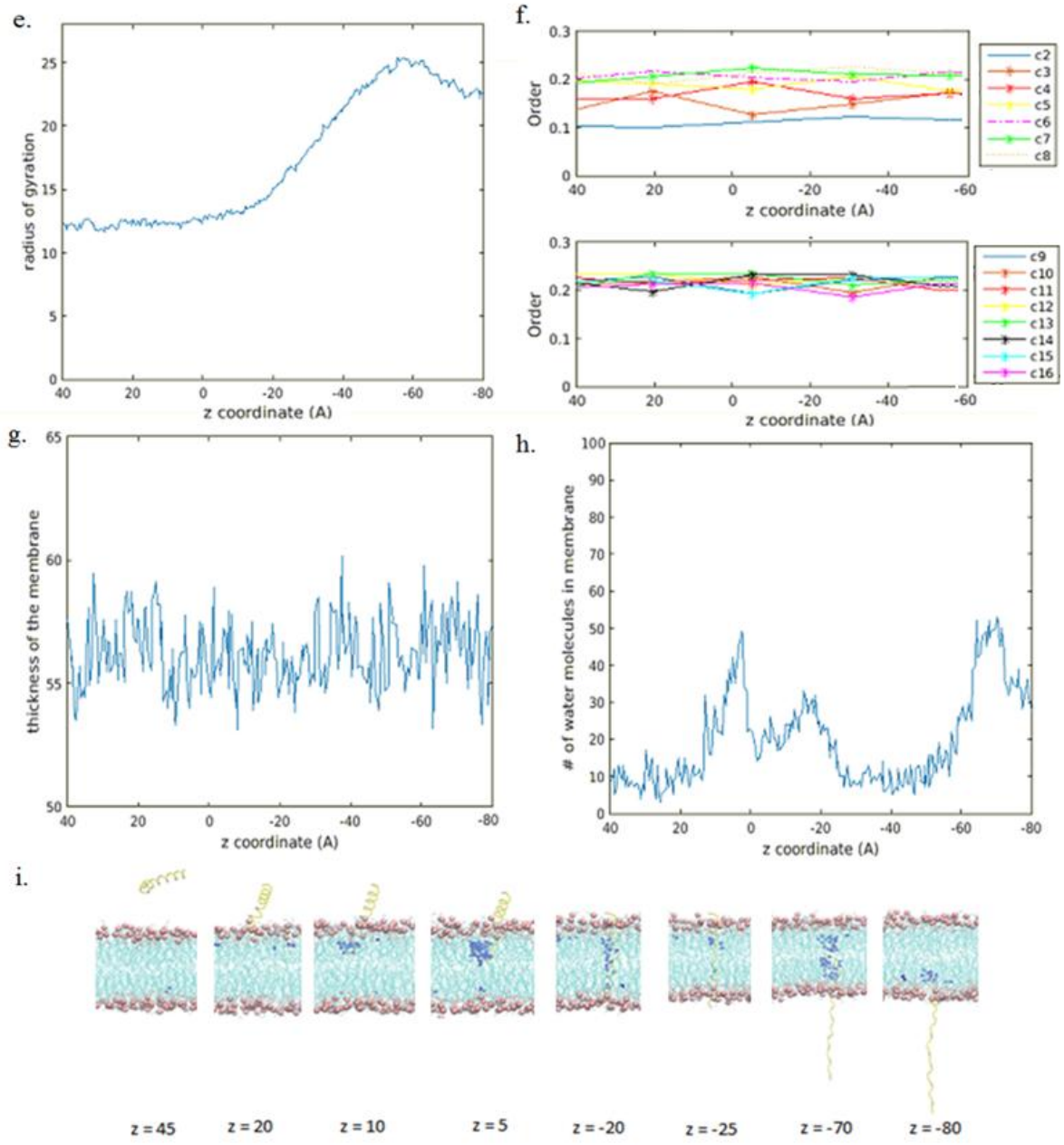

Figure A.1. The analysis graphics of the first melittin POPE SMD simulation. (a) The NAMD energy graph. (b) The electrostatic energy vs. z coordinates of Gly1 graph. (c) The force vs. z coordinates of Gly1 graph. (d) The work vs. z coordinates of Gly1 graph. (e) The radius of gyration vs. z coordinates of Gly1 graph. (f) The order of lipids vs. z coordinates of Gly1 graph. (g) The thickness of membrane vs. z coordinates of Gly1 graph. (h)The water in membrane vs. z coordinates of Gly1 graph. (i) The snapshots of the simulation showing the water molecules inside the membrane at certain z positions of Gly1.

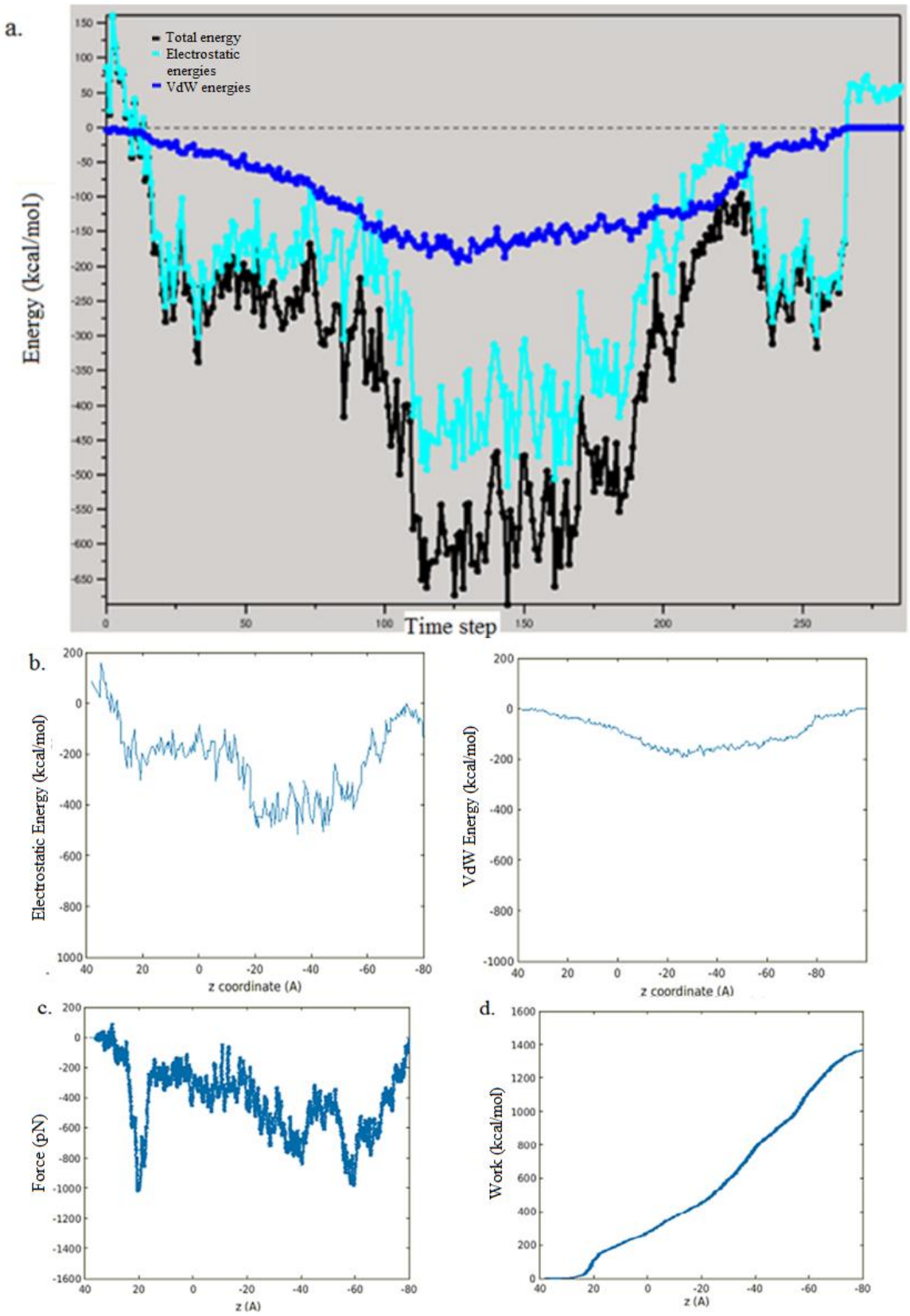
a.
Total energy
Electrostatic energies
VdW energies
Energy (kcal/mol)
Time step
b.
Electrostatic Energy (kcal/mol)
z coordinate (A)
VdW Energy (kcal/mol)
z coordinate (A)
c.
Force (pN)
z (A)
d.
Work (kcal/mol)
z (A)

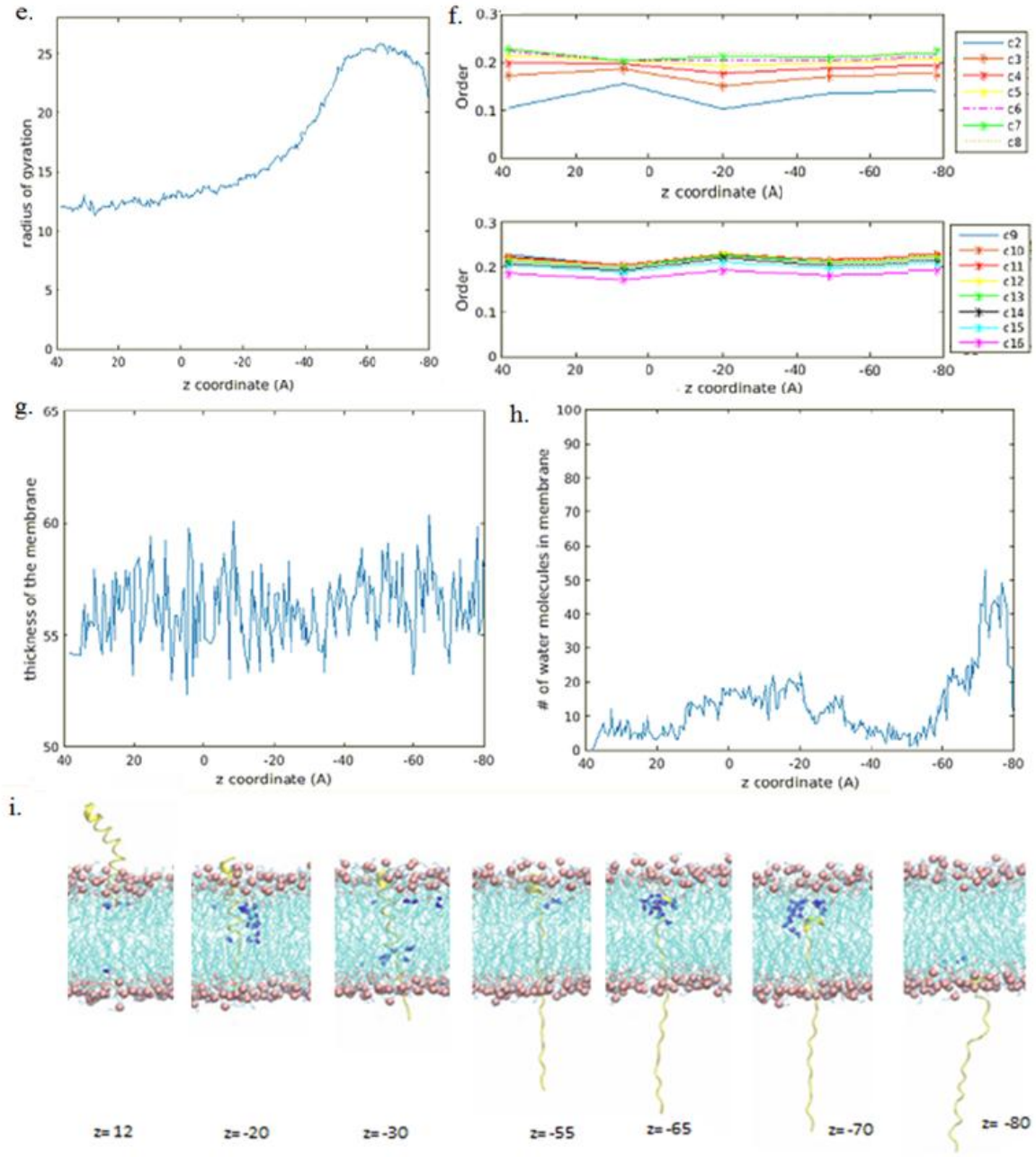

Figure A.2. The analysis graphics of the second melittin POPE SMD simulation. (a) The NAMD energy graph. (b) The electrostatic energy vs. z coordinates of Gly1 graph. (c) The force vs. z coordinates of Gly1 graph. (d) The work vs. z coordinates of Gly1 graph. (e) The radius of gyration vs. z coordinates of Gly1 graph. (f) The order of lipids vs. z coordinates of Gly1 graph. (g) The thickness of membrane vs. z coordinates of Gly1 graph. (h)The water in membrane vs. z coordinates of Gly1 graph. (i) The snapshots of the simulation showing the water molecules inside the membrane at certain z positions of Gly1.

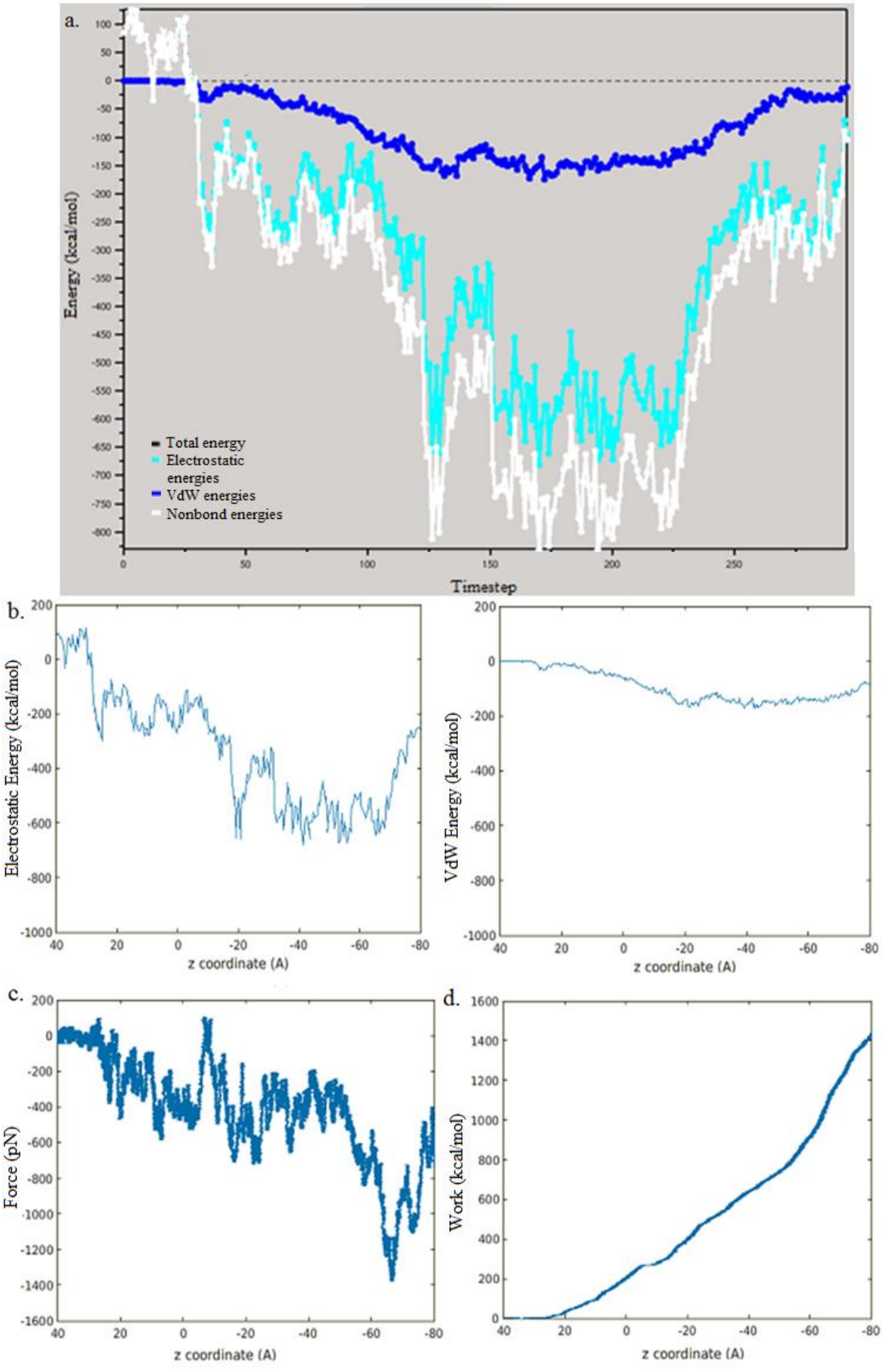
a.
Energy (kcal/mol)
Timestep
Total energy
Electrostatic energies
VdW energies
Nonbond energies
b.
Electrostatic Energy (kcal/mol)
z coordinate (A)
VdW Energy (kcal/mol)
z coordinate (A)
c.
Force (pN)
z coordinate (A)
d.
Work (kcal/mol)
z coordinate (A)

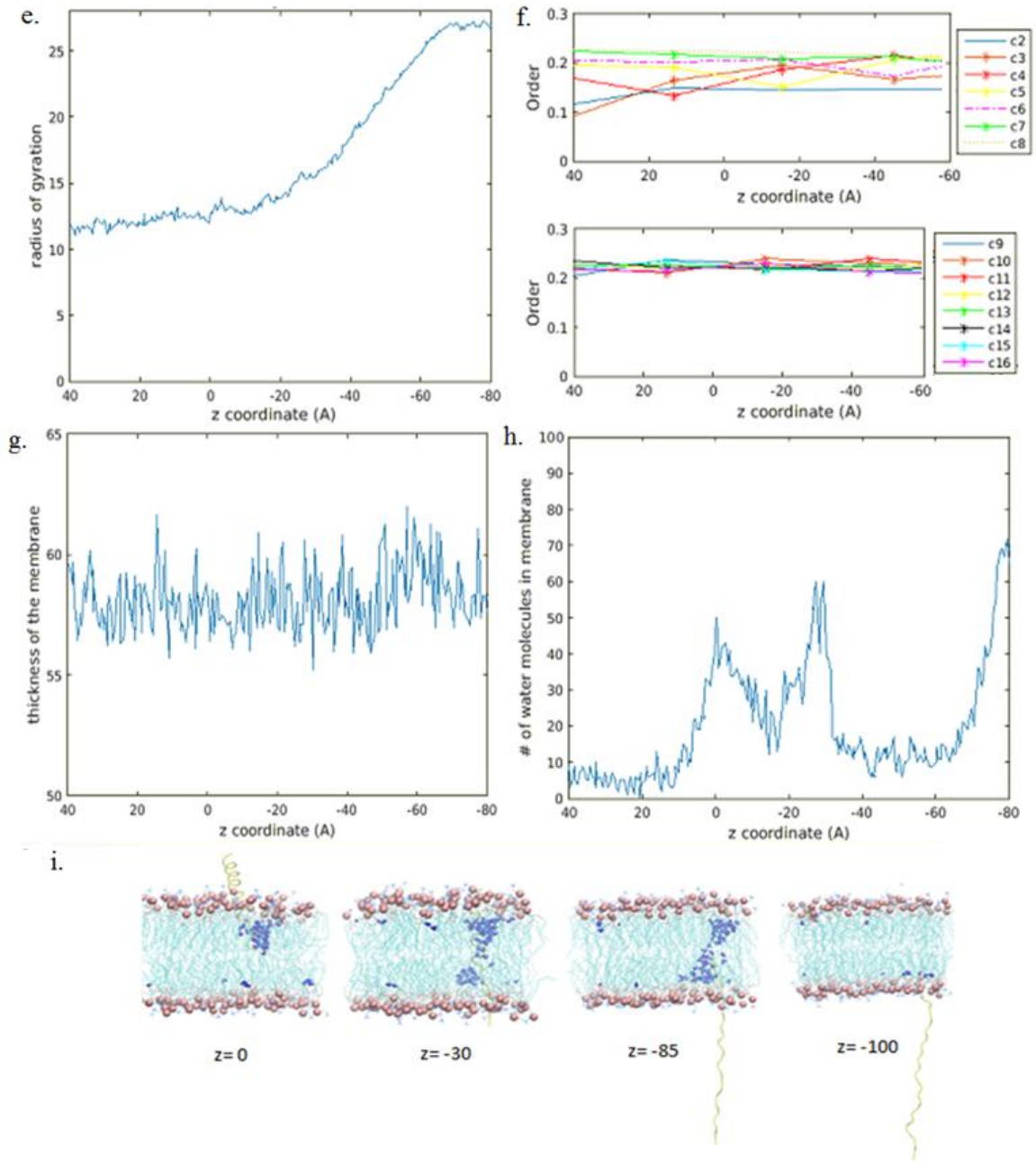

Figure A.3. The analysis graphics of the first melittin POPC SMD simulation. (a) (a) The NAMD energy graph. (b) The electrostatic energy vs. z coordinates of Gly1 graph. (c) The force vs. z coordinates of Gly1 graph. (d) The work vs. z coordinates of Gly1 graph. (e) The radius of gyration vs. z coordinates of Gly1 graph. (f) The order of lipids vs. z coordinates of Gly1 graph. (g) The thickness of membrane vs. z coordinates of Gly1 graph. (h)The water in membrane vs. z coordinates of Gly1 graph. (i) The snapshots of the simulation showing the water molecules inside the membrane at certain z positions of Gly1.

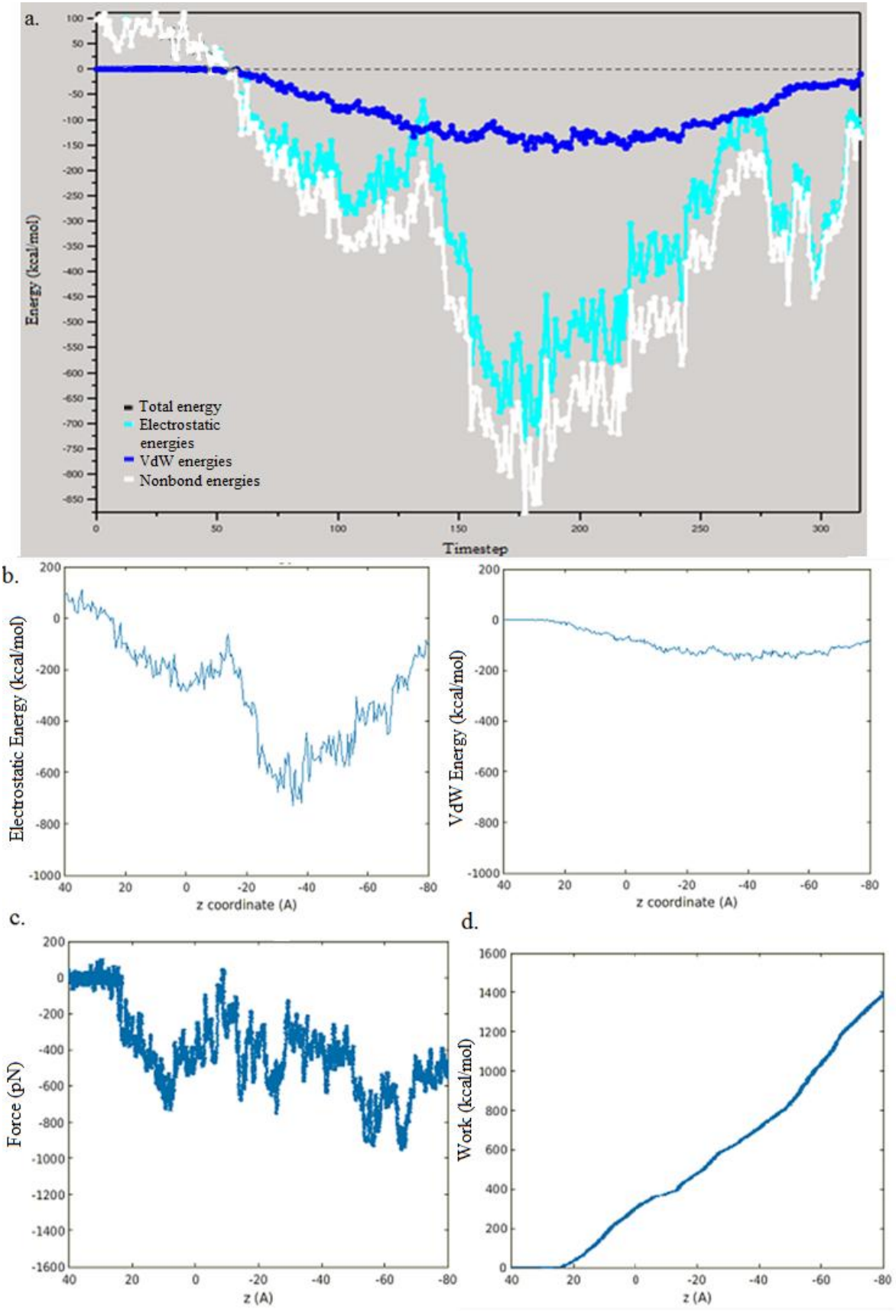
a.
Energy (kcal/mol)
Timestep
Total energy
Electrostatic energies
VdW energies
Nonbond energies
b.
Electrostatic Energy (kcal/mol)
z coordinate (A)
VdW Energy (kcal/mol)
z coordinate (A)
c.
Force (pN)
z (A)
d.
Work (kcal/mol)
z (A)

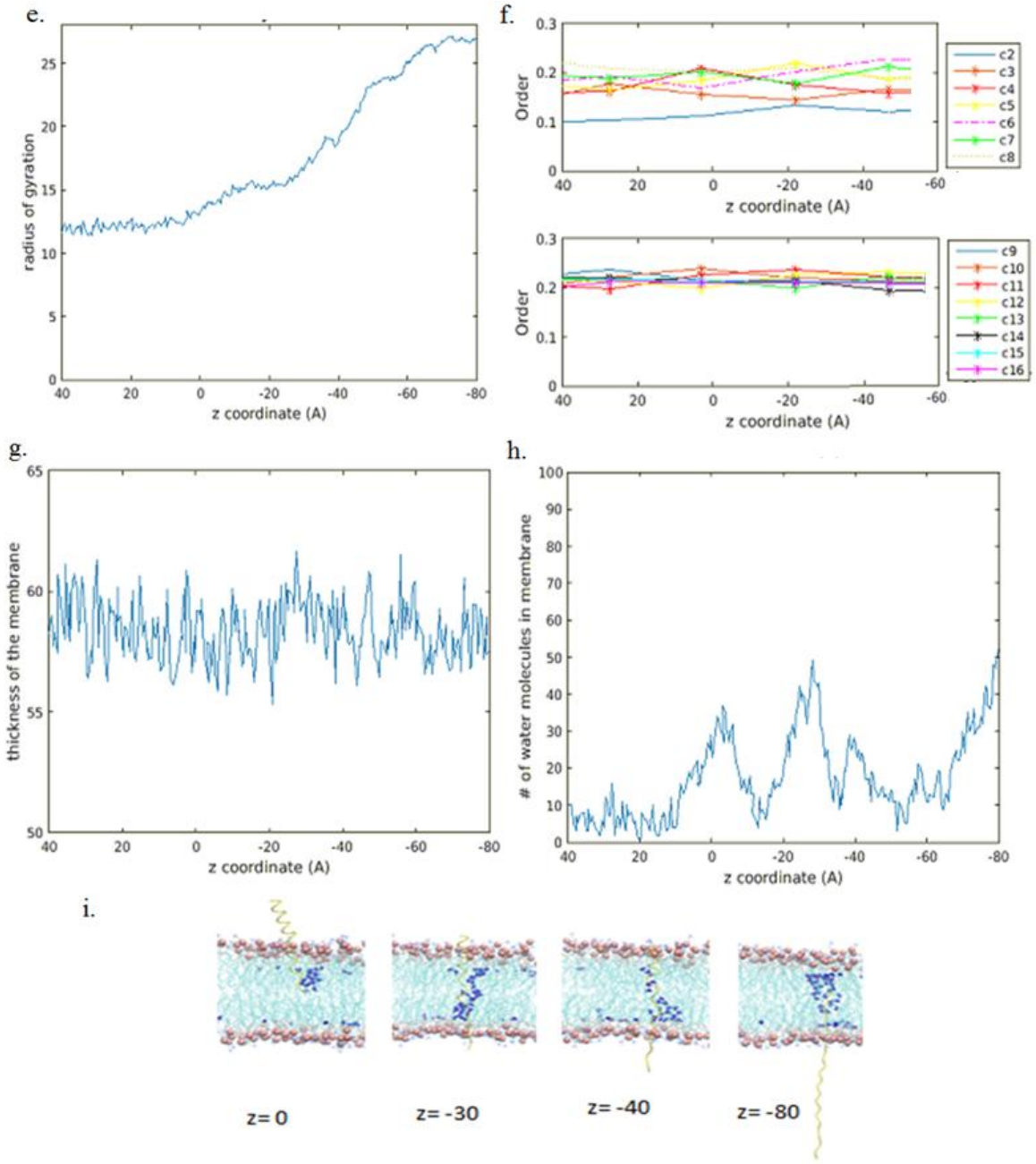

Figure A.4. The analysis graphics of the second melittin POPC SMD simulation. (a) The NAMD energy graph. (b) The electrostatic energy vs. z coordinates of Gly1 graph. (c) The force vs. z coordinates of Gly1 graph. (d) The work vs. z coordinates of Gly1 graph. (e) The radius of gyration vs. z coordinates of Gly1 graph. (f) The order of lipids vs. z coordinates of Gly1 graph. (g) The thickness of membrane vs. z coordinates of Gly1 graph. (h)The water in membrane vs. z coordinates of Gly1 graph. (i) The snapshots of the simulation showing the water molecules inside the membrane at certain z positions of Gly1.

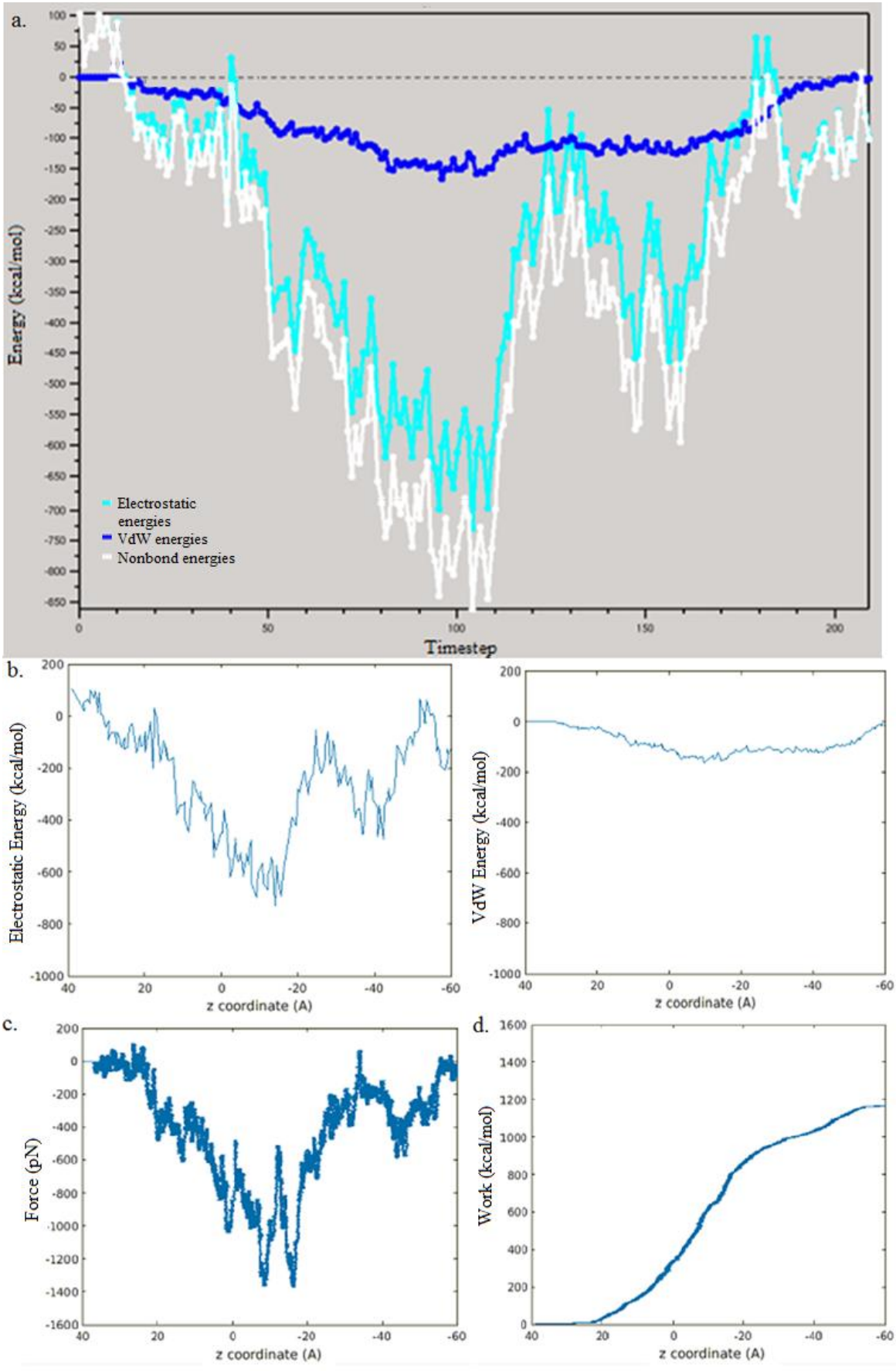
a.
Energy (kcal/mol)
Timestep
Electrostatic energies
VdW energies
Nonbond energies
b.
Electrostatic Energy (kcal/mol)
z coordinate (A)
VdW Energy (kcal/mol)
z coordinate (A)
c.
Force (pN)
z coordinate (A)
d.
Work (kcal/mol)
z coordinate (A)

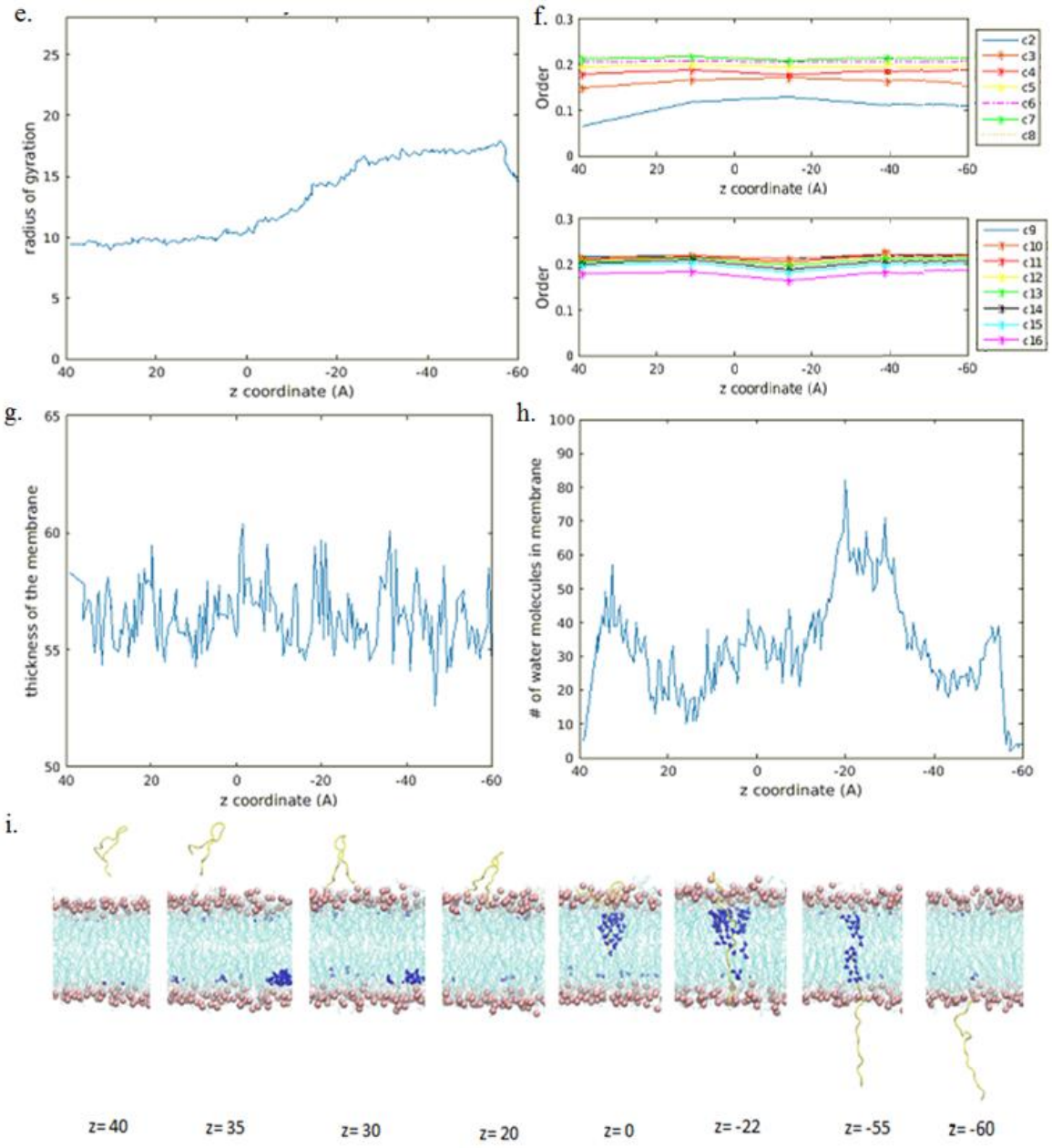

Figure A.5. The analysis graphics of the first pVEC POPE SMD simulation. (a) The NAMD energy graph. (b) The electrostatic energy vs. z coordinates of Leu1 graph. (c) The force vs. z coordinates of Leu1 graph. (d) The work vs. z coordinates of Leu1 graph. (e) The radius of gyration vs. z coordinates of Leu1 graph. (f) The order of lipids vs. z coordinates of Leu1 graph. (g) The thickness of membrane vs. z coordinates of Leu1 graph. (h) The water in membrane vs. z coordinates of Leu1 graph. (i) The snapshots of the simulation showing the water molecules inside the membrane at certain z positions of Leu1.

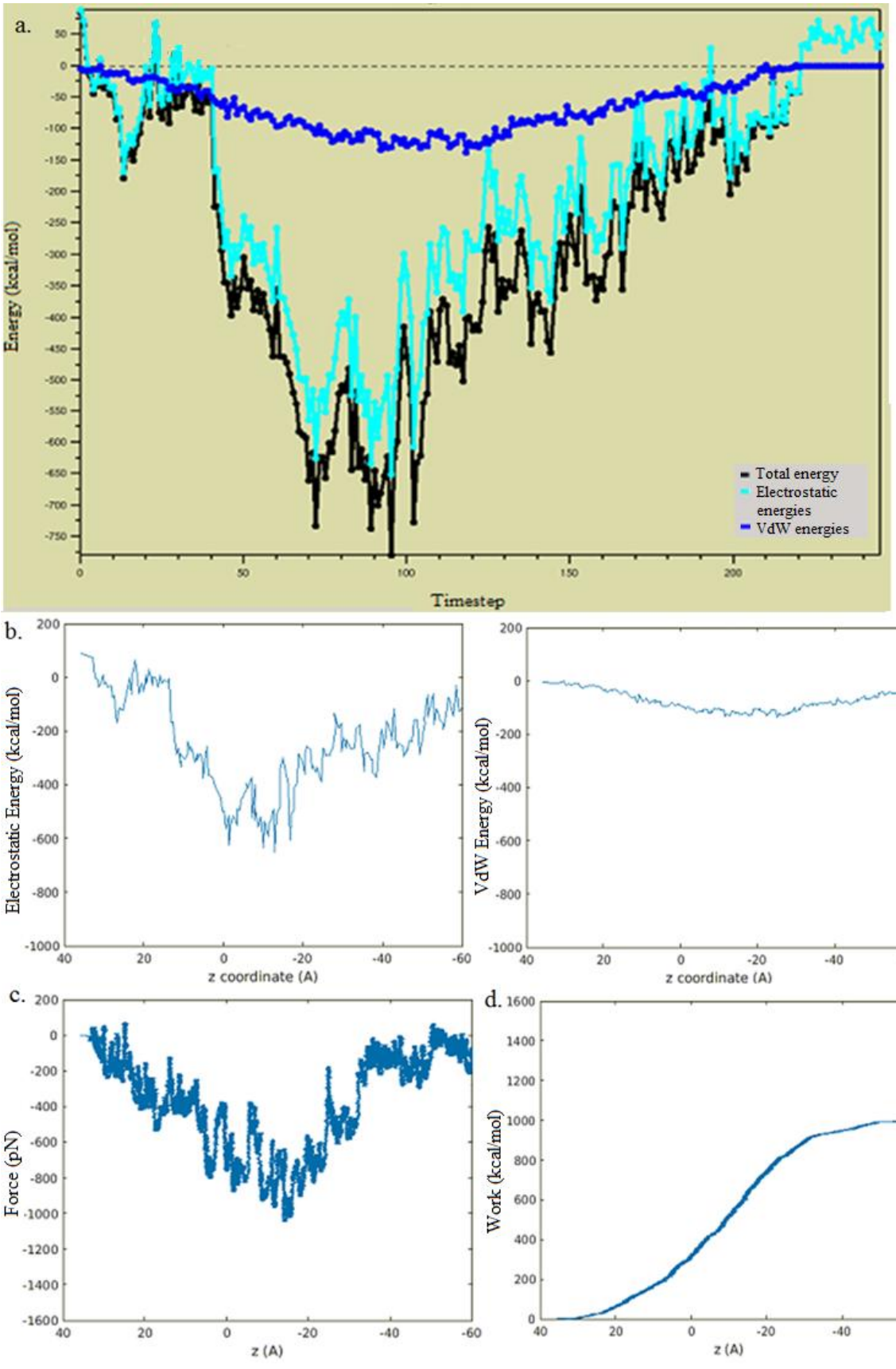
a.
Energy (kcal/mol)
Timestep
Total energy
Electrostatic energies
VdW energies
b.
Electrostatic Energy (kcal/mol)
z coordinate (A)
VdW Energy (kcal/mol)
z coordinate (A)
c.
Force (pN)
z (A)
d.
Work (kcal/mol)
z (A)

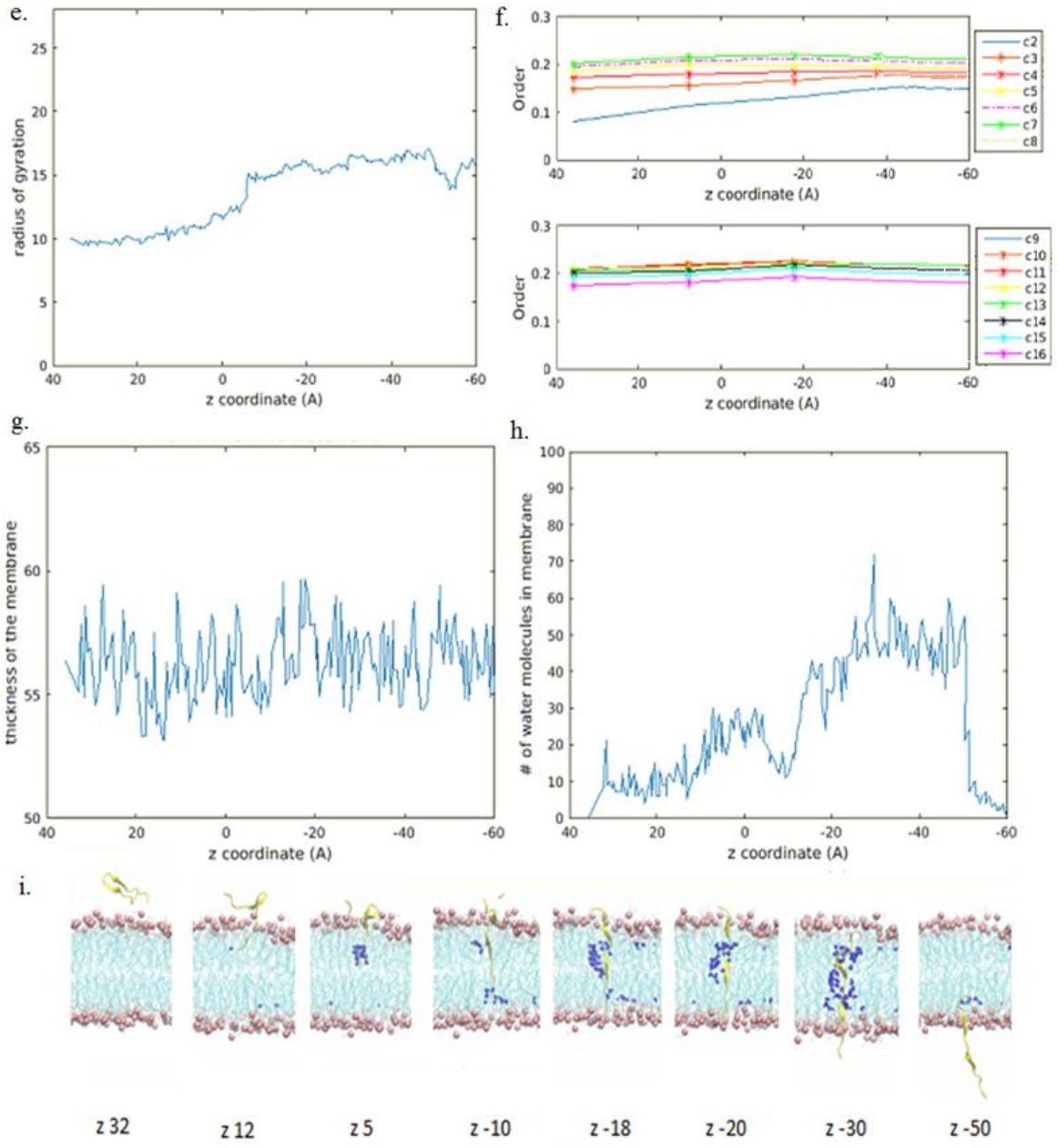

Figure A.6. The analysis graphics of the first pVEC POPE SMD simulation. (a) The NAMD energy graph. (b) The electrostatic energy vs. z coordinates of Leu1 graph. (c) The force vs. z coordinates of Leu1 graph. (d) The work vs. z coordinates of Leu1 graph. (e) The radius of gyration vs. z coordinates of Leu1 graph. (f) The order of lipids vs. z coordinates of Leu1 graph. (g) The thickness of membrane vs. z coordinates of Leu1 graph. (h) The water in membrane vs. z coordinates of Leu1 graph. (i) The snapshots of the simulation showing the water molecules inside the membrane at certain z positions of Leu1.

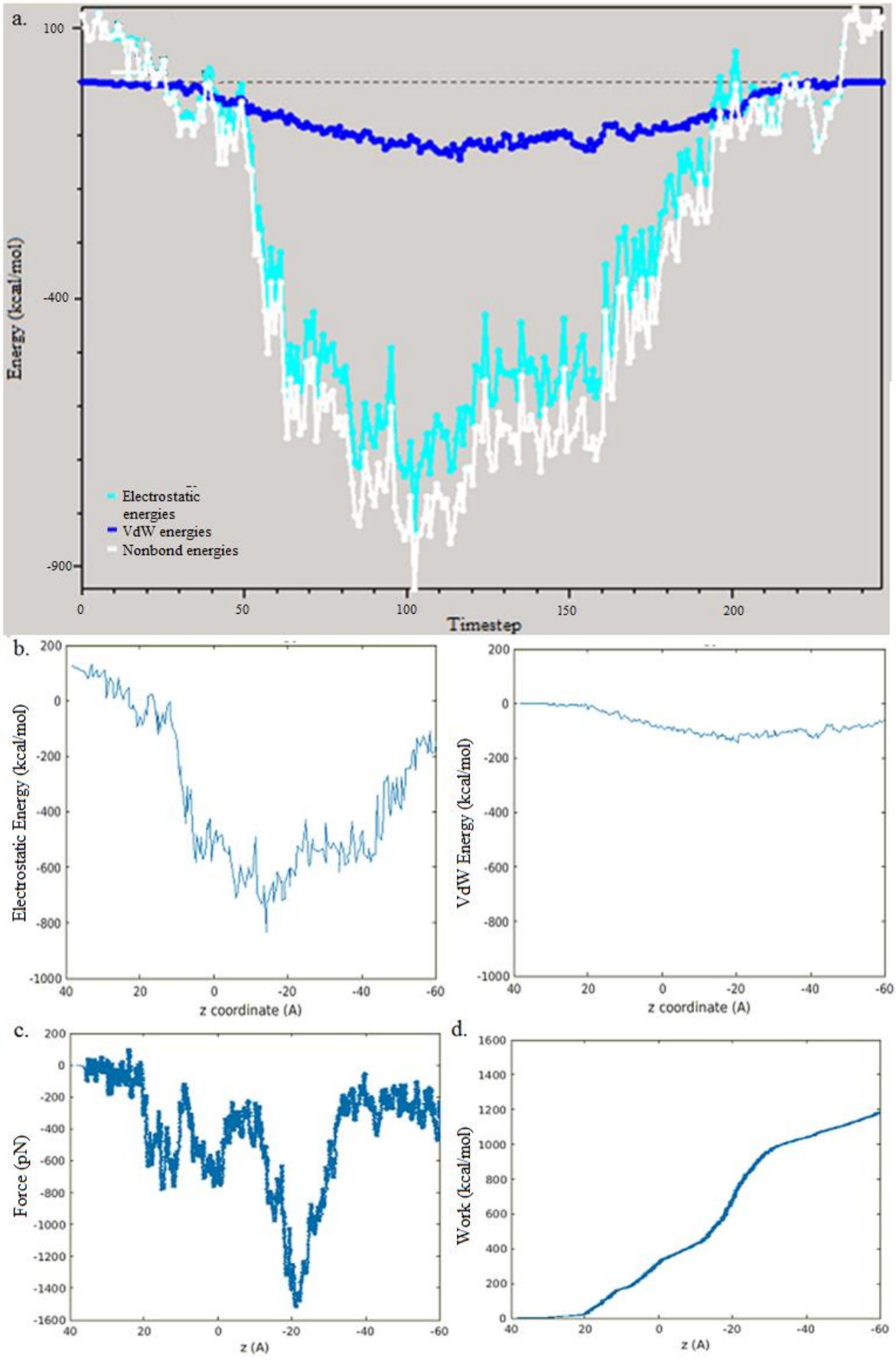
a.
Energy (kcal/mol)
Timestep
Electrostatic energies
VdW energies
Nonbond energies
b.
Electrostatic Energy (kcal/mol)
z coordinate (A)
VdW Energy (kcal/mol)
z coordinate (A)
c.
Force (pN)
z (A)
d.
Work (kcal/mol)
z (A)

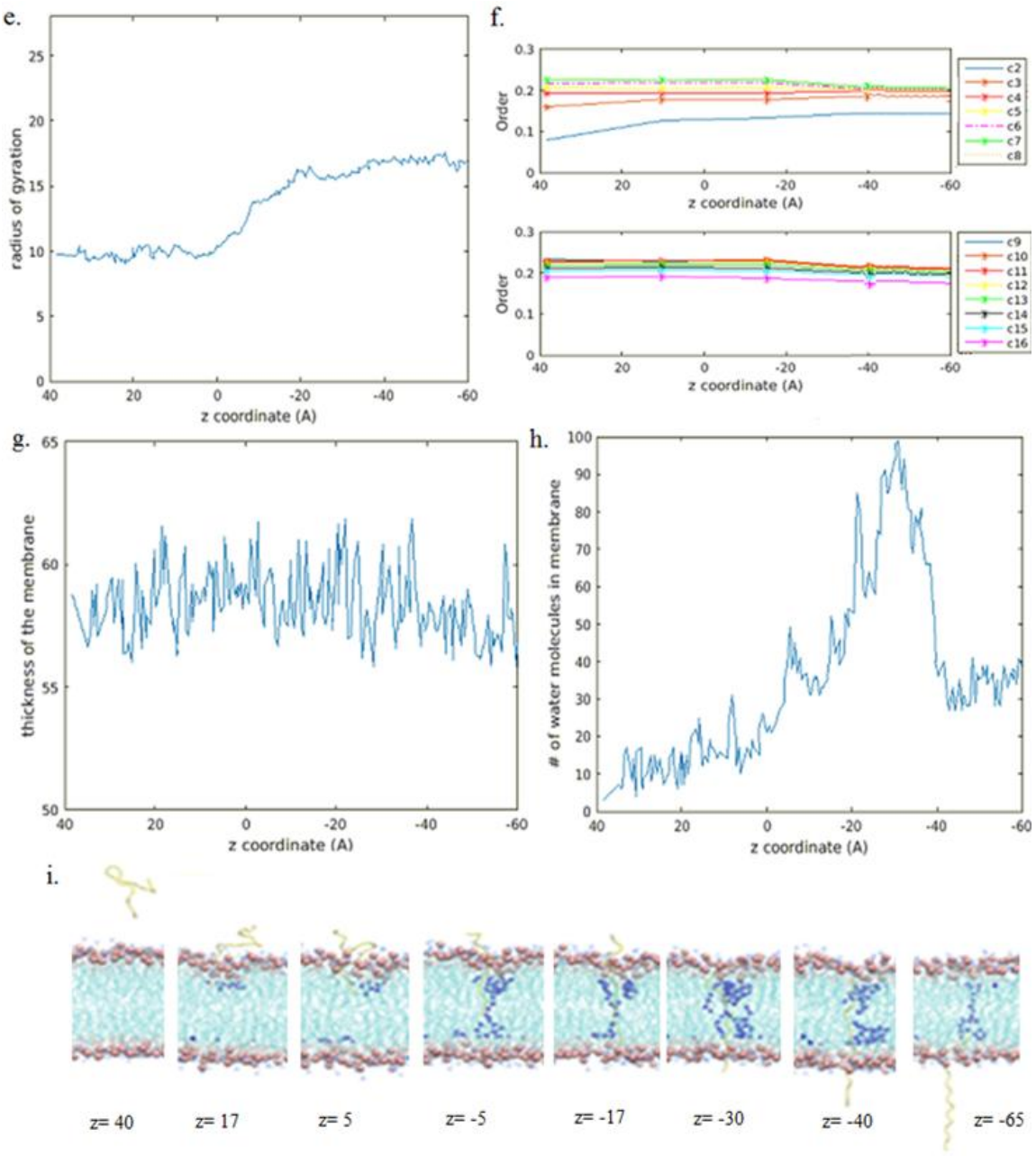

Figure A.7. The analysis graphics of the first pVEC POPC SMD simulation. (a) The NAMD energy graph. (b) The electrostatic energy vs. z coordinates of Leu1 graph. (c) The force vs. z coordinates of Leu1 graph. (d) The work vs. z coordinates of Leu1 graph. (e) The radius of gyration vs. z coordinates of Leu1 graph. (f) The order of lipids vs. z coordinates of Leu1 graph. (g) The thickness of membrane vs. z coordinates of Leu1 graph. (h) The water in membrane vs. z coordinates of Leu1 graph. (i) The snapshots of the simulation showing the water molecules inside the membrane at certain z positions of Leu1.

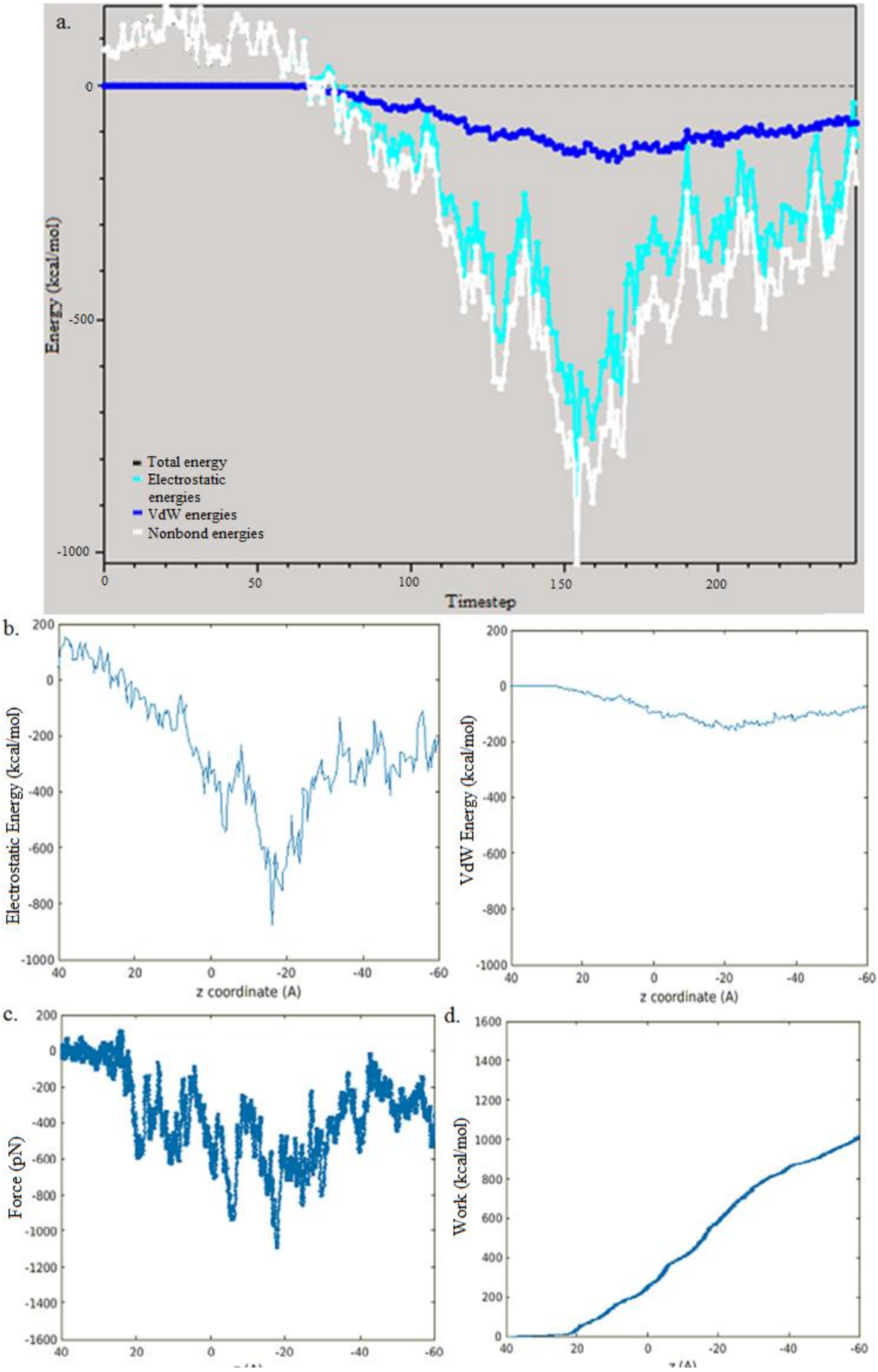
a.
Energy (kcal/mol)
0
-500
-1000
0
50
100
150
200
Timestep
Total energy
Electrostatic energies
VdW energies
Nonbond energies
b.
Electrostatic Energy (kcal/mol)
z coordinate (A)
VdW Energy (kcal/mol)
z coordinate (A)
c.
Force (pN)
d.
Work (kcal/mol)

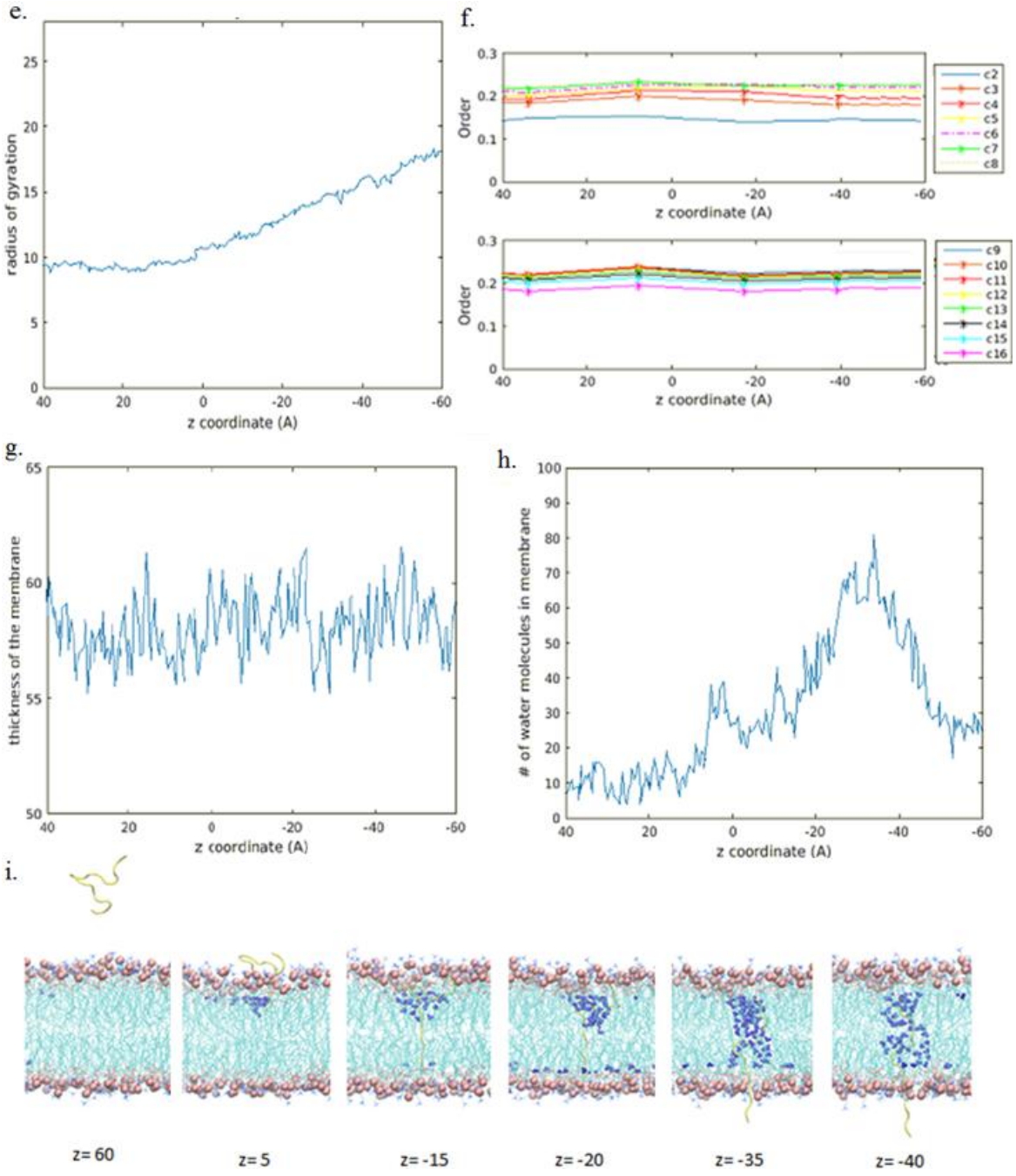

Figure A.8. The analysis graphics of the second pVEC POPC SMD simulation. (a) The NAMD energy graph. (b) The electrostatic energy vs. z coordinates of Leu1 graph. (c) The force vs. z coordinates of Leu1 graph. (d) The work vs. z coordinates of Leu1 graph. (e) The radius of gyration vs. z coordinates of Leu1 graph. (f) The order of lipids vs. z coordinates of Leu1 graph. (g) The thickness of membrane vs. z coordinates of Leu1 graph. (h) The water in membrane vs. z coordinates of Leu1 graph. (i) The snapshots of the simulation showing the water molecules inside the membrane at certain z positions of Leu1.

APPENDIX B: RESIDUE ENERGY ANALYSIS OF SMD SIMULATIONS

B. SMD Residue Analysis Graphs

B.1. Melittin in POPE - NAMD Energy Analysis of Protein Residues

The NAMD energy analysis gives the electrostatic energies of each residue with the system. The analysis of these results gives clues as to which residues play more important roles and which residues have less interactions with its surroundings. Understanding the roles of residues will help in designing more effective drugs. The following graphs show the electrostatic energy vs. z-coordinate of the α-carbon of the first residue of the peptide. The electrostatic energy plays a greater role then VDW and non-bond energies. The energies correlate to the interaction levels of the residues with its surroundings. Melittin is composed of the following residues: GIGAVLKVLTTGLPALISWIKRKRQQ

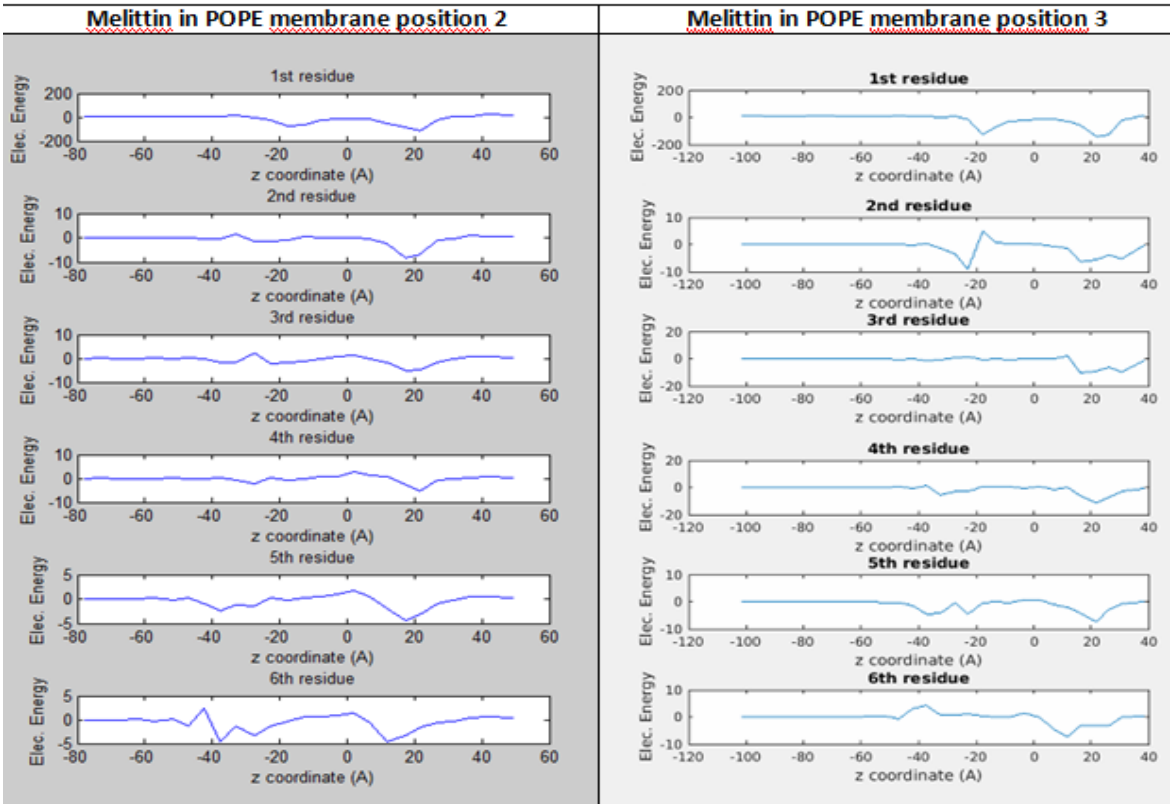

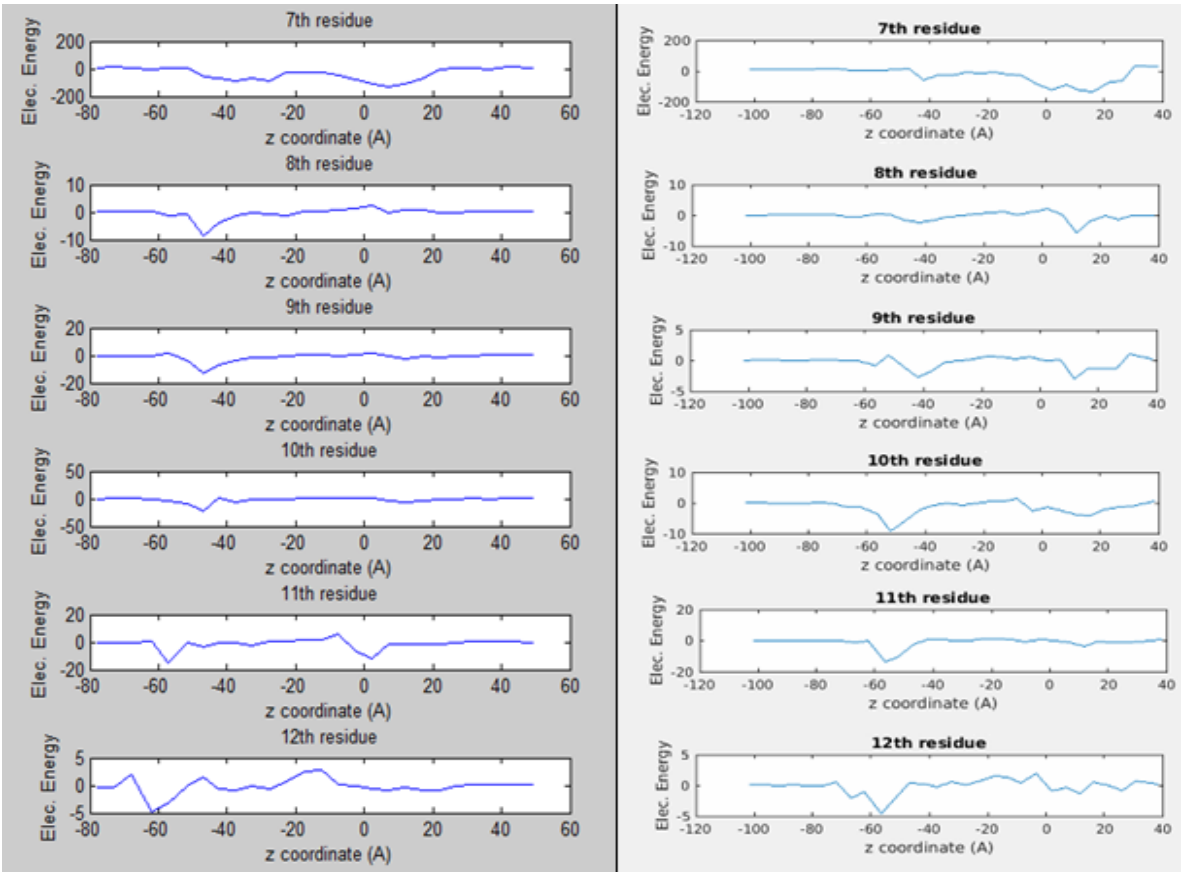
7th residue
8th residue
9th residue
10th residue
11th residue
12th residue
Elec. Energy
z coordinate (A)

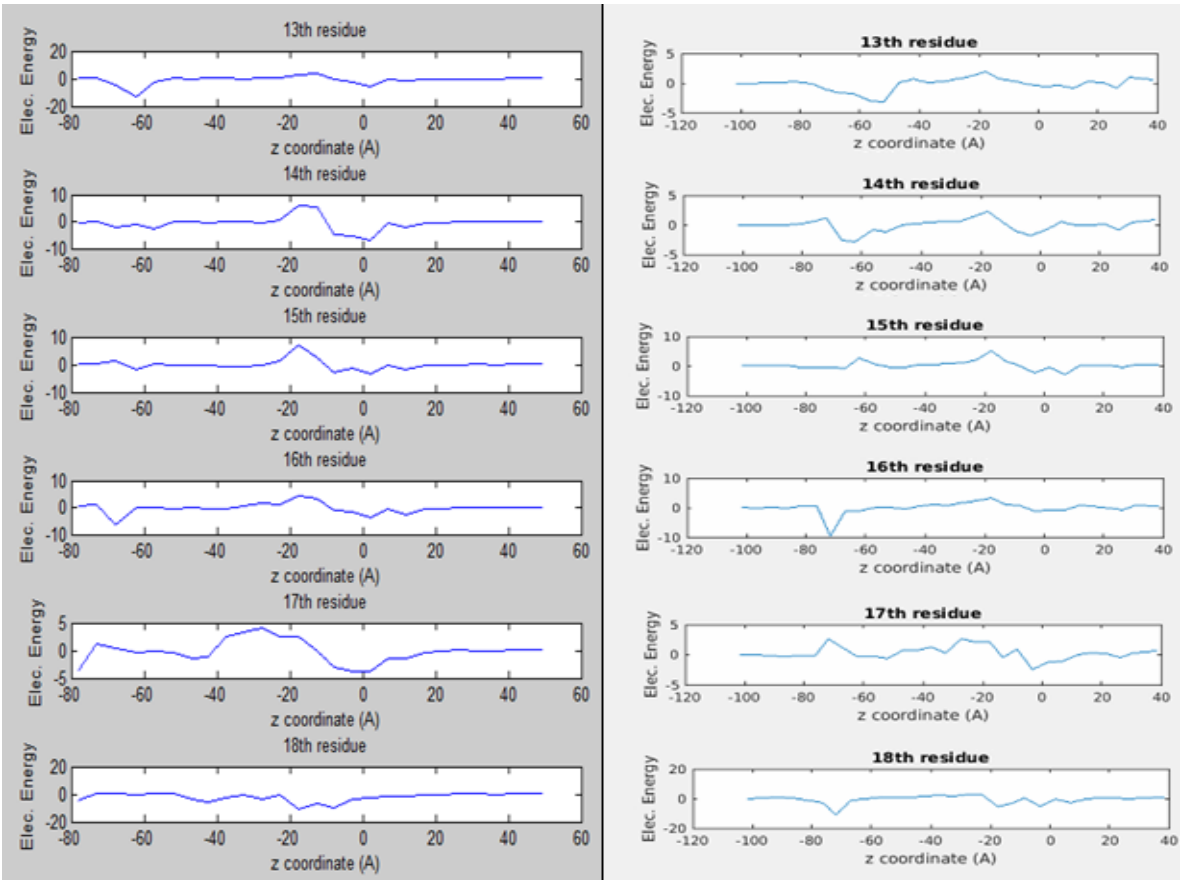
13th residue
14th residue
15th residue
16th residue
17th residue
18th residue
Elec. Energy
z coordinate (A)

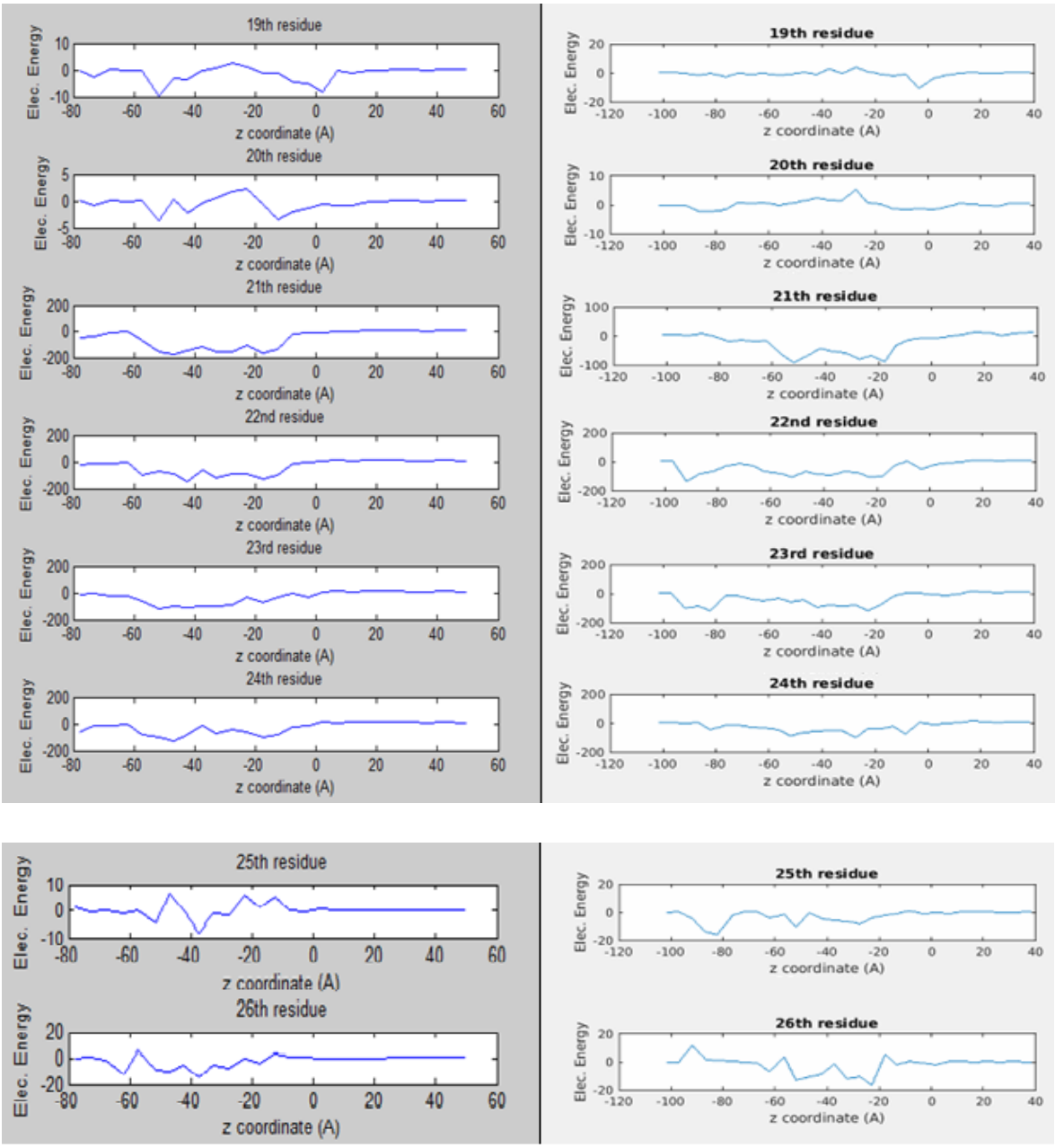

Figure B.1. The residue NAMD Energy graphs of Melittin in POPE SMD simulations. z is the position of the α-carbon of the first residue of the peptide which is glycine (units Å).

1-Gly: Glycine residue energy increases between z [-30, 30] Å for Pos1 simulation. For Pos1 peaks are at z -18 Å and 20 Å. For Pos2, the energy increase is at range z [35, -30] Å. Two peaks are at z -18 Å and z 25 Å. Overall, the first residue Glycine is active in the range z [-30, 35] Å. And most activity is in range z [20, 25] Å and around z [-18] Å.

2-Ile: Isoleucine residue energy increases between z [-40, 40] Å for Pos1 simulation. For Pos1 a peak is at z 18 and a drop of energy at z -35 Å. For Pos2, the energy increase is at range z [-40, 40] Å. Peaks are at z -22 Å and in range z [15, 30] Å. Also a drop of energy is at z -18 Å. Overall, the second residue Isoleucine is active in the range z [-40, 40] Å. And most activity is at range z [15, 30] Å and z [-35, -18] Å.

3-Gly: Glycine residue energy increases between z [-45, 40] Å for Pos1 simulation. For Pos1 a peak is at z 20 Å and drop of energy at z -25 Å. For Pos2, the energy increase is at range z [-50, 40] Å. A peak is at range z [10, 40] Å. Overall, the residue is active in the range z [-50, 40] Å. And most activity is in range z [10, 40] Å and around z -25 Å.

4-Ala: Alanine residue energy increases between z [-40, 30] Å for Pos1 simulation. For Pos1 peaks are at z 22 Å and z -2 Å 7. For Pos2, the energy increase is at range z [-45, 40] Å. Peaks are at z -35 Å and z 22 Å. Overall, the residue is active in the range z [-45, 40] Å. And most activity is in the range z [-35, -27] Å and around z [22] Å.

5-Val: Valine residue energy increases between z [-50, 40] Å for Pos1 simulation. Peaks are at z 18 Å and in range z [-45, -30] Å. Decrease in energy is at z 0. For Pos2, the energy increase is at range z [-45, 30] Å. Peaks are at z 22, -22 and -35 Å .Overall, the Valine residue is active in the range z [-50, 40] Å. And most activity is in ranges z [18, 22] Å and z [-45, -30] Å.

6-Leu: Leucine residue energy increases between z [-60, 40] Å for Pos1 simulation. For Pos1 peaks are at z -12, -27 and -38 Å. Drop of energy is at z 0 and -42 Å. For Pos2, the energy increase is at range z [-60, 25] Å. A large peak is at range z [0, 30] Å . Drop of energy is at range z [-45, -35] Å. Overall, the Leucine residue is active in the range z [-60, 40] Å. And most activity is in around z [-12] Å and ranges z [-45, -27] Å, z [0, 30] Å.

7-Lys: Lysine residue energy increases between z [-50, 40] Å for Pos1 simulation. For Pos1 peaks are at ranges z [-10, 20] Å and z [-50, -23] Å. For Pos2, the energy increase is at range z [-50, 35 Å]. Peaks are at range z [-10, 30] Å and at -42 Å. Overall, the Lysine residue is active in the range z [-50, 40] Å. And most activity is in ranges z [-50, -23] Å and z [-10, 30] Å.

8-Val: Valine residue energy increases between z [-60, 30] Å for Pos1 simulation. Peaks are at z 5 and -45 Å. For Pos2, the energy increase is at range z [-60, 30] Å. Peaks are at z 25, 15 and -42 Å. Overall, the Valine residue is active in the range z [-60, 30] Å. And most activity is in ranges z [-45, -42] and z [5, 25] Å.

9-Leu: Leucine residue energy increases between z [-60, 20] Å for Pos1 simulation. For Pos1 a peak is at z -45. For Pos2, the energy increase is at range z [-60, 40] Å. Peaks are at z -42 Å and range z [10, 30] Å. And a drop of energy is at z -55 Å. Overall, the Leucine residue is active in the range z [-60, 40] Å. And most activity is in range z [-55 ,-42] Å and z [10, 30] Å.

10-Thr:Threonine residue energy increases between z [-60, 20] Å for Pos1 simulation. For Pos1 a peak is at z -45. For Pos2, the energy increase is at range z [-65, 40] Å. Peaks are at z 18, -5 and -55 Å. Overall, the Leucine residue is active in the range z [-65, 40] Å. And most activity is in range z [-55,-45] Å and around z [18] Å and z[-5] Å.

11-Thr: Threonine residue energy increases between z [-65, 10] Å for Pos1 simulation. For Pos1 peaks are at z 2 and -58 Å. For Pos2, the energy increase is at range z [-65, 20] Å. A peaks is at z -58. Overall, the Threonine residue is active in the range z [-65, 20] Å. And most activity is in around z [2] Å and z [-58] Å.

12-Gly: Glycine residue energy increases between z [-75, 30] Å for Pos1 simulation. For Pos1 there is a large peak at z -62 Å. Energy drops are at z -15, -45 and -70 Å. For Pos2, the energy increase is at range z [-75, 40] Å. Little peaks are seen throughout the range, however, the largest peak is at z -57 Å. Overall, the Glycine residue is active in the range z [-75, 40] Å. And activity is throughout the range, however, the most significant activity is in range z [-62, -57] Å.

13-Leu: Leucine residue energy increases between z [-70, 15] Å for Pos1 simulation. For Pos1 peaks are at z -62 and 2 Å. For Pos2, the energy increase is at range z [-80, 40] Å. Peaks are at z 25, 15 and -55 Å. At z -20 the energy decreases. Overall, the Leucine residue is active in the range z [-80, 40] Å. And most activity is in ranges z [15, 20] Å and z [-62, -55] Å and around z [2] Å and z[-20] Å.

14-Pro: Proline residue energy increases between z [-80, 25] Å for Pos1 simulation. For Pos1 peaks are at range z [-5, 5] and a large peak at -57 Å. Energy decreases at z -15 Å. For Pos2, the energy increase is at range z [-80, 40] Å. Peaks are at z 25, -62 Å and at range z [-5, 5] Å. Decrease in energy is at z -18 and -75 Å. Overall, the Proline residue is active in the range z [-80, 40] Å. And most activity is in ranges z [-5, 5], z [-18, -15] and z [-75, -57] Å.

15-Ala: Alanine residue energy increases between z [-70, 20] Å for Pos1 simulation. For Pos1 peaks are at z 10, 2 -5 and -62 Å. Energy drop is at z -18 Å. For Pos2, the energy increase is at range z [-70, 30] Å. Peaks are at z 5 and -2 Å. Drop of energy are at z -18 and -60 Å. Overall, the Alanine residue is active in the range z [-70, 30] Å. And most activity is in ranges z [-5, 10] and z [-62, -60] and around z [-18] Å.

16-Leu: Leucine residue energy increases between z [-75, 25] Å for Pos1 simulation. For Pos1 peaks are at z 10, 2 and -68 Å. Decrease in energy at z -18 Å is also . For Pos2, the energy increase is at range z [-80, 40] Å. A peak is at z -70. Decrease in energy is at z -18. Overall, the Leucine residue is active in the range z [-80, 40] Å. And most activity is in ranges z [2, 10] and z [-70, -68] and around z [-18] Å.

17-Ile: Isoleucine residue energy increases between z [-80, 30] Å for Pos1 simulation. For Pos1 peaks are at z -70 Å and at range z [-10, 5] Å. Energy decrease is at z [-42, -15] Å. For Pos2, the energy increase is at range z [-80, 40] Å. Peaks are seen throughout the range z [-55, -5] Å. Decrease is at z -70 Å. Overall, the Isoleucine residue is active in the range z [-80, 40] Å. And most activity is in range z [-55, 5] and around z [-70] Å.

18-Ser: Serine residue energy increases between z [-60, 20] Å for Pos1 simulation. For Pos1 peaks are at z -18, 8 and at range [-50, 5] Å. For Pos2, the energy increase is at range z [-85, 10] Å. Peaks are at z -70, -18, -5 and 5 Å. Overall, the Serine residue is active in the range z [-85, 20] Å. And most activity is in ranges z [-50, 8] and around z [-70] Å.

19-Trp: Tryptophan residue energy increases between z [-80, 20] Å for Pos1 simulation. For Pos1 a peak is at z 2, -50 and -70 Å. For Pos2, the energy increase is at range z [-90, -20] Å. A peak is at z -5. Overall, the Tryptophan residue is active in the

range z [-90, 20] Å. And most activity is in ranges z [-5, 2] and around z [-50] and z[-75] Å.

20-Ile: Isoleucine residue energy increases between z [-80, 20] Å for Pos1 simulation. For Pos1 peaks are at z -15, -42 and -50 Å. Decrease is at z -22 Å. For Pos2, the energy increase is at range z [-90, 25]. Peak is at range z [-75, -85] Å . Overall, the Isoleucine residue is active in the range z [-90, 25] Å. And most activity is in ranges z [-25, -15], z [-50, -42] and [-80, -75] Å.

21-Lys: Lysine residue energy increases between z [-80, 15] Å for Pos1 simulation. For Pos1 large peaks are at range [-65, -10] Å. For Pos2, the energy increase is at range z [-90, 20] Å. Large peaks are at range [-65, -10] and at z -18 and -52 Å. Overall, the Lysine residue is active in the range z [-90, 20] Å. And most activity is in range z [-65, -10] Å.

22-Arg: Arginine residue energy increases between z [-70, 0] Å for Pos1 simulation. For Pos1 large peaks are at range [-65, -10] especially at -18, -35 and -42 Å. For Pos2, the energy increase is at range z [-100, 15] Å. Peaks are at z -2, -20,-40, -50 and -90 Å. Overall, the Arginine residue is active in the range z [-100, 15] Å. And most activity is in ranges z [-65, -2] and around z -90 Å.

23-Lys: Lysine residue energy increases between z [-65, 10] Å for Pos1 simulation. For Pos1 peaks are at z -5, -18 and -50 Å. For Pos2, the energy increase is at range z [-100, 0] Å. Peaks are at z -22, -42 and range z [-90, -82] Å. Overall, the Lysine residue is active in the range z [-100, 10] Å. And most activity is in range z [-22, -5], z [-50, -42] and z [-90, -82] Å.

24-Arg: Arginine residue energy increases between z [-80, 10] Å for Pos1 simulation. For Pos1 peaks are at range z -18, -37 and -45 Å. For Pos2, the energy increase is at range z [-90, 0] Å. Peaks are at z-10, -25, -50 and -82 Å. Overall, the Arginine residue is active in the range z [-90, 10] Å. And most activity is at range z [-25, -10], z [-50, -37] and around z [82] Å .

25-Gln: Glutamine residue energy increases between z [-80, 5] Å for Pos1 simulation. For Pos1 peaks are at z -38 and -50 Å. Energy decrease is at z -15, -22 and -45 Å. For Pos2, the energy increase is at range z [-100, -5] Å. Peaks are at range z -25, -50 and -82 Å.

Overall, the Glutamine residue is active in the range z [-100, 5] Å. And most activity is at range z [-50, -15] and around z [-82] Å.

26-Gln: Glutamine residue energy increases between z [-75, -10] Å for Pos1 simulation. For Pos1 peaks are at z -18, -38, -50 and -62 Å. Energy drop is at z -58 Å. For Pos2, the energy increase is at range z [-100, -10] Å. A peak is at z -22, -32, -55 and -62 Å. Energy drops are at z -18, -38, -58 and -95 Å. Overall, the Glutamine residue is active in the range z [-100, -10] Å. And most activity is at range z [-62, -18] and around z [-95] Å.

B.2. Melittin in POPC - NAMD Energy Analysis of Protein Residues

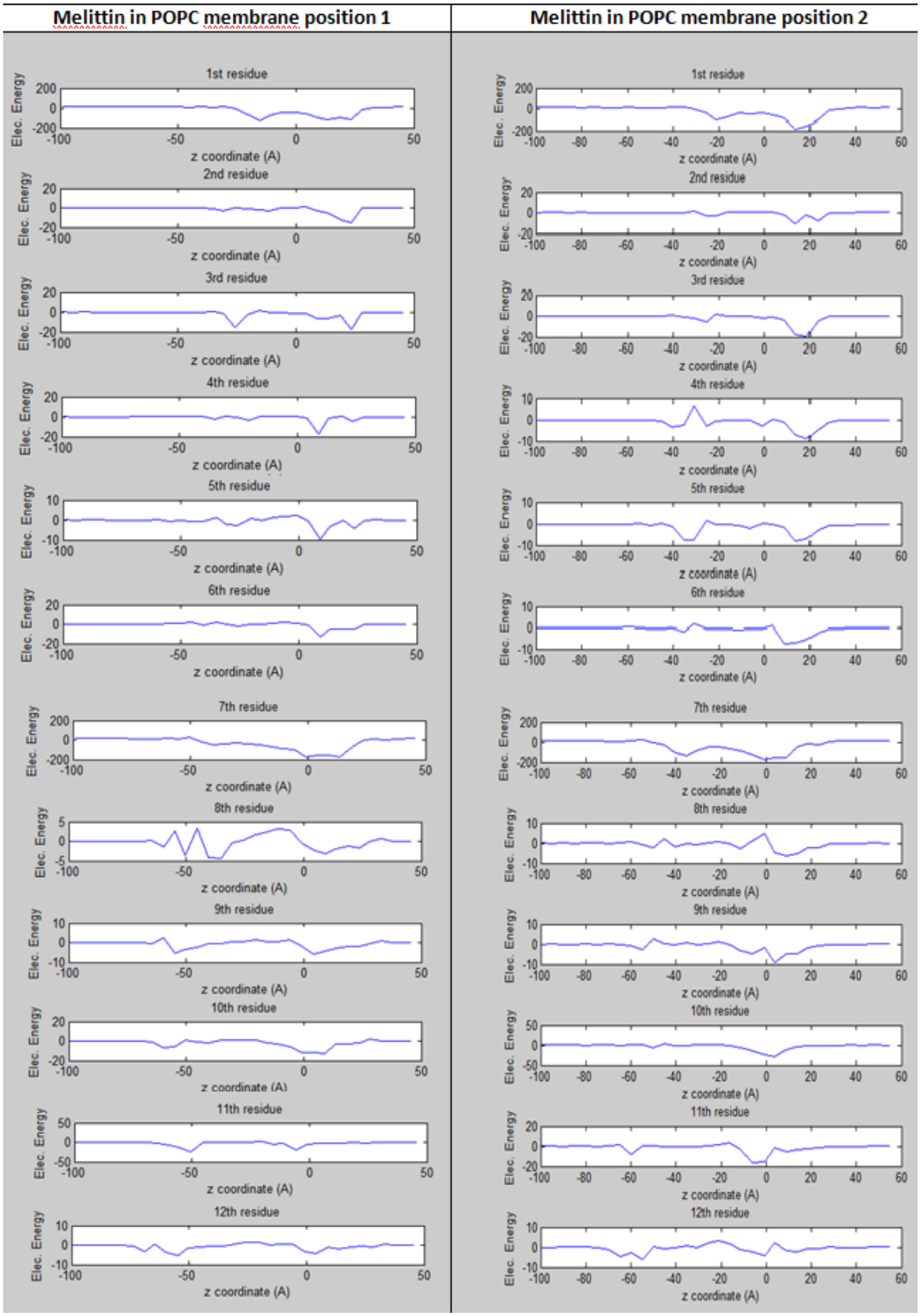

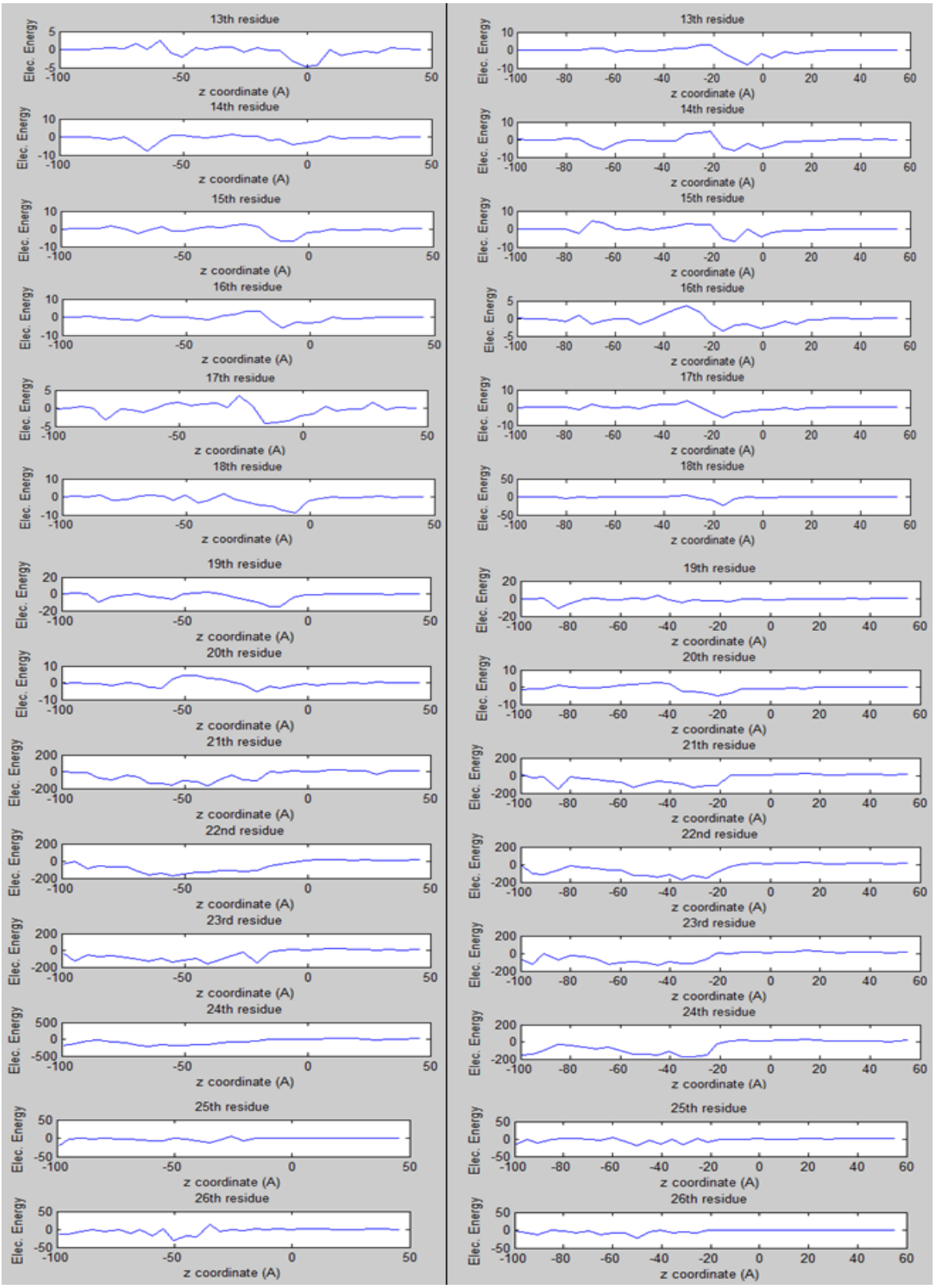

Figure B.2. The residue NAMD energy graphs of melittin in POPC SMD simulations. z is the position of the α-carbon of the first residue of the peptide which is glycine (units Å).

1-Gly: Glycine residue energy increases between z [25, -25] Å for the Pos1 simulation. For Pos1 peaks are at z -18 and 20 Å. For Pos2, the energy increase is at range z [25, -30] Å. Two peaks are at z -20 and z 15 Å. Overall, the first residue Glycine is active in the range z [25, -30] Å. And most activity is in ranges z [-18, -20] and z [20, 15] Å.

2-Ile: Isoleucine residue energy increases between z [-40, 25] Å for Pos1 simulation. For Pos1 a large peak is at z 25 Å and little peaks are at z -12 and z -30 Å. For Pos2, the energy increase is at range z [-35, 30] Å. Peaks are at z 22, 15 and -25 Å. Overall, the second residue Isoleucine is active in the range z [-40, 30] Å. And most activity is at range z [15, 25] Å and although less dominant in the range z [-30, -12] Å.

3-Gly: The Glycine residue energy increases between z [-40, 30] Å for Pos1 simulation. For Pos1 peaks are at z 24 and z -25 Å. For Pos2, the energy increase is at range z [-40, 30]. A high peaks is at z 18 and a low peak at z -25 Å. Overall, the residue is active in the range z [-40, 30] Å. And most activity is in range z [18, 24] Å and around z -25 Å.

4-Ala: Alanine residue energy increases between z [-45, 30] Å for Pos1 simulation. For Pos1 peaks are at z -30, z -20, z 25 Å and a large peak at z 10 Å. For Pos2, the energy increase is at range z [-45, 30] Å. Peaks are at z -40, z 0, a large peak at z 18 Å and a large drop of energy at z -30 Å. Overall, the residue is active in the range z [-45, 30] Å. And most activity is in the range z [10, 18] Å and least activity is at z 30 Å.

5-Val: Valine residue energy increases between z [-60, 25] Å for Pos1 simulation. Large peaks are at z 20 , 7 Å; lower peaks at z -20, -30 Å and decrease in energy is at z 0 and -35 Å. For Pos2, the energy increase is at range z [-60, 30] Å. Peaks are at z 25, 15, -5, -35 Å (15 and -35 being significantly larger) and decrease of energy is at z -25 Å. Overall, the Valine residue is active in the range z [-60, 30] Å. And most activity is in ranges z [7, 20] Å and while in Pos1 the energy decreases at z -35 Å whereas in Pos2 the energy increases.

6-Leu: Leucine residue energy increases between z [-60 30] Å for Pos1 simulation. For Pos1 peaks are at z 10 and -40 Å. For Pos2, the energy increase is at range z [-60, 25]

Å. A large peak is at z 10 Å .Another peak is at -35. Energy decrease is at z -30 Å. Overall, the Leucine residue is active in the range z [-60, 30] Å. And most activity is in around z [10] Å and range z [-35, -40] Å.

7-Lys: Lysine residue energy increases between z [-50 25] Å for Pos1 simulation. For Pos1 a large peak is at z 15-0 Å and a decrease of energy at z -50 Å. For Pos2, the energy increase is at range z [-60 30] Å. Peaks are at z 10-0 and -35 Å. Overall, the Lysine residue is active in the range z [-60 30]. And most activity is in ranges z [15, 0] Å and around z -35 Å. A decrease of energy is at z -50 Å.

8-Val: Valine residue energy increases between z [-70 35] Å for Pos1 simulation. Large peaks are at z -35, -40, -50 Å and a smaller peak at z 10 Å. Energy decrease is at z -10, -45 and -55 Å. For Pos2, the energy increase is at range z [-60, 30] Å. Peaks are at z 10, -10 and -50 Å. And an energy decrease is at z -0 Å. Overall, the Valine residue is active in the range z [-70, 35] Å. And most activity is in ranges z [-35 -50] Å.

9-Leu: Leucine residue energy increases between z [-65 40] Å for Pos1 simulation. For Pos1 peaks are at z 5, -55 Å and decrease of energy at z -60 Å. For Pos2, the energy increase is at range z [-65 30] Å. Peaks are at z 5 and -55 Å.Decrease of energy peaks are at z 0 and -50 Å. Overall, the Leucine residue is active in the range z [-65 40] Å. And most activity is in ranges z [0, 5] Å and z [-50,-60] Å.

10-Thr: Threonine residue energy increases between z [-65 30] Å for Pos1 simulation. For Pos1 peaks are at z-60 Å and range 0-10 Å. For Pos2, the energy increase is at range z [-55, 20] Å. Peaks are at z 5 and -50 Å. Overall, the Threonine residue is active in the range z [-65, 30] Å. And most activity is in ranges z [0, 10] and z [-50, -55] Å.

11-Thr: Threonine residue energy increases between z [-65 0] Å for Pos1 simulation. For Pos1 peaks are at z -5 and -50 Å. For Pos2, the energy increase is at range z [-65 10] Å. Peaks are at z -60 Å and range [0 -5] Å. Overall, the Threonine residue is active in the range z [-65 10] Å. And most activity is in ranges z [0 -5] and z [-60 -50] Å.

12-Gly: Glycine residue energy increases between z [-70, 30] Å for Pos1 simulation. For Pos1 peaks are at z 5, -55 and -70 Å. For Pos2, the energy increase is at range z [-70, 20] Å. Peaks are at z 0, -55, -65 Å and energy decrease is at z 5 and -20 Å. Overall, the

Glycine residue is active in the range z [-70, 30]. And most activity is in ranges z [0, 5] Å and z [-70, -55] Å.

13-Leu: Leucine residue energy increases between z [-75 40] Å for Pos1 simulation. For Pos1 peaks are at z -50, -65 Å and a large peak at range 0-5 Å. Decrease of energy is at z 10 and -60 Å. For Pos2, the energy increase is at range z [-65 20] Å. Peaks are at z 5 , -60 Å and a large peak at z -5 Å. At z -20 Å the energy decreases. Overall, the Leucine residue is active in the range z [-75, 40] Å. And most activity is in ranges z [-5, 5] and z [-60, -50] Å.

14-Pro: Proline residue energy increases between z [-80 15] Å for Pos1 simulation. For Pos1 peaks are at z -5 Å and a large peak at -65 Å. Energy decreases at z 10. For Pos2, the energy increase is at range z [-75, 20] Å. Peaks are at z 0, -10 and -65 Å. A large decrease in energy is at z -20 Å. Overall, the Proline residue is active in the range z [-80, 20] Å. And most activity is in ranges z [0 -10] Å and around z -65 Å.

15-Ala: Alanine residue energy increases between z [-80, 20] Å for Pos1 simulation. For Pos1 a peak is at z -70 Å and a large peak at range z [-10, -5] Å . For Pos2, the energy increase is at range z [-80, 20] Å. Peaks are at z 0 , -10 and -75 Å. Drop of energy are at z -5, -20 and -70 Å. Overall, the Alanine residue is active in the range z [-80, 20] Å. And most activity is in ranges z [-10, 0] and z [-75, -70] Å.

16-Leu: Leucine residue energy increases between z [-65, 20] Å for Pos1 simulation. For Pos1 peaks are at z -40, -60 Å and a large peak at -10 Å. Decrease in energy are at z 10 and -20 Å. For Pos2, the energy increase is at range z [-80, 20] Å. Peaks are at z 15, 0, -18, -50 and -70 Å.Decrease in energy are at z -30 and -75 Å. Overall, the Leucine residue is active in the range z [-80, 20] Å. And most activity is in ranges z [15, 0], z [-10, -20] and z [-40, -75] Å.

17-Ile: Isoleucine residue energy increases between z [-85, 40] Å for Pos1 simulation. For Pos1 peaks are at z -30, -65 Å and large peaks at z -20 and -80 Å. Energy decreases are at z 30, 10 and -25 Å. For Pos2, the energy increase is at range z [-80, 20] Å. Peaks are at z -18 and -75 Å. Decrease is at z -30. Overall, the Isoleucine residue is active in the range z [-85, 40] Å. And most activity is in ranges z [-18, -30] and z [-65, -80] Å.

18-Ser: Serine residue energy increases between z [-80, 10] Å for Pos1 simulation. For Pos1 peaks are at z -5, -45 and -55 Å. Decrease is at z -35. For Pos2, the energy increase is at range z [-80, 10] Å. A Peak is at z -18 Å. Overall, the Serine residue is active in the range z [-80, 10] Å. And most activity is in ranges z [-18, -5] and z [-35, -55] Å.

19-Trp: Tryptophan residue energy increases between z [-90, -5] Å for Pos1 simulation. For Pos1 peaks are at z -55, -85 Å and a large peak at range z [-15, -10] Å. For Pos2, the energy increase is at range z [-90, -20] Å. Peaks are at z -35 Å, a large one at -85 Å and a decrease at z -45 Å. Overall, the Tryptophan residue is active in the range z [-90, -5] Å. And most activity is in ranges z [-15, -10] Å and around z -85 Å.

20-Ile: Isoleucine residue energy increases between z [-80, 5] Å for Pos1 simulation. For Pos1, peaks are at z -20 and -60 Å. Decrease is at z -50 Å. For Pos2, the energy increase is at range z [-90, -10]. Peaks are at range z [-40, -10] Å. Overall, the Isoleucine residue is active in the range z [-90, 5] Å. And most activity is in ranges z [-40, -10] and z [-60, -50] Å.

21-Lys: Lysine residue energy increases between z [-90, 35] Å for Pos1 simulation. For Pos1 peaks are at z -20, -40, -75 and range [-55, -65] Å. For Pos2, the energy increase is at range z [-90, -15] Å. Peaks are at z -55, -85 and at range [-18, -40] Å. Overall, the Lysine residue is active in the range z [-90, 35] Å. And most activity is in ranges z [-40, -18] and z [-85, -55] Å.

22-Arg: Arginine residue energy increases between z [-100, 0] Å for Pos1 simulation. For Pos1 peaks are at z -90 and range z [-60, -20] Å. For Pos2, the energy increase is at range z [-100, -10] Å. Peaks are at z -90 and range z [-20, -60] Å. Overall, the Arginine residue is active in the range z [-100, 0] Å. And most activity is in ranges z [-60, -20] and around z -90 Å.

23-Lys: Lysine residue energy increases between z [-100, -10] Å for Pos1 simulation. For Pos1 peaks are at z -20 Å and range z [-90, -40] Å. Energy decrease is at z -25 Å. For Pos2, the energy increase is at range z [-100, -15] Å. Peaks are at z -95 Å and range z [-80,

-20] Å. Overall, the Lysine residue is active in the range z [-100, -10] Å. And most activity is in range z [-20, -90] Å.

24-Arg: Arginine residue energy increases between z [-100, -20] Å for Pos1 simulation. For Pos1 peaks are at range z [-70, -50]. For Pos2, the energy increase is at range z [-100, -15] Å. Peaks are at range z [-85, -20]. Overall, the Arginine residue is active in the range z [-100, -15]. And most activity is at range z [-85, -20] Å.

25-Gln: Glutamine residue energy increases between z [-100, -20] Å for Pos1 simulation. For Pos1 peaks are at range z [-40, -20] Å. For Pos2, the energy increase is at range z [-100, -15] Å. Peaks are at range z [-50, -20] Å. Overall, the Glutamine residue is active in the range z [-100, -15] Å. And most activity is at range z [-50, 20] Å.

26-Gln: Glutamine residue energy increases between z [-90, -20] Å for Pos1 simulation. For Pos1 peaks are at z [-65, -40] Å. Energy drop is at z -35 Å. For Pos2, the energy increase is at range z [-90, -20] Å. A peak is at z -50 Å. Overall, the Glutamine residue is active in the range z [-90, -20] Å. And most activity is at range z [-65, -40] Å.

B.3. pVEC in POPE - NAMD Energy Analysis of Protein Residues:

The pVEC peptide has 18 residues which are arranged in the following order; LLIILRRRIRKQAHAHSK. The NAMD energy analysis gives the electrostatic energies of each residue with the system. The analysis of these results gives clues as to which residues play more important roles and which residues have less interactions with its surroundings. Understanding the roles of residues will help in designing more effective drugs. The following graphs show the electrostatic energy vs. z-coordinate of the first residue of the peptide. The electostatic energy plays a greater role then VDW and non-bond energies. Therefore it is easy to say that the electrostatic energies correlate to the interaction levels of the residues with its surroundings. pVEC is composed of the following residues: LLIILRRRIRKQAHAHSK

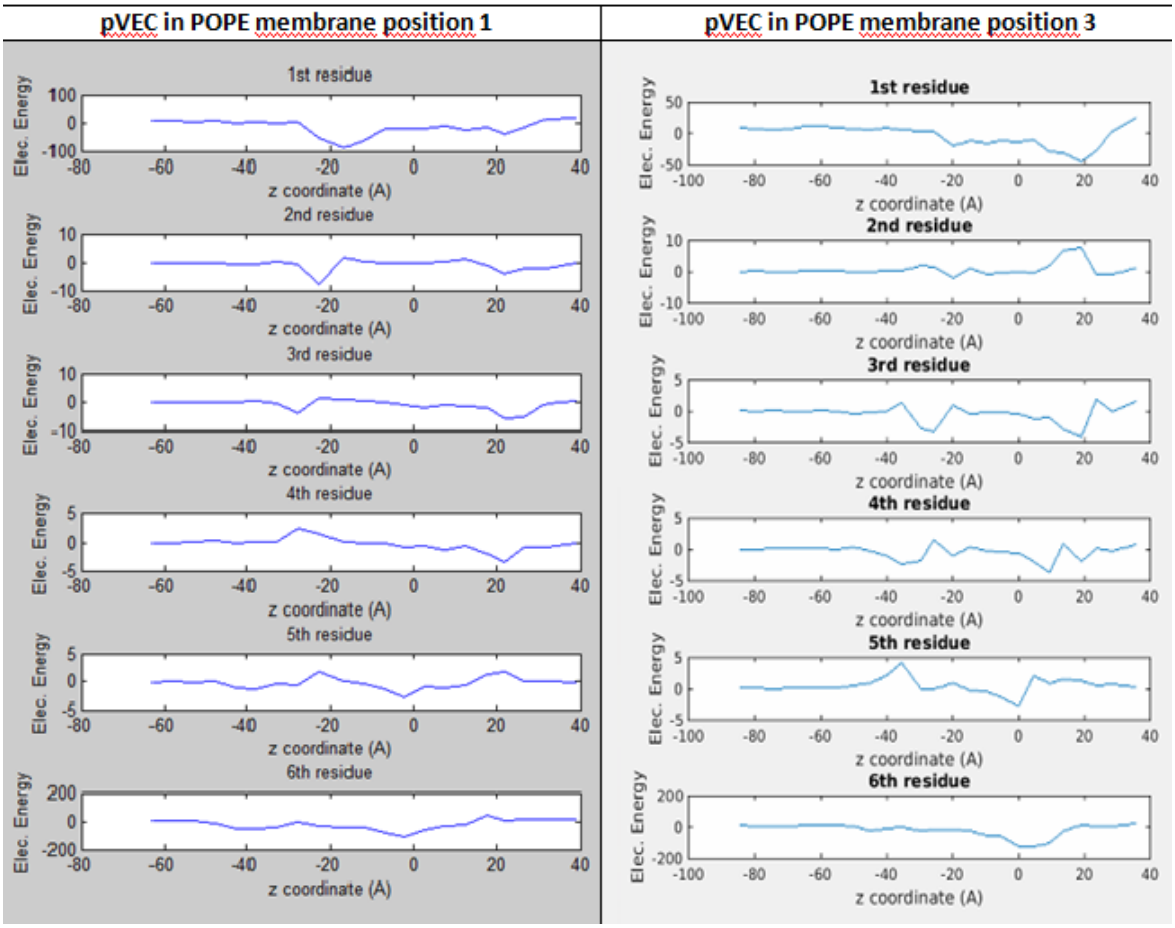

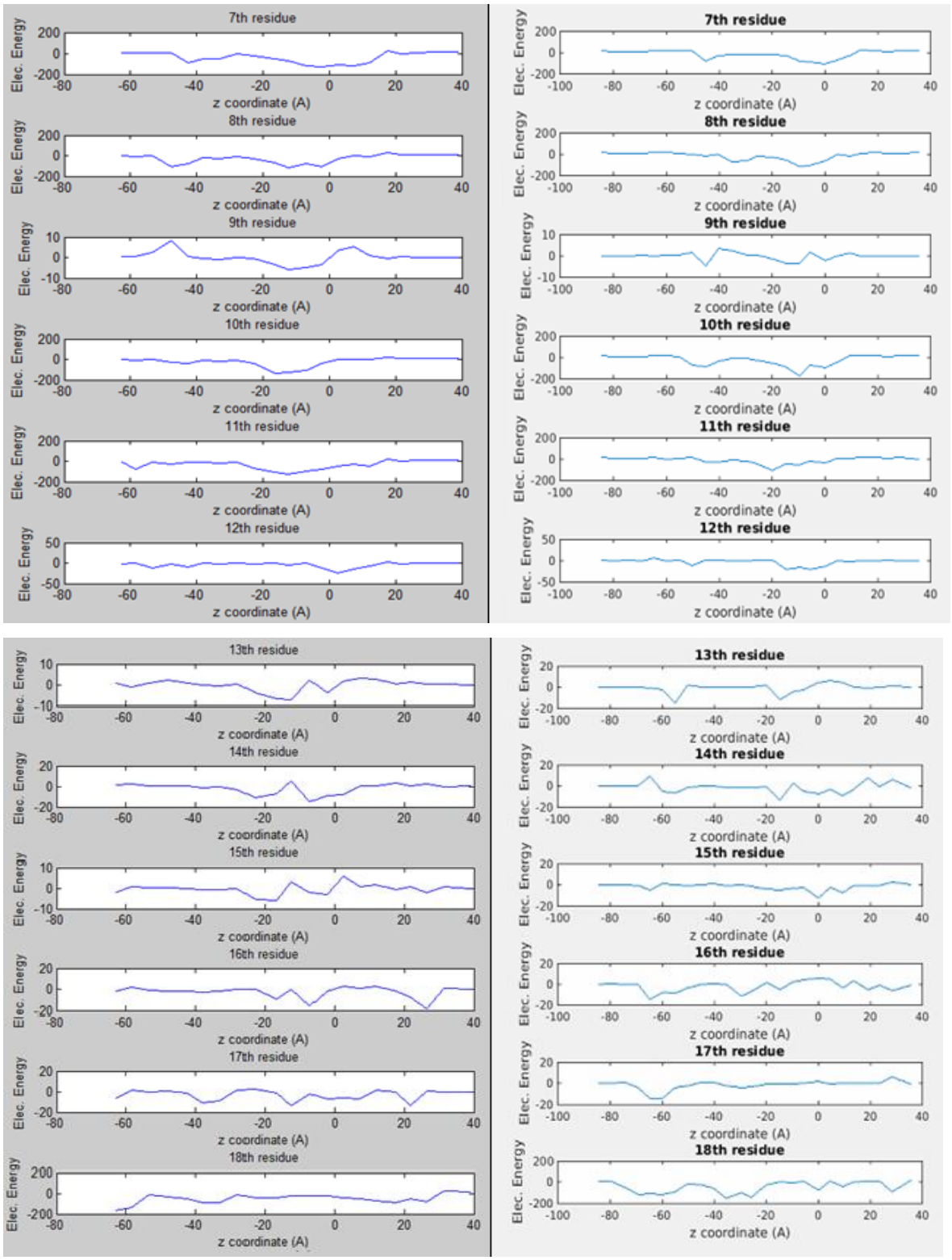

Figure B.3. The residue NAMD energy graphs of pVEC in POPE SMD simulations. z is the position of the α-carbon of the first residue of the peptide which is lyscine (units Å).

1-Leu: The Luecine residue energy increases between z [-30, 30] for the Pos1 simulation. For Pos1 peaks are at z 22 and -18. For Pos2, the energy increase is at range z [-30, 40]. Two peaks are at z 20 and z -20. Overall, the first residue Luecine is active in the range z [-30, 40]. And most activity is in around z 20 and z -20. (Units Å)

2-Leu: The Luecine residue energy increases between z [-30, 30] for the Pos1 simulation. For Pos1 peaks are at z 22 and -22. For Pos2, the energy increase is at range z [-30, 25]. A peak is at z -20, and a large energy drop is at z 20. Overall, the Luecine residue is active in the range z [-30, 30]. And most activity is around z 20 and z -20. (Units Å)

3-Ile: The Isoleucine residue energy increases between z [-40, 30] for the Pos1 simulation. For Pos1 peaks are at z -25 and z 25. For Pos2, the energy increase is at range z [-40, 40]. Peaks are at z 18 and z -25. Drop of energy is at z 25 and z -35. Overall, the Isoleucine residue is active in the range z [-40, 40]. And most activity is in ranges z [18, 25] and z [-35, -25]. (Units Å)

4-Ile: The Isoleucine residue energy increases between z [-35, 25] for the Pos1 simulation. For Pos1 a peak is at z 22 and a drop of energy is at z -25. For Pos2, the energy increase is at range z [-50, 40]. Peaks are at z -35, -20, 10 and 20. Also a drop of energy is at z -25. Overall, the Isoleucine residue is active in the range z [-50, 40]. And most activity is in ranges z [10, 20] and z [-35, -20]. (Units Å)

5-Leu: The Luecine residue energy increases between z [-50, 30] for the Pos1 simulation. For Pos1 peaks are at z -40, -5 and peaks of energy drop at z 20 and -25. For Pos2, the energy increase is at range z [-50, 30]. A peak of energy increase is at z 0 and energy decrease at z 5 and a large decrease of energy at z -35. Overall, the Luecine residue is active in the range z [-50, 30]. And most activity is , in ranges z [-5, 20] and z [-40, -25]. (Units Å)

6-Arg: The Arginine residue energy increases between z [-50, 25] for the Pos1 simulation. For Pos1 peak is at z -5 and a drop of energy at z 18. For Pos2, the energy increase is at range z [-50, 20]. Peaks are at range z [0, 10]. Overall, the Arginine residue is active in the range z [-50, 25]. And most activity is in ranges z [-5, 10] and around z [18]. (Units Å)

7-Arg: The Arginine residue energy increases between z [-50, 25] for the Pos1 simulation. For Pos1 peaks are at z -42 and range z [-5, 10] and an energy drop is at z 18. For Pos2, the energy increase is at range z [-50, 25]. Two peaks are at z -45 and range z [-10, 10]. Overall, the Arginine residue is active in the range z [-50, 25]. And most activity is in ranges z [-10, 18] and z [-45, -42]. (Units Å)

8-Arg: The Arginine residue energy increases between z [-55, 20] for the Pos1 simulation. For Pos1 peaks are at z -47, -15 and -5. For Pos2, the energy increase is at range z [-50, 20]. Two peaks are at ranges z [-10, 5] and range z[-35, -25]. Overall, the Arginine residue is active in the range z [-55, 20]. And most activity is in ranges z [-15, 5] and z [-47]. (Units Å)

9-Ile: The Isoleucine residue energy increases between z [-60, 25] for the Pos1 simulation. For Pos1 peaks are at range z [-15, 5]. And energy drops are at z 5 and z -45. For Pos2, the energy increase is at range z [-55, 15]. Peaks are at z -45, -15 and 0. Energy drops are at z -40 and z -5. Overall, the Isoleucine residue is active in the range z [-60, 25]. And most activity is in ranges z [-15, 5] and z [-45, -40]. (Units Å)

10-Arg: The Arginine residue energy increases between z [-50, 20] for the Pos1 simulation. For Pos1 peaks are at z range [-22, 0]. For Pos2, the energy increase is at range z [-60, 25]. Peaks are at z -10, 0 and z range [-50, -40] . Overall, the Arginine residue is active in the range z [-60, 25]. And most activity is in the range z [-22, 0] and z [-50, -40]. (Units Å)

11-Lys: The Lysine residue energy increases between z [-60, 20] for the Pos1 simulation. For Pos1 peaks are at z -57, -15 and 15. For Pos2, the energy increase is at range z [-50, 30]. A peak is at z -20. Overall, the Lysine residue is active in the range z [-60, 30]. And most activity is in ranges z [-20, -15] and around z[15] and z[-57]. (Units Å)

12-Gln: The Glutamine residue energy increases between z [-60, 25] for the Pos1 simulation. For position a peak is at z 5. For Pos2, the energy increase is at range z [-70, 10]. Two peaks are at z -50 and z range [-20, 5]. Overall, the Glutamine residue is active in the range z [-70, 25]. And most activity is in ranges z [-20, 5] and around z [-50]. (Units Å)

13-Ala: The Alanine residue energy increases between z [-60, 25] for the Pos1 simulation. For Pos1 peaks are at z -57, -2 and range [-20, -15], and an energy drop is at z -7. For Pos2, the energy increase is at range z [-60, 20]. Two peaks are at z-55 and z -17. A drop of energy is at z range [0, 10]. Overall, the Alanine residue is active in the range z [-60, 25]. And most activity is in ranges z [0, 10], z [-20, -2] and z [-57, -55]. (Units Å)

14-His: The Histidine residue energy increases between z [-40, 30] for the Pos1 simulation. For Pos1 peaks are at z -7, -20 and also an energy drop is at z -12. For Pos2, the energy increase is at range z [-70, 40]. Little peaks are at (Units Å)

15-Ala: The Alanine residue energy increases between z [-60, 30] for the Pos1 simulation. For Pos1 a peak is at z -20 and energy drops are at z 5 and -15. For Pos2, the energy increase is at range z [-70, 40]. Peaks are at z 10, 0 and -65. Overall, the Alanine residue is active in the range z [-70, 40]. And most activity is in ranges z [0, 10] and around z [-65] and z [-20]. (Units Å)

16-His: The Histidine residue energy increases between z [-60, 30] for the Pos1 simulation. For Pos1 a large peak is at z 25 and smaller peaks at z -5 and -18. For Pos2, the energy increase is at range z [-70, 30]. Little peaks are at z range [5, 25] and larger peaks at -15, -30 and -65. Overall, the Histidine residue is active in the range z [-70, 30]. And most activity is in ranges z [5, 25], z [-5, -18] and around points z [-30] and z[-65]. (Units Å)

17-Ser: The Serine residue energy increases between z [-60, 30] for the Pos1 simulation. For Pos1 peaks are at z range [-40, -35] and z 22 and -15. For Pos2, the energy increase is at range z [-70, 40]. Peaks are at z range [-65, 60] and energy drop is at z 30. Overall, the Serine residue is active in the range z [-70, 40]. And most activity is in the range z [-65,60], z [-40, -35], z[22, 30] and around z [-15]. (Units Å)

18-Lys: The Lysine residue energy increases between z [-60, 30] for the Pos1 simulation. For Pos1 peaks are at z 25, 18, -60 and z range [-40, -30]. Energy drop is at z -25. For Pos2, the energy increase is at range z [-80, 40]. Peaks are at z ranges [-35, -25] and [-80, -55] and around points z 0, 10 and 30. Overall, the Lysine residue is active in the

range z [-80, 40]. And most activity is in ranges z [0, 30], z [-40, -25] and z [-80, -55]. (Units Å)

B.4. pVEC in POPC - NAMD Energy Analysis of Protein Residues

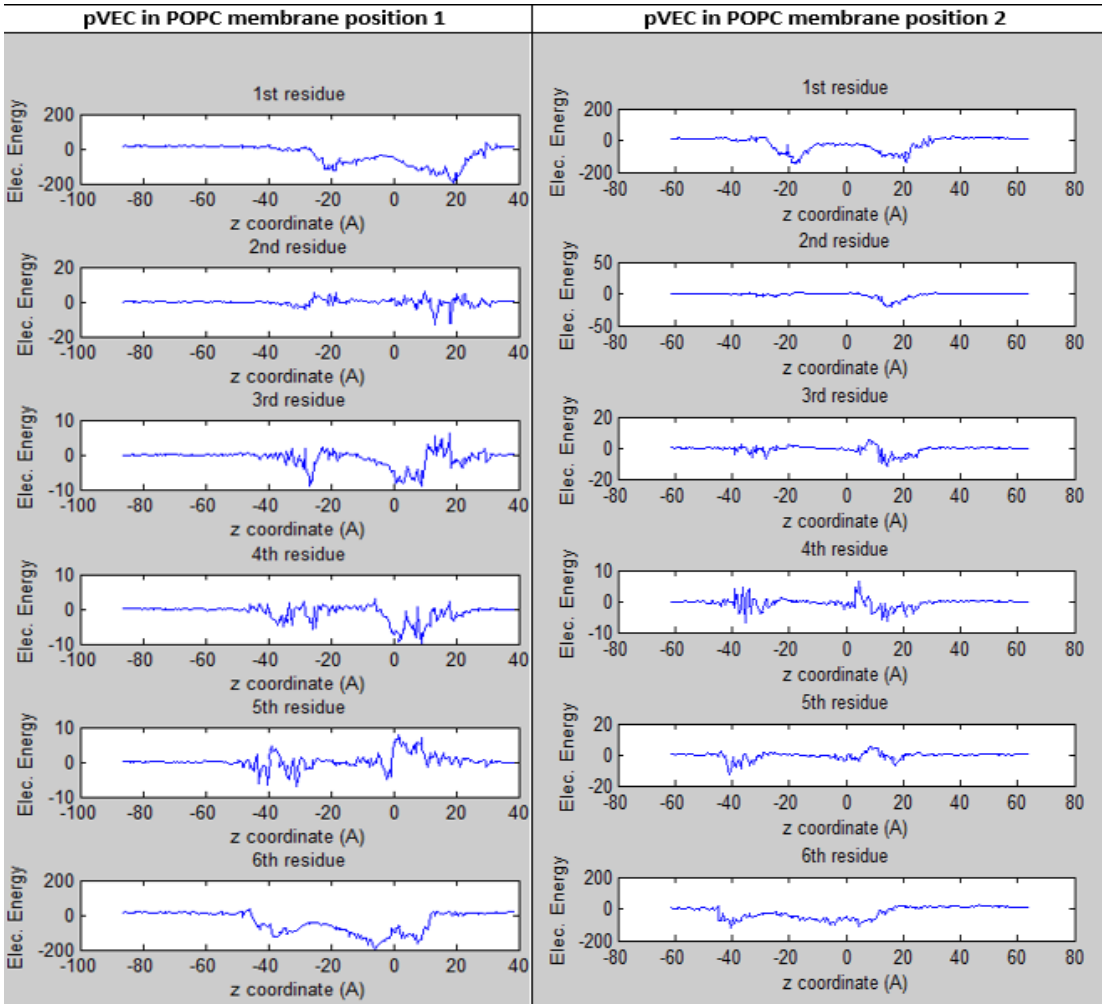

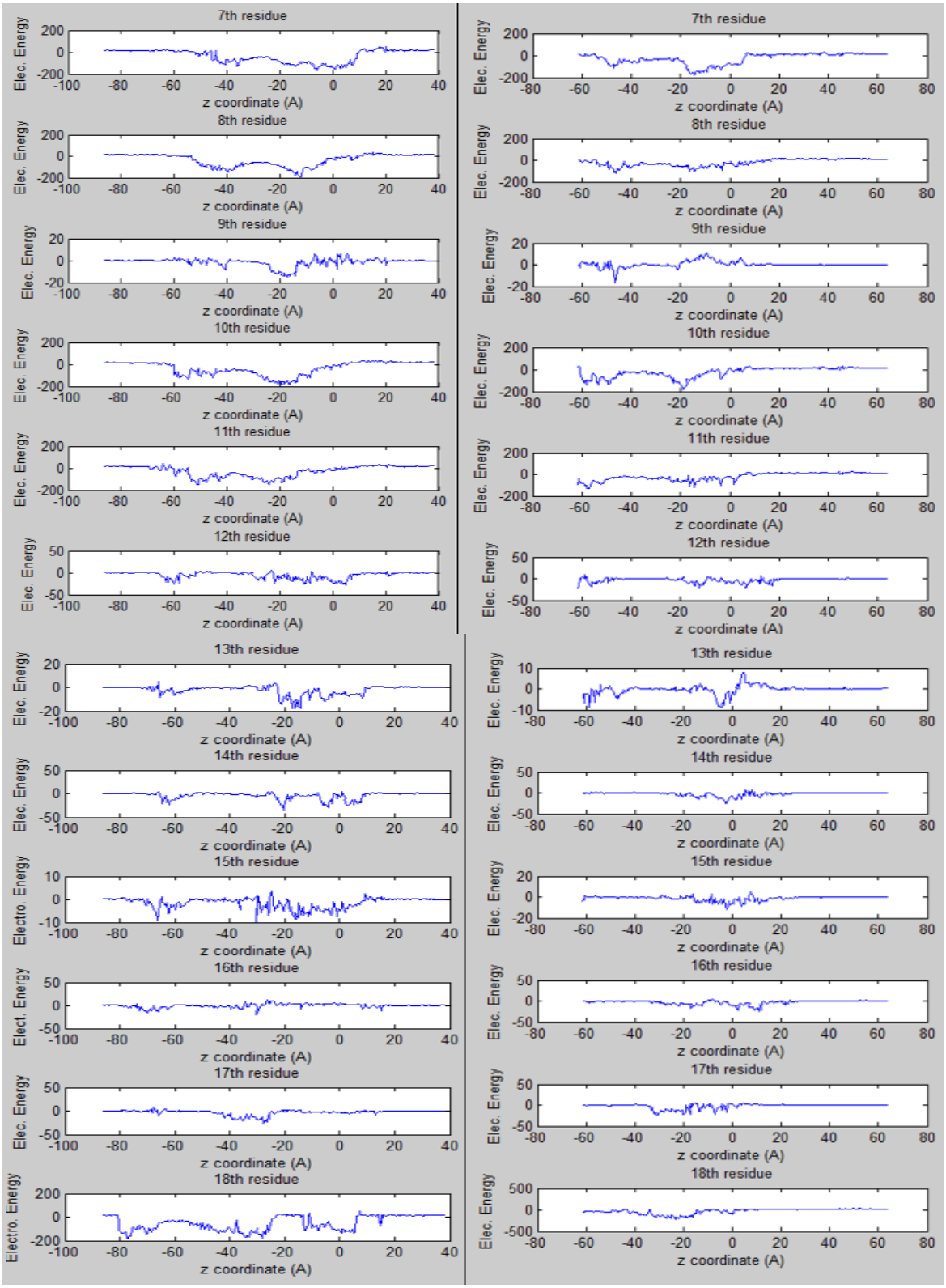

Figure B.4. The residue NAMD energy graphs of pVEC in POPC SMD simulation. z is the position of the α-carbon of the first residue of the peptide which is lyscine (Units Å).

1-Leu: The Leucine residue energy increases between z [-40, 30] for the Pos1 simulation. For Pos1 peaks are at z 20 and -20. For Pos2, the energy increase is at range z [-40, 30]. Two peaks are at z 20 and z -20. Overall, the first residue Luecine is active in the range z [-40, 30]. And most activity is in around z 20 and z -20. (Units Å)

2-Leu: The Luecine residue energy increases between z [-35, 30] for the Pos1 simulation. For Pos1 peaks are at z 15 and 18. And a drop of energy is around z -22. For Pos2, the energy increase is at range z [-35, 30]. A peak is at z 17. Overall, the Luecine residue is active in the range z [-35, 30]. And most activity is in the range z [15, 18]. (Units Å)

3-Ile: The Isoleucine residue energy increases between z [-45, 35] for the Pos1 simulation. For Pos1 peaks are at z -25 and in the range [0,10] . A drop of energy is at z [15-20]. For Pos2, the energy increase is at range z [-40, 30]. A peak is at z [15, 22]. And a drop of energy at z 10. Overall, the Isoleucine residue is active in the range z [-45, 35]. And most activity is in ranges z [0, 22] and around z [-25]. (Units Å)

4-Ile: The Isoleucine residue energy increases between z [-50, 30] for the Pos1 simulation. For Pos1 peaks are at z -35, -25, 0 and 10. For Pos2, the energy increase is at range z [-45, 30]. Two peaks are , an increse in energy at z -35 and a decrease in energy at z 5. Overall, the Isoleucine residue is active in the range z [-50, 30]. And most activity is in ranges z [0, 10] and z [-35, -25]. (Units Å)

5-Leu: The Luecine residue energy increases between z [-50, 35] for the Pos1 simulation. For Pos1 peaks are at z -40, -30, -2 and a peak of energy drop at range [0, 10]. For Pos2, the energy increase is at range z [-45, 25]. Two peaks are , energy increase at z -40 and energy decrease at z 10. Overall, the Luecine residue is active in the range z [-50, 35]. And most activity is, in ranges z [-40, -30] and z [-2]. Energy drop at range z [0, 10]. (Units Å)

6-Arg: The Arginine residue energy increases between z [-50, 15] for the Pos1 simulation. For Pos1 large peaks are at z -10, 10 and -40. For Pos2, the energy increase is at range z [-45, 20]. Two peaks are at z -40 and z 10. Overall, the Arginine residue is active

in the range z [-50, 20]. And most activity is in ranges z [-10, 10] and around z [-40]. (Units Å)

7-Arg: The Arginine residue energy increases between z [-50, 20] for the Pos1 simulation. For Pos1 peaks are at z -40 and range z [-20, 10] . For Pos2, the energy increase is at range z [-50, 15]. Two peaks are at z -45 and range z [-20, 5]. Overall, the Arginine residue is active in the range z [-50, 20]. And most activity is in ranges z [-20, 10] and z [-45, -40]. (Units Å)

8-Arg: The Arginine residue energy increases between z [-55, 15] for the Pos1 simulation. For Pos1 peaks are at z -40 and -10. For Pos2, the energy increase is at range z [-55, 20]. Two peaks are at z -45 and range z [-20, 0]. Overall, the Arginine residue is active in the range z [-55, 20]. And most activity is in ranges z [-20, 0] and z [-45, -40]. (Units Å)

9-Ile: The Isoleucine residue energy increases between z [-60, 20] for the Pos1 simulation. For Pos1 peaks are at z -40, -20 and range z [-10, 5]. For Pos2, the energy increase is at range z [-60, 10]. Two peaks are at z -45 and range z [-20,0] z . Overall, the Isoleucine residue is active in the range z [-60, 20]. And most activity is in ranges z [-20, 5] and z [-45, -40]. (Units Å)

10-Arg: The Arginine residue energy increases between z [-60, 10] for the Pos1 simulation. For Pos1 peaks are at z range [-60, -10]. For Pos2, the energy increase is at range z [-60, 10]. Two peaks are at z -20 and z range [-60, -50] . Overall, the Arginine residue is active in the range z [-60, 10]. And most activity is in the range z [-60, -10], especially at z [-60, -50]. (Units Å)

11-Lys: The Lysine residue energy increases between z [-70, 10] for the Pos1 simulation. For Pos1 peaks are at ranges z [-60, -40] and [-30, -15] . For Pos2, the energy increase is at range z [-60, 10]. Two peaks are at z -60 and z range [-20, 0] . Overall, the Lysine residue is active in the range z [-70, 10]. And most activity is in ranges z [-30, 0] and z [-60, -40]. (Units Å)

12-Gln: The Glutamine residue energy increases between z [-65, 10] for the Pos1 simulation. For Pos1 peaks are at z -60 and z range [-20, 5] . For Pos2, the energy increase is at range z [-60, 20]. Two peaks are at z -60 and z range [-20, 20]. Overall, the Glutamine residue is active in the range z [-65, 20]. And most activity is in ranges z [-20, 20] and around z [-60]. (Units Å)

13-Ala: The Alanine residue energy increases between z [-70, 10] for the Pos1 simulation. For Pos1 peaks are at z -65 and range [-20, 10], however largest peak is at z -20 . For Pos2, the energy increase is at range z [-60, 15]. Two peaks are at z-60 and z -5. Overall, the Alanine residue is active in the range z [-70, 15]. And most activity is in ranges z [-20, 10] and z [-65, -60]. (Units Å)

14-His: The Histidine residue energy increases between z [-70, 10] for the Pos1 simulation. For Pos1 peaks are at z -65, -20 and z range [-10, 10]. For Pos2, the energy increase is at range z [-35, 20]. Peaks are at z range [-20, 10]. Overall, the Histidine residue is active in the range z [-70, 20]. And most activity is in ranges z [-20, 10] and around z [-65]. (Units Å)

15-Ala: The Alanine residue energy increases between z [-70, 20] for the Pos1 simulation. For Pos1 peaks are at z -65 and range [-30, 0] . For Pos2, the energy increase is at range z [-20, 20]. Peaks are at z range [-20, 10] . Overall, the Alanine residue is active in the range z [-70, 20]. And most activity is in ranges z [10, -30] and around z [-65]. (Units Å)

16-His: The Histidine residue energy increases between z [-75, 20] for the Pos1 simulation. For Pos1 a peak is at z -30. For Pos2, the energy increase is at range z [-60, 25]. A peak is at z 10. Overall, the Histidine residue is active in the range z [-75, 25]. And most activity is in around z [-30] and z [10]. (Units Å)

17-Ser: The Serine residue energy increases between z [-70, 15] for the Pos1 simulation. For Pos1 peaks are at z range [-40, -25]. For Pos2, the energy increase is at

range z [-40, 10]. Peaks are at z range [-40, 10] . Overall, the Serine residue is active in the range z [-70, 15]. And most activity is in the range z [-40, 0]. (Units Å)

18-Lys: The Lysine residue energy increases between z [-80, 20] for the Pos1 simulation. For Pos1 peaks are at z 15 and z ranges [-70, -80], [-50, -25] and [-15, 5]. For Pos2, the energy increase is at range z [-50, 10]. Peaks are at z range [-40, -15]. Overall, the Lysine residue is active in the range z [-80, 20]. And most activity is in ranges z [-40, 5] and z [-70, -80] and around z [15]. (Units Å)

APPENDIX C: SIMULATION CODES AND SCRIPTS

This section holds some of the Matlab and tcl scrips used in this study which are presented with further detail in supplementary CD along with software and hardware requirements.

1MELITTINGENERATOR.tcl: is used to form the psf and pdb file for the new peptide.

```
resetpsf

package require psfgen

topology top_all27_prot_lipid.inp


pdbalias residue HIS HSE
pdbalias atom ILE CD1 CD

segment A {
residue 1 GLY
residue 2 ILE
residue 3 GLY
residue 4 ALA
residue 5 VAL
residue 6 LEU
residue 7 LYS
residue 8 VAL
residue 9 LEU
residue 10 THR
residue 11 THR
residue 12 GLY
residue 13 LEU
residue 14 PRO
```

```
residue 15 ALA
residue 16 LEU
residue 17 ILE
residue 18 SER
residue 19 TRP
residue 20 ILE
residue 21 LYS
residue 22 ARG
residue 23 LYS
residue 24 ARG
residue 25 GLN
residue 26 GLN
last CT2
}
coordpdb peptide.pdb A
writepsf newpeptide.psf
guesscoord
writepdb newpeptide.pdb
```

1pVECGENERATOR.tcl: is used to form the psf and pdb file for the new peptide.

```
resetpsf

package require psfgen
topology top_all27_prot_lipid.inp

pdbalias residue HIS HSE
pdbalias atom ILE CD1 CD
segment A {
residue 1 LEU
residue 2 LEU
residue 3 ILE
```

```
residue 4 ILE
residue 5 LEU
residue 6 ARG
residue 7 ARG
residue 8 ARG
residue 9 ILE
residue 10 ARG
residue 11 LYS
residue 12 GLN
residue 13 ALA
residue 14 HSE
residue 15 ALA
residue 16 HSE
residue 17 SER
residue 18 LYS
last CT2
}
coordpdb peptide.pdb A
writepsf newpeptide.psf
guesscoord
writepdb newpeptide.pdb
```

2_code.tcl: used to solvate the protein.

```
mol delete all

package require solvate
solvate newpeptide.psf newpeptide.pdb -o new_pep_sol -t 20
mol load psf new_pep_sol.psf pdb new_pep_sol.pdb
set all [atomselect top all]
$all set beta 0
set clash [atomselect top "resname TIP3 and same residue as (within 2.8 of protein)"]
```

```
$clash set beta 1
set clashwater [atomselect top "name OH2 and beta > 0"]
set seglist [$clashwater get segid]
set reslist [$clashwater get resid]
mol delete all
package require psfgen
readpsf new_pep_sol.psf
coordpdb new_pep_sol.pdb
foreach segid $seglist resid $reslist {
delatom $segid $resid
}
#set all [atomselect top all]
#$all moveby [vecinvert [measure center $all]]
#display resetview
writepdb pep_VdW.pdb
writepsf pep_VdW.psf
mol delete all
mol load psf pep_VdW.psf pdb pep_VdW.pdb
```

3_fix_protein.tcl: to fix protein.

```
mol delete all
resetpsf
mol load pdb pep_VdW.pdb psf pep_VdW.psf
set all [atomselect top "all"]
$all set beta 0

set prot [atomselect top "protein"]
$prot set beta 1
$all writepdb pep_consk.pdb
```

equil2.conf: is used to equilibrate melittin in solvate.

```
#############################################################
## ADJUSTABLE PARAMETERS                                   ##
#############################################################
structure          pep_VdW.psf
coordinates        pep_VdW.pdb
outputName         equil2

set temperature    310

# Continuing a job from the restart files
if {0} {
set inputname      minimization
binCoordinates     $inputname.restart.coor
binVelocities      $inputname.restart.vel  ;# remove the "temperature" entry if you use this!
extendedSystem     $inputname.restart.xsc
}
firsttimestep      0

#############################################################
## SIMULATION PARAMETERS                                   ##
#############################################################
# Input
paraTypeCharmm      on
parameters          par_all27_prot_lipidNBFIX.prm

# NOTE: Do not set the initial velocity temperature if you
# have also specified a .vel restart file!
temperature         $temperature

# Periodic Boundary Conditions
# NOTE: Do not set the periodic cell basis if you have also
```

```
# specified an .xsc restart file!
if {1} {
cellBasisVector1    74.08500289916992 0.   0.0
cellBasisVector2     0.0  67.77099990844727  0.0
cellBasisVector3     0.0    0   55.35799980163574
cellOrigin          -0.000499666144605726 5.660824172082357e-6
0.00032934488262981176
}
wrapWater           on
wrapAll             on

# Force-Field Parameters
exclude             scaled1-4
1-4scaling          1.0
cutoff              12.
switching           on
switchdist          10.
pairlistdist        13.5

# Integrator Parameters
timestep            2.0  ;# 2fs/step
rigidBonds          all  ;# needed for 2fs steps
nonbondedFreq       1
fullElectFrequency  2
stepspercycle       20


#PME (for full-system periodic electrostatics)
if {1} {
PME                 yes
PMEGridSizeX        80
PMEGridSizeY        72
PMEGridSizeZ        60
```

```
}

# Constant Temperature Control
langevin            on    ;# do langevin dynamics
langevinDamping     1     ;# damping coefficient (gamma) of 5/ps
langevinTemp        $temperature

# Constant Pressure Control (variable volume)
if {1} {
useGroupPressure      yes ;# needed for 2fs steps
useFlexibleCell       no  ;# no for water box, yes for membrane
useConstantArea       no  ;# no for water box, yes for membrane

langevinPiston        on
langevinPistonTarget  1.01325 ;#  in bar -> 1 atm
langevinPistonPeriod  200.
langevinPistonDecay   50.
langevinPistonTemp    $temperature
}

restartfreq        1000     ;# 1000steps = every 2ps
dcdfreq            1000
xstFreq            1000
outputEnergies      50
outputPressure      50

# Minimization for Constrained Atoms
fixedAtoms      off
constraints  on
consexp 2
consref   pep_VdW.pdb ;# all coordinate file
conskfile  pep_consk.pdb
conskcol B
```

```
margin 3

tclforces on
set waterCheckFreq            100
set lipidCheckFreq            100
set allatompdb                pep_VdW.pdb  ;# all coordinate file
tclForcesScript               keep_water_out.tcl

minimize           1000 ;# 1 ns

# MD for Constrained Atoms
run 1000000 ;# 2 ns

# MD for No Constrained Atoms
constraintScaling 0
run 1000000 ;# 2 ns
```

################### Scripts used in SMD Simulations ###################

1_merge.tcl: is used to create and combine the peptide and the membrane.

```
mol delete all
 resetpsf
 package require psfgen


readpsf popE_membrane_final.psf
coordpdb popE_membrane_final.pdb
readpsf pVECfinal.psf
coordpdb pVECfinal.pdb
writepdb manipulated.pdb
writepsf manipulated.psf
```

2_deleteclashwater.tcl: is used to delete clashing water molecules around the protein.

```
mol delete all
 resetpsf
mol load pdb manipulated.pdb
set all [atomselect top all]
$all set beta 0
set clash [atomselect top "resname TIP3 and same residue as (within 2.8 of protein)"]
$clash set beta 1
set clashwater [atomselect top "name OH2 and beta > 0"]
set seglist [$clashwater get segid]
set reslist [$clashwater get resid]
mol delete all
package require psfgen
readpsf manipulated.psf
coordpdb manipulated.pdb
foreach segid $seglist resid $reslist {
delatom $segid $resid
}
writepdb memb_wat_pep.pdb
writepsf memb_wat_pep.psf
mol delete all
mol load pdb memb_wat_pep.pdb
```

4_fix_peptide.tcl: is used to fix molecules other than the peptide.

```
mol delete all
 resetpsf
 mol load pdb ionized.pdb psf ionized.psf
set all [atomselect top "all"]
$all set beta 0
set fixed [atomselect top "protein"]
```

```
$fixed set beta 1
$all writepdb fixed_peptide.pdb
```

minimization.conf: is used to minimize peptide then to run the system without constraints.

```
#############################################################
## ADJUSTABLE PARAMETERS                                   ##
#############################################################
structure          ionized.psf
coordinates        ionized.pdb
outputName         minimization
set temperature    310

# Continuing a job from the restart files
if {0} {
set inputname      melting_lipid_tails
binCoordinates     $inputname.restart.coor
binVelocities      $inputname.restart.vel  ;# remove the "temperature" entry if you use this!
extendedSystem     $inputname.restart.xsc
}
firsttimestep      0

#############################################################
## SIMULATION PARAMETERS                                   ##
#############################################################
# Input
paraTypeCharmm      on
parameters          par_all27_prot_lipidNBFIX.prm

# NOTE: Do not set the initial velocity temperature if you
# have also specified a .vel restart file!
 temperature         $temperature
```

```
# Periodic Boundary Conditions
# NOTE: Do not set the periodic cell basis if you have also
# specified an .xsc restart file!
# Vectors are calculated all atoms
if {1} {
cellBasisVector1    76.55299758911133 0.   0.
cellBasisVector2     0.   81.41400146484375  0.
cellBasisVector3     0.    0.  180.33999633789063
cellOrigin         0.11416976153850555 -0.10474114865064621 -0.3407750427722931
}
wrapWater           on
wrapAll             on


# Force-Field Parameters
exclude             scaled1-4
1-4scaling          1.0
cutoff              12.
switching           on
switchdist          10.
pairlistdist        13.5

# Integrator Parameters
timestep            2.0  ;# 2fs/step
rigidBonds          all  ;# needed for 2fs steps
nonbondedFreq       1
fullElectFrequency  2
stepspercycle       20

#PME (for full-system periodic electrostatics)
if {1} {
PME                 yes
```

```
PMEGridSizeX       80
PMEGridSizeY       90
PMEGridSizeZ       192
}

# Constant Temperature Control
langevin           on    ;# do langevin dynamics
langevinDamping    1     ;# damping coefficient (gamma) of 5/ps
langevinTemp       $temperature

# Constant Pressure Control (variable volume)
if {1} {
useGroupPressure      yes ;# needed for 2fs steps
useFlexibleCell       yes  ;# no for water box, yes for membrane
useConstantArea       no  ;# no for water box, yes for membrane

langevinPiston        on
langevinPistonTarget  1.01325 ;#  in bar -> 1 atm
langevinPistonPeriod  200.
langevinPistonDecay   50.
langevinPistonTemp    $temperature
}

restartfreq        1000     ;# 1000steps = every 2ps
dcdfreq            1000
xstFreq            1000
outputEnergies      50
outputPressure      50

# Fixed Atoms Constraint (set PDB beta-column to 1)
if {0} {
fixedAtoms          on
fixedAtomsFile      fixed_peptide.pdb
```

```
fixedAtomsCol       B
fixedAtomsForces    on
minimize            1000

reinitvels          $temperature
}
# Minimization for Constrained Atoms

fixedAtoms      off
constraints  on
consexp 2
consref   ionized.pdb;# all coordinate file
conskfile  fixed_peptide.pdb
conskcol B
margin 5

tclforces on
set waterCheckFreq            100
set lipidCheckFreq            100
set allatompdb                ionized.pdb  ;# all coordinate file
tclForcesScript               keep_water_out.tcl

#####################################################################
## EXECUTION SCRIPT                                 ##
#####################################################################

# Minimization
if {1} {
minimize            1000
}
# MD for Constrained Atoms
run 250000   ;# 0.5 ns
```

```
# MD for No Constrained Atoms
constraintScaling 0
run 250000    ;# 0.5 ns
```

5_smd.tcl : is used to create smd_pulled.ref

```
mol delete all
resetpsf
mol load pdb temp.pdb
set all [atomselect top all]
set pro [atomselect top "name P"]
$all set beta 0
$pro set beta 1
$all writepdb fixed_p.pdb
set all [atomselect top all]
$all set beta 0
$all set occupancy 0
set pro [atomselect top "protein and resid 1 and name CA"]
$pro set occupancy 1
$all writepdb smd_pulled.ref
#set a [atomselect top all]
#measure minmax $a
```

smd_zM_equil_pep.conf: is used to run SMD simulation.

```
#############################################################
## ADJUSTABLE PARAMETERS                                   ##
#############################################################
structure          ionized.psf
coordinates        ionized.pdb
outputName         smd_zM_equil_pep
```

```
set temperature    310

# Continuing a job from the restart files
if {1} {
set inputname      minimization
binCoordinates     $inputname.restart.coor
binVelocities      $inputname.restart.vel  ;# remove the "temperature" entry if you use this!
extendedSystem    $inputname.restart.xsc
}
firsttimestep      501000

#############################################################
## SIMULATION PARAMETERS                                   ##
#############################################################
# Input
paraTypeCharmm      on
parameters          par_all27_prot_lipidNBFIX.prm

# NOTE: Do not set the initial velocity temperature if you
# have also specified a .vel restart file!
#temperature         $temperature

zeroMomentum on

# Periodic Boundary Conditions
# NOTE: Do not set the periodic cell basis if you have also
# specified an .xsc restart file!
if {0} {
cellBasisVector1    60.79100036621094    0.   0.
cellBasisVector2     0.   57.89000129699707   0.
cellBasisVector3     0.    0.  180.99000549316406
cellOrigin          -0.0674348771572113 -0.02197032980620861 -0.5652348399162292
}
```

```
wrapWater           on
wrapAll             on

# Force-Field Parameters
exclude             scaled1-4
1-4scaling          1.0
cutoff              12.
switching           on
switchdist          10.
pairlistdist        13.5

# Integrator Parameters
timestep            2.0  ;# 2fs/step
rigidBonds          all  ;# needed for 2fs steps
nonbondedFreq       1
fullElectFrequency  2
stepspercycle       10

#PME (for full-system periodic electrostatics)
if {1} {
PME                 yes
PMEGridSizeX        80
PMEGridSizeY        80
PMEGridSizeZ        180
}


# Constant Temperature Control
langevin            on    ;# do langevin dynamics
langevinDamping     1     ;# damping coefficient (gamma) of 5/ps
langevinTemp        $temperature

# Constant Pressure Control (variable volume)
```

```
if {1} {
useGroupPressure      yes ;# needed for 2fs steps
useFlexibleCell       yes  ;# no for water box, yes for membrane
useConstantArea       no ;# no for water box, yes for membrane

langevinPiston        on
langevinPistonTarget  1.01325 ;#  in bar -> 1 atm
langevinPistonPeriod  200.
langevinPistonDecay   50.
langevinPistonTemp    $temperature
}

restartfreq        1000     ;# 1000steps = every 2ps
dcdfreq            1000
xstFreq            1000
outputEnergies      50
outputPressure      50

# Fixed Atoms Constraint (set PDB beta-column to 1)
if {0} {
fixedAtoms          on
fixedAtomsFile      nottails.fix.pdb
fixedAtomsCol       B
fixedAtomsForces    on
}
#############################################################
## EXTRA PARAMETERS                                        ##
#############################################################

constraints     on
consexp 2
consref         ionized.pdb     ;# all coordinate file
conskfile       fixed_p.pdb
```

```
conskcol B
selectConstraints  on
selectConstrX off
selectConstrY off
selectConstrZ on
margin 3

SMD    on
SMDFile    smd_pulled.ref
SMDk    10
SMDVel     0.0000050
SMDDir   0 0 -1
SMDOutputFreq  10

#eFieldOn yes
#eField 0 0 -0.155

#################################################################
## EXECUTION SCRIPT                                            ##
#################################################################
run 25000000 ;# 40 ns
```

################### Scripts used in MD Simulations ####################

4_fix_peptide.tcl: is to fix molecules other than the peptide

minimization.conf: is used to minimize then obtain MD simulation.

################### MD simulations analysis Scripts ###################

z_center_of_mass.tcl: gives the center of mass of lipids coordinates vs time frames.

```
set mol [molinfo top]
set out [open z_center_of_mass_of_lipids.txt w]
set total_frame [molinfo $mol get numframes]
set sel [atomselect top "lipids"]

for {set frame 0} {$frame < $total_frame} {incr frame} {
$sel frame $frame
set m [measure center $sel]
puts $out "$frame $m"
}
close $out
```

get_zdata.tcl: gives z coordinates of SMD atom (N terminus, 1st residue, Ca atom) or any atom chosen. Gives output zdata.txt

```
set mol [molinfo top]
set out [open zdata.txt w]
set total_frame [molinfo $mol get numframes]
set smd [atomselect top "protein and resid 1 and name CA"]

for {set frame 0} {$frame < $total_frame} {incr frame}  {
$smd frame $frame
set coords [$smd get {z}]
puts $out "$frame $coords"
}
```

```
close $out
```

distance_vs_frame.m: gives distance vs. frame profile.

```
clear all
clc
x=load('zdata.txt');
y=load('z_center_of_mass_of_lipids.txt');
frame=x(:,1);
z_p=x(:,2);
z_l=y(:,4);
dist= z_p - z_l ;
plot(frame, dist)
xlabel('frame')
ylabel('Distance between 1st res. & center of mass of lipids')
title('Distance vs. Frame')
axis([0 30 -40 40])
```

energy_coor.m: gives Elec','Total','VdW','Nonbond' energy profiles vs. frame.

```
clear all
clc
x=load('energy_profile');
Elec=x(:,3);
VdW=x(:,4);
Nonbond=x(:,5);
Total=x(:,6);
frame=x(:,1);
plot(frame,Elec)
xlabel('Frame')
ylabel('Energy (kcal/mol)')
hold on
plot(frame, Total, '*')
```

```
hold on
plot(frame, VdW, ':')
hold on
plot(frame, Nonbond, '-.')
axis([0 50 -1300 100])
legend('Elec','Total','VdW','Nonbond')
title('NAMDEnergy Plot ')
```

helicity.tcl: gives the secondary structure of the protein.

```
mol delete all
resetpsf
mol new ionized_p.psf
mol addfile minimization_p.dcd waitfor all
set outfile [open helicity.dat w]
set sel [atomselect top "protein and name CA"]
molinfo top set frame 0
set n [molinfo top get numframes]
 for { set i 0 } { $i < $n } { incr i } {
 animate goto $i
 display update ui
 $sel frame $i
 mol ssrecalc top
 set secstruct [$sel get structure]
 puts $outfile "$secstruct"
}
 close $outfile
```

helicity.tcl is run to obtain helicity.dat

main.cpp

```
#include <iostream>
```

```
#include <vector>
#include <fstream>
#include <string>
#include <string.h>
#include <stdio.h>
using namespace std;
int main ( )
{
  vector< string > v;
  string line;
  ifstream inputFile ("helicity.dat");

  if (inputFile.is_open())
  {
    while ( getline (inputFile,line) )
      {
      v.push_back(line);
      }
      inputFile.close();
    ofstream outputFile;
    outputFile.open ("output.txt");

    for(int j=0; j<v.size(); j++)
    {
      char a[100];
      strcpy(a, v[j].c_str());
      int countH=0;

      for(int y =0; a[y]!='\0'; y++)
      {
        if(a[y]=='H')
        {
          countH++;
```

```
        }
      }
      outputFile <<countH<<"\n";
    }
    outputFile.close();
    }
    else cout << "Unable to open file";
    return 0;
```

main.cpp is copied into the file containing helicity.dat file

open terminal

type:

g++ -o a main.cpp

./a

output.txt file will be formed.

Run helicity.m on matlab to obtain helcity percentage vs. frame profile.

```
clear all
clc
x=load('output.txt');
P= (x/26)*100;
plot((1:1:length(x)), P)
xlabel('Frame')
ylabel('Helicity Percentage')
y= 0;
i=1;
while i < length(x) +1
    y= y + x(i);
    i=i+1;
```

```
end

T = y/length(x);
Tp= (T/26)*100;
title(['Helicity Percentage vs. Frame'])
text(40,85,{'Overall Helicity is ',num2str(T), 'which is ',num2str(Tp),'%'})
axis([0 60 0 100])
```

################### SMD simulations analysis scripts ######################

smdforces.out: is obtained from .log file of the SMD simulation.

energy_profile: is obtained from NAMD energy plugin.

count_water_in_membrane.tcl: outputs number of water molecules insie the membrane. Gives count_water_in_membrane.out output file.

```
puts "count_water_in_active_site {{molid top} {outputfile
count_water_in_membrane.out}}"
puts "For Example"
puts "count_water_in_membrane top  count_water_in_membrane.out \n"
proc count_water_in_membrane {{molid top} {outputfile
count_water_in_membrane.out}} {

set selection ""
set selection " z< 15 and z>-10 and water and name OH2"
set fid [open $outputfile "w"]
set total_frame [molinfo $molid get numframes]
for {set frame 0} {$frame < $total_frame} {incr frame} {
  set sel1 [atomselect top $selection frame $frame]
  set a [$sel1 get resid]
  puts $fid [llength $a]
  set a ""
```

```
}
close $fid
}
```

count_water_in_membrane_vs_z.m: MATLAB code generates water in membrane vs. z profile.

```
clear all
clc
y=load('count_water_in_membrane.out');
z=load('smdforces.out');
plot(z(1:9993.9947:end,4),y)
xlabel('z coordinate (A)')
ylabel('# of water molecules in membrane')
set ( gca, 'xdir', 'reverse' )
axis([0 40 0 100])
title('Water in Membrane vs. z  ')
```

thickness_of_memb.tcl: outputs thickness of membrane vs. frame. Gives thickness_of_memb.out output file.

```
puts "thickness_of_memb {{molid top} {outputfile thickness_of_memb.out}}"
puts "For Example"
puts "thickness_of_memb top  thickness_of_memb.out \n"
proc thickness_of_memb {{molid top} {outputfile thickness_of_memb.out}} {
set fid [open $outputfile "w"]
set total_frame [molinfo $molid get numframes]
for {set frame 0} {$frame < $total_frame} {incr frame} {
set sel [atomselect top lipid frame $frame]
set m [measure minmax $sel]
set z1 [lindex $m 0 2]
set z2 [lindex $m 1 2]
set r [expr $z2 - $z1]
```

```
puts $fid $r
}
close $fid
}
```

calculate_thickness.m: MATLAB code gives the maximum and minimum thickness values along with standard deviation.

```
clear all
clc
y=load('thickness_of_memb.out');
A= y(:,1);
M=max(A);
Ave=mean(A);
S=std(A);
P = 'The maximum membrane thickness is %8.3f A, and the average membrane thickness is %8.3f A with a standard deviation of %8.3f A. \n';
fprintf(P,M,Ave,S)
```

thickness_of_memb_vs_z.m: MATLAB code gives membrane thickness vs. z profile.

```
clear all
clc
y=load('thickness_of_memb.out');
order= y(:,1);
z=load('smdforces.out');
plot(z(1:9993.9947:end,4),order)
xlabel('z coordinate (A)')
ylabel('thickness of the membrane')
set ( gca, 'xdir', 'reverse' )

axis([0 40 50 65])
```

```
title('Thickness of Membrane vs. z  ')
```

energy_coor.m: gives energy vs. z profile by using energy_profile file obtained from NAMD.

force_coor_av.m: gives force vs. z profile by using data obtained from smd .log file.

```
clear all
clc
x=load('smdforces.out');
windowsize = 5000;
runningavgF=filter(ones(1,windowsize)/windowsize,1,x(:,7));
plot(x(:,4),runningavgF(:,1));
xlabel('z (A)');
ylabel('Force (pN)');
set ( gca, 'xdir', 'reverse' )
axis([0 40 -1600 200])
title('Force vs. z  ')
```

order3_vs_frame.tcl: gives lipid order values vs. frame.

```
  set n [molinfo top get numframes]
  set out [open orderc3_vs_frame.txt w]
  for { set frame 0 } { $frame < $n } { incr frame 50} {
  puts $frame
set sum 0.0
    set nh 0
  for { set i 2 } { $i <= 20 } { incr i } {
#    puts $i
    set cp [atomselect top "lipid and name C3$i"]
       set nres [$cp num]
    if { [$cp num] == 0 } {
#      puts "skipping $i"
```

```
  continue
}
set hx [atomselect top "lipid and name H${i}X"]
set hy [atomselect top "lipid and name H${i}Y"]
set hz [atomselect top "lipid and name H${i}Z"]

  $cp frame $frame
  $hx frame $frame
  $hy frame $frame
  $hz frame $frame
  set cpx [$cp get x]
  set cpy [$cp get y]
  set cpz [$cp get z]

  set hxx [vecsub $cpx [$hx get x]]
  set hxy [vecsub $cpy [$hx get y]]
  set hxz [vecsub $cpz [$hx get z]]
  foreach dx $hxx dy $hxy dz $hxz {
    set norm2 [expr {$dx*$dx + $dy*$dy + $dz*$dz}]
    set sum [expr {$sum + $dz*$dz/$norm2}]
  }
  incr nh $nres

  if { [$hy num] != 0 } {
    set hyx [vecsub $cpx [$hy get x]]
    set hyy [vecsub $cpy [$hy get y]]
    set hyz [vecsub $cpz [$hy get z]]
    foreach dx $hyx dy $hyy dz $hyz {
      set norm2 [expr {$dx*$dx + $dy*$dy + $dz*$dz}]
      set sum [expr {$sum + $dz*$dz/$norm2}]
    }
    incr nh $nres
  }
```

```
    if { [$hz num] != 0 } {
      set hzx [vecsub $cpx [$hz get x]]
      set hzy [vecsub $cpy [$hz get y]]
      set hzz [vecsub $cpz [$hz get z]]
      foreach dx $hzx dy $hzy dz $hzz {
        set norm2 [expr {$dx*$dx + $dy*$dy + $dz*$dz}]
        set sum [expr {$sum + $dz*$dz/$norm2}]
      }
      incr nh $nres
    }
  set order [expr {-1.5*$sum/$nh + 0.5}]
  puts $out "$i $frame $order"
   }
  }
  close $out
```

order3_vs_z_subplot.m: plots lipid carbon orders vs. z coordinates.

rgyr.tcl: gives radius of gyration values with frames. Gives radius_of_gyration.txt output.

```
set mol [molinfo top]
set out [open radius_of_gyration.txt w]
set sel [atomselect top protein]
set frames [molinfo $mol get numframes]
for {set i 0} {$i < $frames} {incr i} {
$sel frame $i
puts $out "$i [measure rgyr $sel]"
}
$sel delete
close $out
```

radius_of_gyration_vs_z.m: MATLAB code gives radius of gyration vs. z coordinate profiles.

```
clear all
clc
y=load('radius_of_gyration.txt');
order= y(:,2);
z=load('smdforces.out');
plot(z(1:9993.9947:end,4),order)
xlabel('z coordinate (A)')
ylabel('radius of gyration')
set ( gca, 'xdir', 'reverse' )
axis([0 40 0 28])
title('Radius of Gyration vs. z  ')
```

Trp19_z_vs_t.tcl: gives z coord of SMD atom Trp19 alpha carbon vs frame profile. gives Trpzdata.txt output.

```
set mol [molinfo top]
set out [open Trpzdata.txt w]
set total_frame [molinfo $mol get numframes]
set smd [atomselect top "protein and resid 19 and name CA"]
for {set frame 0} {$frame < $total_frame} {incr frame}  {
$smd frame $frame
set coords [$smd get {z}]
puts $out "$frame $coords"
}
close $out
```

Trp19_distance_vs_frame.m: plots Trp19 z coordinates vs. frame profile.

vdw_z.m: gives VdW energy profile vs. z coordinates.

work_z_50.m: gives work profile vs. z coordinates.

```
clear all
clc
load smdforces.out;
ftemp = smdforces(:,7)/69.479;
fsum = 0;
v = -1*0.0000050;
dt = 20;

for i = 1:length(smdforces)
   fsum(i+1) = fsum(i) + ftemp(i)*v*dt;
   w(i) = fsum(i);
end

A = smdforces;
z = A(:,4);
plot(z,w);
xlabel('z (A)')
ylabel('Work (kcal/mol)')

set ( gca, 'xdir', 'reverse' )

axis([0 40 0 1600])
title('Work vs. z  ')
```